3-2001

A System Dynamics Approach to Modeling Temperature Effects in Solid Waste

David A. Jokinen

A SYSTEM DYNAMICS APPROACH TO MODELING TEMPERATURE EFFECTS
IN SOLID WASTE LANDFILLS

THESIS

David A. Jokinen, 2nd Lt, USAF

AFIT/GEE/ENV/01M-05

DEPARTMENT OF THE AIR FORCE
AIR UNIVERSITY
AIR FORCE INSTITUTE OF TECHNOLOGY

Wright-Patterson Air Force Base, Ohio

APPROVED FOR PUBLIC RELEASE; DISTRIBUTION UNLIMITED.

20010508 090

The views expressed in this thesis are those of the author and do not reflect the official policy or position of the United States Air Force, Department of Defense, or the U. S. Government.

A SYSTEM DYNAMICS APPROACH TO MODELING TEMPERATURE EFFECTS IN SOLID WASTE LANDFILLS

THESIS

Presented to the Faculty

Department Systems Engineering and Management

Graduate School of Engineering and Management

Air Force Institute of Technology

Air University

Air Education and Training Command

In Partial Fulfillment of the Requirements for the

Degree of Master of Science in Engineering and Environmental Management

David A. Jokinen, B.S.
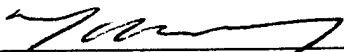
2nd Lt, USAF

March 2001

AFIT/GEE/ENV/01M-05

A SYSTEM DYNAMICS APPROACH TO MODELING TEMPERATURE EFFECTS IN SOLID WASTE LANDFILLS
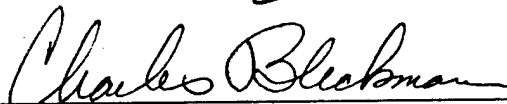
David A. Jokinen, BS
2nd Lt, USAF

Approved:

_____   _5 Ma-01_
Dr. Michael L. Shelley (Chairman)   date
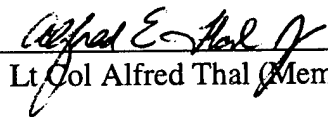
_____   _5 Mar 01_
Dr. Charles A. Bleckmann (Member)   date

_____   _5 MAR 01_
Lt Col Alfred Thal (Member)   date

<u>Acknowledgements</u>

Table of Contents

List of Figures and Tables

Abstract

The amount of municipal solid waste discarded to landfills is continually increasing even with extensive recycling efforts. The need to understand the behavior of waste in landfills is increased due to the decreasing number of active landfills, communities concern to the potential hazards associated with landfills, and companies or installations with landfills on-site need to understand landfill behavior because they must comply with new legislation concerning design and detecting hazardous material movement of-site.

This research is focused on increasing the understanding of landfill behavior by examining the effects of temperature in a landfill system. A system dynamics approach was used in this research to develop and build structure to produce landfill behavior. Two reference modes using gas generation and a basic microbial growth curve were used as verification mechanisms. Initial verification and validation were preformed in separate sections then added to Shelley's landfill model to verify that the additional temperature structure more accurately modeled landfill behavior.

Results show that an equation responsive to temperature effects on microbial growth and death, more accurately depicts landfill behavior. Increased understanding of how heat is lost from a landfill will increase the usefulness of this model. An inclusive model will help landfill operator's build and manage landfills to optimize performance and biodegradation over the lifetime of a landfill.

A SYSTEM DYNAMICS APPROACH TO MODELING TEMPERATURE EFFECTS

IN SOLID WASTE LANDFILLS

I. Introduction

Background

Landfills are an important part of solid waste management with approximately 55 percent of generated waste being disposed of in landfills (EPA, 1996). The number of active landfills in the United States has declined over the past two decades, putting an increased strain on existing landfills. Landfills have a number of concerns associated with their operation: (1) build-up of landfill gas can cause on-site explosions, (2) landfill gas increases greenhouse effects, (3) leachate isreleased into surrounding groundwater and surface waters, and (4) trace gases from hazardous materials escape into the atmosphere (Tchobanoglous et al., 1993: 370).

The declining number of active landfills is partially attributed to the above concerns expressed by local communities. Communities have the "not in my backyard" mind frame which prevents many new landfills from being built. New ways need to be researched to expand the longevity of the existing landfills. According to Murphy, new efforts such as "exploring methods to enhance degradation rates of municipal solid waste, and subsequently mining landfills to recover mineral and landfill space" are becoming increasingly popular.

One method to enhance biodegradation rates is to promote the onset of biodegradation. Landfill gases, which can be used as a metric to model the stages of

1

waste degradation, has been the focus of numerous landfill studies. A benefit of promoting methane production is that it reduces the strength of leachate, thus reducing leachate treatment costs. A second benefit of enhancing degradation rates is revenue received from gas collection facilities. Regulations requiring landfills to collect landfill gases while giving tax incentives for using the collected gas to generate energy has led to a rise in gas collection facilities at landfills from approximately 75 facilities in 1984 to over 500 in 1998 (Barlaz, 1990: 557; Wheeler, 1998). A final benefit is that the landfill will be at a stable state once gas production is completed thereby reducing the cost of long-term maintenance (Barlaz, 1988:1-20).

In order to make methane to energy facilities profitable it is necessary to obtain and keep a high methane gas production rate. Methane production is often limited by the size of the landfills and other parameters such as temperature, pH, moisture content, and substrate availability. These parameters will affect landfill processes throughout each stage of degradation and play an important role in determining the time spent in each stage. According to Rees and Grainger, temperature is one of the first parameters that can be changed resulting in significant changes in methane production (Barlaz, 1988: 56). Studies have shown that raising the temperature from 22-33°C can increase gas production as much as 70 percent (Verstraete, 1984). Hartz investigated short-term studies on temperature affects on methane generation from solid waste and concluded the optimal temperature was 41°C (1982: 629).

The temperature of the refuse is affected by a number of factors. The temperature of the refuse at placement and subsequent solar radiation before coverage can impact the beginning of degradation. This initial temperature is also an important factor in microbial

2

growth along with other factors such as moisture and density of the waste (Senior, 1990: 99-100); a high temperature can create an unsuitable environment for the bacteria. Models have shown the growth rate for a microbial population to be optimum just before 40°C, with the value going to zero as the temperature rises to 45°C (Zwietering, 1990: 1096).

Temperature losses in a landfill can be attributed to heat losses to the atmosphere and surrounding soil. The thermodynamic properties of waste and soil such as specific heat and heat capacity and flow affect the amount of heat available for temperature gain. The type of soil, climate, and seasonal fluctuations in temperature can affect soil thermodynamic properties resulting in a change in heat loss or gain in the landfill.

To effectively model landfill processes, a system dynamics approach has been utilized in the past by Colborn, Benter, and Eck, in which gas generation was used as a validation metric for the system's behavior. Colborn's model began the research by looking at the entire landfill system with respect to solid waste degradation (Colborn, 1997). Benter added to the work by researching the effect of substrate availability for microorganisms (Benter, 1999). Eck's contribution consisted of incorporating the effects of moisture on the landfill system (Eck, 2000). The system dynamics model used in this study is an improved form of Colborn's and Benter's created by Shelley after review of their models.

The current model has not been expanded to include temperature factors. In order to represent the landfill system fully, temperature effects on the system must be studied to show that the model will continue to demonstrate reasonable behavior patterns.

Purpose Statement

The purpose of this thesis is to model the effects of temperature on the degradation process in a landfill system. Understanding temperature effects on microbial processes will provide a clearer picture of the behavior of a landfill system. The finalized model will provide a means to explore landfill behavior, which will enable landfill managers to explore methods to optimize methane production, reduce leachate, decrease time for landfill management, or to optimize landfill space.

Research Questions

1. How does the internal landfill system effect temperature?

2. What effects do external influences such as climate and seasonal variation have on waste degradation?

3. How does the landfill temperature affect the microorganisms in the landfill and the byproducts formed from their activity?

Scope/Limitations

The current system model will be expanded to include temperature effects on microbial activity, degradation process, and gas generation. The model will investigate the source of heat generation in a landfill, how temperature influences the microbial processes, and how heat is lost/gained from a landfill. These items will be built and tested outside of Shelley's model to validate their behavior, and then added to the model to more accurately describe and represent landfill behavior.

The exploration of what occurs at various levels in a landfill, along with the fact that solid waste composition varies in a landfill, complicates the research and values to be used in the model. Gas generation, more specifically methanogenesis, has been

4

demonstrated to vary under psychrophilic, mesophilic, and thermophilic conditions (Senior, 1990: 99). Studies have been done looking at one specific microbial group, but there are other microbial populations that will influence the degradation process. The compounding nature of uncertain parameters will complicate validation of the model, thus the temperature structure of the model will be kept simple, until testing proves a more intricate structure is needed to represent temperature behavior in the landfill.

II. Literature Review

Biodegradation Sequences in a Landfill

According to the Environmental Protection Agency (EPA) approximately 62 percent of the waste discarded in landfills is biodegradable (EPA, 1996). This waste percentage is organic matter that can be broken down into simpler substances such as cellulose, hemicellulose, lignin, and volatile solids (Barlaz, 1988: 542). A typical breakdown of municipal solid waste (MSW) excluding waste that is recycled and ground up in garbage disposals is shown in Table 1. Considering the readily degradable percentages of organic matter from Table 1, 59.5 percent is obtained for waste that is degradable which corresponds with the EPA value.

Component			
Organic	Percentage	Inorganic	Percentage
Food wastes	9.0	Glass	8.0
Paper	14.0	Tin cans	6.0
Cardboard	6.0	Aluminum	0.5
Plastics	7.0	Other metal	3.0
Textiles	2.0	Dirt, ash, etc.	3.0
Rubber	0.5		
Leather	0.5		
Yard Wastes	18.5		
Wood	2.0		

TABLE 1. PERCENT BY WEIGHT BREAKDOWN OF RESIDENTIAL MSW IN THE UNITED STATES IN 1990
(TCHOBANOGLOUS ET AL., 1993: 52)

It is important to know the types of waste going into a landfill in order to calculate the potential amount of energy that will be released during biodegradation. Knowing the quantity of the final products of biodegradation will aid in designing the correct gas and leachate collection systems. As the initial MSW composition is transformed into the end products, the waste must go through a series of degradation reactions.

Aerobic Degradation

Aerobic degradation occurs from the first placement of the waste in a landfill until the available oxygen is depleted. This process usually lasts around one week. Soluble sugars in the waste provide the energy for microbial activity; nitrate and oxygen are also consumed producing less complex sugars, heat energy, new bacteria and gases. A general equation that describes the aerobic transformation of waste is provided by (Tchobanoglous et al., 1993:677):

$$\text{Organic matter} + O_2 + \text{nutrients} \longrightarrow \text{new cells} + \text{resistant organic matter} + CO_2 + H_2O + NH_3 + SO_4^{-2} + \ldots + \text{heat}$$
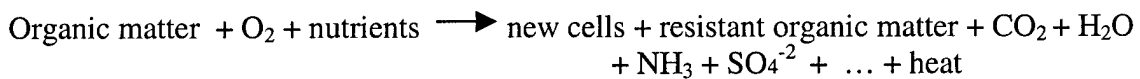
Limited studies have been undertaken to study aerobic degradation in landfills since the process lasts for such as short time period. Research has been accomplished to compare the benefits that might occur if waste was continuously left under aerobic conditions. An aerobic system was found to contain 2-3 times more organisms than in a similar anaerobic system with benefits of increased degradation rates and completion of degradation, elimination of the need to buffer leachate, and elimination of the need for a gas collection system since there was no formation of methane or hydrogen sulfide (Murphy and Stessel, 1994: 492). However, more monitoring of leachate levels would be required. If landfill mangers could extend the aerobic degradation phase, the total time for managing the landfill site could decrease.

Anaerobic Degradation

More time and research focus has been given to the study of anaerobic degradation stages are well document by (Barlaz, Adeel, Tchobanoglous et al.). There

7

are typically three stages to anaerobic degradation: (1) hydrolysis reduces complex

polymers to alcohols, ketones, and acids; (2) acetogenesis (fermentation) converts these

first stage end products to hydrogen, CO_2, and acetate; and (3) methanogenesis reduces

CO_2, acetate, and methyl amines and converts these to methane and CO_2 (Adeel,

1994:694). A flow diagram of the anaerobic degradation process is shown in Figure 1.
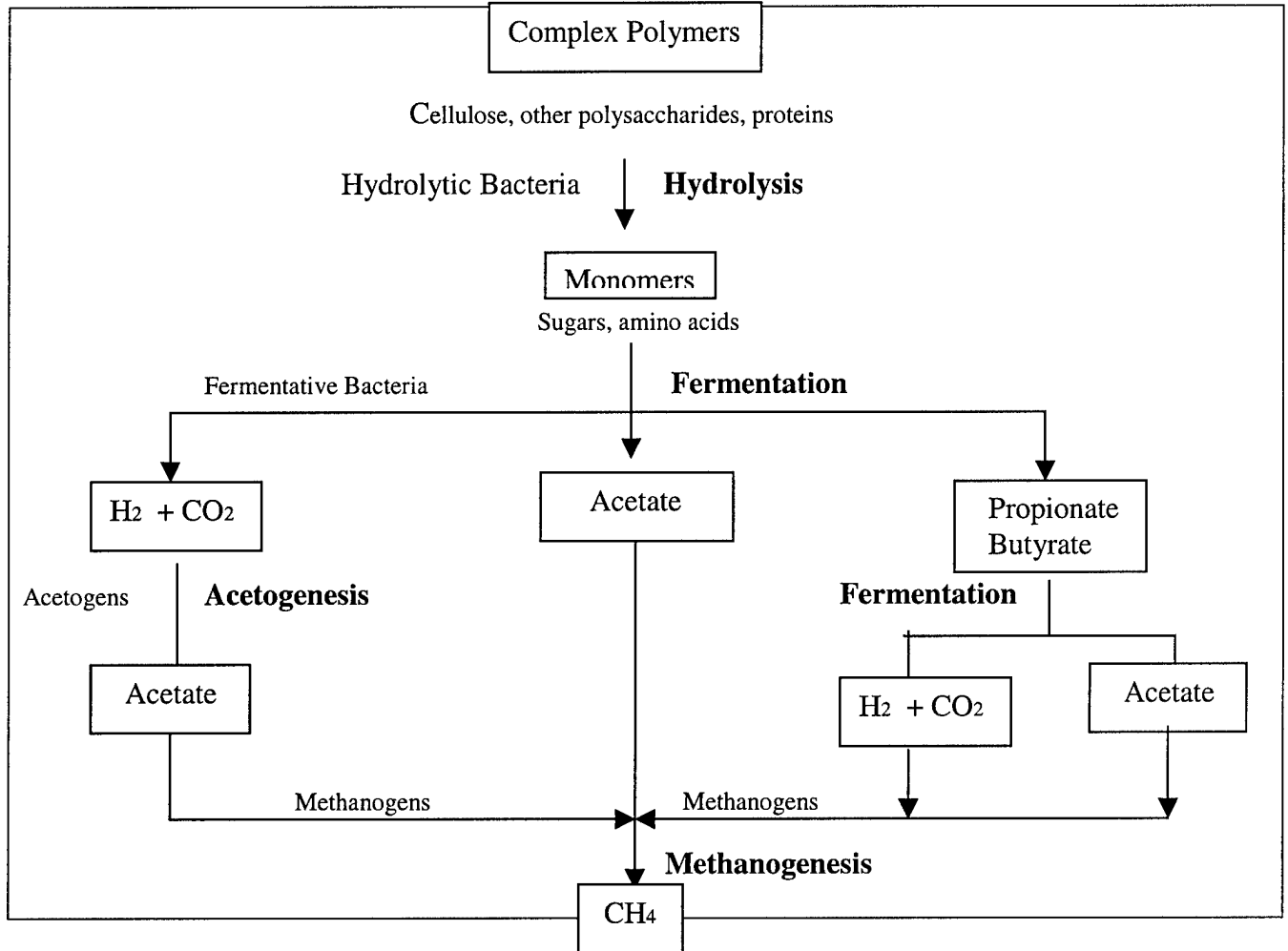
FIGURE 1. OVERALL PROCESS OF ANAEROBIC DECOMPOSITION (AFTER BARLAZ AND PALMISANO, 1996:38)

A general equation that describes the anaerobic transformation of waste is also provided by Tchobanoglous et al. (1993:681):

$$\text{Organic matter} + \text{nutrients} \longrightarrow \text{new cells} + \text{resistant organic matter} + CO_2 + CH_4 \\ + NH_3 + H_2S + \ldots + \text{heat}$$
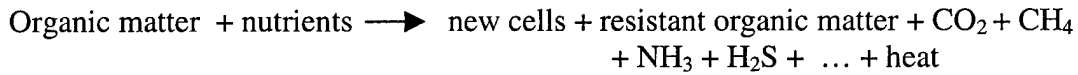
Hydrolysis. Hydrolytic microorganisms are responsible for the breakdown of waste to structural components. Lipids, polysaccharides, proteins, and nucleic acids are broken down to fatty acids, monosaccharides, amino acids, purines and pyrimidines, and simple aromatics (Tchobanoglous et al., 1993:680). Hydrolytic and fermentative microorganisms are responsible for further degradation of waste to carboxyl acids, carbon dioxide, and hydrogen. An important factor that affects the rest of waste degradation is the concentration of hydrogen in the system. If hydrogen is allowed to build-up, the formation of acetate, and ultimately, methane will be hindered for other compounds such as propionate, butyrate, ethanol, and lactate (Barlaz, 1988:5).

Acetogenesis. Acetogens oxidize the products of hydrolysis to acetate, carbon dioxide and water. Acetate formation is important because it is one of the large pathways for the completion of degradation to methane and carbon dioxide. Acetogenesis relies on the methanogenesis process to consume hydrogen to achieve favorable conditions to form acetate.

9

Methanogenesis. Methanogens utilize a limited number of substrates in the formation of methane. Recognized pathways for the formation of methane are (Tchobanoglous et al., 1993:680):

$$4H_2 + CO_2 \Rightarrow CH_4 + 2H_2O$$
$$4HCOOH \Rightarrow CH_4 + 3CO_2 + 2H_2O$$
$$CH_3COOH \Rightarrow CH_4 + CO_2$$
$$4CH_3OH \Rightarrow CH_4 + CO_2 + 2H_2O$$
$$4(CH_3)_3N + 6H_2O \Rightarrow 9CH_4 + 3CO_2 + 4NH_3$$
$$4CO + 2H_2O \Rightarrow CH_4 + 3CO_2$$
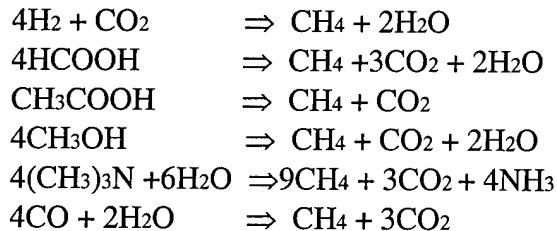
Methanogens perform three important functions in the landfill (Zeikus, 1979: 61):

1. Control of pH by the consumption of acetate.

2. Regulation of flow of electrons by the consumption of hydrogen. This creates thermodynamically favorable conditions for the catabolism of alcohols and acids.

3. Excretion of organic growth factors including vitamins and amino acids, which are used by other heterotrophic bacteria in the system.

Landfill Gas as a Metric

Since the degradation process of waste can be characterized and measured by the gas generated during the stages of aerobic and anaerobic degradation recent research has used methane gas generation as a metric. Landfill gas production has been well documented over the life span of a landfill. Gas production is described and broken down into distinct phases based on the gases produced during the biodegradation of waste. There are two widely accepted descriptions of the gas phases: the four-phase approach and the five-phase approach. The phases and description shown in Table 2 of landfill gas generation match up with the stages in aerobic and anaerobic degradation described above.

10

Four-Phase	Five-Phase	Phase Description	Degradative Steps
Aerobic	Initial Adjustment	Beginning of decomposition under Aerobic conditions; O2 depleted; CO2 produced (3-10 days).	Aerobic Degradation
----	Transition	O2 completely depleted; anaerobic Decompositions begins	Begin Hydrolysis Begin Fermentation
Anaerobic Acid	Acid	Anaerobic decomposition; organic acids accumulate; CO2 principal gas generated; H2 also produced; pH decreases (10-50 days)	Hydrolysis, Fermentation, Begin Acetogenesis and Methanogensis
Accelerated Methane	Methane Fermentation	Rapid accumulation of methane; CO2 also produced; organic acids consumed; pH increases (90 days to several years)	Hydrolysis, Fermentation, Acetogenesis, Methanogensis
Decelerated Methane	Maturation	Production of methane remains steady until organic matter is depleted (90 days to several years)	Reduced Hydrolysis, Fermentation, Acetogenesis, and Methanogensis

TABLE 2. SUMMARY OF LANDFILL GAS GENERATION PHASES AND DEGRADATION STEPS (AFTER COLBORN, 1997:14-20)

An important aspect of modeling a complex system such as a landfill is to have a metric by which to interpret experimental results. Researchers have used these phases to explain experimental observations. A base case condition has been proposed that shows the theoretical gas generation output of a landfill throughout its lifetime. Figure 2 shows the theoretical gas production of the five-phase model. This is the basic condition that this research will try to achieve and demonstrate in order to show confidence in the model and the proposed relationships.

11
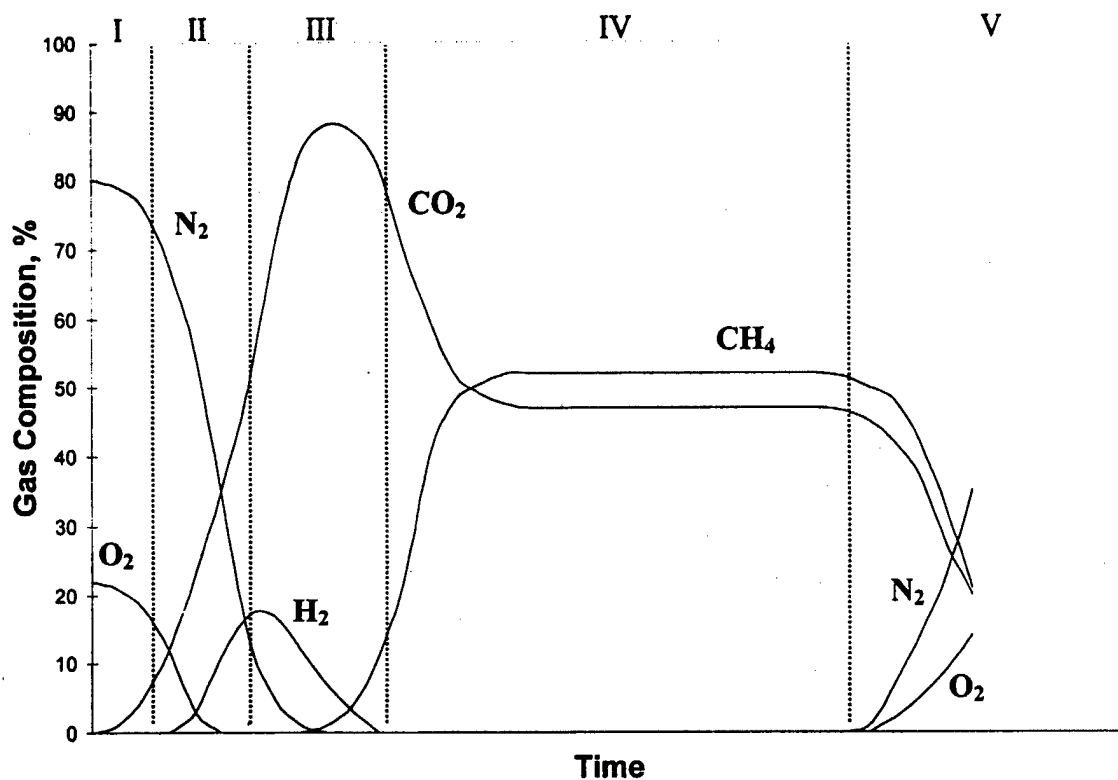
FIGURE 2. GENERALIZED PHASES OF LANDFILL GAS GENERATION DURING DECOMPOSITION (AFTER TCHOBANOGLOUS ET AL., 1993: 385; PALAMISANO AND BARLAZ, 1996:40)

Microbial Dynamics

Understanding internal reactions in a landfill is necessary to develop an accurate model of the landfill under dynamic conditions. A model must represent how the microbial populations will grow and die for the aerobic and anaerobic degradation processes. Three potential models for describing microbial growth are Blackman kinetics, Exponential growth and Monod kinetics.

Blackman Model

The Blackman equation recognizes that there is a maximum specific growth rate for a population under given conditions, which cannot be exceeded even if there is a greater substrate potential. The general equation is (Bazin, 1982:14).

12

$$\frac{dX}{dt} = (\frac{\mu}{2} * \frac{S_1}{K_1})x \quad \text{for } S_1 < 2K_1$$

$$\frac{dX}{dt} = \mu x \qquad \text{for } S_1 \geq 2K_1$$

where μ = specific growth rate

                                x = concentration of microorganism

                                S_1 = concentration of substrate

and K_1 = half-saturation constant

This model is good at representing experimental data but is discontinuous at $S_1 = 2K_1$.

Monod Kinetics

Monod kinetics relates microbial growth and substrate concentration based on enzyme kinetics. This model suggests that there is a single enzyme that limits the growth of a microbial population. The general equation is (Bazin, 1982:14):

$$\frac{dX}{dt} = (\mu \frac{S_1}{K_1} + S_1)x$$

This model is well understood because it follows Michaelis-Menten kinetics.

Exponential Kinetics

The exponential model falls between the others. The general equation is (Bazin, 1982:16)

$$\frac{dX}{dt} = \mu\ (1 - \exp\{-0.6931\frac{S_1}{K_1}\})x$$

This model seems to be able to represent experimental data more accurately and saturates more rapidly than the Monod model, but can be difficult to manipulate.

These microbial models are representative of systems with one substrate. Systems with more than one substrate add increased complexity with a separate S and K value for each substrate. The models represent the growth of microorganisms at the basic

13

level and are affected by environmental factors of the system. In a landfill system the factors that can manipulate microbial growth are pH, moisture content, substrate availability, temperature, and refuse density.

Factors that Influence Temperature

Temperature effects on methane production and microbial growth have been studied but rarely simulated in a model. Temperature is recognized as a first-tier variable in its role in anaerobic decomposition and has been found to have significant effects on interrelated metabolic processes of acidogenesis, solventogenesis, and methanogenesis (Kasil, 1989:31). A number of factors may influence the internal landfill temperature, such as initial refuse temperature, chemical heat given off through neutralization and microbiological interactions, exothermic microbial activity, specific surface area of refuse, availability of electron acceptors, solar radiation, and heat loss to surrounding soil and into the atmosphere (Senior, 1990:99).

<u>Microbial Growth</u>

Temperature may immediately affect microbial populations or slowly affect populations over an extended period of time. Landfill temperatures vary from initial refuse temperature to lethal temperature values for each microorganism population. This temperature range typically encompasses three of the four groups of microorganisms; psychrophiles, mesophiles, thermophiles. Figure 3 illustrates the temperature ranges for each group and the relative influence of temperature on growth rates.
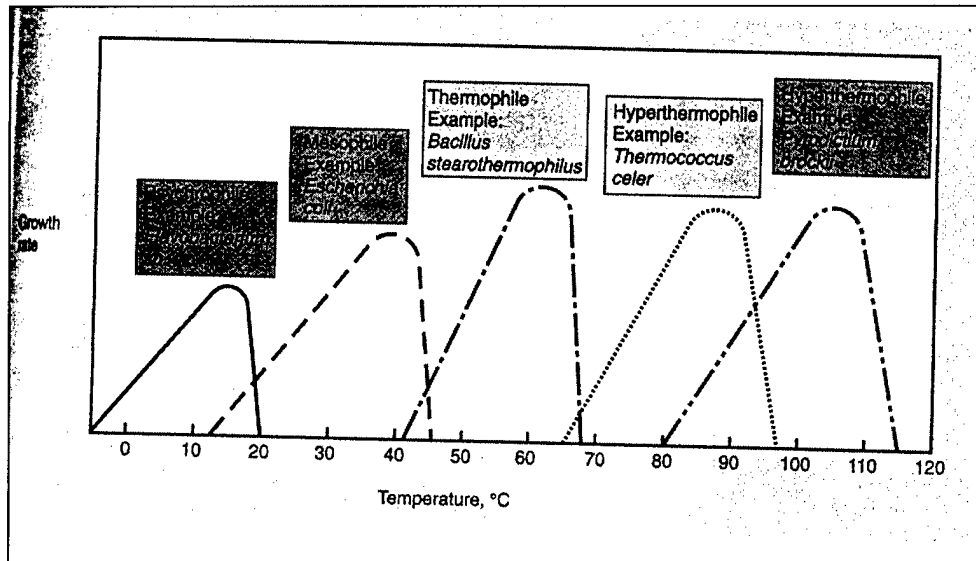
FIGURE 3. RELATION OF TEMPERATURE TO GROWTH RATES (FROM BROCK AND OTHERS, 1994:333)

The shape of the curve represents the effect of temperature from the minimum amount needed to begin growing to an optimal value for sustained growth and an extreme value where no growth can occur for that microorganism. Figure 4 illustrates this general description of the effect of temperature on growth rate.
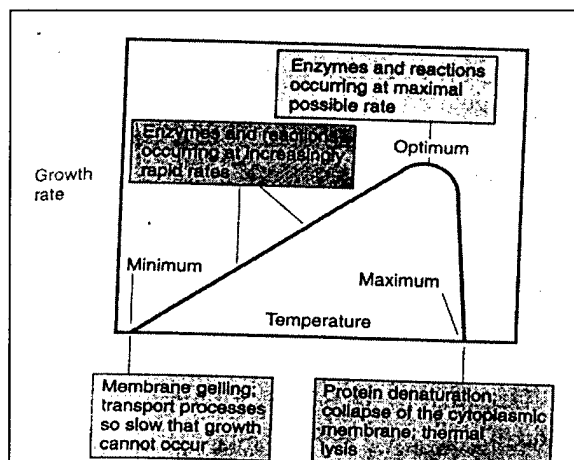
FIGURE 4. EFFECT OF TEMPERATURE ON GROWTH RATE AND THE MOLECULAR CONSEQUENCES (AFTER BROCK AND OTHERS, 1994:333)

One of the first industries in which temperature was studied as a function of microbial growth was in food processing. The temperature of chilled food is an

15

important variable for microbial safety in the production and distribution chain of food substances. The response of organisms plays a role in modeling the lag time, specific growth, and growth yield as a function of temperature (Zwietering, 1991:1094). A number of mathematical models were discussed with varying limitations. All of the models showed that the growth rate was similar to the shape illustrated in Figure 3, with initial growth beginning at 5°C, continued growth to an optimum rate at 35°C, and no growth at temperatures in excess of 45°C. These models all considered growth and death rates of microorganisms in separate equations.

Peleg proposed that the two equations could be combined and demonstrated that, even though the kinetics are different in growth and death, they can overlap. The term that is used to describe this overall equation is the propagation/destruction rate constant. The general form of the equation is (Peleg, 1994:83):

$$k(T) = \ln((1 + b \exp{-((T - T_m)/a_1)^2}))/(1 + \exp((T - T_c)/a_2)))$$

where

b= dimensionless constant that accounts for peak height
T= current temperature deg C
T_m= temperature at which peak height is obtained
a_1= temperature span of the curve
T_c= critical lethal temperature of the population
and
a_2= lethal decay steepness

The range and contribution of each kinetic parameter varies independently among microorganisms of different types (Peleg, 1994: 88). Researchers are still trying to understand microbial growth as a function of temperature in important processes such as food preservation in order to increase safety.

Another industry or process in which temperature plays an important function is in wastewater treatment. The same anaerobic reactions that occur in a landfill occur in

16

the degradation of organic fecal matter. The optimum temperatures in anaerobic digestion are 35°C and 55°C in the mesophilic and thermophilic zones, respectively (Cha and Noike, 1997: 247). Cha and Noike researched the effects of rapid temperature drops on the characteristics of substrate degradation and bacterial population levels in anaerobic acidogenesis. An important conclusion was that the numbers of acidogens, homo-acetogens, and H2 utilizing methanogens were not affected in the first three days after a rapid temperature drop. However, the number of acetate-utilizing methanogens remarkably decreased in the first three days, when the temperature rapidly dropped from 30°C to 25°C, and were completely elimianted when the temperature rapidly dropped from 20°C to 15°C (Cha and Noike, 253). The landfill system is vastly more complicated with more variables affecting microbial growth and temperature compared to the food processing, but there are many similar relationships and reactions found in wastewater treatment.

An early view of temperature effects on microbial growth in a landfill is presented by Hartz using the Arrhenius equation (1982:630).

$$K = Ae^{\frac{-EA}{Rt}}$$

$$\ln \frac{K_2}{K_1} = Ea(T_2 - T_1)/R(T_1 T_2)$$

where   A = proportionality constant
             K_1, K_2 = reaction rates at each temperature
             T_1 and T_2=temperature deg K
             Ea = activation energy
and   R =gas constant

Hartz used this equation to study the effects of temperature on methane production. A significant finding was that the optimum temperature, for short-term timeframes was

17

41°C, with methane evolution ceasing between 48°C and 55°C (Hartz, 1982:637). Many researchers have followed up on Hartz's work to determine the effect of temperature on methanogenic rates of production.

Gordon examined the relationship of three species of methanogens on temperature. These three species were the only methanogens known to have optimal growth below 30°C: Methanolobus tindarius, Methanogenium cariaci, and Methanogenium marisnergri (Gordon, 1996:334). Thus, landfill sites with temperatures greater than 30°C are capable of generating significant amounts of methane. An optimal temperature range of 30-35°C, with significant inhibitory responses occurring between 45-55°C was found in the study. One vessel showed no methane production inhibition in the temperature range of 20-25°C. However, substrate availability from acidogenic and acetogenic populations seemed to limit methanogenic production at 20°C in two other vessels.

Recent work by El-Fadel investigates the Arrhenius equation by using different activation energies for acidogen and methanogen growth rates, half saturation rates, and death rates. Proportionality constants are also given for each acidogen and methanogen rate. El-Fadel notes that the normal range of temperature for a sanitary landfill is between 25-40°C with temperatures rarely exceeding 70°C. The Arrhenius equation is assumed to fail beyond this value (El-Fadel, 1996:499).

Temperature Increase from Refuse Degradation

The energy in waste can be determined by analyzing the landfill waste composition. BTU values can be approximated by using a modified Dulong formula

(Tchobanoglous et al., 1993:86): BTU/lb = 145 C + 610 (H_2 –1/8 O_2) +40S +10N, each

variable is % by weight. Table 3 shows the energy available for various categories of

waste found in a landfill.

Component		Inert Residue	
Organic		% Range	Typical Energy, Btu/lb
Food wastes		2-8	2000
Paper		4-8	7200
Cardboard		3-6	7000
Plastics		6-20	14000
Textiles		2-4	7500
Rubber		8-20	10000
Leather		8-20	7500
Yard Wastes		2-6	2800
Wood		0.6-2	8000
Inorganic			
Glass		96-99+	60
Tin Cans		6-99+	300
Aluminum		90-99+	-
Other metals		94-99+	300
Dirt, ashes, etc.		60-80	3000

TABLE 3. TYPICAL VALUES FOR INERT RESIDUE AND ENERGY CONTENT OF RESIDENTIAL MSW (FROM
TCHOBANOGLOUS ET AL., 1993:84)

The energy released from the breakdown of waste can also be calculated

by looking at the free energy released during the stages of biodegradation. This release

of energy in a closed system such as a landfill increases the temperature of the system.

Free energy values released during typical anaerobic reactions are shown in Table 4.

Energy	Change (kJ/reaction)	
Reaction Type	ΔG^{0b} (Std Conditions)	ΔG^c
Fermentation of glucose to acetate, H2, and CO2	-207	-319
Fermentation of glucose to butyrate, CO2, and H2	-135	-284
Fermentation of butyrate to acetate and H2	+48.2	-17.6
Fermentation of propionate to acetate, CO2, and H2	+76.2	-5.5
Methanogenesis from H2 + CO2	-136	-3.2
Methanogenesis from acetate	-31	-24.7
Acetogenesis from H2 + CO2	-105	-7.1

TABLE 3. MAJOR REACTIONS OCCURRING IN THE ANAEROBIC CONVERSION OF ORGANIC COMPOUNDS TO METHANE (FROM BROCK AND OTHERS, 1994:651)

Depth in Landfill

Temperature will vary with landfill depth because the waste is increasingly insulated at greater depths from heat losses additionally, there is more circulation of leachate and nutrients. The first six meters of a landfill is generally considered to be in the mesophilic temperature range. From 6 meters to 20-25 meters the temperature increases to the thermophilic range (Chiampo et al., 1996:39). The following figures show the general temperature profile of the investigated landfill and the specific temperatures at different bore depths.

Figure 5 shows a water lens at a depth of 16m. Vehicles driving over the daily cover of a landfill cell in order to reach the current operational cell form a water lens. When future cells are placed on this packed layer it acts as an impermeable layer where moisture can collect. The higher moisture content in this area allows the organic waste to rapidly decompose creating unfavorable biodegradable conditions. The layers of waste

underneath the lens will have less moisture and characteristically less degradation than the layers above. The high temperature value of the waste at the water lens was attributed to drilling friction since no biodegradation was occurring.
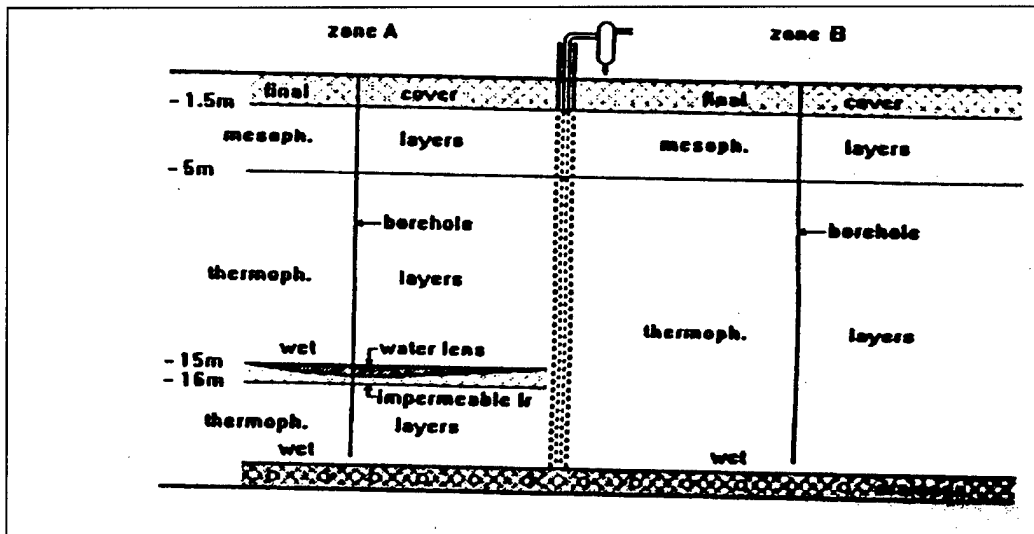
FIGURE 5. SECTION OF LANDFILL PROFILE (CHIAMPO ET AL., 1996:39)
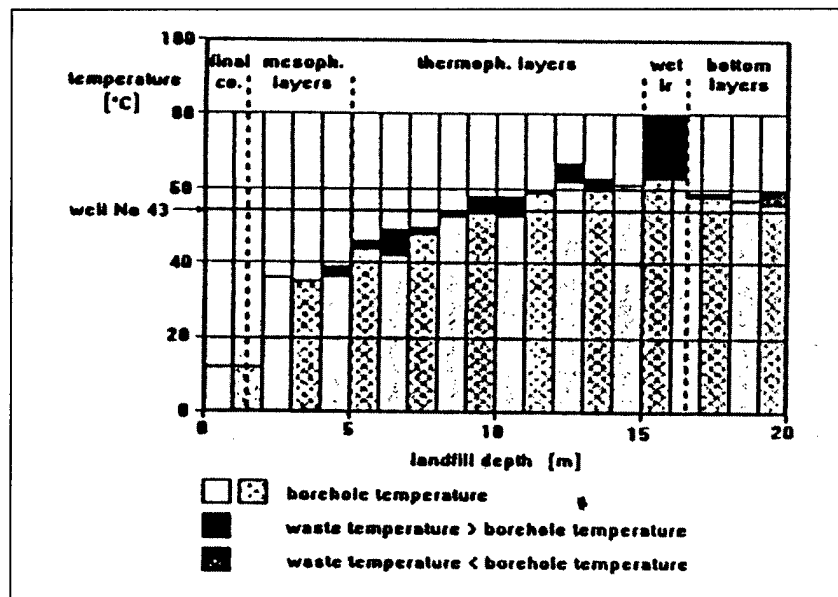
FIGURE 6. TEMPERATURE PROFILE VS. DEPTH IN A LANDFILL (CHIAMPO ET AL., 1996:39)

21

A previous study also examined the effect of temperature vs. landfill depth, and

methane percentage vs. landfill depth. The results are similar to Chiampo in that the first

six meters were under mesophilic influences with the remainder of the landfill falling

under thermophilic influences. The results in Figure 7 show that the temperature

increases from 26°C to 50°C as the depth goes from 2 to 10 m. The temperature remains

steady, around 50°C ,for the remaining 15 meters of the landfill (Attal et al., 1992:249).

Figure 8 illustrates how the methane percentage changes with respect to temperature at

the varying burial depths. If methane percentage is used to describe the degree of landfill

waste decomposition, one conclusion that could be drawn is that waste at greater depths

has had more time to decompose compared with the waste closer to the surface, thus

creating more methane. However, this is hard to determine due to gases closer to the

surface being released into the atmosphere.
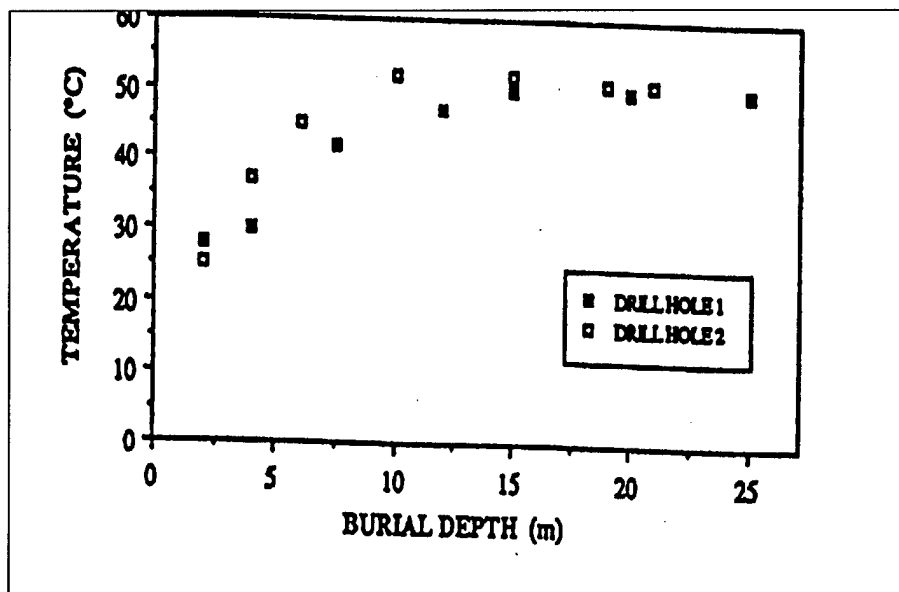
FIGURE 7. TEMPERATURE CHANGES AS A FUNCTION OF BURIAL DEPTH
(AFTER ATTAL ET AL., 1992:249)
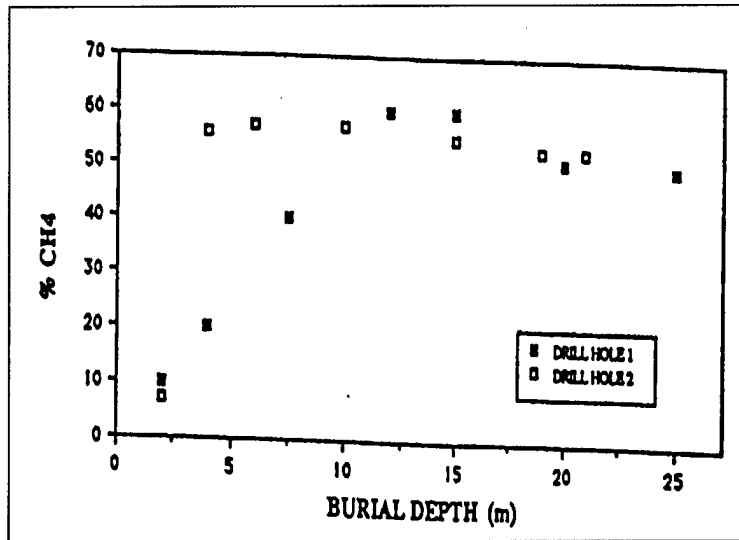
FIGURE 8. PERCENT METHANE AS FUNCTION OF BURIAL DEPTH
(AFTER ATTAL ET AL., 1992:249)

Gurijala and Suflita looked at environmental factors affecting methanogensis in a

landfill through samples taken from Fresh Kills Landfill. Their research focused on

moisture content, pH levels, and sulfate levels (Gurijala and Suflita, 1993: 1175) The

initial data for the landfill samples had burial depths with temperature values and rate of

methanogenesis for each depth. Table 5 shows the characteristics of the samples. Figure

9 graphs burial depth against temperature in order to compare this set of data to the

studies discussed previously. Notice that there is not a clear distinction in the

temperature between 7-10 m, with temperatures varying from 14°C to 42°C. The

temperature at intermediate depths might vary because some of the refuse might be under

different phases of degradation.

Sample No.	Temp (°C)	Sampling Depth(m)	Rate of Methanogenesis (μmol(dry kg)$^{-1}$day^{-1})	Sample No.	Temp (°C)	Sampling Depth(m)	Rate of Methanogenesis (μmol(dry kg)$^{-1}$day^{-1})
1-2	29.4	3.08	0	6-3	28.9	6.15	0
1-3	42.2	6.15	262.5	6-4	27.8	9.85	302
1-4	ND	9.23	0	7-1	21.1	3.08	0
1-5	37.2	13.54	335.2	8-1	ND	3.08	79.9
1-6	37.7	15.69	272.3	8-2	43.3	6.76	56.8
2-1	ND	4.62	0	8-3	40.5	9.23	149.8
2-2	ND	10.15	1.6	8-4	ND	15.38	26.3
3-2	22.2	4.31	520.3	9-2	21.7	4.62	702.5
3-3	25	6.77	435.1	10-2	21.7	3.08	17.2
3-4A	14.4	9.23	124.9	11-2	21.7	4.92	52.2
3-4B	14.4	9.23	297.5	12-2	21.7	5.23	148.1
3-5	ND	ND	116.1	13-4	31.7	8.62	377.8
4-1	16.1	3.38	219.3	13-5	10.5	9.8	316.3
5-2	22.2	3.38	371.8	14-2	57.8	13.85	109.4
5-2A	22.2	3.38	302	14-4	45.5	20.31	24.1
5-3	18.3	6.76	274.9	14-S	62.8	12.31	0
6-2	21.1	3.08	0	14-M	45.5	21.53	298.3

TABLE 5. SELECTED CHARACTERISTICS OF MUNICIPAL REFUSE COLLECTED FROM THE FRESH KILLS LANDFILL (AFTER GURIJALA ET SUFLITA, 1993:1177)
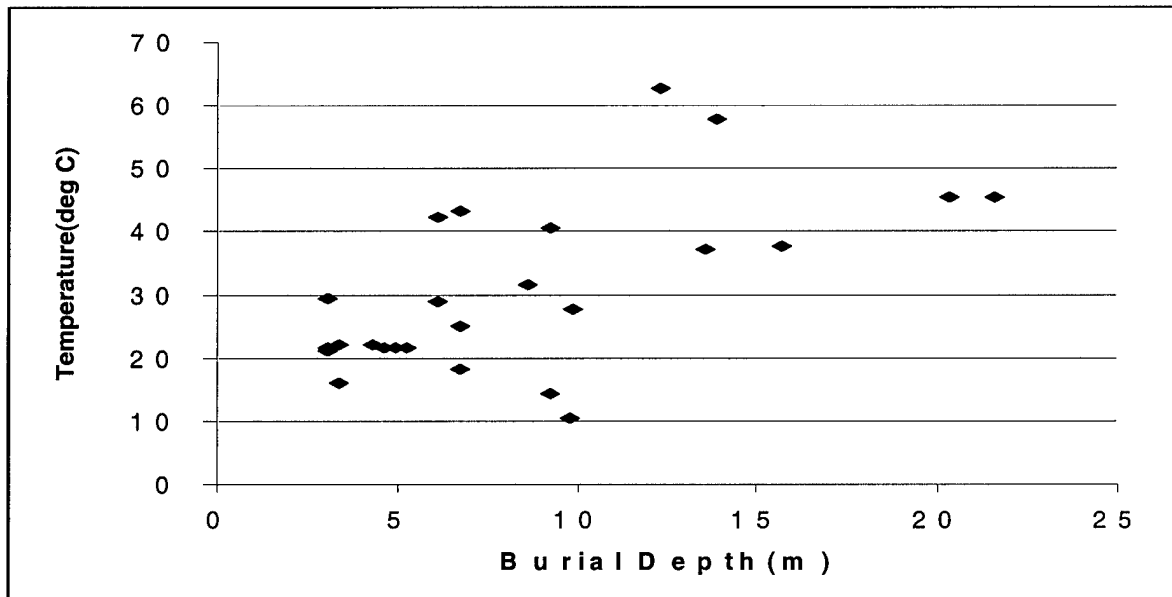
FIGURE 10. TEMPERATURE CHANGES AS A FUNCTION OF BURIAL DEPTH

24

Seasonal Temperature Changes

An extensive study on the effects of daily and seasonal temperature changes has not been performed on an entire landfill. Borjesson and Svensson investigated seasonal and diurnal methane emission from Hokhuvud landfill in Sweden. The experiment went from 1992-1994; soil and air temperatures were taken along with methane and carbon dioxide emissions (Borjesson and Svensson, 1997: 39-40). Experimental results are depicted in Table 6.

Date	Gas flux (mmol m^{-2} h^{-1}) CH$_4$		CO$_2$		Soil moisture 0–0.60 m (% wetness)		Temperature (°C) Air	Soil (0.85 m)
1992 13 May	0.31	(64.1)	12	(67.1)	22	(41)	1.5	—
5 June	0.037	(164)	35	(64.2)	12	(70)	5.5	—
23 July*	1.2	(169)	22	(60.3)	15	(75)	33.0	19.5
3 Sept.*	1.3	(200)	3.4	(93.5)	18	(49)	27.0	16.8
1993 18 May*	0.048	(200)	16	(67.3)	6.9	(79)	24.0	12.8
21 June*	0.83	(240)	8.1	(69.5)	12	(59)	18.5	14.8
21 July*	0.68	(172)	23	(40.3)	5.0	(65)	24.5	19.8
19 Aug.*	0.82	(200)	25	(71.6)	6.8	(33)	17.5	18.0
28 Sept.*	9.8	(176)	10	(85.1)	13	(135)	10.5	12.1
18 Nov.*	13	(188)	5.7	(120)	12	(74)	−2.8	4.5
29 Dec.	3.2	(85.5)	14	(30.5)	18	(52)	−2.0	2.1
1994 28 Jan.	0.88	(200)	0.56	(200)	22†		−7.0	0.4
25 Feb.	6.9	(198)	3.9	(146)	39	(47)	−6.0	—
12 Mar.	0.034	(59.7)	−0.42	(−200)	14	(58)	4.0	0.6
19 Apr.*	20	(102)	12	(94.5)	9.1	(64)	5.0	3.4
16 May*	2.7	123)	25	(79.1)	5.9	(79)	12.2	10.4
15 June*	0.77	(123)	11	(116)	6.8	(56)	16.5	14.1
26 July*	0.23	(204)	33	(64.9)	5.8	(96)	26.0	22.6

* = Measurements made during frost-free periods, and with gas and temperature probes installed.
† = Only measured at 0–0.10 m depth.
— = Not measured.

TABLE 6 MEAN GASEOUS EMISSIONS FOR FOUR CHAMBERS, SOIL MOISTURE AND TEMPERATURE MEASURED AT THE HOKHUVUD LANDFILL 1992-1994(% COEFFICIENT OF VARIATION IN PARENTHESES) (FROM BORJESSON AND SVENSSON, 1997:40)

The ground was covered with snow and ice from December 1993 through March 1994.

Methane emissions appear to have been greater during the winter months (September-

April) compared to emissions taken during the summer (May-August), excluding April 19th and November 18th. There was a negative correlation between methane emission and soil temperature at a depth of 0.6 m (Borejesson and Svensson, 1997: 46). Jones and Nedwell (1983), in a study in Britain, found the opposite results with higher methane emission in the summer months, while Kunz and Lu (1980), at the Freshkills landfill in New York, obtained their highest methane emission during February (Borejesson and Svensson, 1997: 33-34). A lot of seasonal variation seems to be dependent on climatic variations. Soil covering particle size, moisture content level, and compaction play important roles in the ability of gases to escape through the landfill cover. Specific studies concerning emissions from landfill cover soils have been done by Whalen et al., 1990; Bogner, 1992; Jones and Nedwell, 1993; Boeckx and Cleempt, 1996. The optimal temperature range for methane oxidation was from 25°C to 30°C (Boeckx and Cleempt, 1996:180), which corresponds to the Whalen et al. (1990) optimum value of 31°C.

Solar Radiation

A large portion of the internal heat of a landfill comes from the decomposition of waste. A significant portion of heat can be added by solar radiation. The average solar constant has been calculated to be 2.00 cal/cm^2 min (langley/min) with an error of two percent (Chang, 1958:44). Houghton calculated the amount of solar radiation reaching the surface based on degrees of cloud cover and the vegetation at the ground surface. Actual daily solar radiation absorbed depends upon geographical location, the season of the year, the character of the ground, and the weather conditions (Chang, 1958: 46). The energy that is absorbed by the earth surface is consumed in evaporation or radiated back out into the atmosphere with remainder energy being transferred into the soil

Thermal Properties

The porosity of soil and waste allow movement of gases and water in the landfill through a convection system. The soil/waste temperature will change due to radiant, conductive, and latent energy exchanges. Internal processes and thermal properties of various waste cells and soil coverings will affect the degree of temperature change. The combinations of waste layers and soil have thermal property characteristics such as thermal conductivity, heat capacity, and latent heat (Cox, 1995: 27). Thermal conductivity is defined as the quantity of heat, Q, flowing through a unit area of a substance of unit thickness in unit time under a unit temperature gradient, dT/dz, and coefficient of thermal conductivity, K, of the ground (Johnson, 1981: 114). The K value will be different for each soil type and is affected by moisture content. Thermal conductivity will increase as the soil's dry density increases, as the moisture content increases, and when the ground is more solid (Johnston, 1981:109-11). In a dry state the soil and waste will be surrounded by air which will insulate the passage of heat. However, when air is replaced by water, the thermal contact increases, causing an increase in thermal conductivity (Chang, 1958:33).

Heat capacity, c, is the amount of heat required to raise a unit mass temperature of substance by one degree where $c = Q/\Delta T$ (Johnston, 1981:115). A soil's heat capacity is dependent upon its mineral and organic makeup, moisture content, and bulk density (Smith and Hinchee, 1993:8). This applies to all three phases that are present in a landfill: solid, liquid, and gas.

Current Model

Shelley and others created the landfill model to be expanded in this research. The research is focused on enhancing the biodegradation in a landfill in order to reduce the stabilization time of the waste (Shelley, 2000). All of the previous models have used the system dynamics perspective to represent landfill behavior. The models were developed using a numerical integration software STELLA® version 5.0.1 Research (High Performance Systems Inc). The system dynamics methodology compares the relationships of different parameters to a given behavior. The model was tested by comparing output data to the known observed behavior shown in Figure 3. This process allows the "big picture" of the system to be modeled in a manner that can be used by landfill managers (Shelley, 2000). Monod kinetics was used to characterize the degradation reactions in the landfill with a focus on mass balance.

A system dynamics approach was utilized to explain the complex relationships, behavior, and interrelationships of a landfill over an extended period of time. The primary assumption of the system dynamics paradigm is that the relationships in the system arise from a causal structure, which is formed by constraints, goals, and feedback loops (Meadows, 1980:31). Once the relationships are defined, simulations can be run to determine the sensitivity of parameter values and to explore and predict emergent behavioral patterns based on internal and external forces.

System dynamics is a methodology that provides an organized process to build and explore system behavior. The first step in the modeling process is to develop a mental view of the behavior in the system, which is believed to be important to the objectives of the model. Once an understanding of the system behavior is achieved,

28

gathering relevant data will help define parameter values and possible relationships. This information is used to form logic diagrams showing the cause-and-effect relationships needed to define the system and its boundaries (Shelley, 2000). After the relationships are defined, the structure of the model may be built. Throughout the building of the structure, revisions to the structure are changed through new understanding of the mental model or logic diagrams. The final step of the modeling process is to perform numerous tests to verify the model structure and values as well as to validate the system boundaries and logic.

The system dynamics process allows for an efficient means of exploring any system, no matter the complexity of the system. Modelers can first look at the whole system in a simple manner; and once relationships and behavior are understood, more complex aspects may be added. The modeling process is broken down into four stages: conceptualization, formulation, testing, and implementation. Each stage can be reiterated as new information is added to define the system's behavior.

Conceptualization

An initial literature review of the basic concepts that describe and comprise the system will help develop a mental view of important parameters. The conceptualization stage should be a time when questions are continuously being asked to ensure a thorough investigation of the system. Why is this system behaving in this manner? What is causing a change in behavior? Are the changes in the system internal or external? What is the effect of these changes on the system? Questions such as these will lead to the formulation of a reference mode.

The reference mode is the behavior of the system over a given range of interest (Shelley, 2000), which can be hypothesized or well documented in the literature. The biodegradation of waste in a landfill has historically been measured by landfill gas generation. Numerous researchers have used landfill gas as a metric to describe the extent of waste degradation in a landfill, energy potential, and longevity of existing landfills (Tchobanoglous et al., 1993:385; Barlaz et al.). The reference mode is a cornerstone for the model through its indication of important structure. The rise of relationships describing the reference mode is called the basic mechanism (influence diagram), which along with the reference mode forms the dynamic hypothesis for the system (Shelley, 2000). The dynamic hypothesis is what must be tested, and in the end, validated to ensure that the proposed model of the system is a good representation of the system's behavior.

The basic mechanisms of the model are developed through causal relationships and feedback loops. Arrows between parameters indicate a relationship between them. A positive arrow into a parameter indicates that it has a positive relationship with the other parameter; as the other parameter increases, so will the parameter with the positive arrow. The opposite is true with a negative arrow. Multiple arrows can be drawn from and into a parameter creating feedback loops. A feedback loop with an overall positive relationship is representative of a reinforcing behavior and indicates the relationship is unstable, while a negative feedback loop is representative of a compensating behavior and indicates the relationship is stable. These feedback loops give rise to the system's behavior. Once the basic mechanism is understood, application to a model format is

necessary. The software package used to model this system is the numeric integration software STELLA from High Performance Systems (STELLA 5.1.1, 1998).

Formulation

Transferring the basic mechanisms into STELLA requires the parameters be separated into levels or stocks and flow rates. Stocks represent an initial level of an object in the system, which can accumulate or decrease in size depending on the flow rate of the substance into and out of the stock. The flow rates are formed by equations that describe the relationship of the stock with other parameters per unit of time. The connection of two or more stocks formulates the feedback loops present in the influence diagram. Detail is added in order to define the relationships and formulate the flow rate equations. This detail cannot add logic that is not present in the influence diagram.

Testing

Once the structure of the model adequately represents the influence diagram and all the parameters are defined, testing of the model may begin. Testing encompasses verification, validation, and credibility of the model. Verification of the model tests whether the model is performing as intended, compared to the logic presented in the influence diagram. Validation of the model compares the model's output to empirical data. The reference mode can be compared here to develop confidence in the model. The primary objective of validation in system dynamics is to ensure confidence in the model's soundness and usefulness as a policy tool (Forrester, 1980:211).

Verification can be divided into small tests performed while building the model or before the addition of more complex aspects to the model. There are two main types of tests, structure tests and behavior tests. Structure tests include structure verification,

parameter verification, extreme conditions test, boundary adequacy test, and dimensional consistency test. The testing process is very iterative and can be broken up into small steps as the model is being built to ensure that the structure and behavior of the section is valid. This process was used in the model to test for the correct behavior of the transfer coefficient, life cycle curves with respect to temperature, and the Peleg equation.

Structure Tests. Structure verification compares the model to the real system it represents. Knowledge of the real system must not be contradicted in the model (Forester, 1980:212). This test is done by comparing assumptions to information found in literature and ensures that the stocks and flows are interacting in the real system as described in the model. Extending the model to professional criticism or advice adds validation to the model's structure.

Parameter verification is similar to structure verification in that it justifies the constants used in the model to the real system. A constant or parameter must be studied over the time frame of the model to ensure that the structure using that parameter is able to handle any changes. Parameter and structure tests often overlap but the bottom line is to ensure knowledge of the real system is never contradicted.

Extreme conditions tests ensure that there are not abnormalities in the model by testing at reasonable, extreme values, which should produce a well-defined outcome. For example, if the temperature in the landfill remains below microbial activity levels, then biodegradation will not occur. Extreme conditions testing are essential for two reasons. First, any abnormalities in the test might indicate problems in the model's structure and formulation. Second, the documented range of a system in reality might extend beyond

any observations (Forrester, 1980:214). Modeling extreme conditions may provide new insight to a system's behavior that might increase the system's productivity or resilience.

Boundary-adequacy tests are included in the testing of the model structure and behavior. The main purpose is to reinforce the concept that there is enough information built into the model to satisfy the purpose of the model and to represent the real system. The test allows for criticism of the model for parameters that have been omitted that may be important factors in the model based on the model's purpose. If a defense for not including the parameter in the model can be developed and represented by model output, the test passes. However, if output from the model indicates that more structure needs to be added to the model to fulfill its purpose, then the test fails.

Behavioral Tests. Behavioral tests ensure that model structure performs adequately in order to represent the behavior of the real system. Verification of behavioral tests and structural tests seem to overlap in that each of their definitions includes the other. Behavioral tests focus on the output derived from the model's structure and not on the structure itself. There are numerous tests for model behavior, which include, behavior anomaly test, family member test, boundary adequacy test, and behavior sensitivity test.

Behavior-anomaly tests allows for the investigation of behavior in the model that is contradictory to the behavior found in the real system. The anomalous behavior can be traced to model structure, which then can be evaluated for flaws. If no flaws can be found in the structure or assumptions then the model behavior might just represent a new range of behavior that has not been experienced before in the real system.

Boundary-adequacy (behavior) tests look at comparing model behavior based on the presence and absence of additional structure. This test builds confidence that the structure present adequately models the desired behavior. The test passes if the additional structure does not change the behavior.

The behavior sensitivity test compares the range of a parameter's values. If the behavior of the model drastically changes over a defined range of values of a parameter that is defined in the real system, then the modeler must go back and see where this behavior is developed. In order to build confidence, a modeler must indicate and explain where a parameter passed one test but failed to pass the sensitivity test for a plausible range of values (Forrester, 1980:223). A modeler often gets caught up in performing numerous sensitivity tests on parameters and never compares these tests with other tests out of fear of invalidating their model. A model is not necessarily invalid if it fails the sensitivity test. Failure may indicate behavior that is actually observed in the real system but has not been documented. A system's model passes the sensitivity test if the output behavior for a parameter's range does not contradict what has already been documented for the real system.

Implementation

The final product of a model is ultimately evaluated by its usefulness to the customer in representing behavior found in the real system. The customer should be able to understand the real system's dynamics based upon model behavior. The model should be user friendly and allow updates as the understanding of the real system changes.

III Methodology

Using the system dynamics approach described previously, structure will be added to Shelley's model to reflect temperature effects in a landfill system. This section will explain how the additional structure was developed and incorporated into the model. Throughout the process of development and incorporation, tests need to be done to verify and validate the system's structure. There are two reference modes that this model will be working from to develop and validate the model. The first reference mode, shown in Figure 2, is showing the mole fraction of gases emitted over the lifetime of the landfill. The second reference mode shown in Figure 3, is showing the temperature effects on microbial growth. From this reference mode, ideas for parameters affecting temperature were developed. Before formulation of model structure can begin, an influence diagram needs to be developed showing the relationships and influences of the parameters in the system. Figure 10 illustrates parameters that affect temperature in a landfill environment.
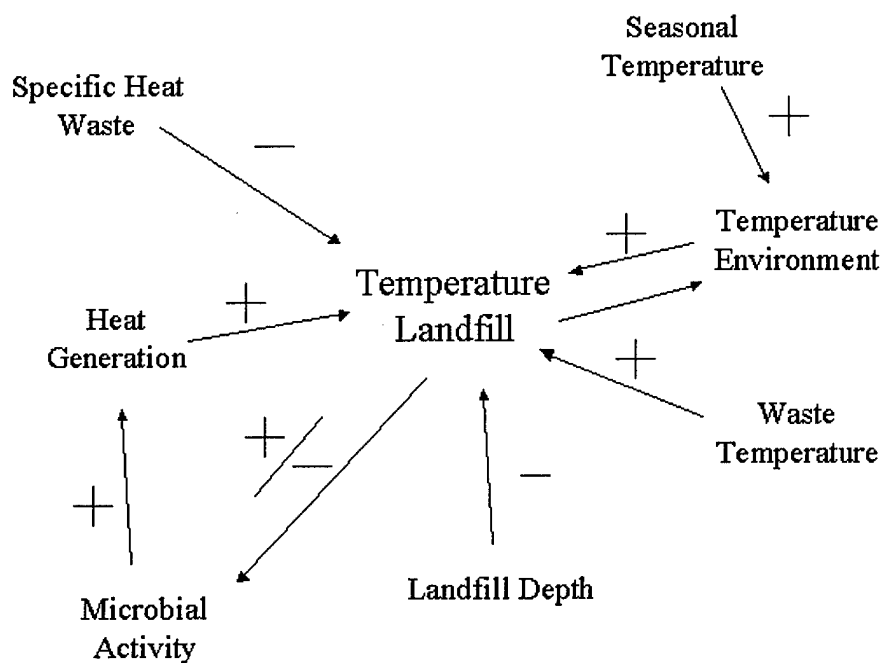
FIGURE 10. TEMPERATURE INFLUENCE DIAGRAM

The initial temperature of waste at arrival and burial is one of the first influences on the landfill temperature. This relationship is positive because the warmer the initial waste, the warmer the temperature of the landfill cells will be when degradation begins. The landfill cell temperature can have a positive or negative affect on the microbial populations. When the temperature is at a low end of a population's growth range, an increase in temperature will allow an increase in the population. However, when temperature rises to the extreme value of a population's growth range an increase in temperature will decrease the population's size. Microbial activity can, in turn, affect the temperature of the landfill by the heat released due to their biodegradation. An increase in microbial activity will have a positive influence on the heat generated. Another factor

that influences the amount of heat generated available for a temperature increase is the specific heat of waste. The specific heat can have a positive or negative impact on the temperature. Specific heat >1 will have a positive impact on the temperature increase while a specific heat value <1 will reduce the potential for temperature increase. The temperature loss from the system is based upon properties of the landfill and the surrounding soil. The temperature of the soil is affected by its depth and by the local air temperature. A lower soil depth is cooler than soil close to the surface, causing more heat to be lost from the landfill. However, in the winter the soil at a deeper depth can be warmer than soil near the surface, which will reduce the heat lost to the atmosphere.

Using the relationships and influences in this structure, model development may begin. Setting up the temperature structure in STELLA will encompass three distinct areas. The first area of development looked at how microbial activity translates into energy, which corresponds to a temperature value. The heat generated is based on the amount of kcal given off for the transformation of one mole of glucose to one of the nine simpler forms found in Shelley's model. The total heat generated in kcal will be transformed to a degree Celsius increase per day using specific heat and the changing landfill's mass.

The second area of development looked at how temperature will, in turn, affect the microbial growth cycle. This process requires an equation to relate temperature to microbial activity. Temperature will affect the U_{max} parameter, the saturation parameter and the death parameter which are all part of Monod kinetics. The behavior of the equation will be checked against the reference mode in Figure 3.

The third area of development investigated how the temperature will be lost from the system. This section will use a temperature differential between the surrounding soil and the changing landfill temperature. This differential will be dissipated with a transfer coefficient.

From these three areas, tests were run to confirm structure and behavior with respect to temperature and with the overall model. Verification began with running the growth and death equations, separated from Peleg's equation, to determine the range of the U_{max} and k_d terms produced for methanogens and acetogens. The system's temperature will be artificially manipulated to gradually and steadily increase over a landfill's normal operating range. The U_{max} and k_d terms will change with respect to the changing temperature in accordance with each population's parameter values. The range for the U_{max} and k_d values will be compared to values found in the literature and values being used in the current model.

After verification of the equation representing, U_{max} and k_d it is important to test for a good growth curve for an acetogen and methanogen population over the population's temperature range. A series of simulations will be run to verify that the acetogen and methanogen populations' biomass curves have the correct behavior over their temperature range. The correct behavior in this case is a curve showing a population growth with unlimited substrate to a peak point where the population will begin to decline due to the approach of the population's critical temperature. The system's temperature will be artificially manipulated to gradually and steadily increase over a landfill's normal operating range. This test will be performed outside the main model using microbial equations and an acetogen and methanogen population structure.

Extreme boundary tests will be run at low and high temperature extremes to observe any anomalous behavior.

Another test that can be performed outside the model is for the transfer coefficient. The transfer coefficient defines the rate of heat loss from the landfill. A plausible range of values for the transfer coefficient will be defined by testing the time it takes for a high initial landfill temperature to come to equilibrium with a fixed soil temperature when no other system influences are allowed to affect temperature. The test will be done using a sensitivity analysis approach for the transfer coefficient parameter.

Once verification of the microbial equation, biomass curves, and transfer coefficient parameter are validated these structures can be implemented into the larger model. The microbial equations now can be tested against the entire model for effects on the mole fraction of gases generated and the amount of waste degraded. The growth equation will be tested by looking at the height parameter, current temperature, peak temperature, and temperature span. Testing the sensitivity of all the parameter values in the Peleg equation will be accomplished by comparing the mole fraction of gases produced to the mole fraction of gases seen in the reference mode The range for each parameter will be determined by comparing the mole fraction of gases generated to the reference mode. The temperature span parameter will be tested initially using a sensitivity test running four simulations in the 5-30°C range. After observing the results of these simulations further simulations may be needed. The equations representing the methanogens will be tested similarly to the acetogens but the ranges initially used will be different due to the higher temperature these populations require for growth. The height variable affects the U_{max} variable and ultimately affects the time when the population will

reach its maximum value. The initial sensitivity test will have four simulations covering a height range of 2-10. The peak temperature controls the temperature value at which the population will reach its largest size. The sensitivity test will run four simulations in the temperature range of 20-35°C. The last parameter in the U_{max} equation is the current temperature. What will be changing in this test is the starting landfill temperature. The sensitivity test will run four simulations in the starting temperature range of 5-25°C. The total number of initial simulations testing the U_{max} equation is 2(methanogen and acetogen) * 4 parameters* 4 simulations in each range = 32 simulations.

The decay rate equation is affected by the decay steepness, current temperature, and critical temperature parameters. These tests will be run for both acetogen and methanogen populations. The decay steepness is a constant that controls how fast the population will die off once the critical temperature is reached. The sensitivity test will run four simulations covering a range of 1-12°C. The critical temperature constant is the temperature value at which the population will begin to die off in large numbers. The sensitivity test will run four simulations in the temperature range 30-55°C. The same simulations will be performed for the starting temperature value in the growth equation. The total number of initial simulations testing the kd equation is 2 (methanogen and acetogen) * 4 parameters* 4 simulations in each range = 32 simulations.

There are nine microbial processes transforming glucose into simpler substances. Each of these reactions has an associated heat generation value based on the number of moles of glucose converted into simpler substances. The current value being used, found in El-Fadel's work for heat generation, is on the order of 50 kcal/mol of heat generated per mole of glucose transformed. In order to test the heat generation, the nine heat

generation constants will be manipulated by changing one constant that is applied to all of them. A sensitivity analysis will be run for this one heat generation constant to determine the effects of the nine populations on the heat generated. The sensitivity test will run four simulations in the range of 10-50 kcal/mol. This number of simulations may depend on the first sensitivity test. The heat generation constant is important because it directly affects the temperature increase in the system, which then affects all the other parameters in the system.

The specific heat of waste is a variable not well documented in the literature and a sensitivity analysis should be run. The initial value is 0.5 cal/gm-deg C taken from Chang for the specific heat of peat. Four simulations will be run for the specific heat using values of 0.2, 0.8, 1.4, 2.0 cal/gm-deg C. The tests will see how much of an effect specific height has on the temperature increase. Specific heat, along with the heat generation constants, affects the rate of temperature increase in the landfill. These two parameters may need to be varied to determine if the temperature increase in the landfill is accurate.

The temperature differential between the landfill cell and surrounding soil temperature could impact the amount of heat lost depending on the location and time of year. Three different soil profiles will be investigated representing a cold climate, a temperate climate and a warm climate. Each profile will be run using a sensitivity test for different TC's, which will be defined in the transfer coefficient testing. A total of 12 simulations will be run. A summary of the tests that will be initially performed to verify and validate the model are shown in Table 7.

	# Simulations
Initial Arrhenius	32
Microbial Growth Curves	2
Peleg test	1
Transfer Coeff	5
Sensitivty on Heat	4
Genertion Constants	
Sensitivty on specific heat	4
Peleg in entire model	64
Soil Temperature	12
Total	**124**

time for each simulation is 5 minutes

TABLE 7. SUMMARY OF TESTS

IV. Results and Discussions

This chapter will focus on the actual tests performed using the system dynamics process. For a further description of the system dynamic process, see thesis done by Colborn and Benter (Colborn, 1997 and Benter, 1999). The purpose of this research was to investigate temperature effects inside a landfill in order to understand its effects on landfill behavior. Temperature effects on microbial populations and their subsequent release of energy from the degradation of waste are the key research questions that will be discussed in this chapter. A secondary research question is how landfill temperature changes affect the percentage of landfill gas produced. The analysis of the relationship between temperature and microbial activity will use the diagram in Figure 3 as a reference mode. This reference mode is one view of the relationship between microorganism's growth rates and temperature. An equation that has been proposed in the literature to represent the relationship between microbial activity and temperature is the Arrhenius equation.

Arrhenius Equation Testing

The first test conducted was the Arrhenius equation generation of values for U_{max}, the saturation constant, and the death constant. The test was run setting the initial landfill temperature to 0°C and raising the temperature incrementally over time across actual landfill temperature ranges.

The values obtained from the equation are reported below with corresponding literature values next to them. The model values were taken from output in Figures 42-45 of Appendix A.

Model Results	Literature Values (El-Fadel, 490)
Acidogen:	**Acidogen:**
Death constant: 0.0 – 0.6 (day^{-1})	Death constant: 0.01 – 0.4(day^{-1})
Umax: 0.0-6.0 (day^{-1})	Umax: 2.0-30.0(day^{-1})
K: 0 .7- 0.02	K:10-150 (mg COD^{-1})
Methanogen:	**Methanogen:**
Death constant: 0.0-0.0036 (day^{-1})	Death constant: 0.01-0.04 (day^{-1})
Umax: 0.15 –0.46 (day^{-1})	Umax: 0.1 –0.5 (day^{-1})
K: 0.9 –0.4	K:10-2500 (mg COD^{-1})

TABLE 7. COMPARISON OF ARRHENIUS MODEL RESULTS TO LITERATURE VALUES

These values corresponded well for the death constants and U_{max} values reported by El-Fadel but were off by three orders of magnitude for the saturation constant. The verification of the Arrhenius equation representing microbial activity as a function of temperature was accomplished by taking a portion of Shelly's model representing butyrate activity and setting up a separate structure to test its behavior (see Appendix B).

Butyrate Growth Curve Test Using Arrhenius Equation

The purpose of this separate structure was to see if the growth curve reflected the curve present in Figure 3 with respect to the landfill temperature. The output of the Arrhenius equation initially behaved similarly to the reference mode. Figure 11 shows a well-defined biomass curve with respect to temperature, peaking at 19°C and decaying to zero at 40°C.
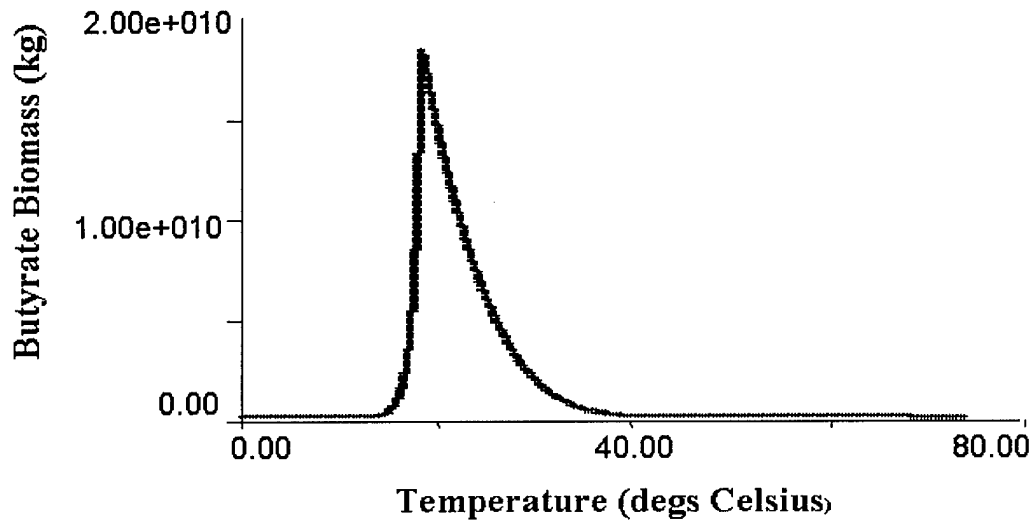
FIGURE 11. BUTYRATE BIOMASS CURVE VS TEMPERATURE USING ARRHENIUS EQUATION

Noticeable differences in values for U_{max}, K, and, k_d were observed. The U_{max} started at zero but rose with increasing temperature until a value of 15 was reached. The k_d term likewise rose form zero to a value near 1.5. Both terms never decreased, even if temperatures not typical for that microbial population were reached. The problem with this basic model was in the structure. The substrate level, glucose, was not held constant so temperature was not the only value changing.

A second model was developed to hold glucose constant and to have microbial growth cut off at 70°C. The biomass curve in Figure 12 rises to an extremely high value 8.24 E167 due to the U_{max} growth not being offset by the k_d term. Once the cutoff was reached at 70°C, the biomass curve dropped to zero.

45
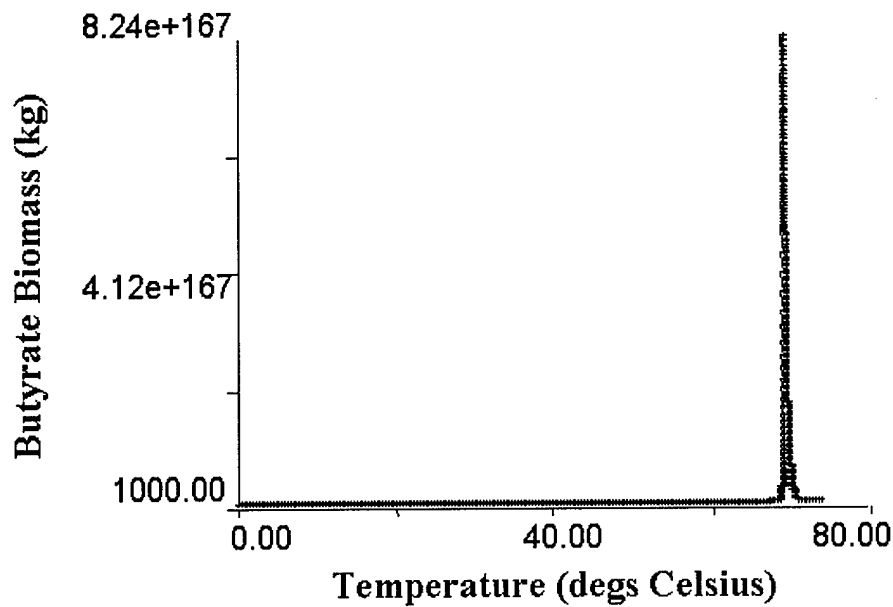
FIGURE 12. BUTYRATE BIOMASS CURVE VS TEMPERATURE USING ARRHENIUS EQUATION

A conclusion drawn from this test was that the values of the Arrhenius equation did not

represent the death rate of microorganism with respect to temperature. Since the biomass

growth curve is a reference mode for the system, it was necessary to go back to the

literature to find an equation that accurately represents the overall microbial growth

curve.

The Peleg Structure and Parameter Test

The Peleg equation represents microbial activity with respect to temperature. This test looks at the range in values for the growth and death parameters. The values for the equation and other initial parameter values are shown in Table 8.

$$k(T) = \ln((1 + b\exp-((T - T_m)/a_1)^2))/(1 + \exp((T - T_c)/a_2)))$$

Peleg equation parameters:
B height Acidogen- 3
Temperature span-34 deg C
Temperature Peak-38 deg C
Temperature Critical- 46 deg C
Decay Steepness-6
B height Methanogen-4
Temperature span- 25 deg C
Temperature Peak-60 deg C
Temperature Critical- 70 deg C
Decay Steepness-5
Initial Waste Temperature-15 deg C
Fixed Temperature increase- starting at 0.1 deg C/day to 0.3 deg C/day

TABLE 8. INITIAL PELEG EQUATION PARAMETER VALUES USED

Results show the U_{max} and k_d terms change with temperature and follow normal behavior. When the temperature is within the temperature span and less than the critical temperature the U_{max} value will increase. After the temperature reaches its critical temperature, the U_{max} term decreases while the k_d term increases. Figures 46-52 of Appendix A show the behavior described for the Peleg equation.

Butyrate Growth Curve Test Using the Peleg Equation

The same structure that was used to test microbial activity using the Arrhenius

equation was used to test the Peleg equation (see Appendix C for model structure). The

microbial populations that use butyrate are controlled by U_{max}, saturation, and decay

terms. The U_{max} and death terms are affected by the Peleg equation, which is controlled

by a fixed temperature increase variable. The parameter values used by Shelley to model

the saturation influence were left in the model. The important parameters were set at the

following initial values shown in Table 9.

Glucose Stock- 1E12 kg
Butyrate-0
Butyrate biomass-100
Peleg equation parameters
B height Acidogen- 3
Temperature span-20 deg C
Temperature Peak-25
Temperature Critical- 46
Decay Steepness-6
Initial Waste Temperature-10 deg C
Fixed Temperature increase starting at 0.1 deg C/day to 0.3 deg C/day

TABLE 9. PELEG EQUATION INITIAL PARAMETERS USED TO MODEL BUTYRATE ACTIVITY

The purpose of setting aside this piece of the model was to test the structure of the Peleg

equation, comparing the biomass present in the model to a known reference, Figure3.

The test was set up with fixed temperature increase that would cover the full temperature

range found in a landfill. The temperature started at 10°C and rose to 71°C. The

important parameter tested was the butyrate biomass stock level. The test did a time

series comparison of temperature vs biomass.
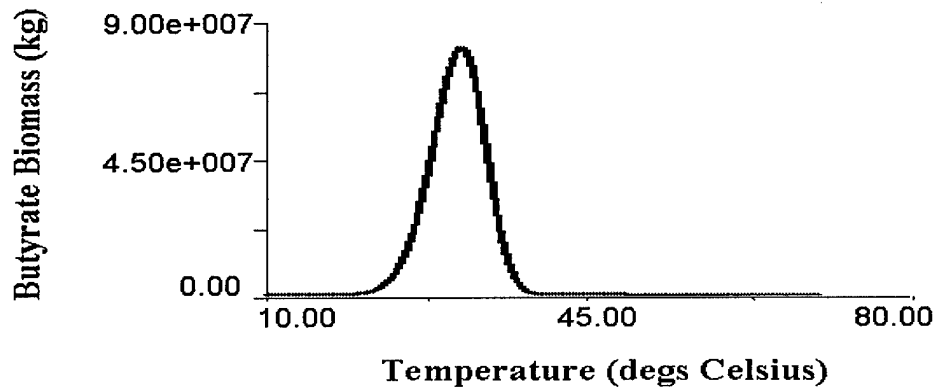
FIGURE 13. BUTYRATE BIOMASSS CURVE VS TEMPERATURE USING THE PELEG EQUATION

Figure 13 shows that the butyrate population has low initial growth until a

temperature value defined by the temperature range is reached, then the population

begins to rapidly grow. There is no substrate limitation in this structure; therefore only

temperature limits the population's growth. As the temperature reaches the defined

critical temperature value, the death parameter is greater than the growth parameter,

causing the population to decline to zero.

Formate Basic Structure Testing Biomass Growth Curve

The basic structure for the formate biomass is from the Shelley model for formate

(see Appendix C for model structure). The structure indicates how glucose is broken

down into other simpler products with some portion being transformed into formate. The

microbial populations that use formate are controlled by U_{max}, saturation, and decay

terms. The U_{max} and death terms are affected by the Peleg equation, which is controlled

by a fixed temperature increase variable. The important parameters were set at the initial

values shown in Table 9.

Glucose Stock- 1E12 kg
Butyrate-0
Butyrate biomass-100
Peleg equation parameters:
B height Acidogen- 3
Temperature span-20 deg C
Temperature Peak-25
Temperature Critical- 46
Decay Steepness-6
B height Methanogen-3
Temperature span- 30 deg C
Temperature Peak-40
Temperature Critical- 55
Decay Steepness-5
Initial Waste Temperature-10 deg C
Fixed Temperature increase- starting at 0.1 deg C/day to 0.3 deg C/day

TABLE 9. PELEG EQUATION INITIAL PARAMETERS USED TO MODEL FORMAT ACTIVITY

The purpose of setting aside this piece of the model was to test the structure of the

Peleg equation, comparing the methanogenic biomass to a known reference, Figure 3.

The test was set up with fixed temperature increase that would cover the full temperature

range found in a landfill. The temperature started at 10°C and rose to 71°C. The

important parameter tested was the formate biomass. The test did a time series

comparison of temperature vs formate biomass.
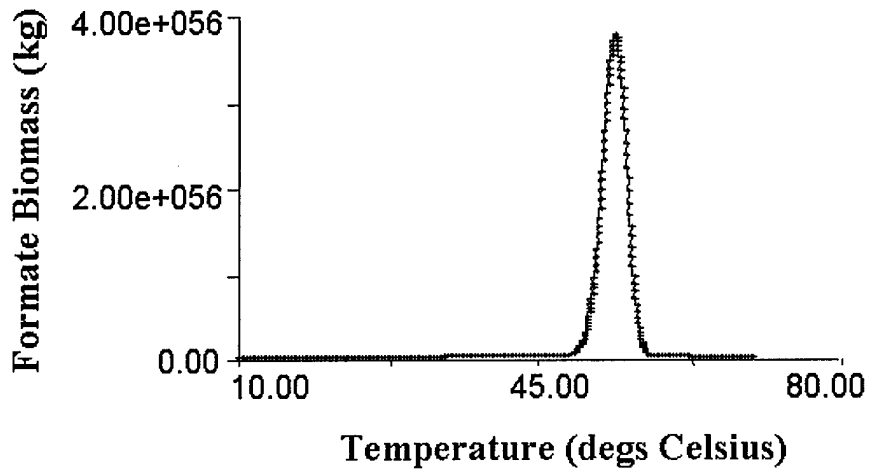
FIGURE 14 FORMATE BIOMASS CURVE VS TEMPERATURE USING PELEG EQUATION

The output shows that the formate population has low initial growth until a

temperature value defined by the temperature range is reached, then the population

begins to rapidly grow. There is no substrate limitation here; therefore temperature is the

only parameter that is limiting the population's growth. As the temperature reaches the

defined critical temperature value, the death parameter is greater than the growth, causing

the population to decline to zero.

Transfer Coefficient

The structure set up to test the transfer coefficient is simple. The concept of

thermodynamic principles and heat transfer are presented in Chapter 2, but the actual

application in a landfill system is not understood thoroughly. Keeping with system dynamics methodology, the structure is kept simple initially until tests can confirm the need for more complex structure. The temperature structure consists of a temperature stock representing the landfill temperature at a high value and a fixed ground temperature. The difference between the two is dissipated at a rate determined by the transfer coefficient (TC). The purpose of the structure was to test the plausible range for the transfer coefficient.

A plausible transfer coefficient range was found by running time simulations to determine how long it would take for the landfill temperature to reach ground temperature. Figure 15 shows a range for the transfer coefficient between 0.1 and 0.0001 which corresponds to a time to equilibrium of 75 days for a TC of 0.1 to well over one year for a TC of 0.00001. Figure 53, of Appendix A, shows in more detail the time for temperature equilibrium for the transfer coefficient range 0.001-0.00001.
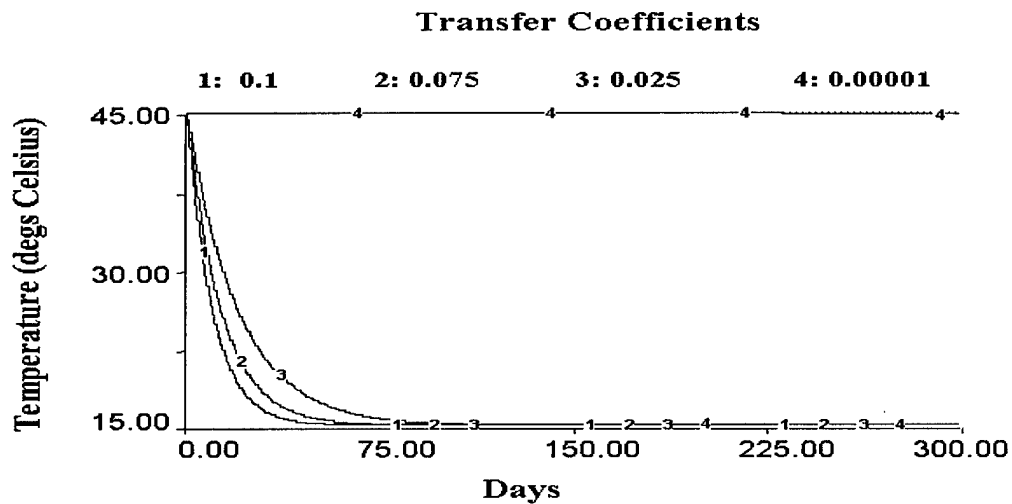
FIGURE 15. TRANSFER COEFFICIENT RANGE DETERMINATION

Heat Constants

The structure of the microbial populations with respect to temperature has been tested as well as the range for the transfer coefficient. The final structural area to test is the generation of heat, which corresponds to a temperature increase per day. The literature review provided information on the heat available for temperature increase based upon the degradation of glucose into simpler substances. For example, for every mole of glucose converted into acetate, there was 20 kcal of heat energy produced. Shelley's model has glucose breaking down into nine simpler substances. This test incorporated the whole model structure presented in Appendix D.

Heat constants were all given the same initial value to evaluate the temperature generated. A sensitivity analysis was performed to check the temperature range. Since the values for the heat generation constant ranges from 20-50 kcal/mol of glucose, a value of 50 was used as the base constant. The sensitivity analysis showed that the temperature rose from an initial value of 15°C to a value close to 60°C for all four simulations, which is within the temperature range of a typical landfill.

However, the temperature rise was too sudden, inhibiting the early stages of anaerobic degradation. Consequently, there was a small amount of glucose degraded, as seen in Figure 16. This clearly does not represent the system behavior and further tests were performed to find the heat constant values, which would produce reasonable system behavior.

Heat Constants (kcal/mole glucose)
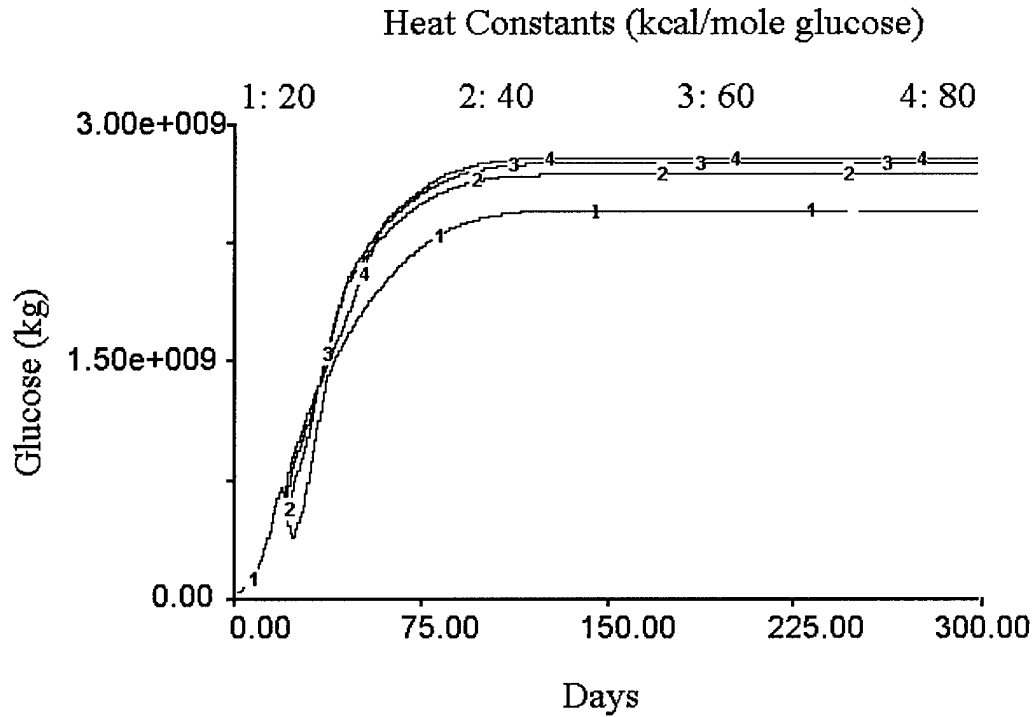
FIGURE 16 LITERATURE HEAT CONSTANTS TESTED SHOWING GLUCOSE

The methane mole fraction was similarly low with the high heat constants, as seen in

Figure 17. Figure 17 is deceptive because it looks like methane is being produced in

appropriate quantities, but this figure is representing the percentage of the total gas in the

system. If there is little glucose being degraded, then there will be less total gas

production, resulting in the relatively normal methane fraction graphs seen in Figure 17.

Heat Constants (kcal/mole glucose)

1: 20   2: 40   3: 60   4: 80
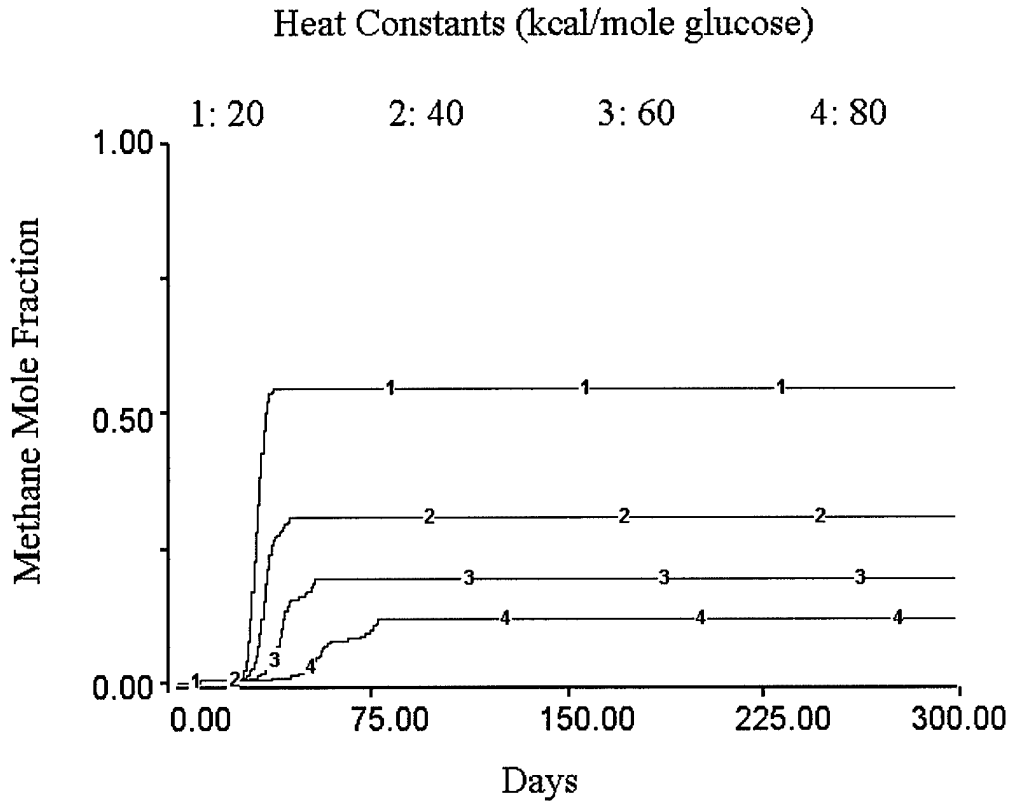
FIGURE 17. LITERATURE HEAT CONSTANTS TESTED SHOWING METHANE MOLE FRACTION

The range of heat constants tested in the next simulations was 1-10 kcal/ mole

glucose. Glucose levels and the reference mode seen in Figure 3 are a good indication of

biodegradation level. If little biodegradation occurs, then the methane mole fraction will

decrease around day 225, seen in Figure 18 for simulation 2, when the temperature drops

due to temperature dissipation. As a result, anaerobic degradation breaking glucose down

into simpler substances begins again. The only value that did not behave in this manner

was 1.0 kcal/mol. Simulation 5 looks like it will have a high methane mole fraction for

the entire period but if the simulation was carried out another couple of days it would too

drop to a lower fraction. Figures 54-56 of Appendix A include graphs of temperature,

temperature increase and total heat gain over the simulation time.
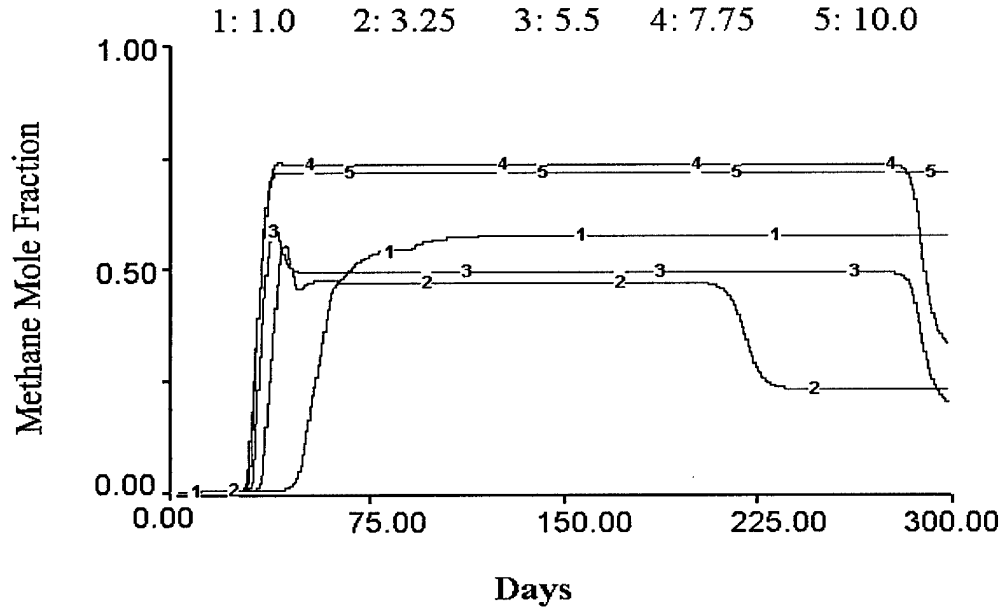
FIGURE 18 HEAT CONSTANTS TEST WITH METHANE MOLE FRACTION, TC 0.001

Specific Heat Constant

Since, a value was found to produce results showing behavior of the reference

mode, a sensitivity test was performed to see how changing the specific heat would affect

the temperature increase. The range chosen for the specific heat constant was 0.3 to 2.00

kcal/kg- deg C, with a set heat constant of 3 kcal/mol. The results in Figure 19 show that

only the first simulation with 0.3 specific heat value, indicated a drop in methane

production due to incomplete degradation of glucose.

Specific Heat (kcal/kg-deg C)

1: 0.3   2: 0.87   3: 1.43   4: 2.0
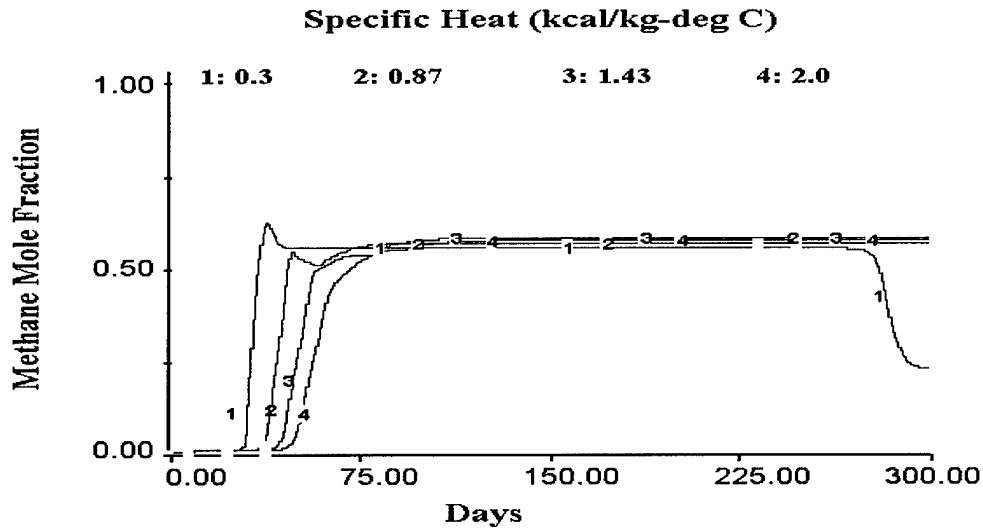
FIGURE 19 SPECIFIC HEAT VALUES SHOWING METHANE MOLE FRACTION

Glucose is formed in the model from a set degradation rate of the solid waste present over time. The solid waste starts at 3.0 E9 kg and is converted at a constant rate until there is no more waste seen in Figure 20. The glucose will rise as the waste is being degraded seen in Figure 21.
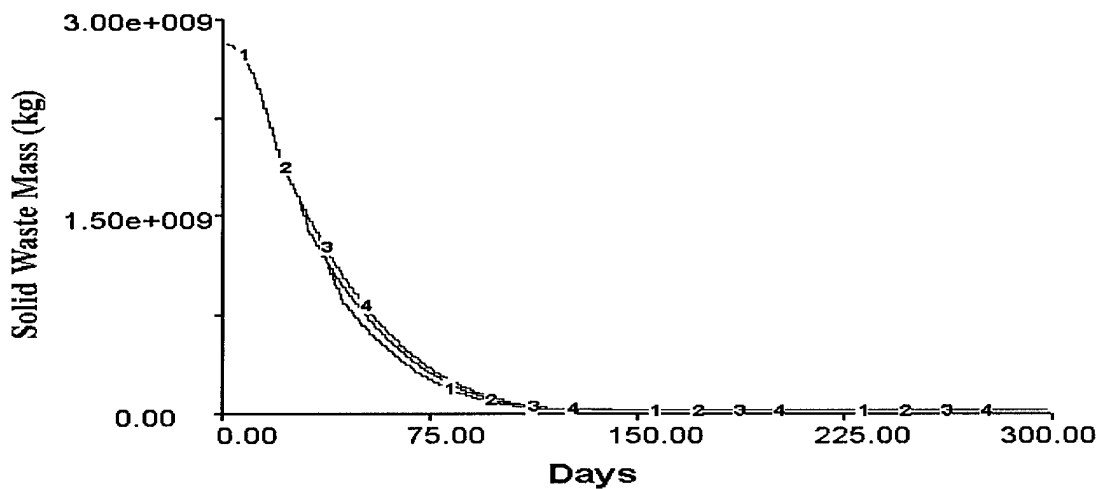
FIGURE 20. SOLID WASTE DEGRADATION TIME SCALE

57

As the solid waste is being degraded, the glucose stock will rise. The temperature of the system controls whether the glucose is converted into simpler forms by affecting the growth of microbial populations. If the temperature is favorable for microbial activity, specifically acetogens and fermentors, then the glucose stock will be used as it is being produced. This behavior can be seen in Figure 21 when the glucose rises but begins to fall around day 15 due to the onset of anaerobic degradation. However, if the specific heat is low, a value of 0.3, it take less heat energy to increase the temperature of the waste, causing the temperature to rise above microbial growth levels. Glucose degradation into simpler substances by microorganisms is stopped; as the remaining solid waste is degraded it is stored as glucose until the temperature drops low enough again for microorganism to become active. The resulting effect on gas production is a decrease in the methane mole fraction, seen in Figure 19, and a subsequent increase in the carbon dioxide mole fraction. Refer to Figures 57-61 in Appendix A for more graphs of U_{max} values and other gas mole fractions.
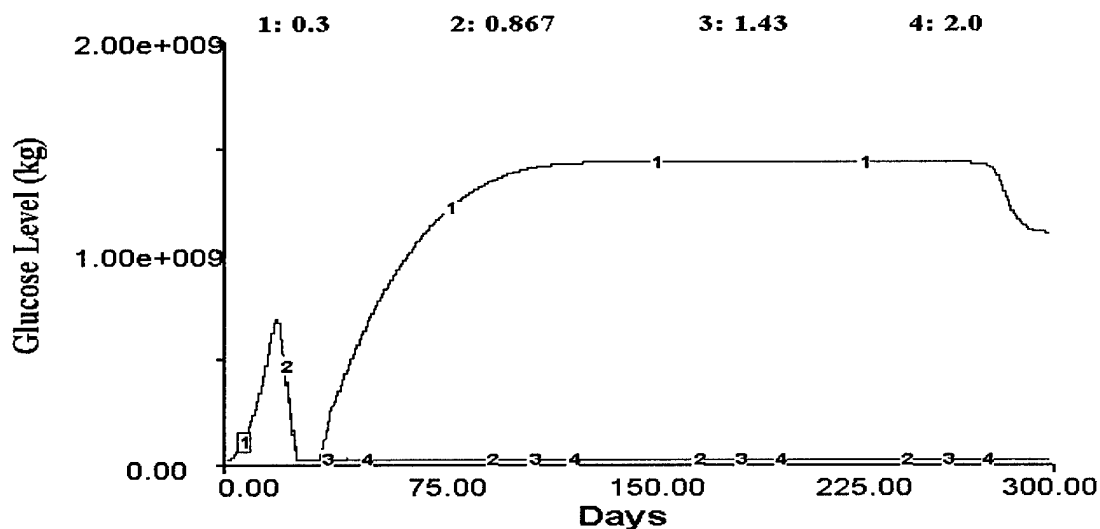
FIGURE 21. GLUCOSE LEVEL WITH CHANGING SPECIFIC HEAT VALUES

The next simulations tested the range of heat constant's with a higher specific heat value,

0.6 kcal/kg- deg C. The range tested for the heat constant was 5-20 kcal/mol glucose.

The test was stopped at the second simulation, after seeing inhibited degradation.

To find what specific heat would be required to get a slower heat rise, using the

literature values for the heat constant, another sensitivity test was run on the specific heat

constant. The heat constant was set at 30 kcal/mol and the sensitivity test values ranged

form 1.00 – 5.00 kcal/kg- deg C. None of the specific heat values allowed

biodegradation to occur in the system.

In order to find a range of values for the heat constant, more sensitivity tests were

performed using values from 1-5 kcal/mol. The simulations representing 1.0 and 2.0

kcal/mol showed the desired behavior, this seems to be the upper range for the heat

constant parameter. Another sensitivity analysis was performed from 1.0 – 0.01. The

59

sensitivity test was stopped after the second simulation when the heat constant of 0.333

kcal/mol failed to produce a high enough temperature increase.

Using the heat constant value of 2.0 kcal/mol, a sensitivity analysis was run to

determine the range for the specific heat parameter. The tests range was from 0.2-2.00

kcal/kg-deg C. The 0.2 specific heat value produced a rapid increase in temperature to

53°C by day 40 while a value of 2.00 only produced a 5°C increase to a temperature

value of 20.0°C. During this low temperature range glucose is depleted but due to a large

hydrogen inhibition gas levels are kept low with most of the mass being stored as acetate

see Figure 22.
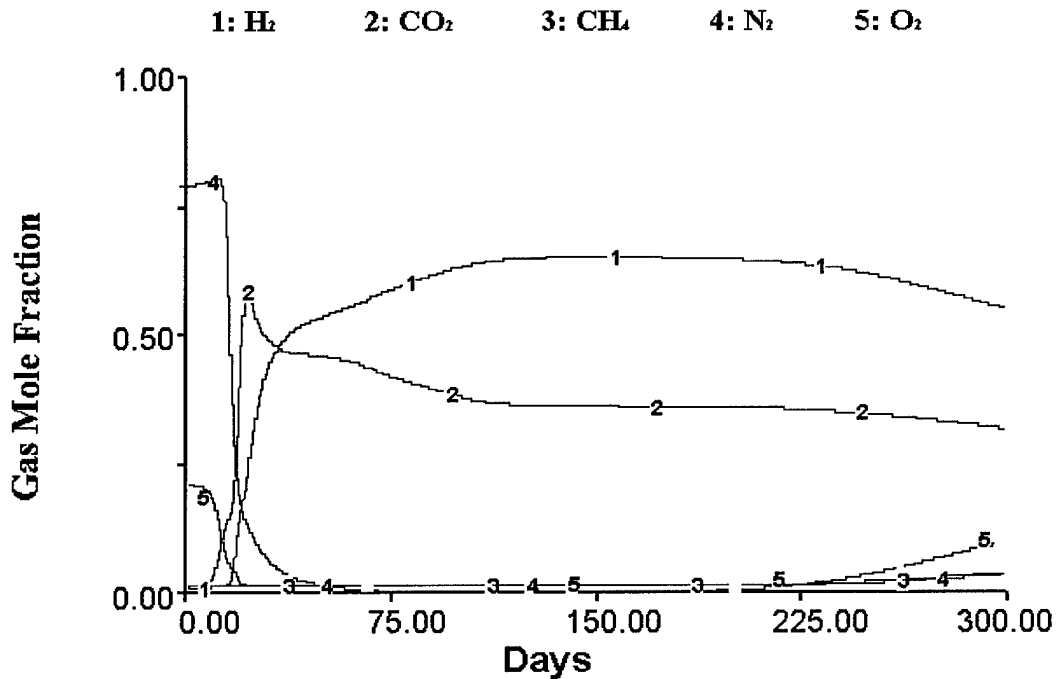
FIGURE 22. MOLE FRACTION OF GASES FOR A 2.00 SPECIFIC HEAT VALUE

All the above simulations running sensitivity tests for the heat constant and specific heat were obtained using only one transfer coefficient. The transfer coefficient was 0.001, which allows for only a small temperature loss out of the system. Using a transfer coefficient at the higher range shown in Figure 19 should increase the rate of heat loss from the system and allow use of a higher heat constant. The following discussions of simulations use a transfer coefficient of 0.1. Figure 23 shows the methane mole fraction of gas produced with different heat constants. These heat constants are similar to the values reported by El-Fadel. A heat constant value of 30 kcal/mole of glucose produces enough heat, to cause the temperature to rise rapidly to the methanogenic critical temperature value. There is little activity at this temperature until transfer to the environment reduces this heat. This is why there is a delay in the methane mole fraction curve for simulation four. Once the temperature reaches a value near 40°C then the acetogens and fermenters begin to degrade glucose. However, since the temperature value is near the critical temperature for these microbial populations the growth of the populations is low. This result is an extended glucose degradation curve over time. The slower glucose degradation results in less substance available for methanogenesis. Figures 62-65 of Appendix A show the CO_2 mole fraction, temperature, and U_{max} values for the simulation.
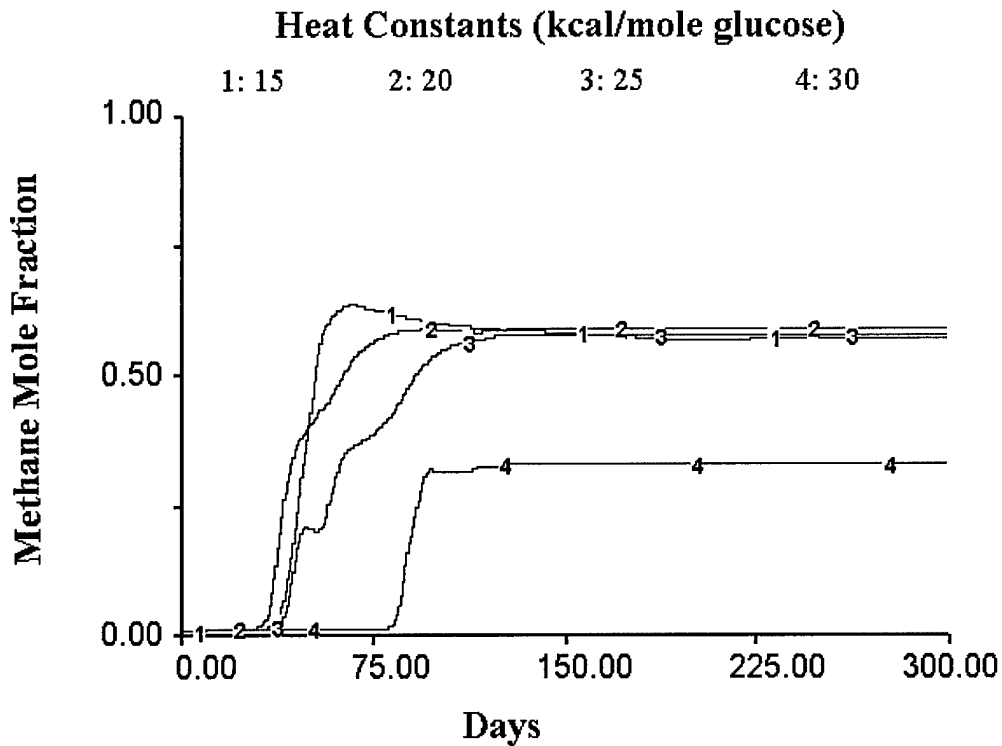
FIGURE 23. HEAT CONSTANTS USING A TC 0.1 SHOWING METHANE MOLE FRACTION

Related Factors with Heat Constants

A heat constant value around 15 kcal/mol glucose with a specific heat of 0.6 kcal/

kg-deg C, using a transfer coefficient of 0.1, produces behavior that is similar to the

behavior seen in the reference mode. Exploring this behavior further by looking at the

initial waste temperature and seasonal soil temperature will help verify and validate the

model. The waste's initial temperature will be affected by the climate where the waste is

disposed. Other factors that might influence initial temperature of the waste is the

amount of time the waste is exposed to ambient air conditions at a transfer station or the

time it takes to transport the waste to the landfill. These factors were not investigated in

this research; therefore, an assumption was made for the initial waste temperature. The

waste is assumed to have a starting temperature close to ambient air temperature.

However, simulations show that with a high heat constant and transfer coefficient the

initial waste temperature, °C, does not effect the landfill temperature or gas production as

seen in Figure 24.
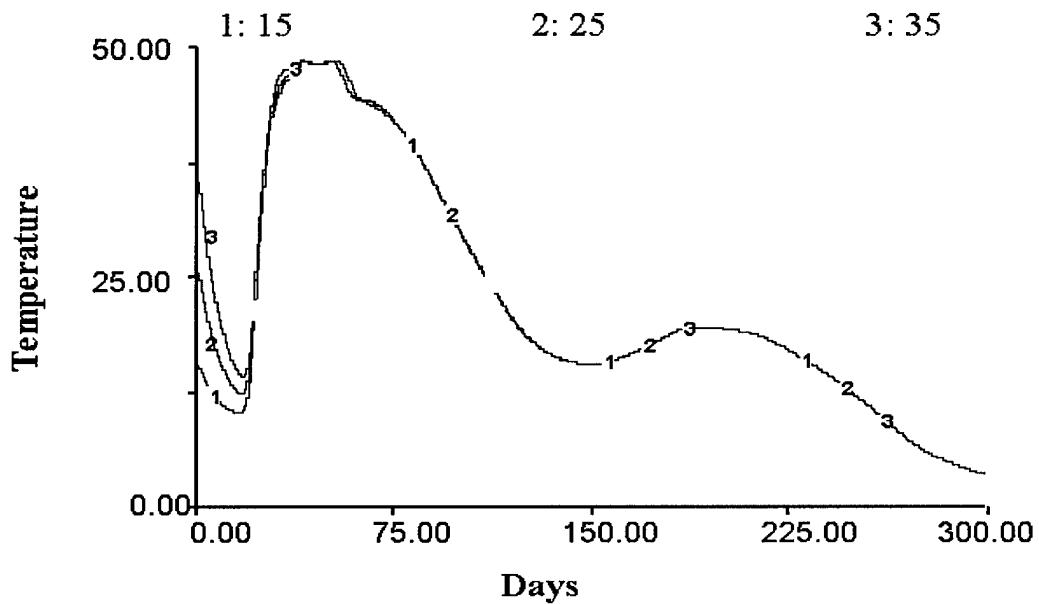
FIGURE 24. INITIAL WASTE TEMPERATURE AFFECTS ON LANDFILL TEMPERATURE, TC 0.1

Initial waste changes affects on other parameter values such as; Umax

methanogen, Umax acidogen, glucose, CO_2 mole fraction and butyrate biomass curve are

presented in Figures 66-71 of Appendix A. These graphs show that all the parameters

have the same behavior for each simulation. The biomass curve is normal until the

critical temperature is reached around 50°C. The curve jumps around here because of the

fluctuations in the temperature, which are being mapped onto a scatter plot.

These observations are different as an alternative transfer coefficient was applied.

Changing the transfer coefficient used in the system changes the heat constant it can be

associated with. A transfer coefficient of 0.01 was proposed to see how an order of

magnitude shift would affect the corresponding heat constant, biodegradation level, gas

production, and temperature. Also, simulations were run to determine if the initial waste

temperature would affect landfill conditions in a different manner due to an order of

magnitude change in the transfer coefficient. Figure 25 illustrates the level of glucose

biodegradation over time based on a transfer coefficient of 0.01, a heat constant value of

10 kcal/mol glucose with a changing initial waste temperature.

Temperature (degs. Celsius)
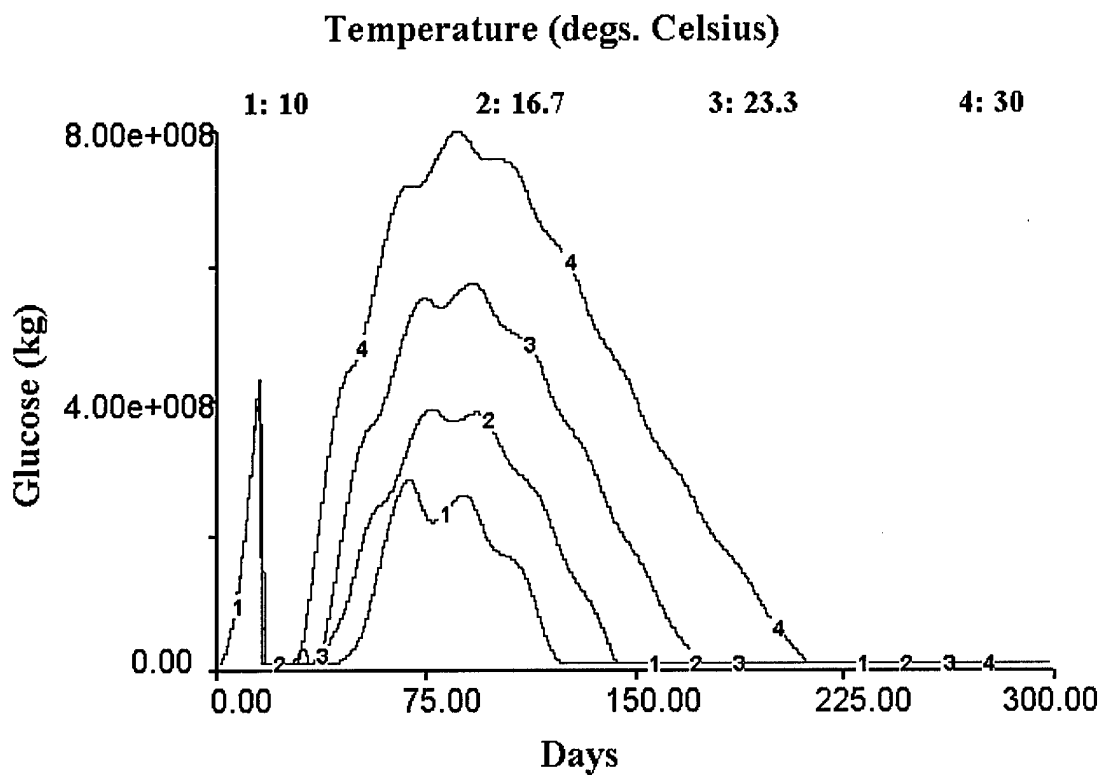
FIGURE 25 INITIAL WASTE TEMPERATURE AFFECTS ON GLUCOSE LEVEL, TC 0.01

The glucose level rises as solid waste is being degraded and is transformed into simpler substances until day 35. The temperature conditions at this time rise higher than the fermentators or acidogens can withstand. As the temperature decreases certain microorganisms become active increasing the temperature. This is why the temperature seems to fluctuate around 60°C seen in Figure 26. These fluctuations in temperature can be seen as small rises and dips in the glucose curves.

Initial Waste Temperature (degs Celsius)
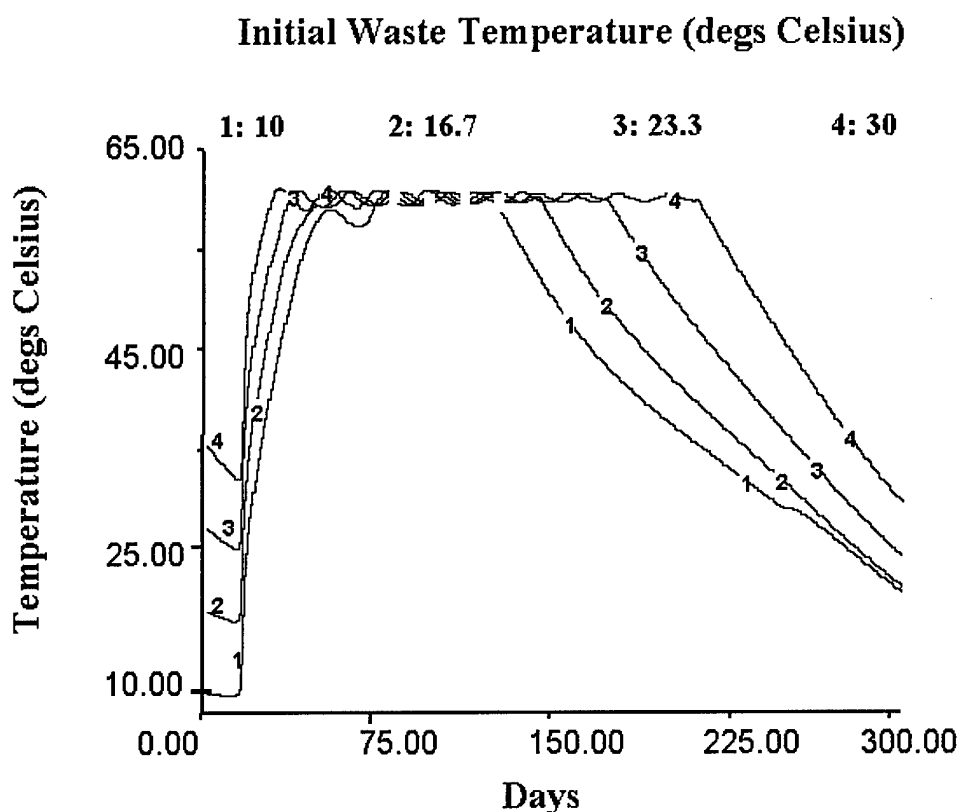
FIGURE 26 INITIAL WASTE TEMPERATURE AFFECTS ON LANDFILL TEMPERATURE, TC 0.01

The majority of gas produced under this simulation is CO_2 with little visible methane production seen in Figure 72 of Appendix A. Figures 74 and 75 of Appendix A illustrate that the acidogen and methanogen U_{max} values have the same oscillations with respect to the temperature oscillation.

The differences in graphs between the transfer coefficients indicate that if a high rate of heat generation and loss occurs in the landfill then the starting temperature will not have any affect on the glucose biodegradation or gas production amounts. The rate of heat loss will probably vary over time and not be at one constant rate. The rate changes in the beginning of the solid waste degradation will determine the significance of the initial waste temperature.

Sensitivity Tests on the Peleg Equation

The main equation in thesis model is the equation describing the growth and decay for the microorganisms in the system. The organisms in the system were assumed to take on the behavior of either an acidogen or methanogen based microorganism. Sensitivity tests were performed on all the variables in the equations for both the acidogens and methanogens.

B Height Parameter

The height parameter for both the acidogen and methanogen microorganisms affects their respective U_{max} value. The original value used by Peleg for microorganisms in the food processing industry had values between 3-5; this range was used as a beginning point for the sensitivity tests. The initial run for the sensitivity tests used a TC of 0.001 with a heat constant of 2 kcal/mol glucose. The sensitivity test for the acidogen height parameter tested the range between 1.0-10.0, using four simulations. The results in Figure 27 show that a low height value produces a lower methane mole fraction than the other three higher values. This is due to the U_{max} value having a low value, which

does not allow the acidogen populations to grow thus reducing the amount of simpler

substances available for the production of methane. Height parameter values do not

appear to be sensitive to values between 4-10 due to the fact that the U_{max} value is closer

to maximizing the glucose available. Figures 76-80 of Appendix A show other model

behavior sensitivity based on the changing height parameter.

Acidogen Height Parameter
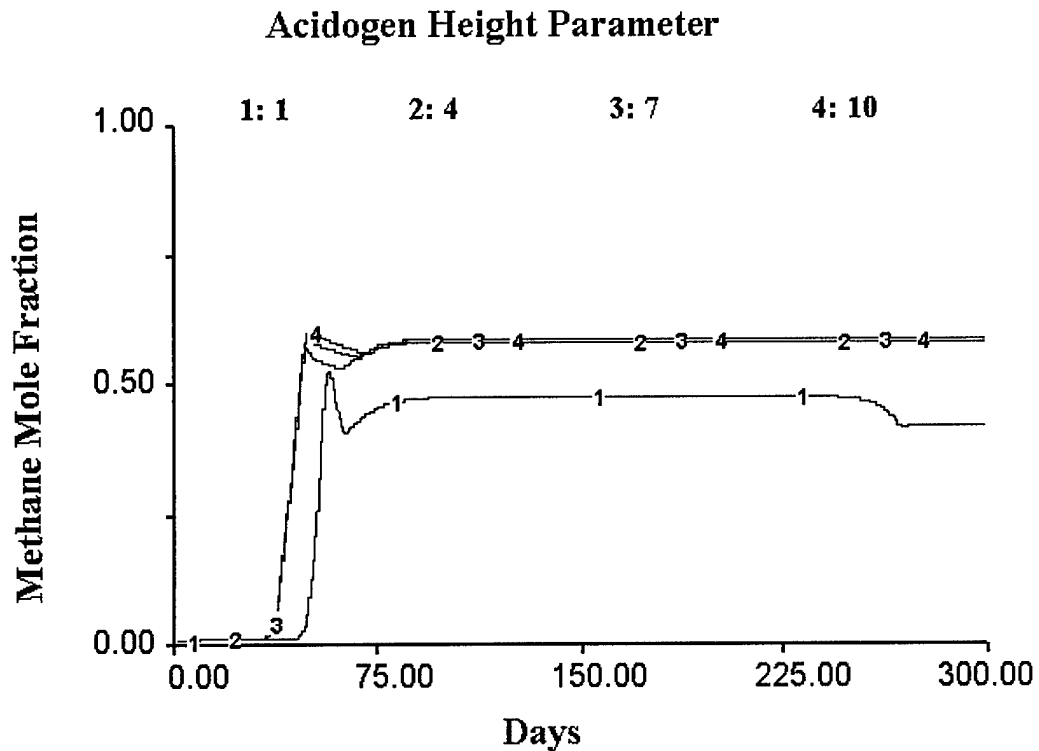
FIGURE 27 ACIDOGEN HEIGHT PARAMETER SHOWING METHANE MOLE FRACTION, TC 0.001

The TC was changed to 0.1, and follow up sensitivity tests were done to see if any

of the Peleg equation parameters would have different effects on the behavior for the

biomass curves and gas production. A simulation was run to compare various extreme

values for the b height parameter seen in Figure 28. When the TC was 0.1 the height

parameter needed to be above 3.0, which produced good results for the TC of 0.001.

The height parameter effects the U_{max} value for microbial growth. The U_{max} values produced from the height parameters tested in Figures 27 are not within the range reported in the literature, presented in Table 6, while Figure 28's height values produced Umax values within the literature range for simulations two, three and four. The low Umax values cause the glucose level, for TC of 0.001, in Figure 71 to remain high over the degradation process. Figures 81-85 of Appendix A include more model behavior for the changing acidogen height parameter.
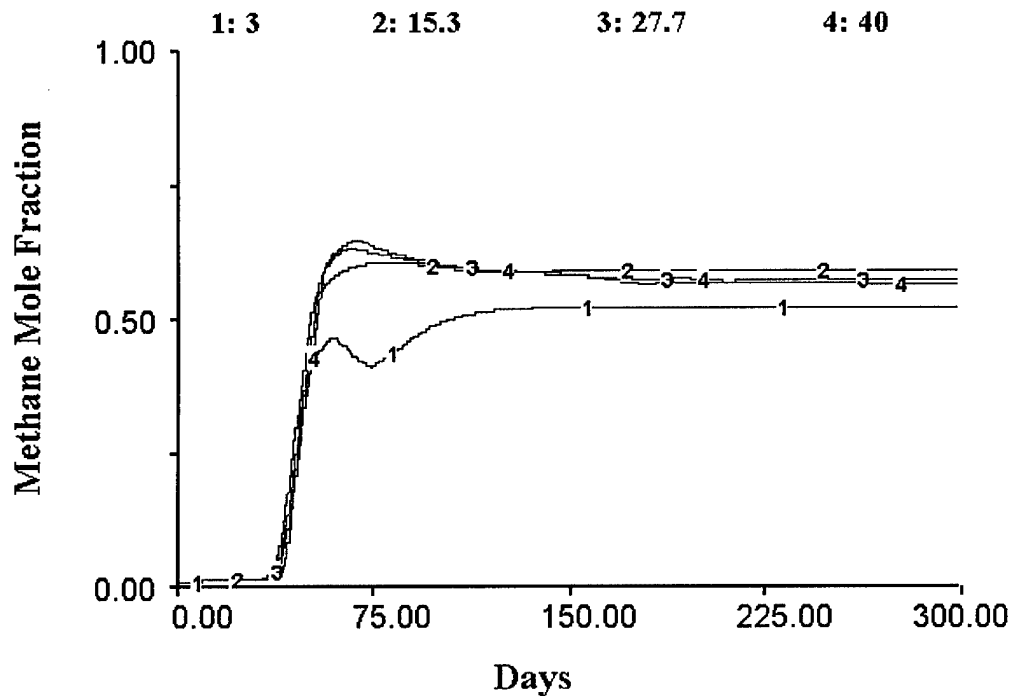
FIGURE 28 ACIDOGEN HEIGHT PARAMETER SHOWING METHANE MOLE FRACTION, TC 0.1

The methanogen height parameter behaved similarly to the acidogen height parameter with a low height value resulting in a lower methane mole fraction while higher height values seemed to produce methane mole fraction slightly above 50 percent,

see Figure 86 in Appendix A. A low height parameter, 1.0, in Figure 29 allows the U_{max}

value for methanogens to maintain a value presented in literature, presented in Table 6.

Also, the height parameter seems to have an effect on the shape of the biomass curve

shown in Figure 30.
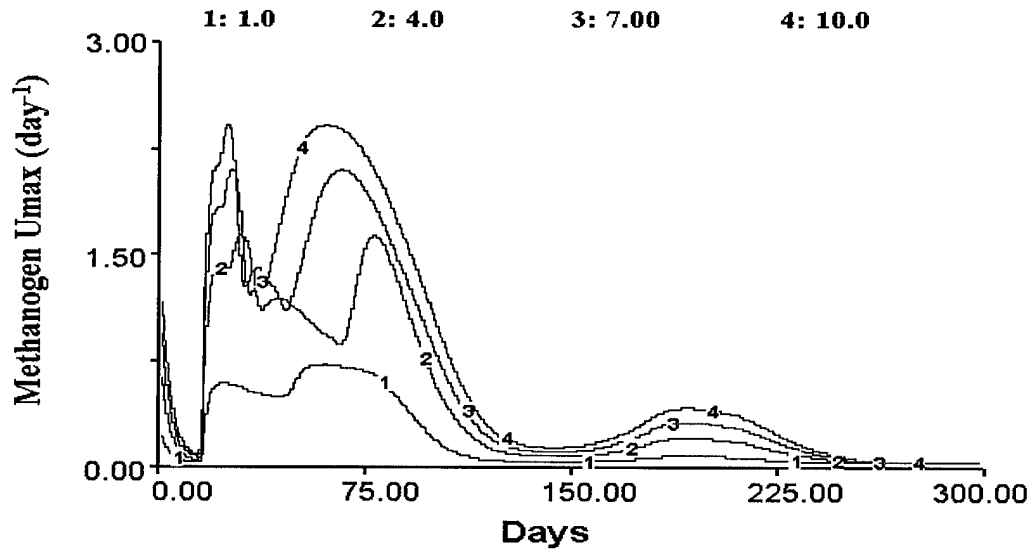
FIGURE 29. METHANOGEN UMAX VALUE WITH CHANGING METHANOGEN HEIGHT PARAMTER

Figure 30 shows that a lower methanogen height pushes the methanogen biomass curve

to a higher temperature range, which corresponds to the reference mode in Figure 3.
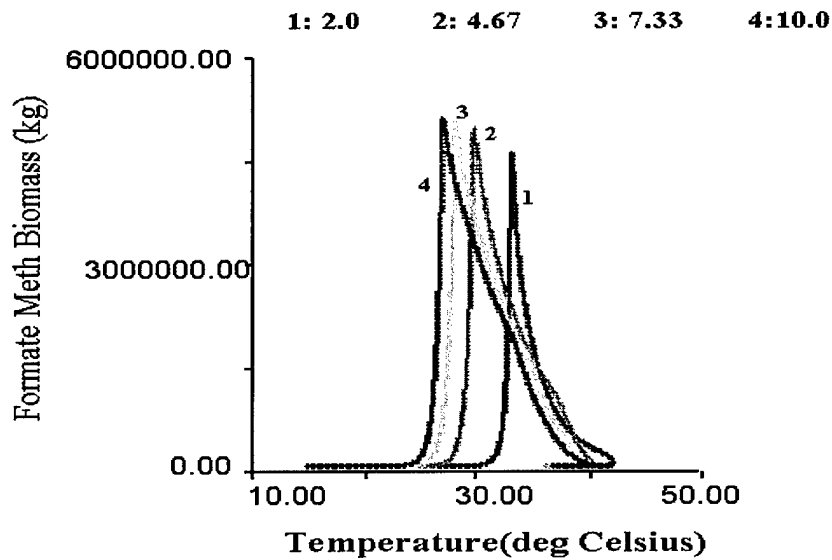
FIGURE 30 METHANOGEN HEIGHT PARAMETER WITH METHANE MOLE FRACTION, TC 0.001

Decay Steepness

The decay steepness affects the death rate constant and was reported by Peleg to

range from 1-7 °C. There seemed to be little effect of the acidogen decay steepness on

the mole fraction of methane and carbon dioxide produced or the shape of the biomass

curves. Figure 31 illustrates the insensitivity of methane production to the decay

steepness parameter.

Decay Steepness

1: 1.0   2: 4.67   3: 8.33   4: 12.0
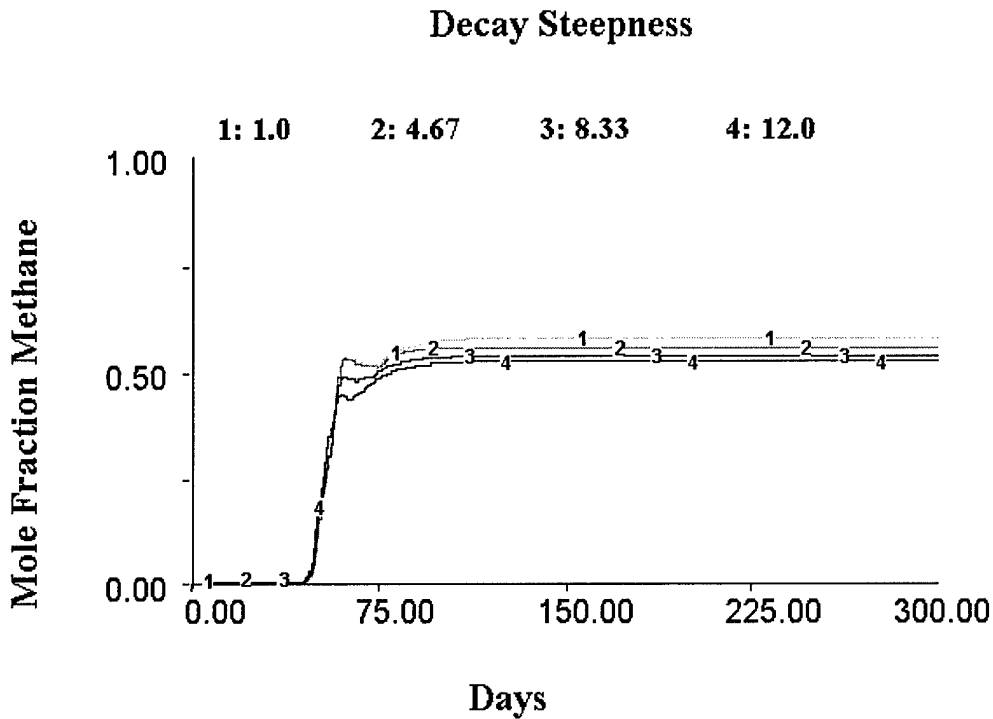
FIGURE 31 ACIDOGEN DECAY STEEPNESS SHOWING METHANE MOLE FRACTION

The methanogen decay parameter changes produced no noticeable behavior differences

between values. Appendix A Figures 87-89 has the remaining acidogen graphs and the

methanogen graphs can be seen in Figures 90-93.

Temperature Span

The temperature span affects the U_{max} value and also affects the biomass curve

shape. A larger range for the temperature span will produce a higher U_{max} value. The

first sensitivity test used an acidogen temperature range from 5-45°C. A value of 5°C did

not produce a high enough U_{max} to support population growth resulting in no biomass

growth. A second set of simulations was run when the TC was changed from 0.001 to

0.1. Similarly to the first set of simulations the second showed that a value of 5°C

71

produced no noticeable biomass growth. Methane production, as well as the other gases, have similar mole fraction traces, seen in Figure 95 of Appendix A, with just a slightly higher mole fraction early in the biodegradation process with a TC of 0.1.

Methane populations are more sensitive to temperature span changes. The big difference is that the methane biomass curves visibly shift with changing temperature span ranges as shown in Figure 32. Figures 32-34 are running sensitivity tests for the formate methane biomass curve by changing the temperature span range, °C.

1: 5   2: 13.3   3: 21.7   4: 30
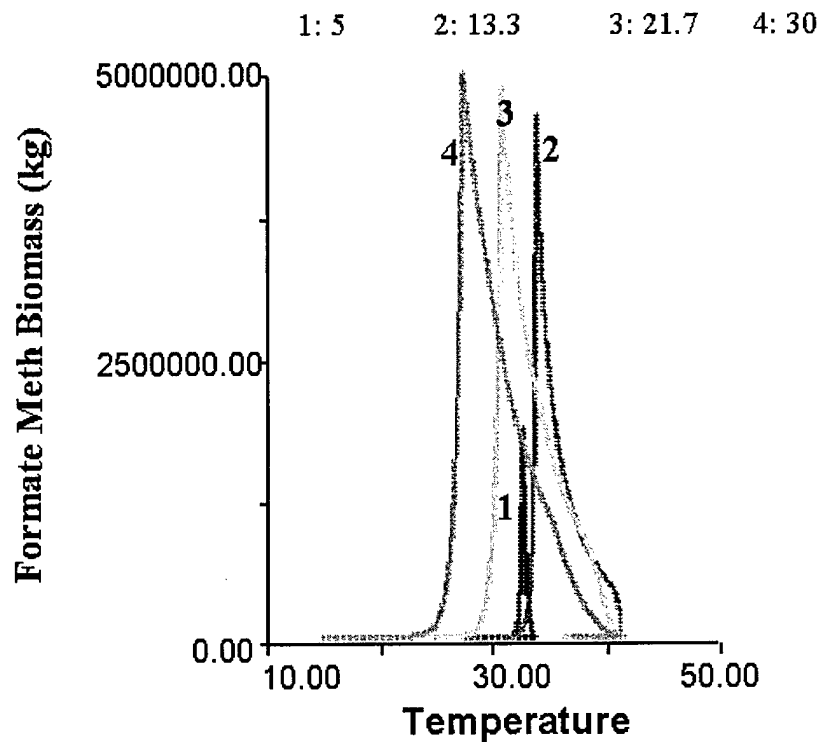
FIGURE 32. METHANOGEN TEMPERATURE SPAN WITH FORMATE BIOMASS

The low temperature span value of 5 °C produces a stunted biomass curve, which affects the amount of biomass produced compared to the other curves. As the temperature span increases, the base of the biomass curves shift to the left indicating increased activity at

72

lower temperatures. Simulation 2 with a temperature span of 13.3 produced a biomass

curve that is more characteristic of methane populations. Figures 97 and 98 show the

U_{max} and k_d values for the methanogen populations.

A change in the TC has a large impact on the methane biomass curve. The curves

in Figure 33 begin to slope to the right and are not a distinct curve shown in Figure 32.
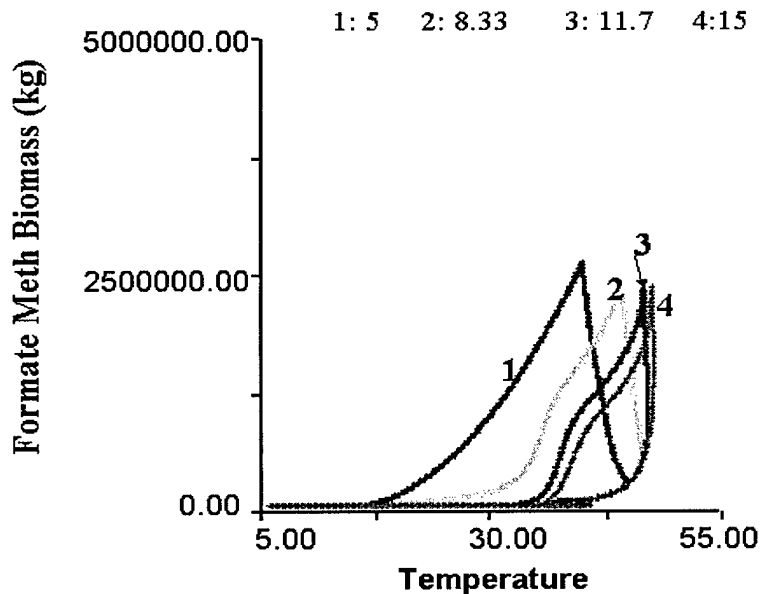
FIGURE 33. METHANOGEN TEMPERATURE SPAN WITH FORMATE BIOMASS, TC 0.1

An explanation for this behavior is that a higher TC bleeds off heat faster causing

the temperature to stay below 50 °C. Since the temperature never reaches the critical

temperature for the methane populations, the curves appear skewed. As the food source

and temperature decline the populations begins to die off due to lower extreme

conditions. Since there has not been time for glucose to degrade there is little food for

the methanogens. Once the temperature falls below 46°C, the critical temperature for

acidogens, acidogen growth begins allowing glucose to be broken down into simple substances. When the glucose is depleted the temperature rapidly drops and the remaining amount of simpler substances are converted to CO_2 and CH_4. Figures 99-102 show other parameters are sensitive to the changing temperature span for a heat constant of 15 kcal/mol glucose.

Since the biomass curves were not representative of the whole range, due to the temperature maintaining at a value below the critical temperature for the methanogen populations, a third sensitivity test was run with a heat constant of 25 kcal/mol glucose. Figure 34 shows more distinct curves for the same temperature span simulations. The other parameters run is this test can be seen in Figures 103-106.
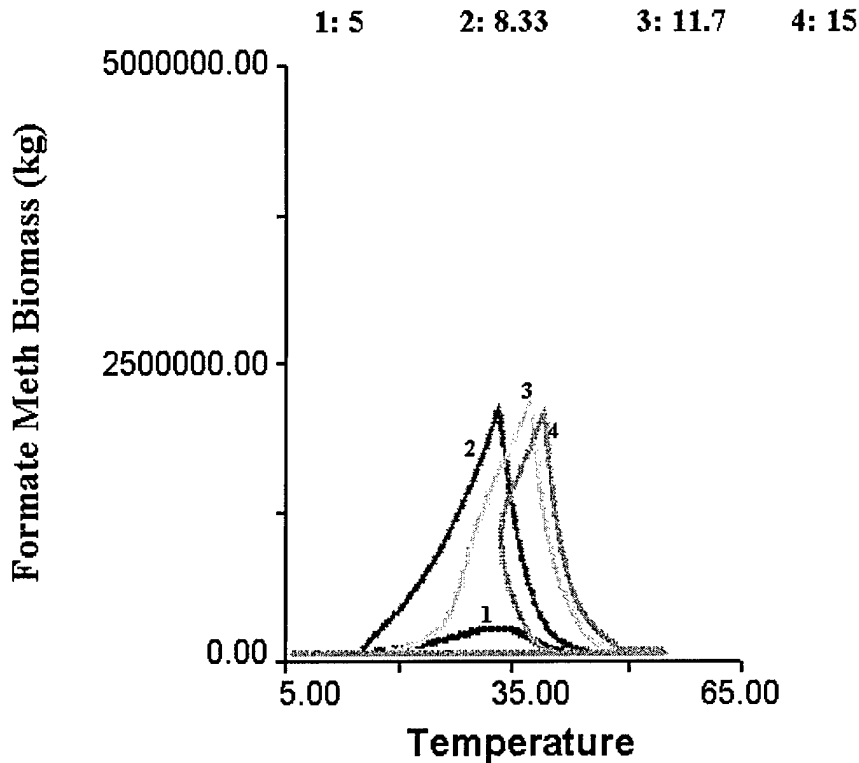
FIGURE 34. METHANOGEN TEMPERATURE SPAN WITH FORMATE BIOMASS

The value used in the final model was 12 due to simulation 3 having a complete curve that was representative of methanogenic behavior, based on temperature.

Peak Temperature

The peak temperature controls the characteristic peak for each population. Simulations for the acidogen populations show that the range for the peak temperature running between 20-35 °C has no effect on the U_{max}, biomass curve or mole fraction of gases produced, see Figures 107-109. The peak temperature used in the final model is 30°C. The peak temperature used for the methanogen populations has an impact on the system's behavior. One reason for the methanogens having an effect is that the temperature range for their peak temperature is higher and conditions are reached in the system that go above this temperature range. The temperature range used in the sensitivity test for the methanogen peak temperature was 30-55°C. Figure 35 shows the methane mole fraction for this range.
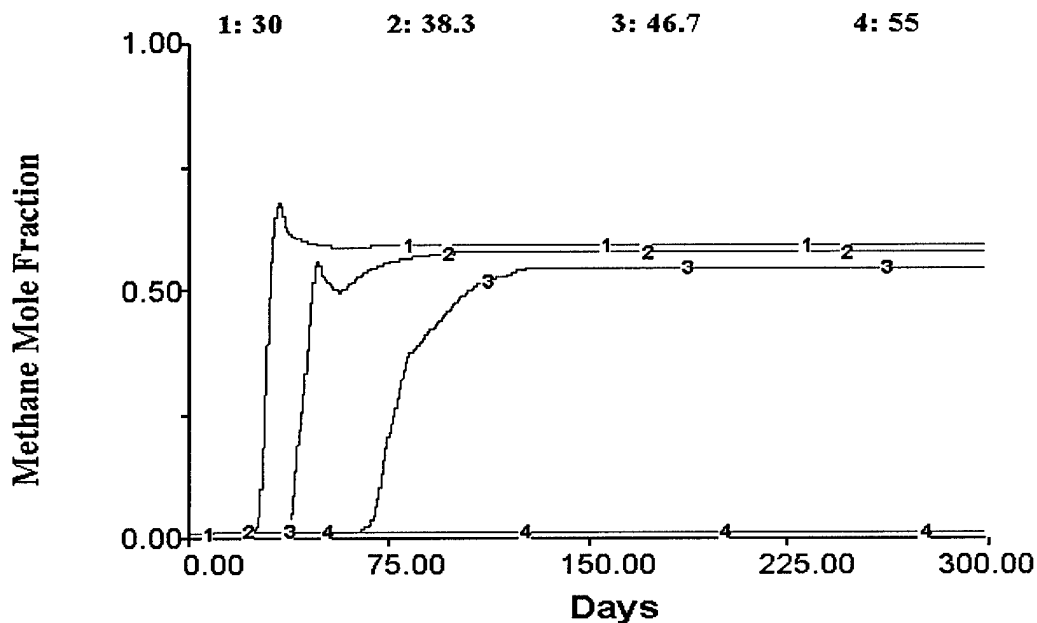
FIGURE 35. METHANOGEN PEAK TEMPERATURE WITH METHANE MOLE FRACTION

The first simulation produces the highest methane fraction but it is not characteristic

of methanogenic populations. Simulation two has a methane mole fraction similar to the

first but its peak temperature is closer to values reported in literature. Simulation three

shows a decline in the methane mole fraction because the temperature is too high for

actual temperature in the landfill. The last simulation's temperature is not reached in the

system so the U_{max} value would always be negative resulting in no biomass growth. The

U_{max} graph along with others can be seen in Figures 110-113.

Critical Temperature

The critical temperature is an important parameter in the death rate constant that was lacking in the Arrhenius equation. The acidogen populations are mainly affected by this parameter in the lower extreme range. The sensitivity test range was between 30-55 °C shown in Figure 36.
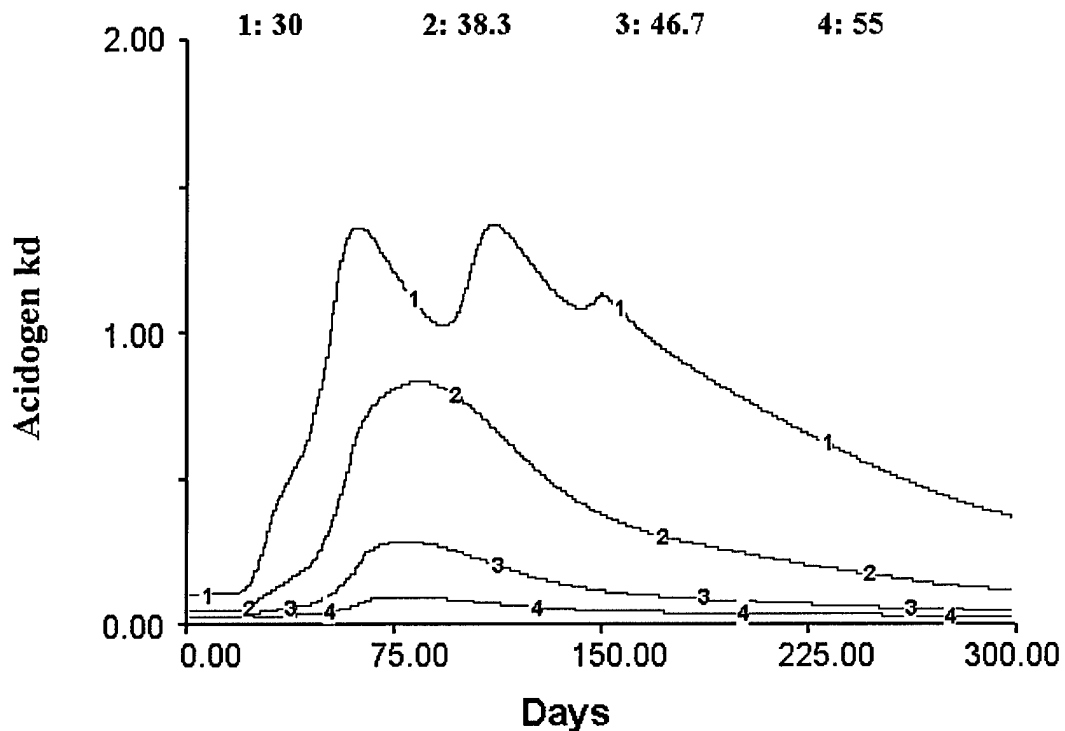
FIGURE 36. ACIDOGEN CRITICAL TEMPERATURE WITH DEATH RATE CONSTANT

A value of 30°C for the critical temperature is unrealistic if the system begins at 25°C. The Peleg equation generates a high k_d in this case resulting in less glucose being degraded seen in Figure 114 of Appendix A. The second simulation produces a distinct k_d curve with no oscillations which indicates that a large glucose stock is not built up or

is not being depleted over a long time period. The fourth simulation has a temperature value that is reached in a very short time so the k_d term for this value is low, meaning there is a small amount of acidogen death occurring in the system.

The methanogen critical temperature parameter did not affect the system due to temperatures not rising or sustaining at this high level. The temperature range tested in the sensitivity test was between 50-70°C; results are shown in Figure 117-120 of Appendix A. The temperatures needed for effects to be seen would have to occur over special circumstances. The temperature would have to gradually increase allowing for glucose depletion through fermentation then increase throughout methanogensis. This occurred when the model structure was tested separately with the temperature gain being manually controlled. Using a high transfer coefficient does not allow the system to maintain any kind of sustained temperature level to reach the methanogen critical temperature.

Climate Influences

The location of the landfill can have a significant effect on the biodegradation process. The temperature at the beginning of biodegradation can be affected by the seasonal variations in soil temperature in one location and between different climate locations. Data was collected on the seasonal soil temperature from three different climate locations. The temperature readings are based on a 1.2 m depth; temperature values beyond this depth appear to level off at this value (Chang, 1958:82-84). All the temperature profiles begin with the month of January and go through the month of October to account for the 300 days in the system simulations. Cairo was used as a warm

climate whose soil temperature maintains relatively the same temperature the whole year, roughly 20°C. Kansas was chosen as a moderate temperature climate with moderate temperature fluctuations between 5-20°C. A Moscow soil temperature profile was used to represent a cold climate; its soil temperature range is from 2-13°C. The main element explored with these soil profiles was the methane mole fraction produced and the landfill temperature profile. Each climate location was compared using a TC of 0.1 and 0.01 over the same range of heat constants, 5.0-15.0 kcal/mol glucose.
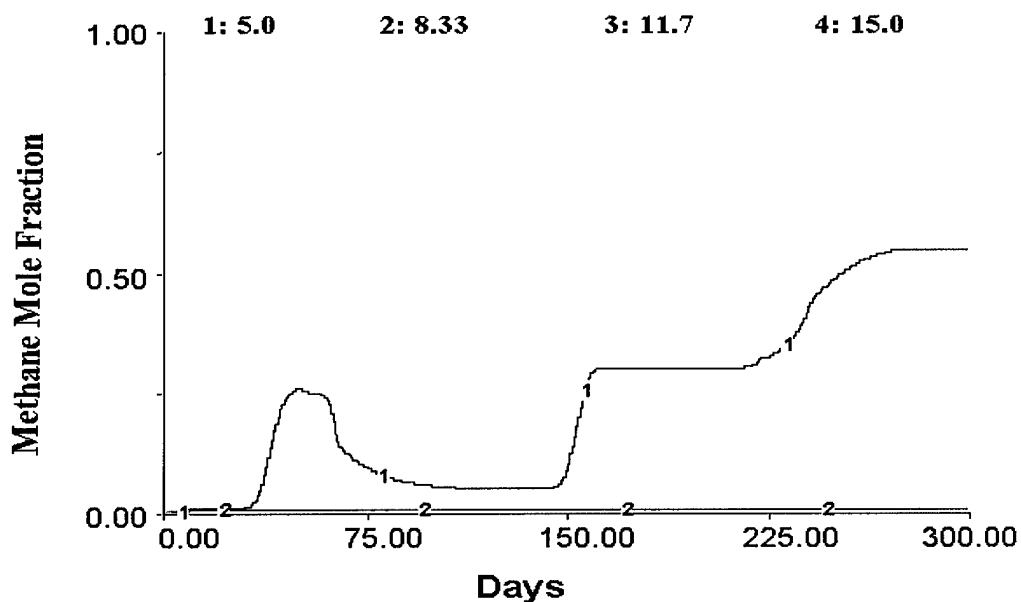
FIGURE 37. CAIRO SOIL PROFILE WITH A TC OF 0.01

The TC of 0.01 does not reduce the heat fast enough for most of the heat constants. The block like methane curve for simulation one is from a changing temperature value going in and out of the range for methane production. The colder climates produced less methane with this TC. Kansas and Moscow soil profile behavior results are in Appendix A, Figures 121-125 and 126-131 respectively. Figure 38 shows

the difference that a higher transfer coefficient can make. The 5.0 kcal/mol glucose heat constant now does not provide enough heat energy compared to the heat lost for the microorganisms to grow. All of the other heat constants produce normal methane curves.
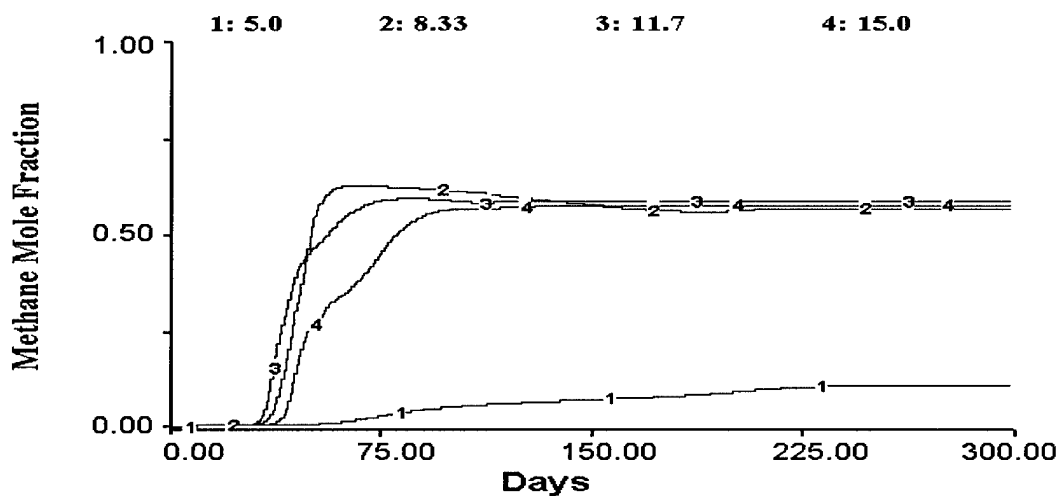
FIGURE 38. CAIRO SOIL PROFILE WITH A TC OF 0.1
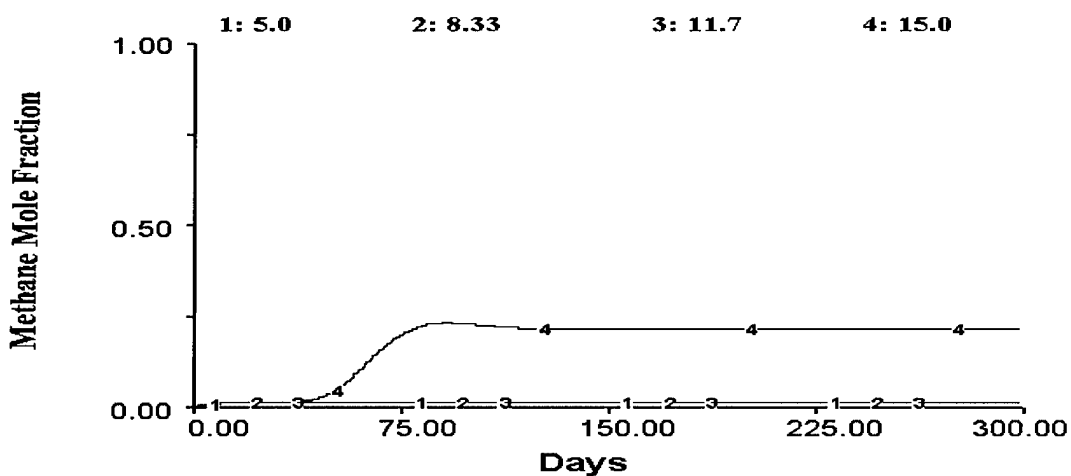
FIGURE 39. KANSAS SOIL PROFILE WITH A TC OF 0.1
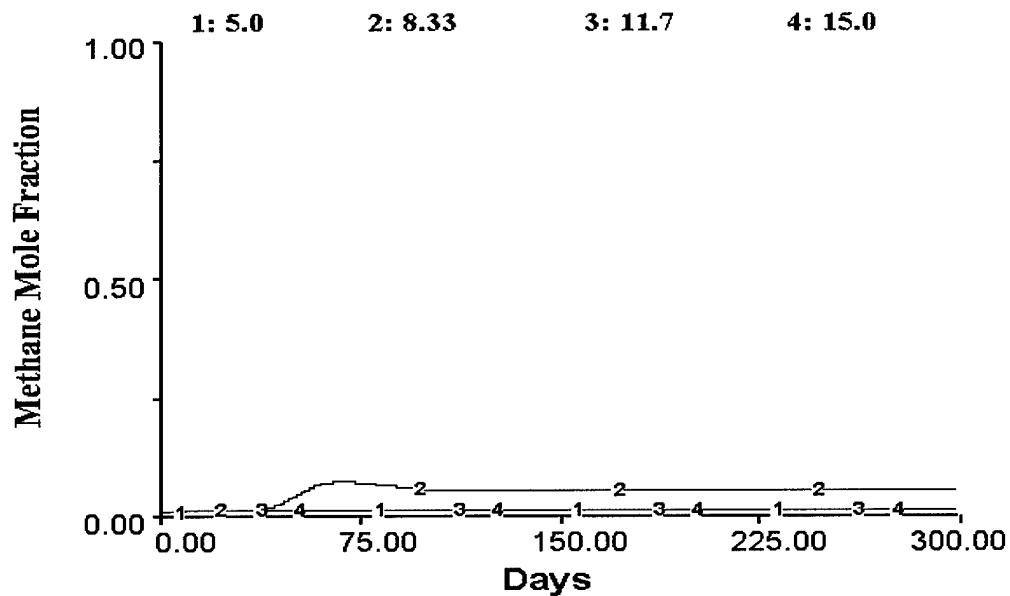
FIGURE 40 MOSCOW SOIL PROFILE WITH A TC OF 0.1

The methane graphs for the three climates show that climate does have a significant impact on the methane mole fraction for a TC of 0.1. Cairo, having the warmest soil temperature does not lose a lot of heat during the week to two weeks of aerobic degradation so the temperature is warm enough for acidogen microorganism to begin growing immediately at the onset of anaerobic degradation. All the heat constants show some level of methane production. The soil in Kansas during January is much cooler than Cairo, which causes larger temperature loss early in the degradation process. When the heat constant is activated at the beginning of anaerobic degradation the temperature rise is rapid allowing for limited acidogen microbial growth thus limiting that substance needed for methanogensis. Refer to Figures 132-136 for more parameters of Kansas and Figures 137-141 for more parameters of Moscow.

Seasonal Influences

Results show that climate can influence gas generation. Expanding this concept, seasonal temperature shifts were investigated to examine the effect of degradation of waste based on the month it is put into the landfill. The seasonal shift was accomplished starting the soil profile simulation with June's temperature instead of January's. Cairo was not changed due to its relative constant soil temperature throughout the year. Figures 41 and 42 show the methane production with the seasonal shift for Kansas and Moscow. Seasonal shifts of the parameters influencing this shift and other parameters affected by it refer to Figures 142-146 for Kansas and 152-157 for Moscow.
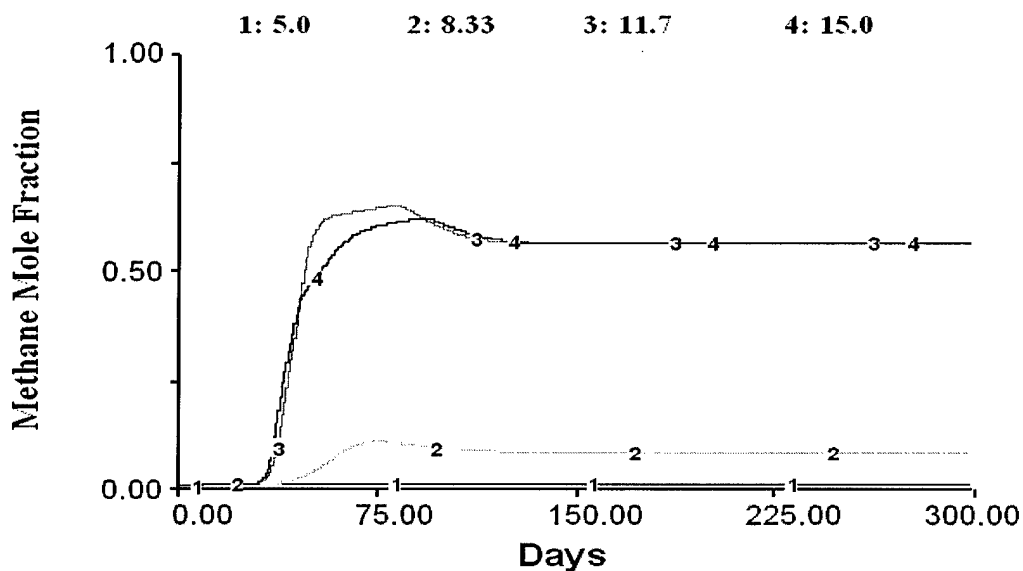
FIGURE 41. KANSAS SEASONAL SOIL PROFILE, TC 0.1

82
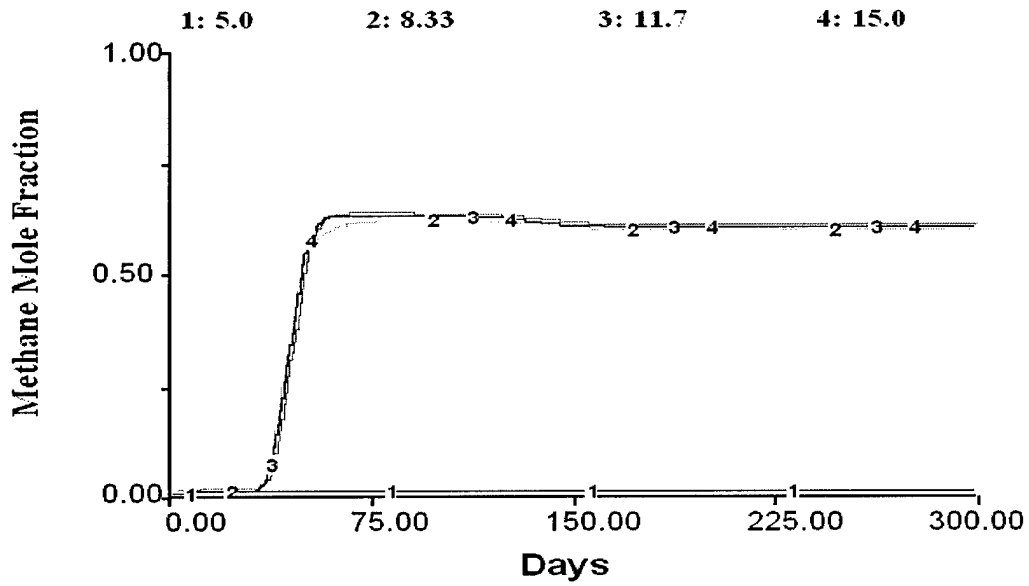
FIGURE 42. MOSCOW SEASONAL SOIL PROFILE, TC 0.1

These figures, when compared to Figures 39 and 40, show that landfilling waste in

June will produce more methane than waste landfilled in January for a TC of 0.1. This

seasonal change causes similar methane fraction levels to those seen for Cairo in Figure

38. The behavior for a lower TC showed similar results with a higher gas production if

biodegradation began in the summer months. Refer to Figures 147-151 and Figures 158-

163 to see results for Kansas and Moscow respectively, using a 0.01 TC.

V. Conclusions and Recommendation for Further Study

Microbial Activity

The individual structure verification and validation for the Arrhenius and Peleg equations ensured that proper growth and death rates were modeled for the acidogens and methanogens. A clear relationship between microbial behavior in a landfill and temperature has not been documented in the literature with reference to each population's growth curve. Literature information on the temperature progression from one population becoming dominant to another is not known. It is clear that the Arrhenius equation often used by other researchers to model microbial growth fails to represent adequate structure when there are unlimited substrate conditions. This leads to questions concerning the Arrhenius equation accuracy when substrate is limited and what other parameters might be affecting the microbial activity. The Peleg equation, utilizing system dynamics principles, allows exploration of microbial activity solely based on temperature through its parameter values. However, starting information on the suspected or hypothesized range for various microbial populations would be helpful in the future to build accuracy for representing behavior observed in a real landfill. This research has only looked at grouping the landfill microbial populations into two groups: acidogens (including fermenters and acetogens) and methanogens.

Temperature Generation

The most difficult concept to model was the temperature rise due to heat gain and its loss due to internal processes and diffusion out of the landfill. Information on free energy and heat constants gets confusing when trying to determine a temperature change. Free energy looks at total energy available through certain degradation steps but does not

84

inform one how much energy is available to increase the temperature of a system or how much is used for other processes, such as microbial growth. Heat constants allow for the calculation of the energy in the form of heat available to increase the temperature. Literature is available to describe the heat released from anaerobic reactions along certain pathways. This information was taken and modified to fit Shelley's model by assuming the same heat constant for all nine microbial processes breaking glucose down into simpler substances. This simplifying assumption allowed for more thorough sensitivity testing on a value that is not well defined in the literature. Results show that values for the heat constant found in literature can be modeled to produce documented behavior if a high transfer coefficient is used.

Transfer Coefficient

The transfer coefficient is a simple mechanism that allows for the calculation of diffusion of heat from the landfill. Incorporated into this number are several more complex relationships. Thermodynamic properties mentioned in the literature review were not applied in order to keep the number of unknown parameters and relationships low. There are both internal and external avenues for temperature to be dissipated. For example, the infiltration of rainwater can cause a temperature drop in the system due to the heat lost warming the water or a significant amount of heat could be lost in escaping gases. A simple transfer coefficient allows for an easier understanding of temperature losses in order to see how significant this parameter is on the system's behavior.

A conclusion from testing the transfer coefficient is that it represents the behavior for gas production adequately. A transfer coefficient of 0.1 allows the use of heat constants between 5-25 kcal/ mole glucose, which represent values found in the literature.

A transfer coefficient of one order of magnitude lower, 0.01, allows for a much smaller range of heat constants, 3-10 kcal/ mol glucose, that produce observed behavior. Information on the actual rate of heat loss will always be different between landfills due to landfill characteristics such as heat retention of the waste, effect of the liner on escaping gases as well as movement of heat to the surrounding soil, and the effects of seasonal temperature changes. The main issue from looking at the TCs and heat constants is what amount of energy given off by microbial activities, converting glucose to simpler substances, is actually available to effect the landfill temperature. If the reported literature values by El-Fadel are correct for the heat constants then a high TC is required to maintain a landfill temperature below 50°C. If the landfill is not losing enough heat then conditions will occur that will build up acetate and CO_2. However, if the landfill loses more heat than a TC of 0.1 then the landfill temperature will maintain a temperature of 20°C during anaerobic degradation. Control over the heat being lost from a landfill would increase waste degradation and allow production of desirable byproducts.

Initial Waste Temperature

This factor does not affect the landfill system if a large transfer coefficient is used, such as 0.1. However, an order of magnitude lower transfer coefficient can affect gas generation, based upon the initial waste temperature. This slower break down of glucose might be more realistic due to the amount of waste in a cell degrading at different rates. Different rates for solid waste degradation and glucose degradation occur due to warmer conditions occurring at the center of a landfill cell. The initial waste temperature is due largely to the ambient air temperature at each location and due to the time the

waste remains in a contact with the ambient air. This means that the local climate and season can affect the waste temperature.

Climate/Seasonal Influences

There were significant differences in gas generation between a warm climate compared to a cold climate when the soil temperature profile began in the winter months. The simulations looked at the changing soil temperature but did not take into account that the initial waste temperature would probably be lower during these months. Results still indicate that the warm climate has consistently better gas generation. This information can be expanded and used by landfill mangers by minimizing the time waste sits in trucks and recovery facilities and the time the trucks are on the road during colder months. When the soil profiles were changed so that waste degradation began during a summer month both the cold climates produced more methane, similar to the warmer climate.

Options to Landfill Managers

Keeping the waste at higher temperatures all year round similar to temperatures experienced in the summer, could increase the methane generation and reduce the time required for biodegradation. Besides following recommendations already mentioned, landfill mangers could implement indoor drive up holding facilities for trucks to park while waiting to unload. Engineering practices could be employed in cold climates to trap/reduce the amount of heat lost from a landfill through the design of a membrane liner that also acts as an thermal insulator or put heating rods that monitor landfill temperature and release heat if temperatures drop below minimum biodegradation levels. These devices could monitor the temperature rise during anaerobic degradation. If the

temperature rise is detrimental to methane generation, managers could have a heat sink or increase the recycling flow rate through the cell in order to reduce the heat in the system. A heat sink could be made by running leachate pipes or even water pipes through the landfill. When the heat generation rises to levels inhibiting degradation of waste the flow rate through the pipes could be increased, resulting in a heat loss from the landfill to the fluid in the pipes.

Review of Model Strengths

The addition of a temperature structure to Shelley's model will enable more accurate simulations with respect to microbial behavior. Shelley's model assumed a constant value over the degradation process for microbial growth and death parameters which does not allow behavior to observe the effects of one population affecting another or one population giving over to another based on the landfill temperature. The addition of the Peleg equation will allow easy changes to occur in the model when parameter values become more commonly accepted. The use of a simple transfer coefficient allows for observations in the system describing other uncertain parameters without compounding the uncertainty.

Review of Model Limitations

There is uncertainty in the amount of heat released and available to be transformed into a temperature increase from the degradation of glucose using the heat constant. This uncertainty of heat generation as well as the uncertainty in the amount of heat lost compounds the model's uncertainty. Behavior found in the literature is observed in this model using transfer coefficients; but how much accuracy would be added by including thermodynamic principles, and what would be the consequence as far

as increased complexity? Also, the complexity of the model increases when the temperature structure is included in Shelley's model, creating problems when trying to determine which factors are producing the observed behavior.

Suggestion for Further Study

The above weaknesses raise questions on what could be tested or added that would increase the validation and usefulness of the model. Investigation of energy released from the degradation of glucose or even of the energy released from the degradation of solid waste to glucose is needed. How much of the energy is used by the microbial populations for growth and maintenance? How much of the energy is lost to internal reactions or stored in gases produced? Is there a defined internal temperature diffusion from the center of the cell to the edges, and what waste factors can influence this transfer? Are the process and conditions of aerobic degradation significant to anaerobic process behavior? The transfer of heat across the interface between the landfill cell and soil depends on waste properties and soil properties such as porosity and density. Neither of these is fully understood.

APPENDIX A

ARRHENIUS EQUATION STRUCTURE TESTING   FIGURES 43- 46

1: H2 Mole Fraction   2: CO2 Mole Fract...   3: CH4 Mole Fract...   4: O2 Mole Fraction   5 N2 Mole Fraction
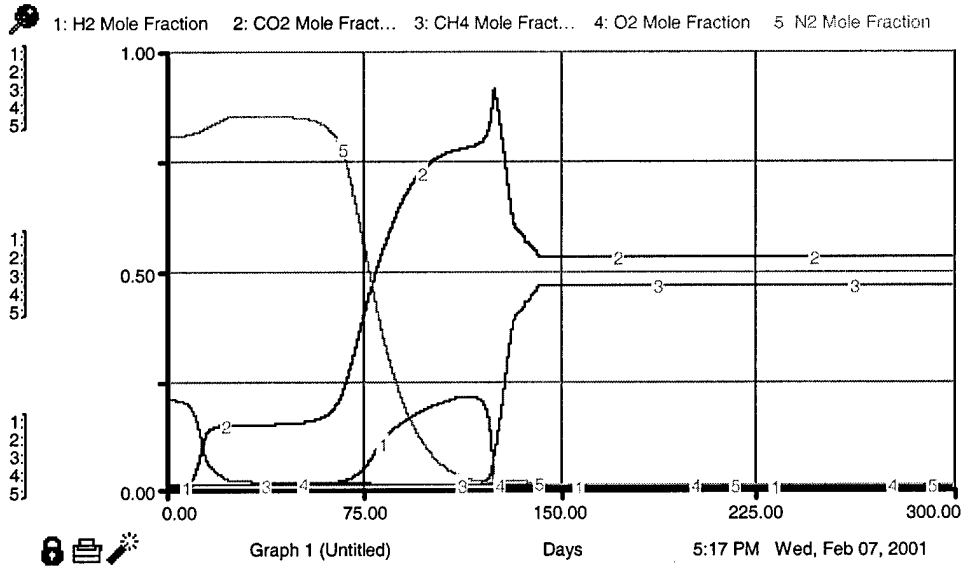
FIGURE 43. MOLE FRACTION OF GASES
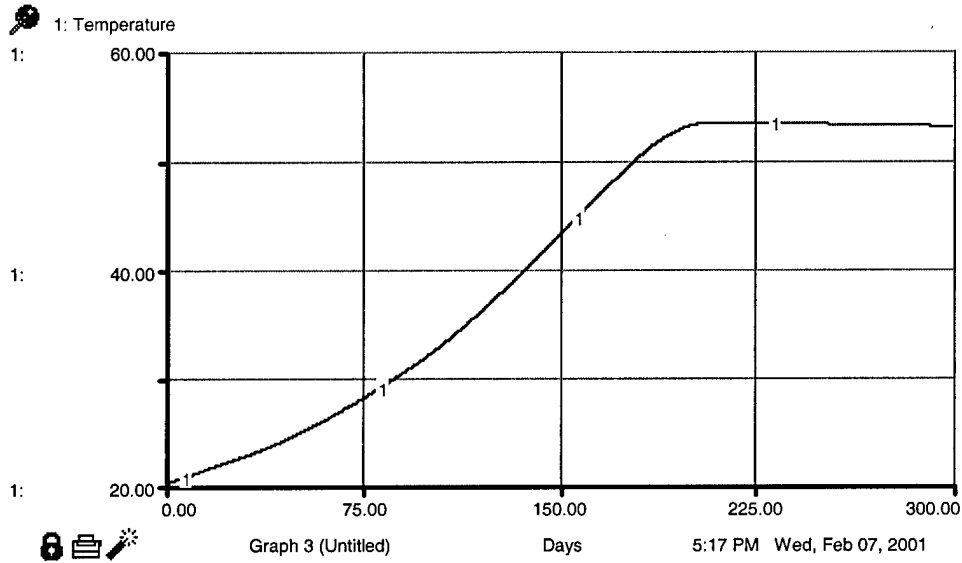
1: Temperature

FIGURE 44. TEMPERATURE
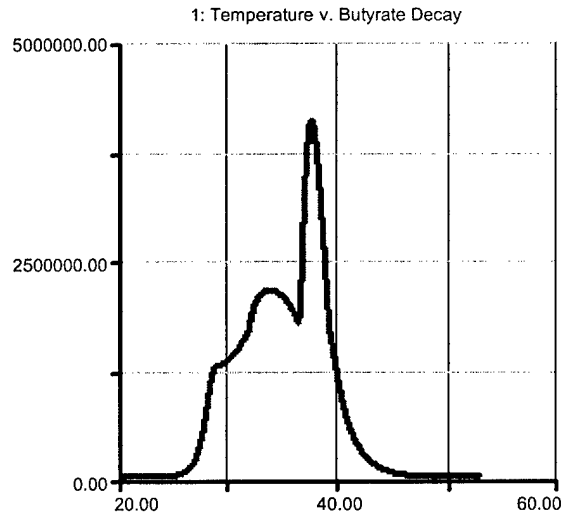
1: Temperature v. Butyrate Decay

FIGURE 45. BUTYRATE DECAY

1: Umax Acidogen   2: Umax Meth
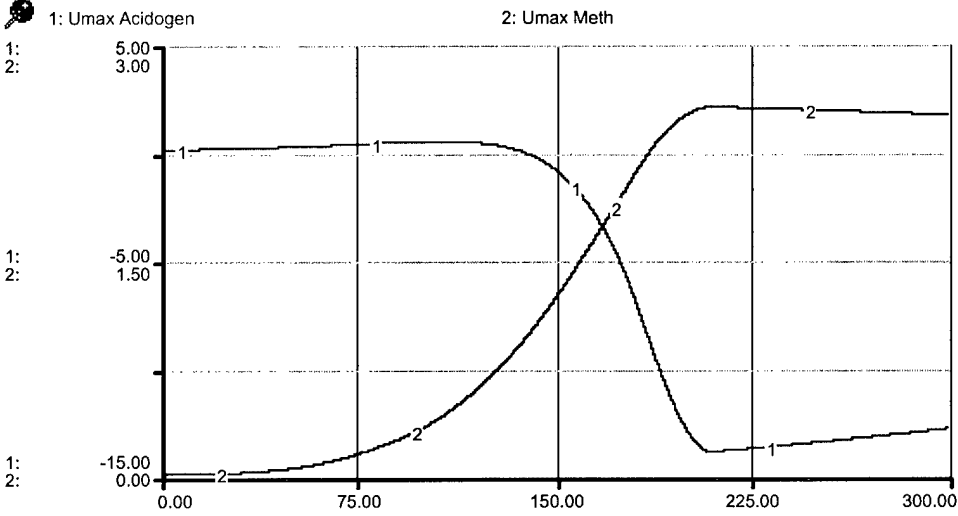
FIGURE 46. U$_{MAX}$ VALUES FOR ACIDOGENS AND METHANOGENS
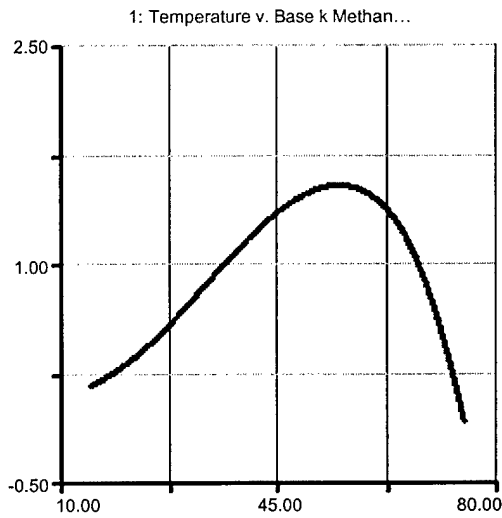
FIGURE 47. TEMPERATURE VS K_D METHANOGEN
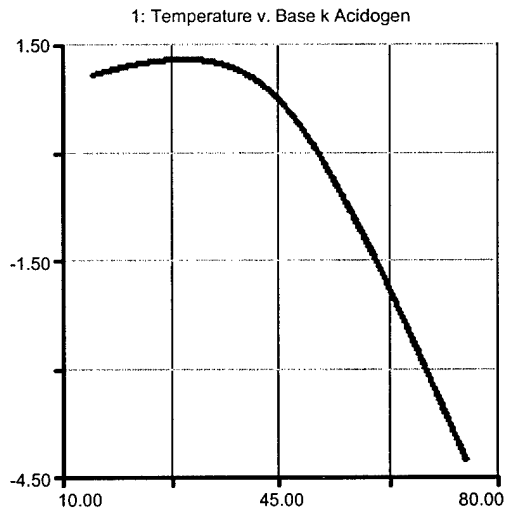
FIGURE 48. TEMPERATURE VS K_D ACIDOGEN
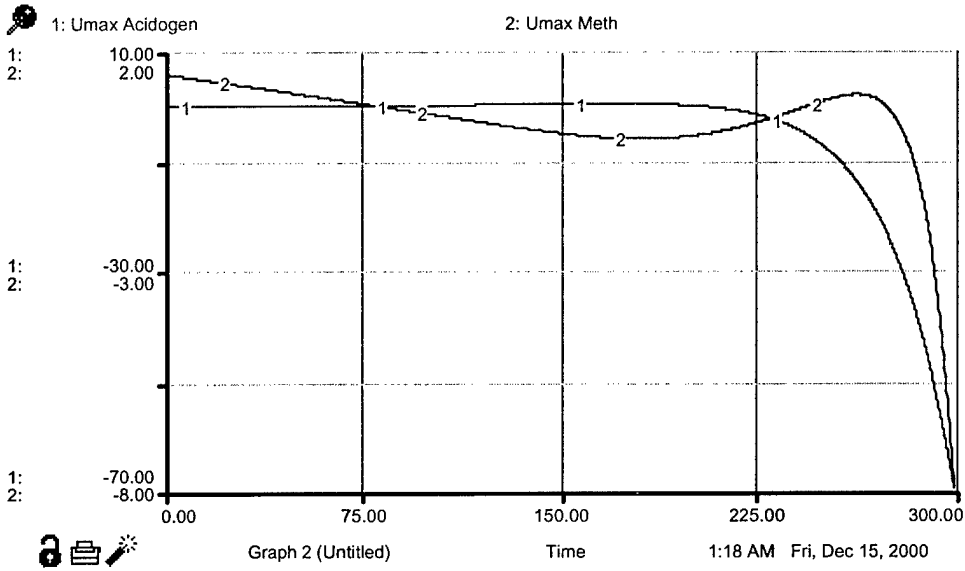
FIGURE 49. U_{MAX} ACIDOGEN AND U_{MAX} METHANOGEN OVER TIME
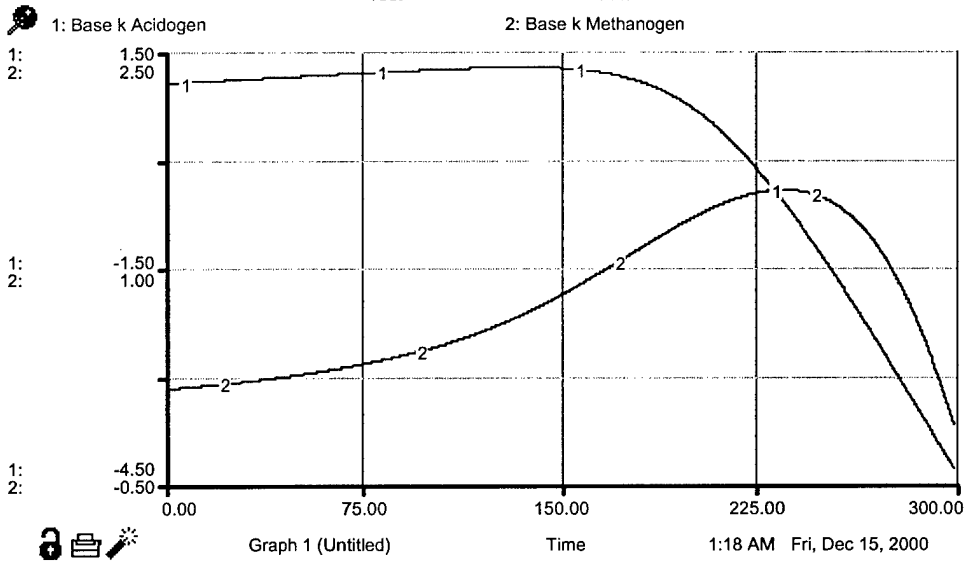
FIGURE 50. K_D ACIDOGEN AND K_D METHANOGEN OVER TIME
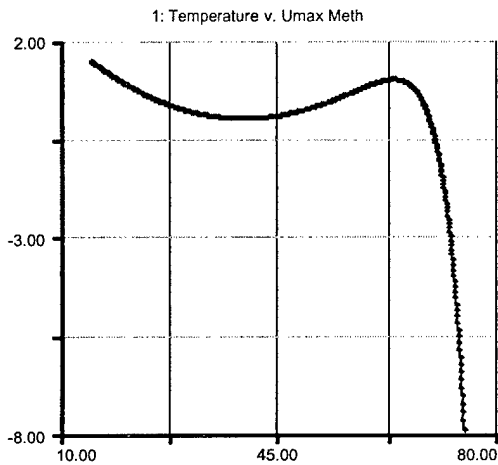
FIGURE 51. TEMPERATURE VS U_{MAX} METHANOGEN
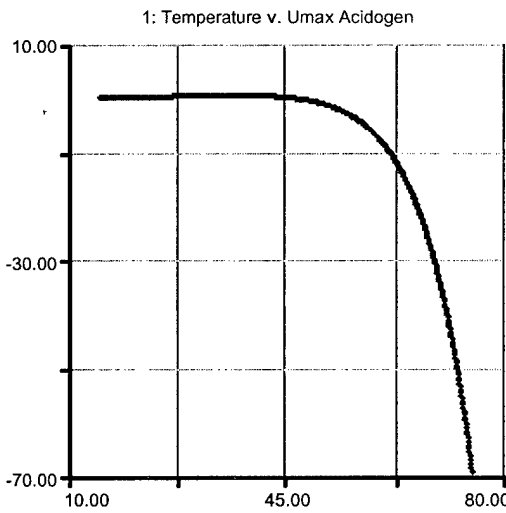
FIGURE 52. TEMPERATURE VS U_{MAX} ACIDOGEN

TRANSFER COEFFICIENT VERIFICATION FIGURE 53

TC: 1: 0.001   2: 0.000753   3: 0.00055   4: 0.000258   5: 0.00001

1: Temperature   2: Temperature   3: Temperature   4: Temperature   5: Temperature
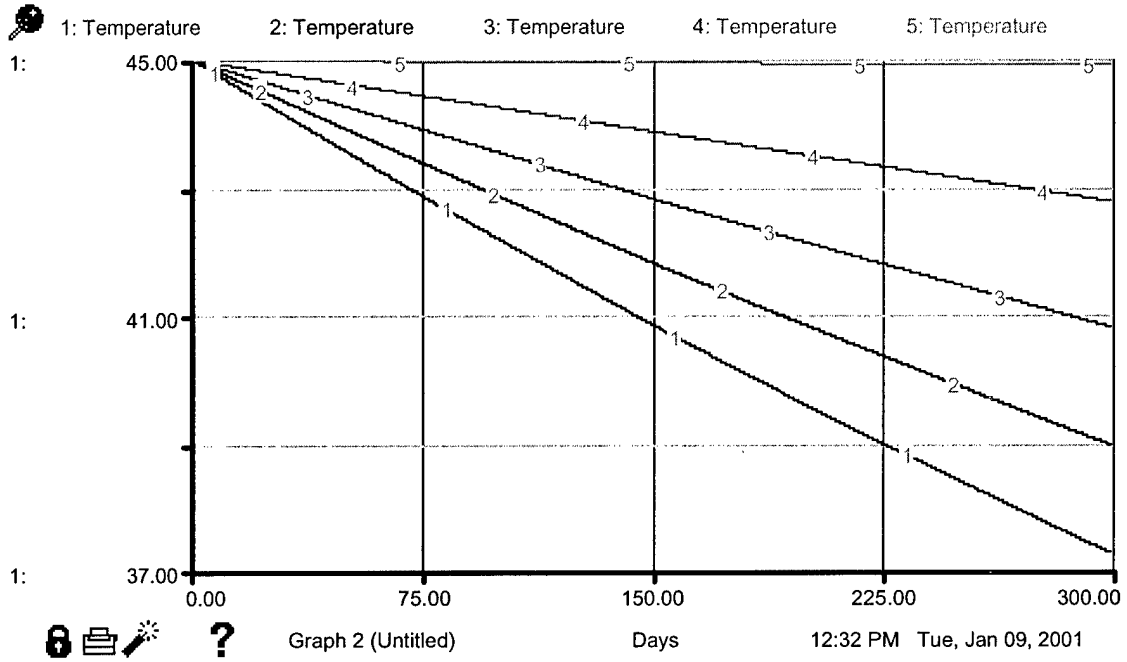
FIGURE 53. TRANSFER COEFFICIENT RANGE 0.001 – 0.00001
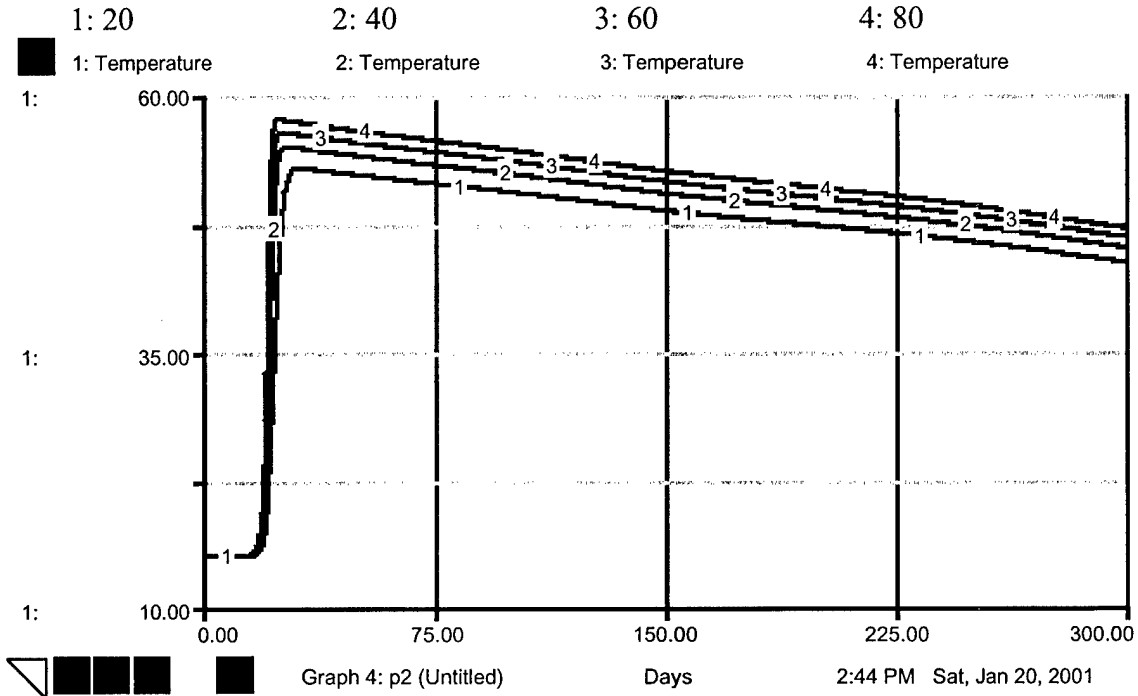
FIGURE 54. TEMPERATURE OVER TIME FOR HEAT CONSTANTS 20-80 KCAL/MOL GLUCOSE
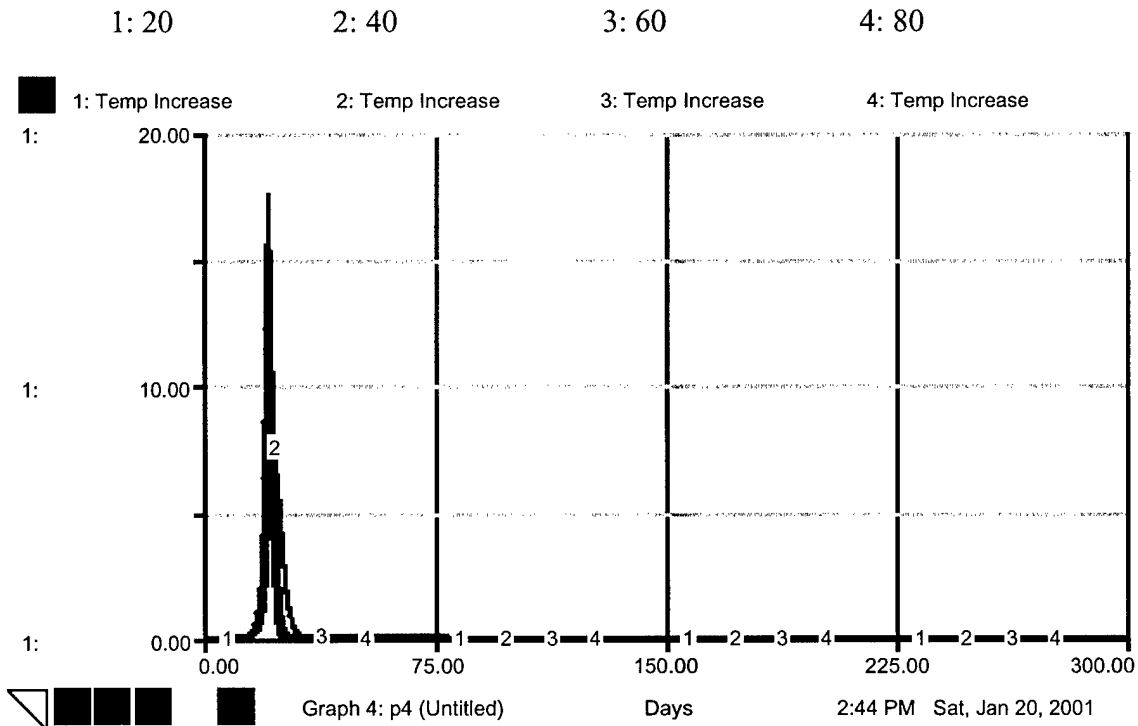
FIGURE 55. TEMPERATURE INCREASE OVER TIME FOR HEAT CONSTANTS 20-80

96

1: Total heat gain   2: Total heat gain   3: Total heat gain   4: Total heat gain

Graph 4: p5 (Untitled)   Days   2:44 PM   Sat, Jan 20, 2001
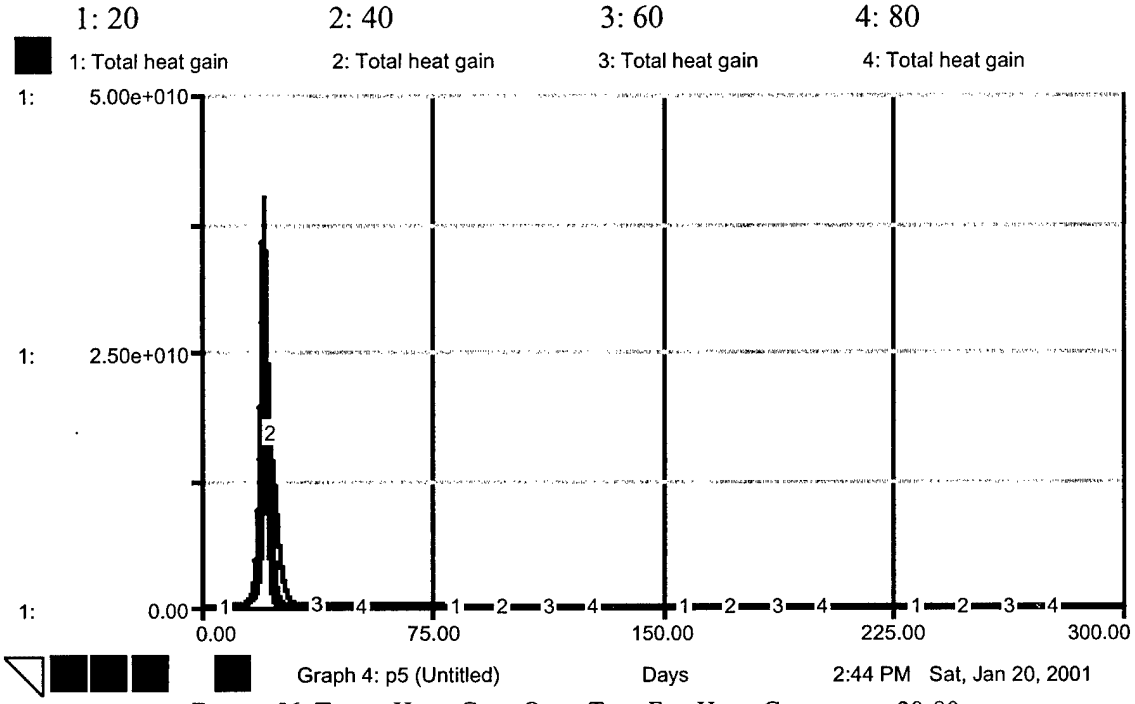
FIGURE 56. TOTAL HEAT GAIN OVER TIME FOR HEAT CONSTANTS 20-80

SPECIFIC HEAT CONSTANTS FIGURES 57-61

1: 0.3   2: 0.87   3: 1.43   4: 2.0

1: CO2 Mole Fraction   2: CO2 Mole Fraction   3: CO2 Mole Fraction   4: CO2 Mole Fraction

Specific Heat Constant: p2 (Unti...   Days   2:15 PM   Sat, Jan 20, 2001
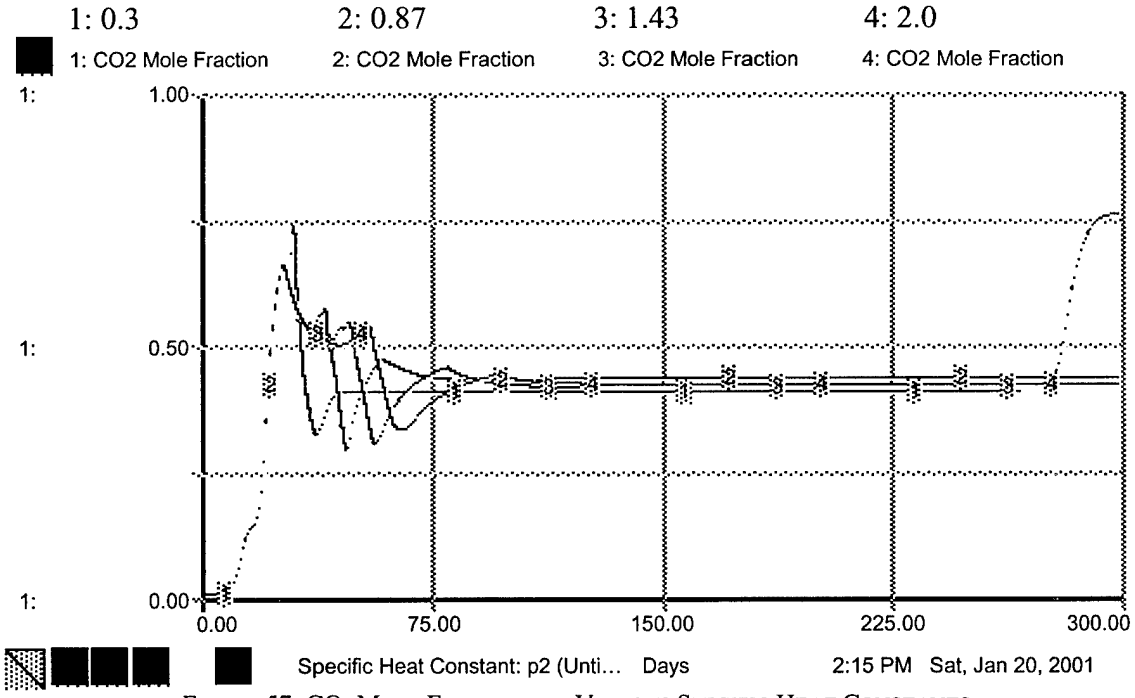
FIGURE 57. CO_2 MOLE FRACTION AT VARIOUS SPECIFIC HEAT CONSTANTS

97

1: 0.3	2: 0.87	3: 1.43	4: 2.0
1: H2 Mole Fraction	2: H2 Mole Fraction	3: H2 Mole Fraction	4: H2 Mole Fraction

Specific Heat Constant: p3 (Unti...   Days   2:15 PM   Sat, Jan 20, 2001
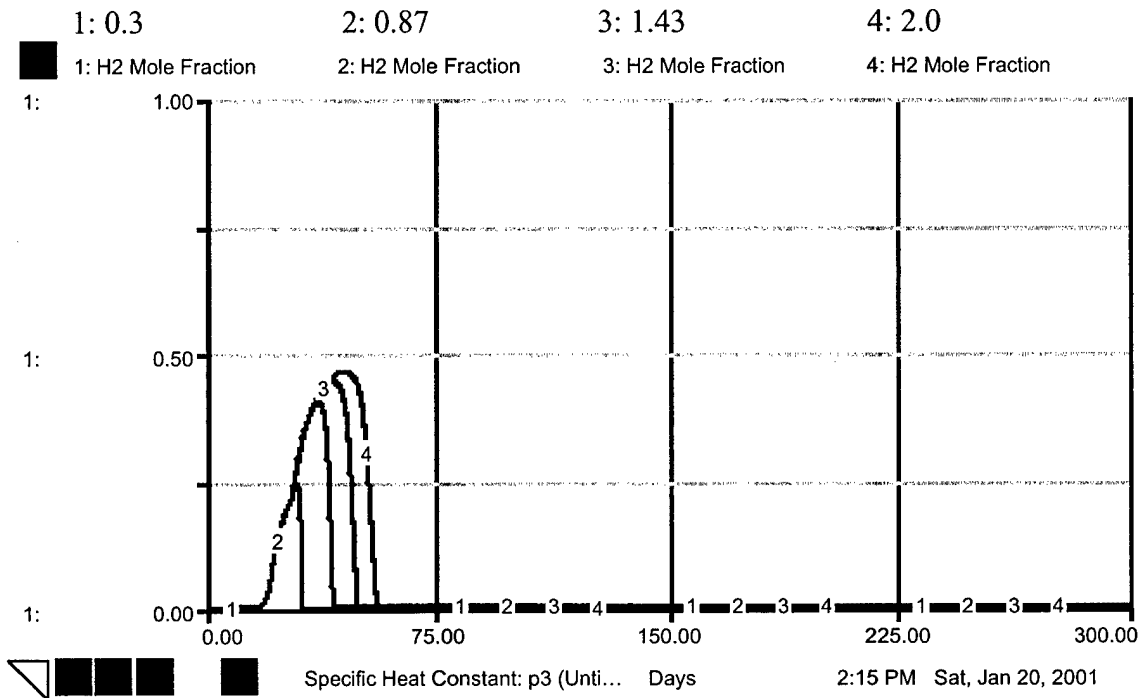
FIGURE 58. H_2 MOLE FRACTION AT VARIOUS SPECIFIC HEAT VALUES

1: 0.3	2: 0.87	3: 1.43	4: 2.0
1: Umax k Acido	2: Umax k Acido	3: Umax k Acido	4: Umax k Acido

Specific Heat Constant: p6 (Unti...   Days   2:15 PM   Sat, Jan 20, 2001
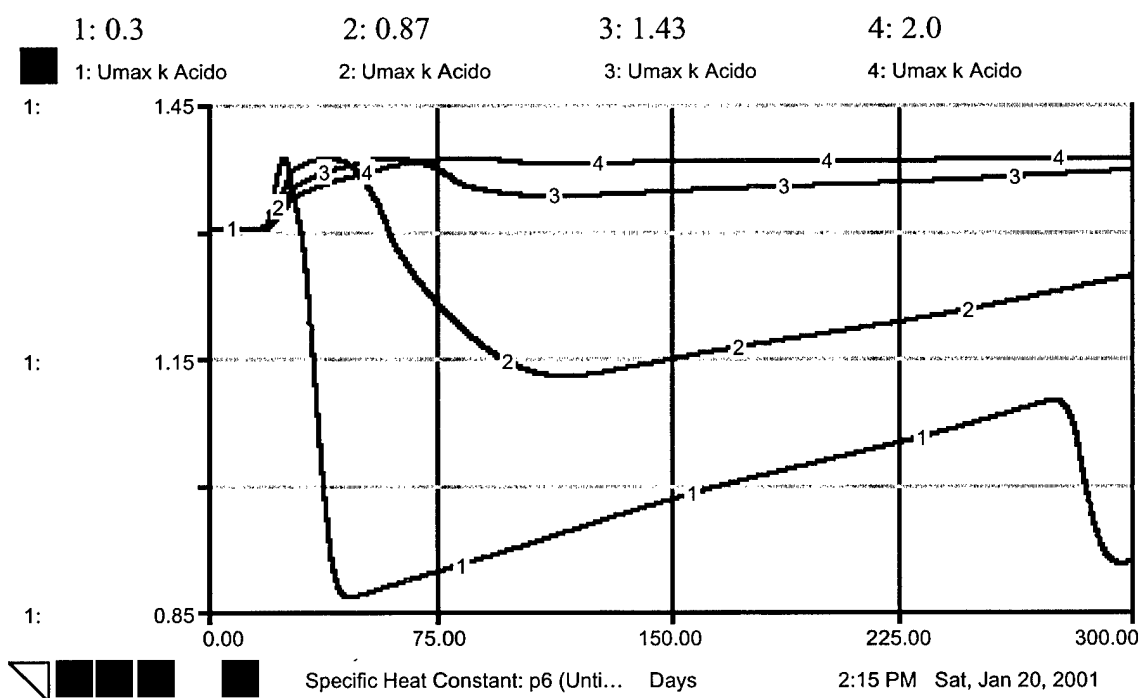
FIGURE 59. U_{MAX} ACIDOGEN AT VARIOUS SPECIFIC HEAT VALUES

98

1: 0.3   2: 0.87   3: 1.43   4: 2.0

■ 1: Umax k Meth   2: Umax k Meth   3: Umax k Meth   4: Umax k Meth

Specific Heat Constant: p7 (Unti...   Days   2:15 PM   Sat, Jan 20, 2001
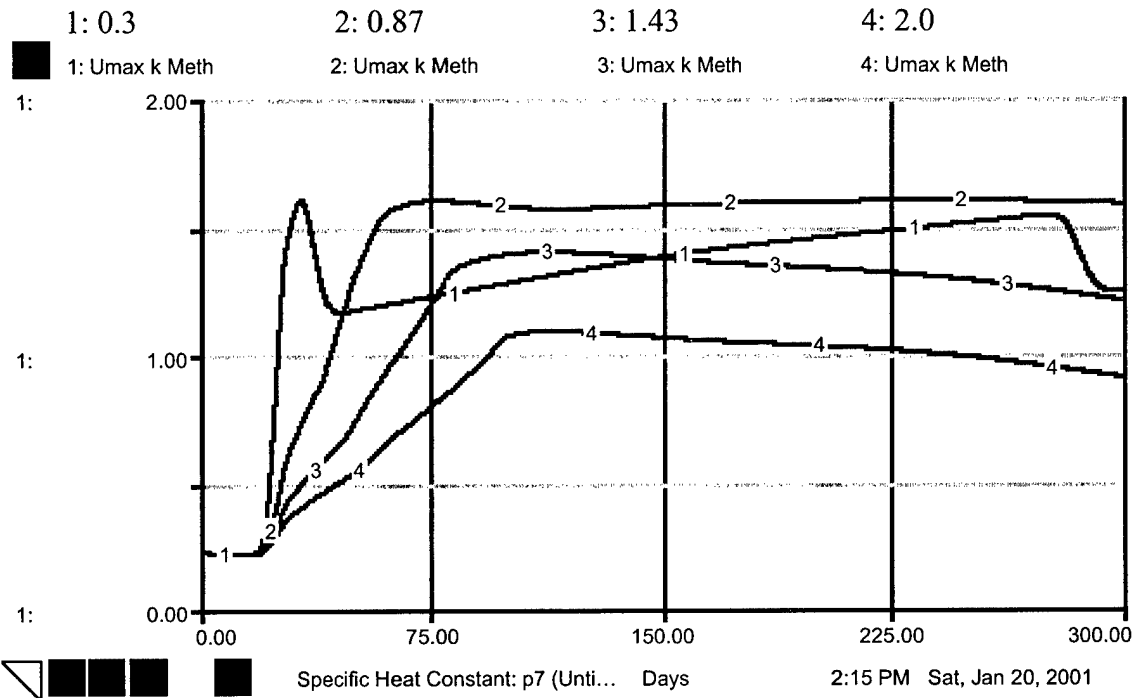
FIGURE 60. U_{MAX} METHANOGEN AT VARIOUS SPECIFIC HEAT VALUES

1: 0.3   2: 0.87   3: 1.43   4: 2.0

■ 1: Glucose   2: Glucose   3: Glucose   4: Glucose

Specific Heat Constant: p8 (Unti...   Days   2:15 PM   Sat, Jan 20, 2001
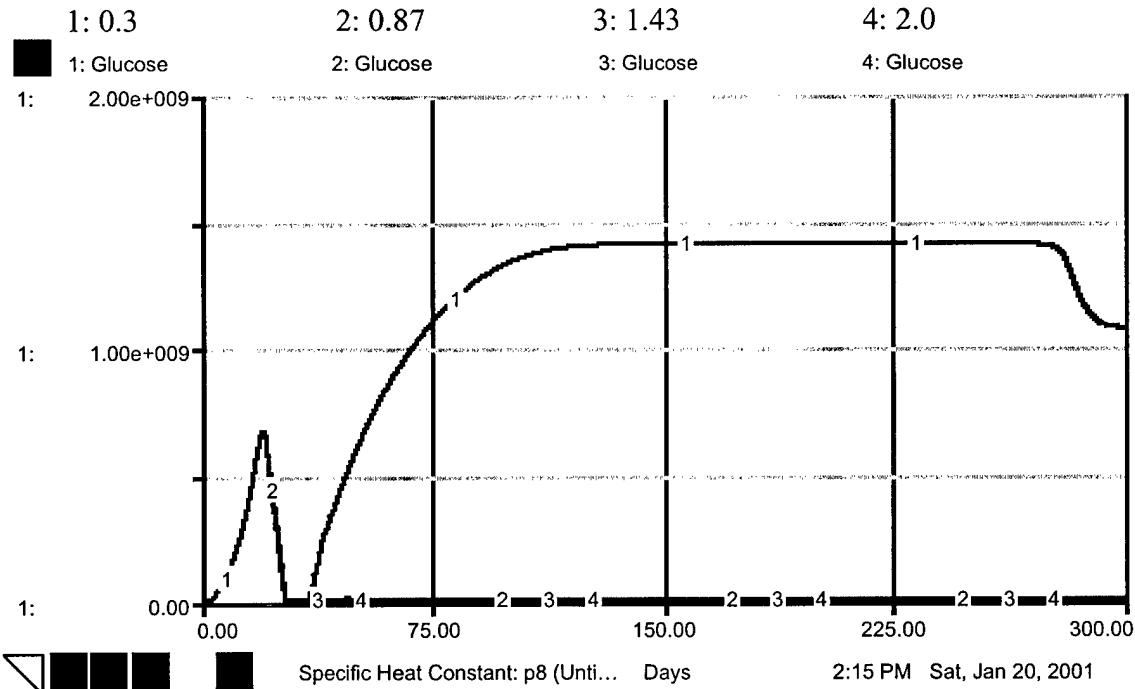
FIGURE 61. GLUCOSE LEVELS AT VARIOUS SPECIFIC HEAT VALUES

99

1: 15   2: 20   3: 25   4: 30

■ 1: CO2 Mole Fraction   2: CO2 Mole Fraction   3: CO2 Mole Fraction   4: CO2 Mole Fraction

TC1intemp25HC1530: p4 (Untitled) Days   3:03 PM Tue, Jan 30, 2001

FIGURE 62. CO_2 MOLE FRACTION AT VARIOUS HEAT CONSTANTS

1: 15   2: 20   3: 25   4: 30

■ 1: Temperature   2: Temperature   3: Temperature   4: Temperature

TC1intemp25HC1530: p2 (Untitled) Days   3:03 PM Tue, Jan 30, 2001

FIGURE 63. TEMPERATURE AT VARIOUS HEAT CONSTANTS

100
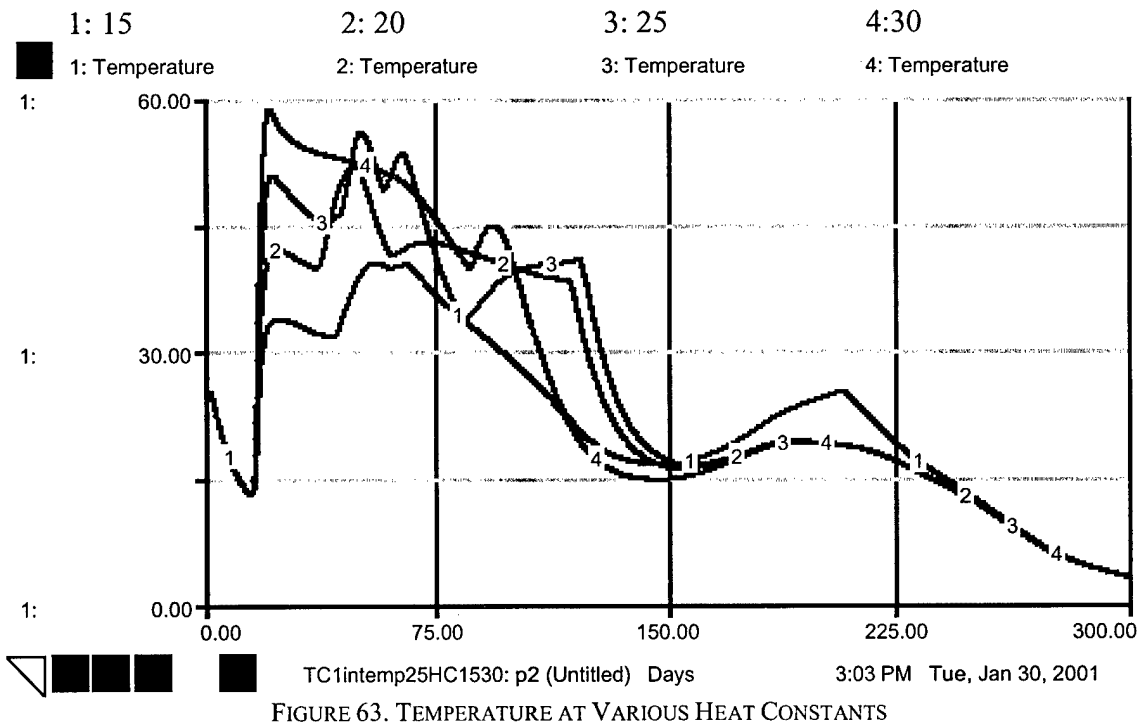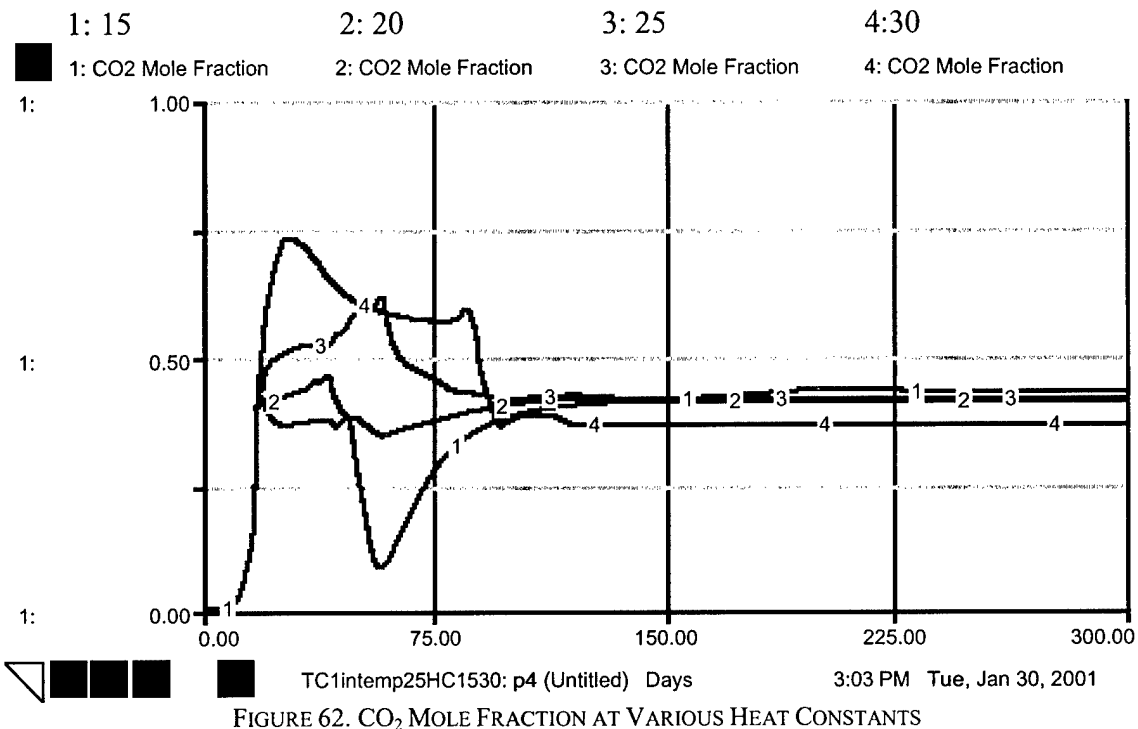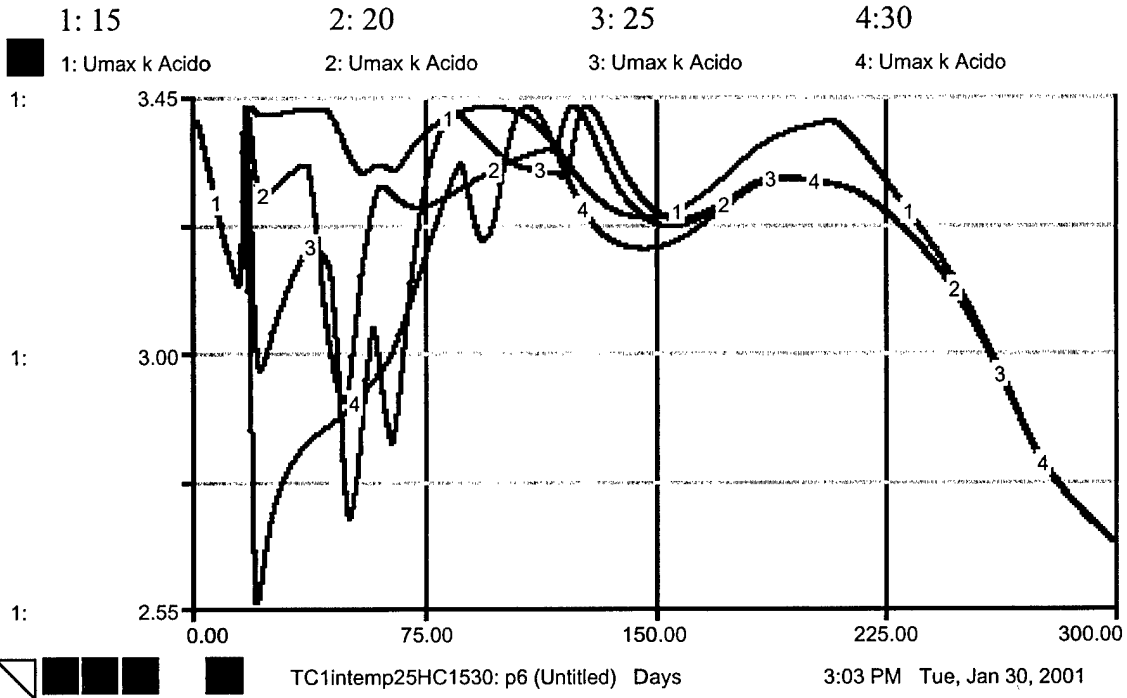
FIGURE 64. U$_{MAX}$ ACIDOGEN AT VARIOUS HEAT CONSTANTS
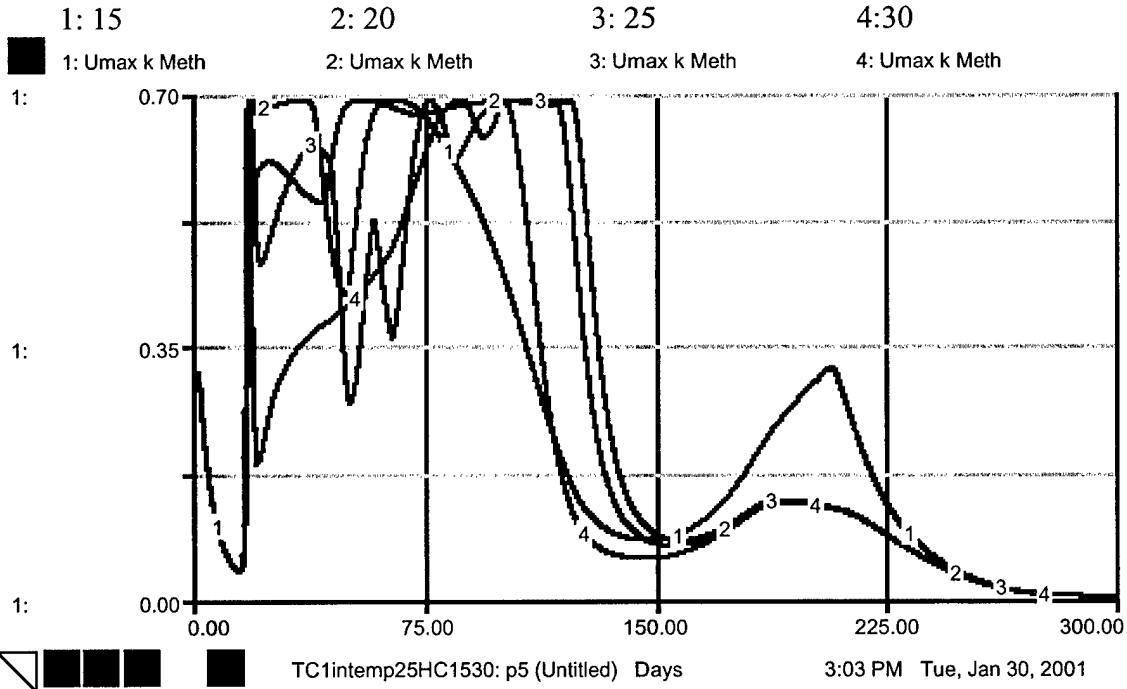
FIGURE 65. U$_{MAX}$ METHANOGEN AT VARIOUS HEAT CONSTANTS
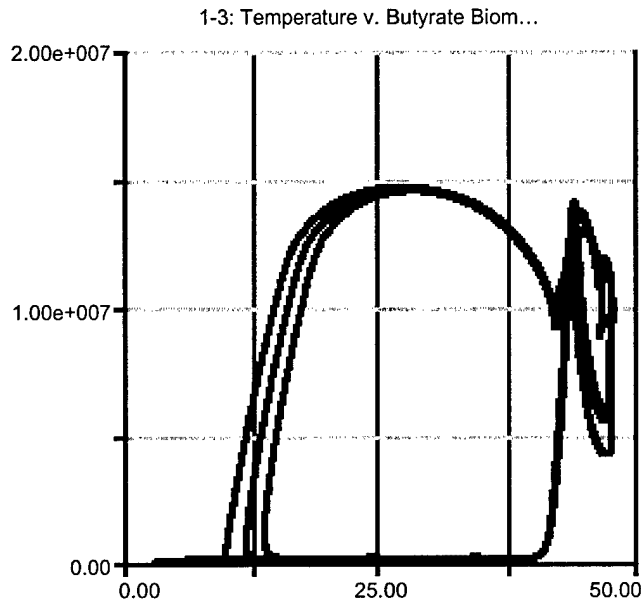
101

FIGURE 66. BUTYRATE BIOMASS WITH VARIOUS INITIAL WASTE TEMPERATURES
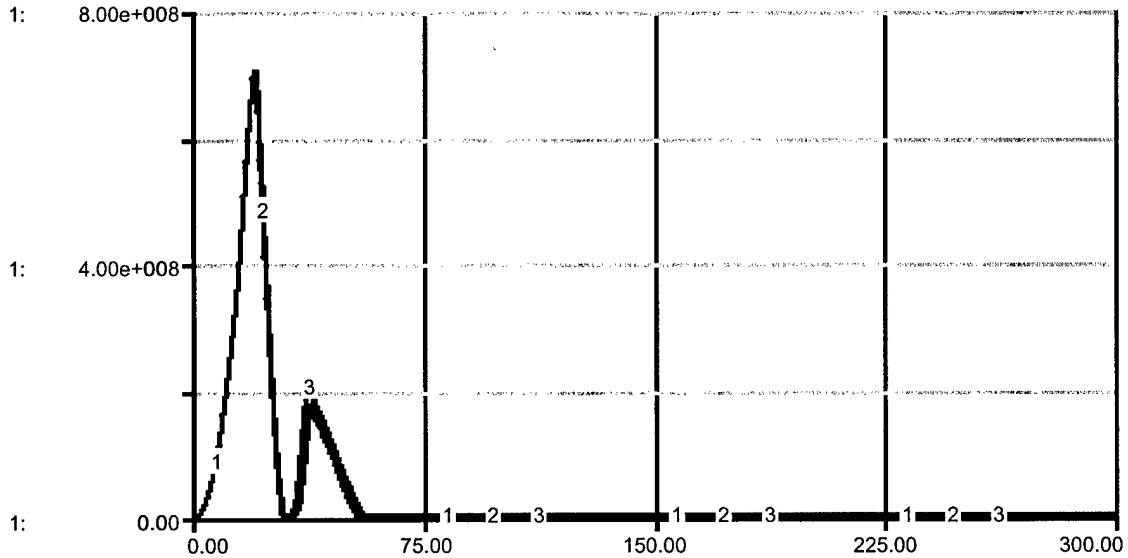
FIGURE 67. GLUCOSE LEVEL WITH VARIOUS INITIAL WASTE TEMPERATURES

1: 15   2: 25   3: 35

■ 1: CH4 Mole Fraction   2: CH4 Mole Fraction   3: CH4 Mole Fraction

1:     1.00

1:     0.50

1:     0.00

0.00   75.00   150.00   225.00   300.00

TC1intemp1535: p5 (Untitled)   Days   12:55 PM   Tue, Jan 30, 2001
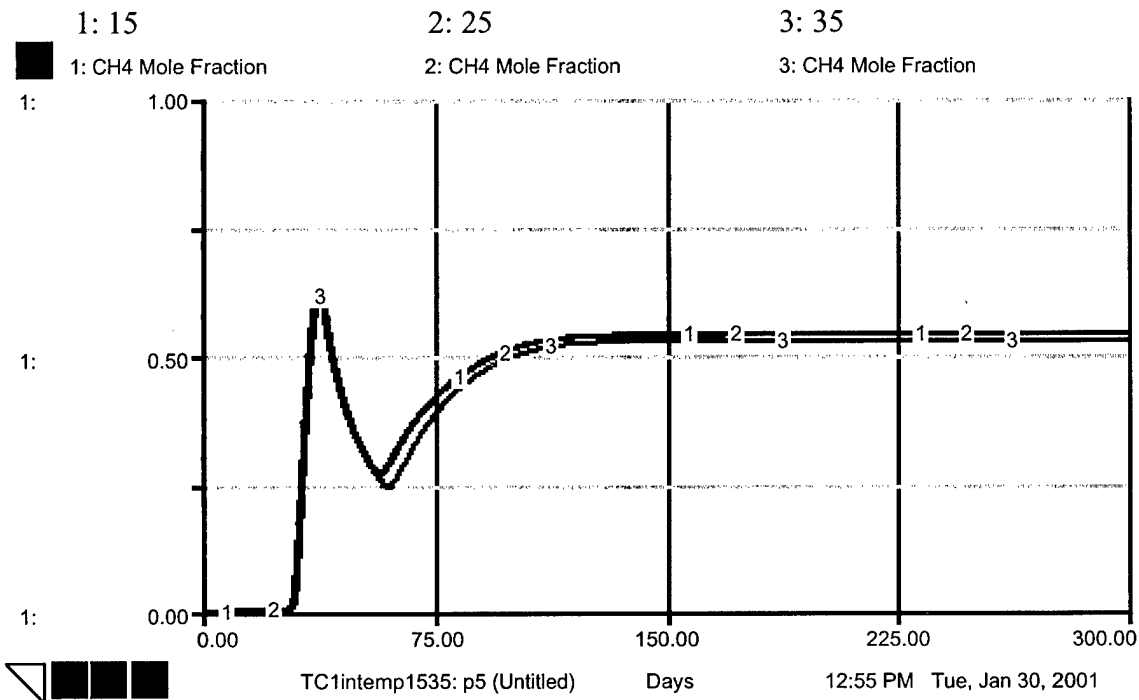
FIGURE 68. CH_4 MOLE FRACTION WITH VARIOUS INITIAL WASTE TEMPERATURES

1: 15   2: 25   3: 35

■ 1: CO2 Mole Fraction   2: CO2 Mole Fraction   3: CO2 Mole Fraction

1:     1.00

1:     0.50

1:     0.00

0.00   75.00   150.00   225.00   300.00

TC1intemp1535: p6 (Untitled)   Days   12:55 PM   Tue, Jan 30, 2001
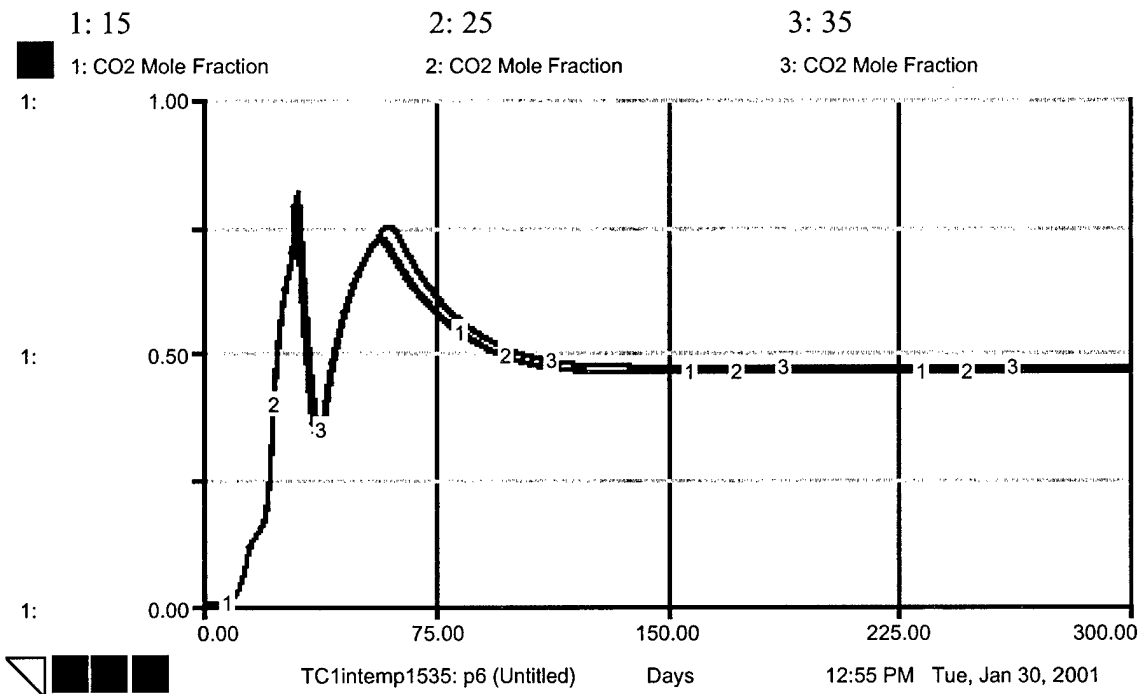
FIGURE 69. CO_2 MOLE FRACTION WITH VARIOUS INITIAL WASTE TEMPERATURES
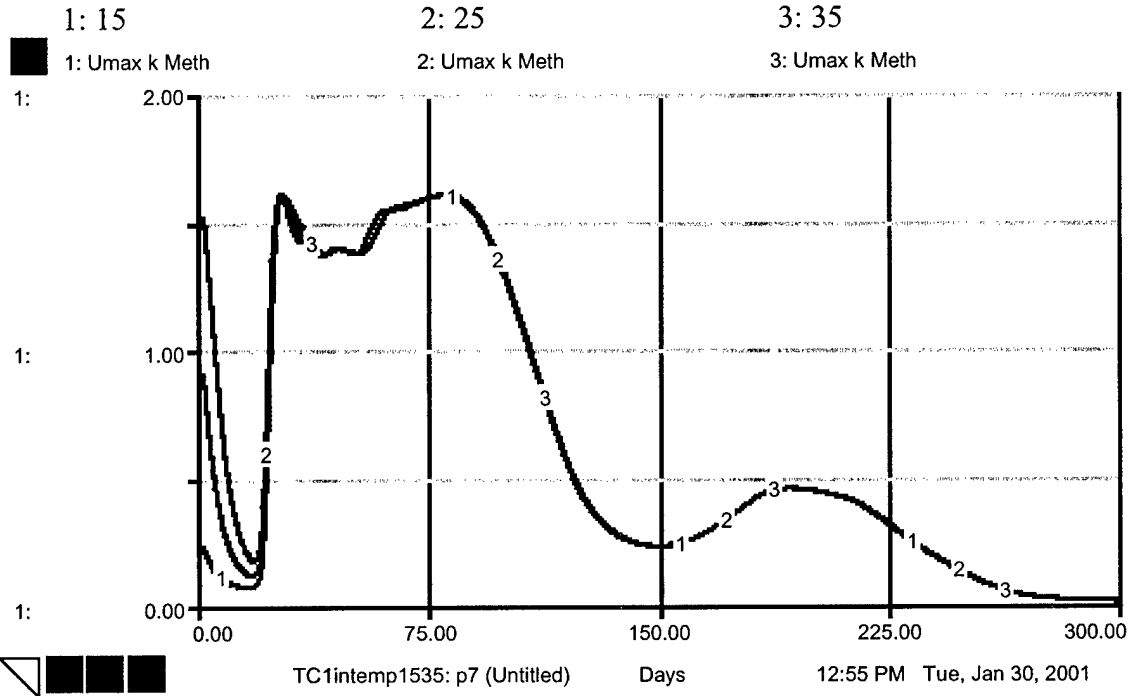
FIGURE 70. U_{MAX} METHANOGEN WITH VARIOUS INITIAL WASTE TEMPERATURES
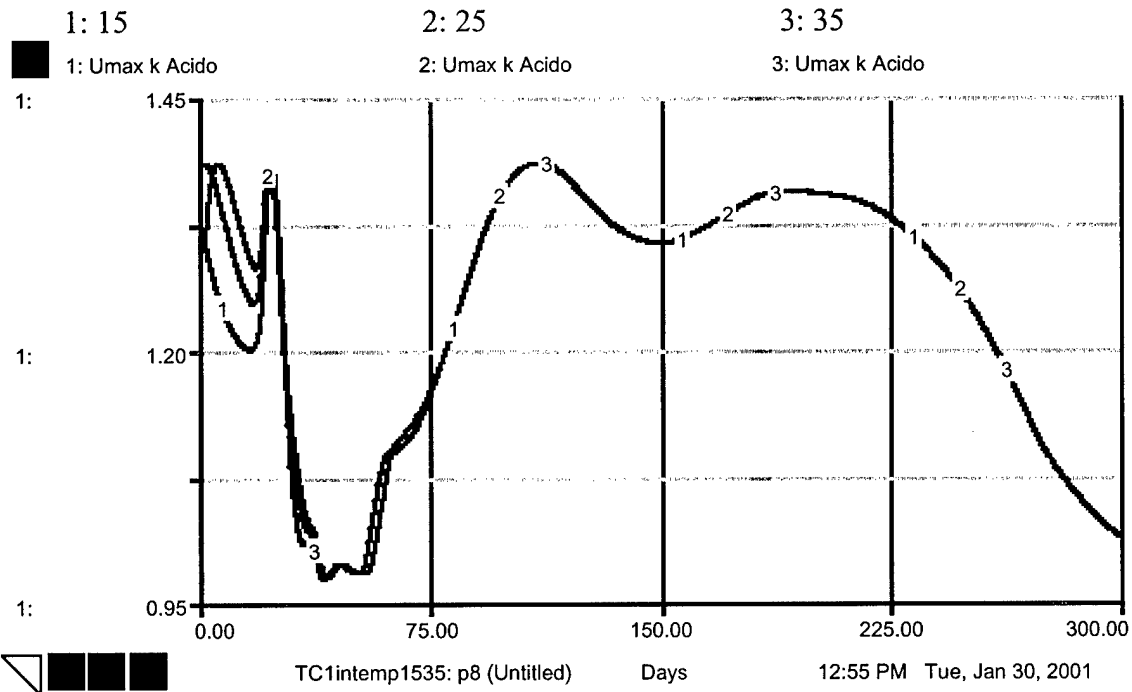
FIGURE 71. U_{MAX} ACIDOGEN WITH VARIOUS INITIAL WASTE TEMPERATURES

1: 10   2: 16.7   3: 23.3   4: 30

■ 1: CH4 Mole Fraction   2: CH4 Mole Fraction   3: CH4 Mole Fraction   4: CH4 Mole Fraction

Tc01HC10tempchanges: p4 (Unti... Days   10:26 AM   Fri, Feb 02, 2001
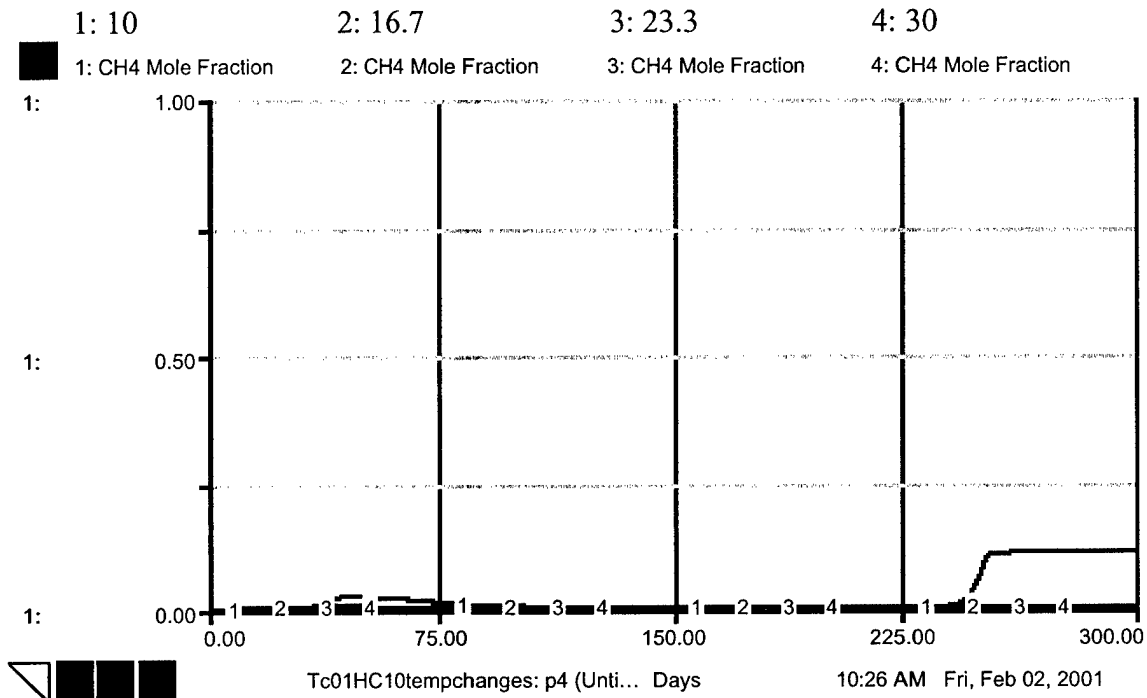
FIGURE 72. CH_4 MOLE FRACTION WITH VARIOUS INITIAL WASTE TEMPERATURES

1: 10   2: 16.7   3:23.3   4: 30

■ 1: CO2 Mole Fraction   2: CO2 Mole Fraction   3: CO2 Mole Fraction   4: CO2 Mole Fraction

Tc01HC10tempchanges: p3 (Unti... Days   10:26 AM   Fri, Feb 02, 2001
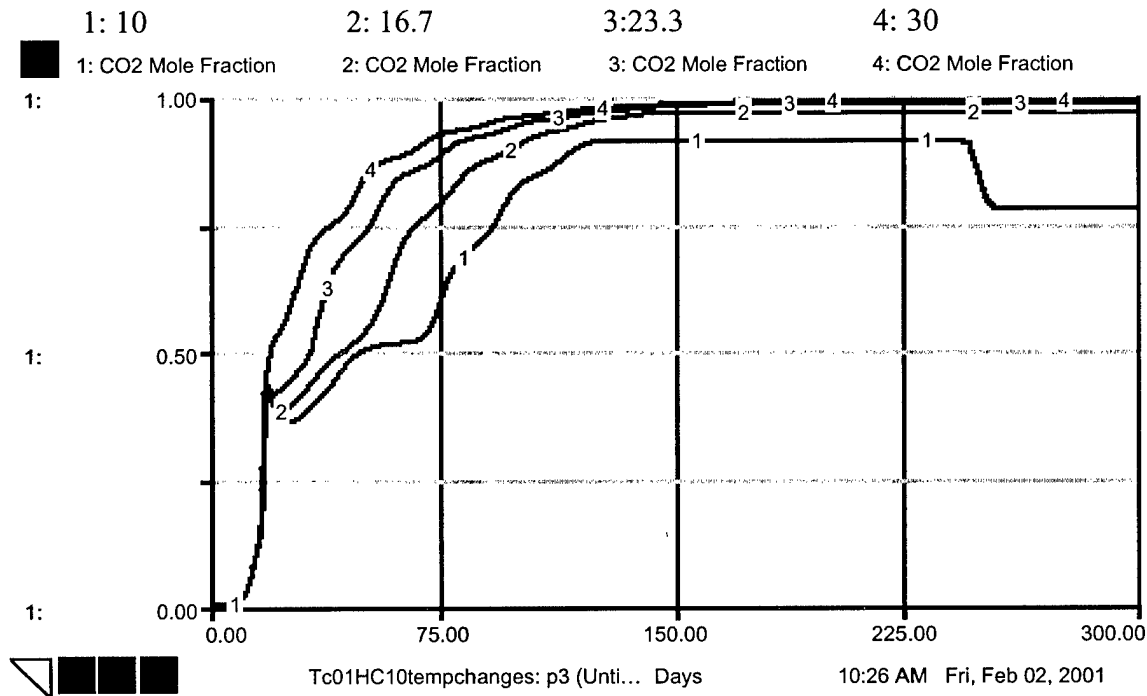
FIGURE 73. CO_2 MOLE FRACTION WITH VARIOUS INITIAL WASTE TEMPERATURES

105
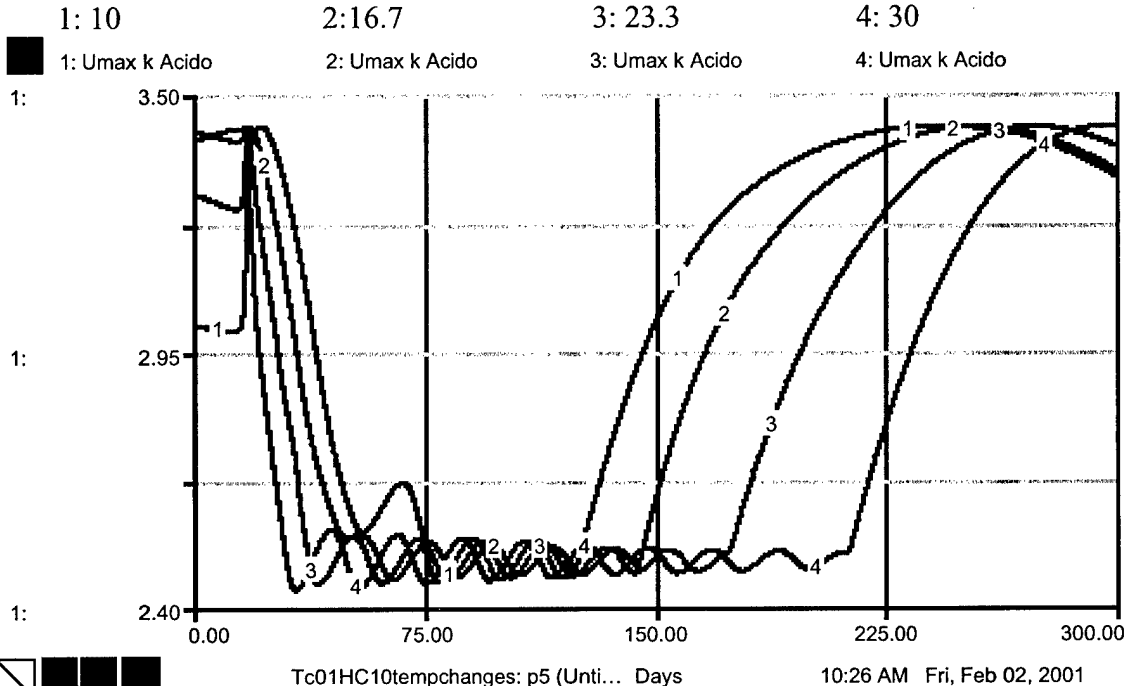
FIGURE 74. U$_{MAX}$ ACIDOGEN WITH VARIOUS INITIAL WASTE TEMPERATURES
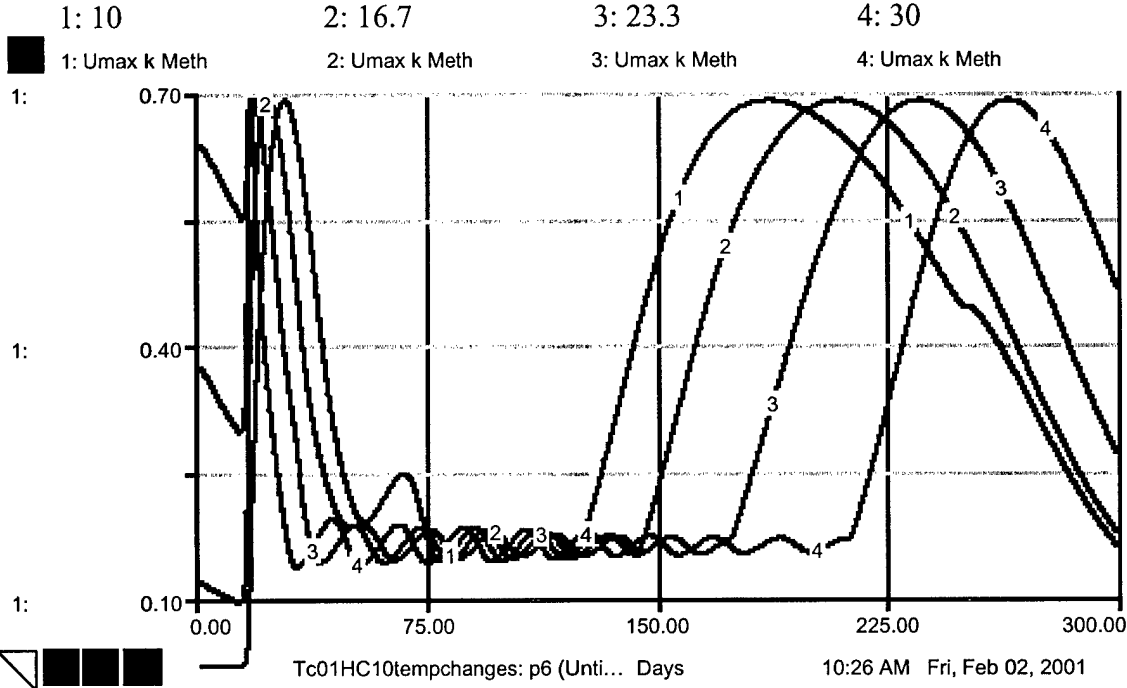
FIGURE 75. U$_{MAX}$ METHANOGEN WITH VARIOUS INITIAL WASTE TEMPERATURES

106

ACIDOGEN HEIGHT: TC 0.001, HC 2.0 KCAL/MOL GLUCOSE, INITIAL WASTE TEMPERATURE 25
FIGURES 76-80
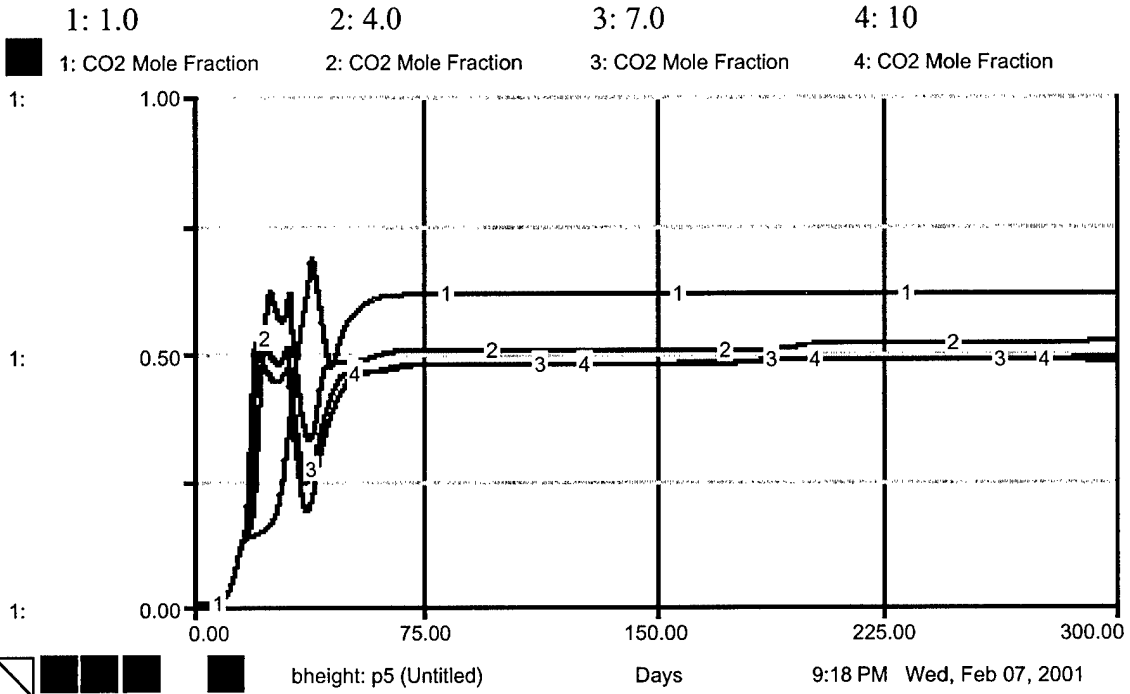
FIGURE 76. CO_2 MOLE FRACTION WITH VARIOUS HEIGHT VALUES
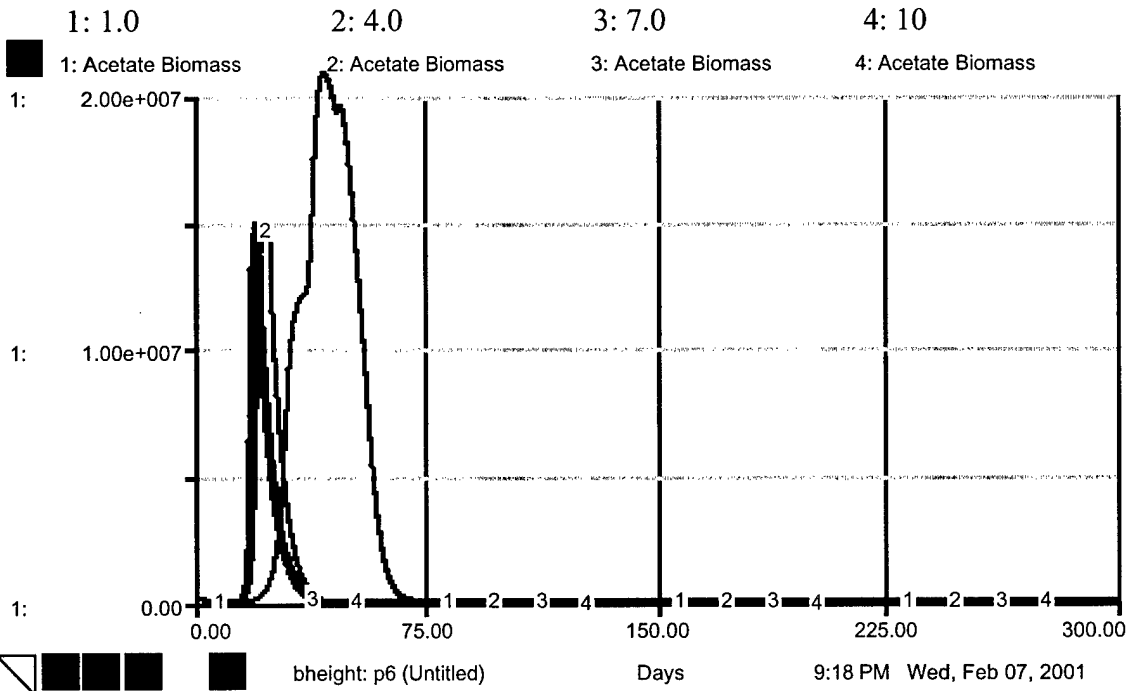
FIGURE 77. ACETATE BIOMASS WITH VARIOUS HEIGHT VALUES
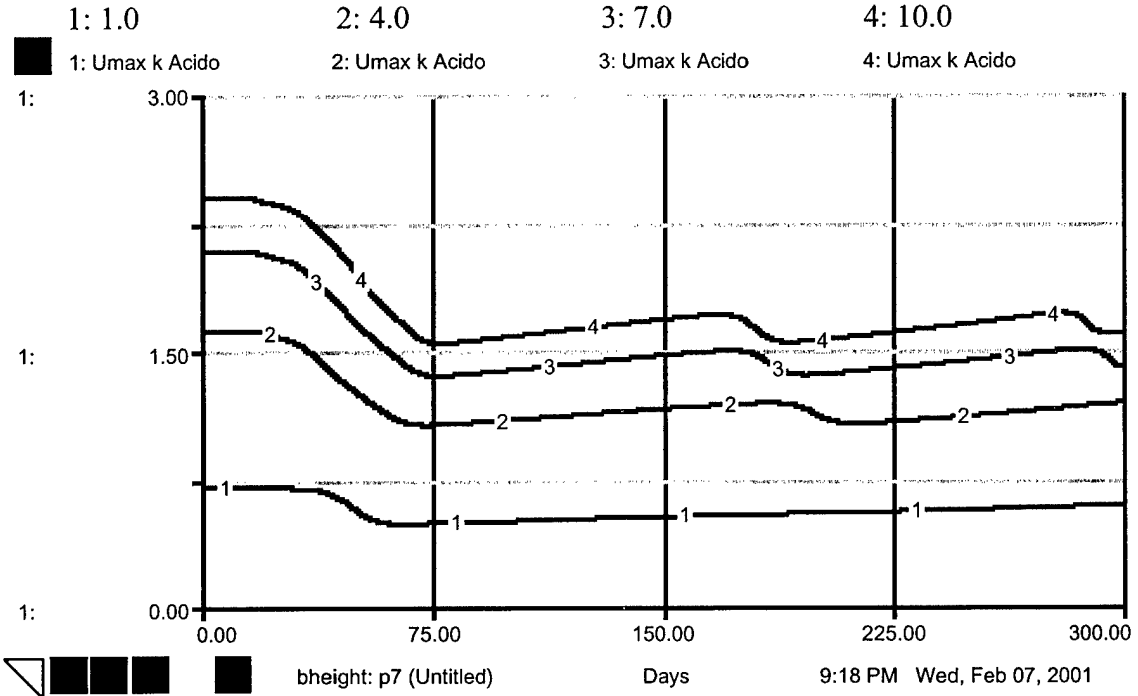
FIGURE 78. UMAX ACIDOGEN WITH VARIOUS HEIGHT VALUES
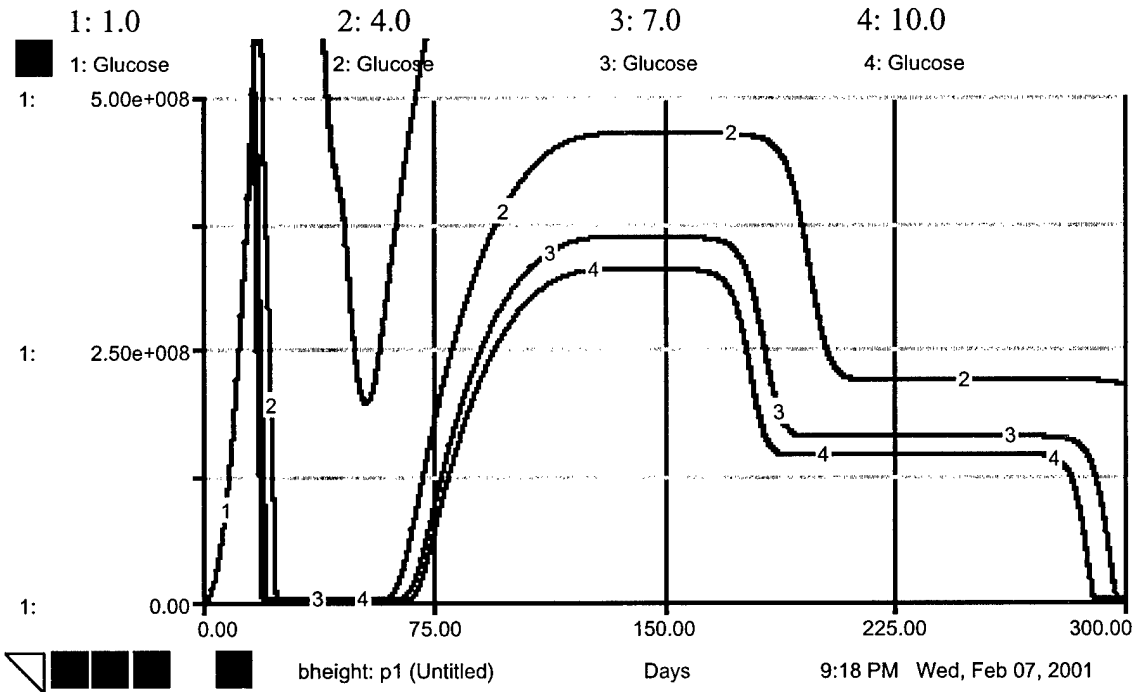
FIGURE 79. GLUCOSE LEVEL WITH VARIOUS HEIGHT VALUES

108

1: 1.0	2: 4.0	3: 7.0	4: 10.0
■ 1: Temp Increase	2: Temp Increase	3: Temp Increase	4: Temp Increase

bheight: p2 (Untitled)   Days   9:18 PM   Wed, Feb 07, 2001

FIGURE 80. TEMPERATURE INCREASE WITH VARIOUS HEIGHT VALUES
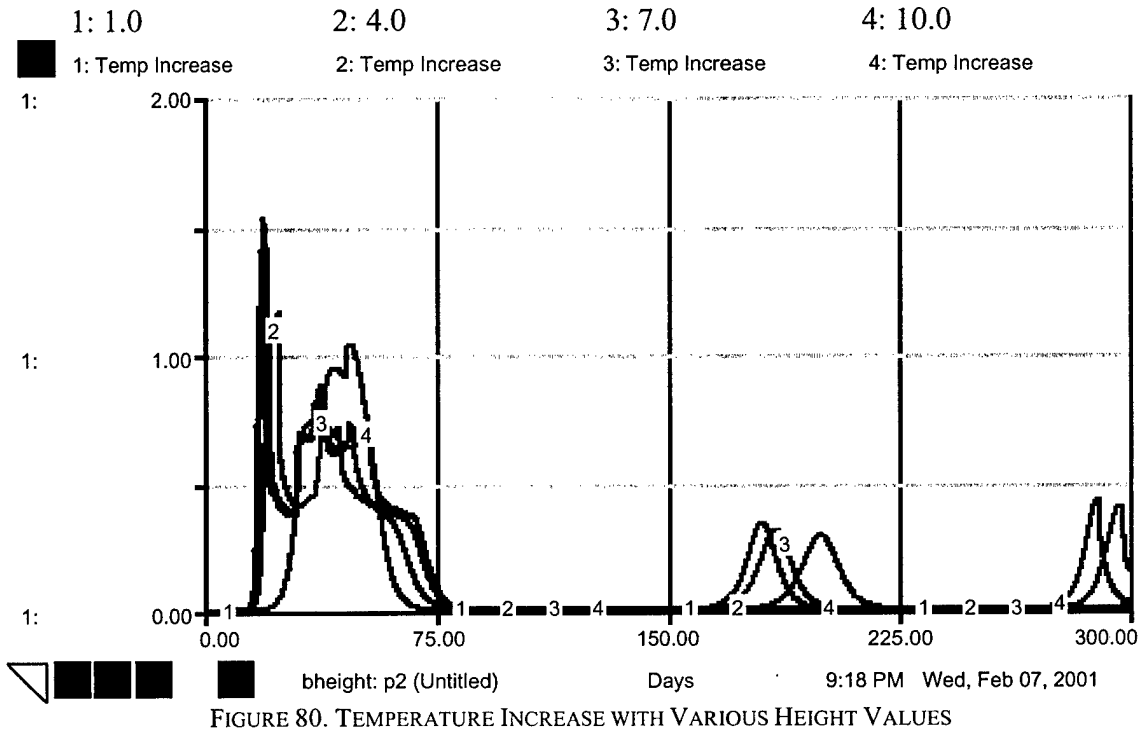
ACIDOGEN HEIGHT: TC 0.1, HC 15 KCAL/MOL GLUCOSE, INITIAL WASTE TEMPERATURE 25°C FIGURES:81-85

1: 3.0	2: 15.3	3: 27.7	4: 40.0
■ 1: Glucose	2: Glucose	3: Glucose	4: Glucose

simcheck: p3 (Untitled)   Days   9:26 PM   Mon, Feb 05, 2001

FIGURE 81. GLUCOSE LEVEL WITH VARIOUS HEIGHT VALUES

109
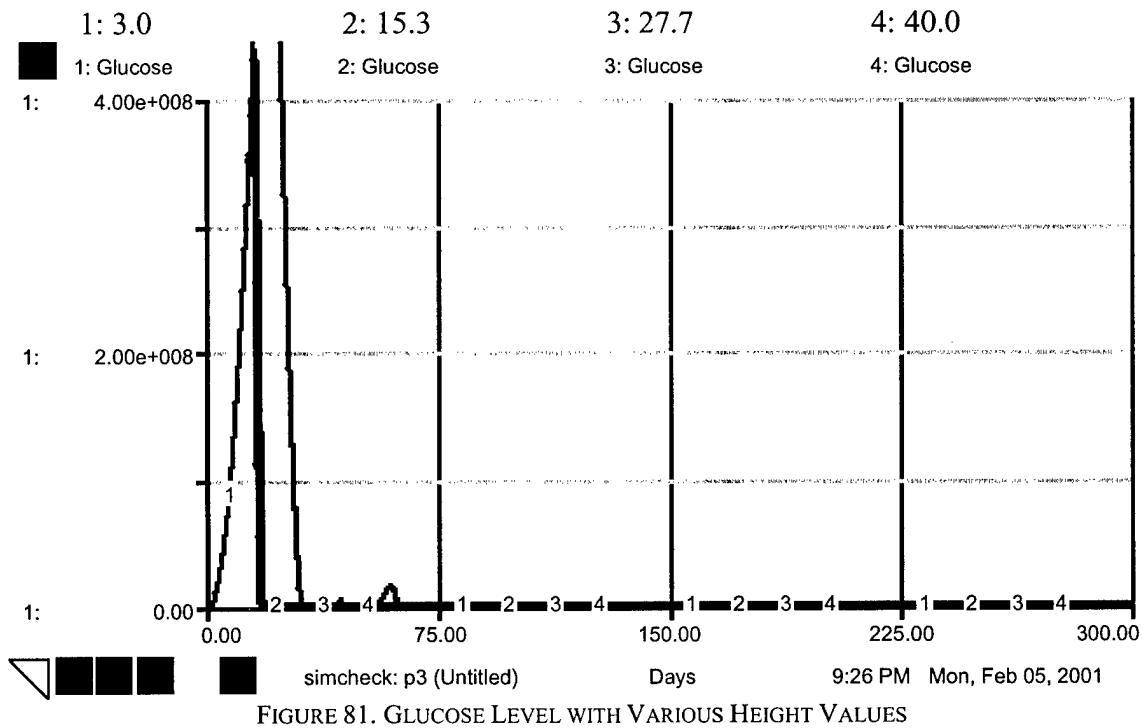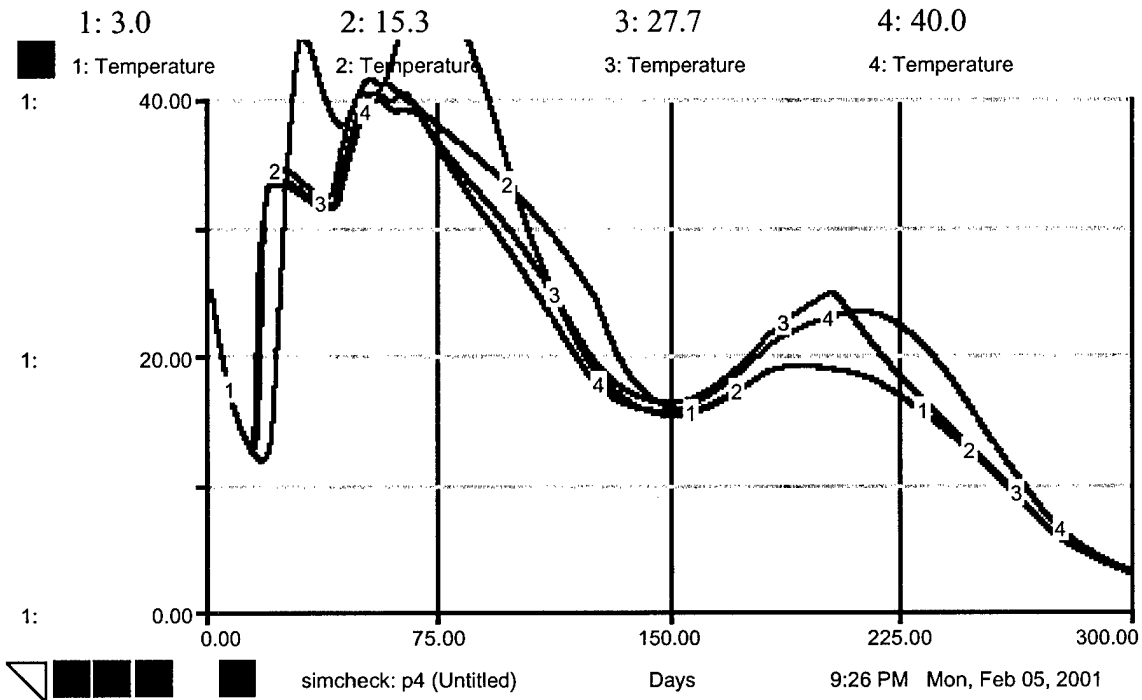
FIGURE 82. TEMPERATURE WITH VARIOUS HEIGHT VALUES
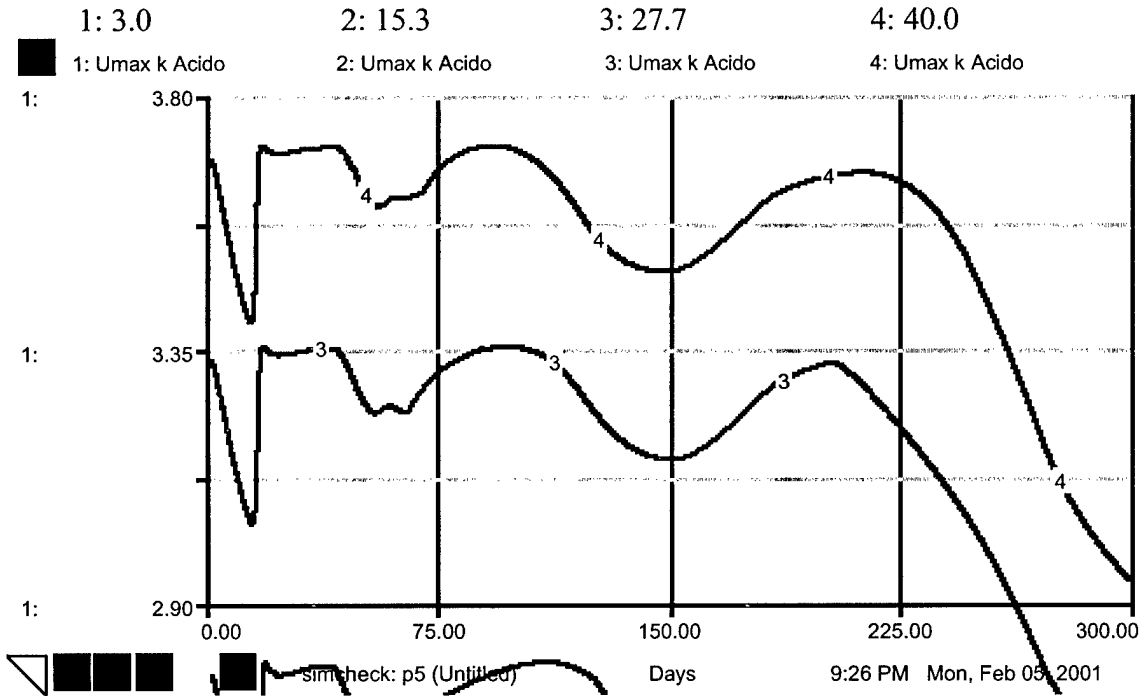
FIGURE 83. U$_{MAX}$ ACIDOGEN WITH VARIOUS HEIGHT VALUES

1: 3.0   2: 15.3   3: 27.7   4: 40.0

1: Umax k Meth   2: Umax k Meth   3: Umax k Meth   4: Umax k Meth

simcheck: p6 (Untitled)   Days   9:26 PM Mon, Feb 05, 2001
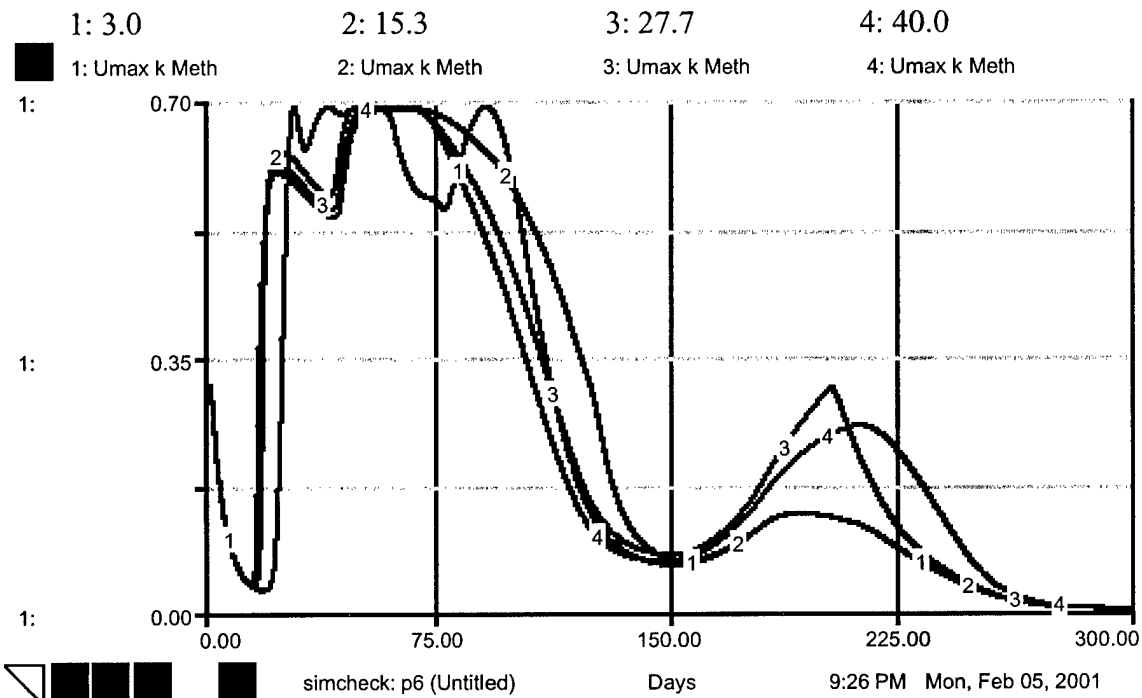
FIGURE 84. U_{MAX} METHANOGEN WITH VARIOUS HEIGHT VALUES

1: 3.0   2: 15.3   3: 27.7   4: 40.0

1: CO2 Mole Fraction   2: CO2 Mole Fraction   3: CO2 Mole Fraction   4: CO2 Mole Fraction

simcheck: p1 (Untitled)   Days   9:26 PM Mon, Feb 05, 2001
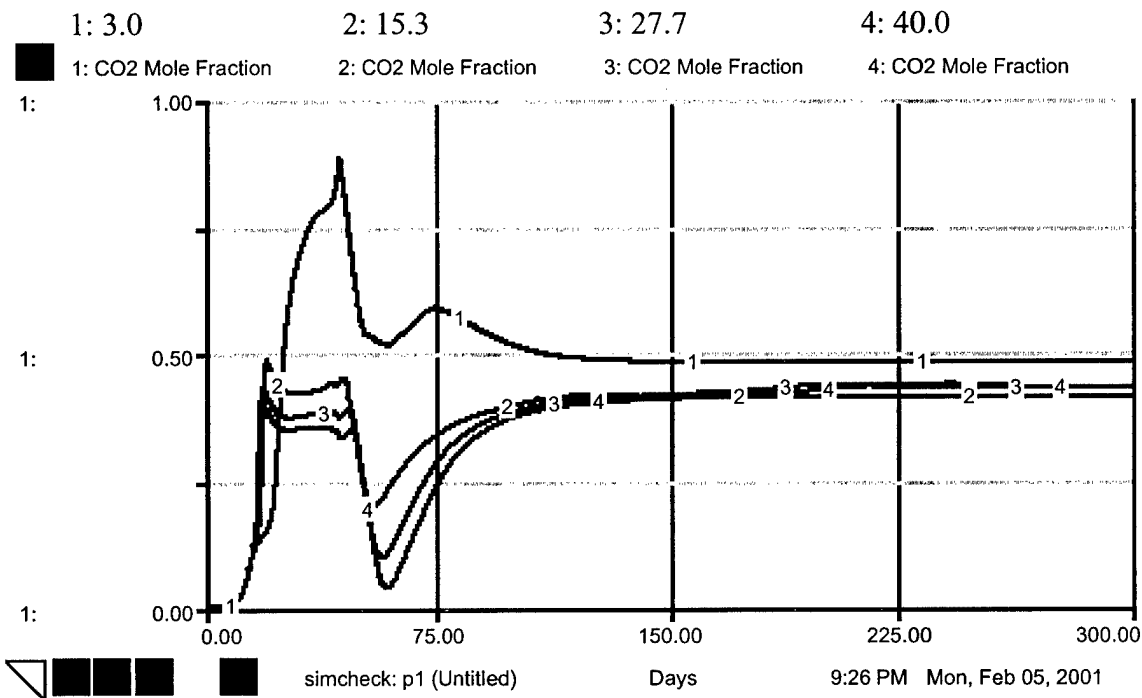
FIGURE 85. CO_2 MOLE FRACTION WITH VARIOUS HEIGHT VALUES

111

METHANOGEN HEIGHT: TC 0.1, HC 15 KCAL/MOL GLUCOSE, INITIAL WASTE TEMPERATURE 25°C
FIGURE 86

1: CH4 Mole Fraction   2: CH4 Mole Fraction   3: CH4 Mole Fraction   4: CH4 Mole Fraction

methbheight: p3 (Untitled)   Days   3:55 PM   Tue, Dec 26, 2000
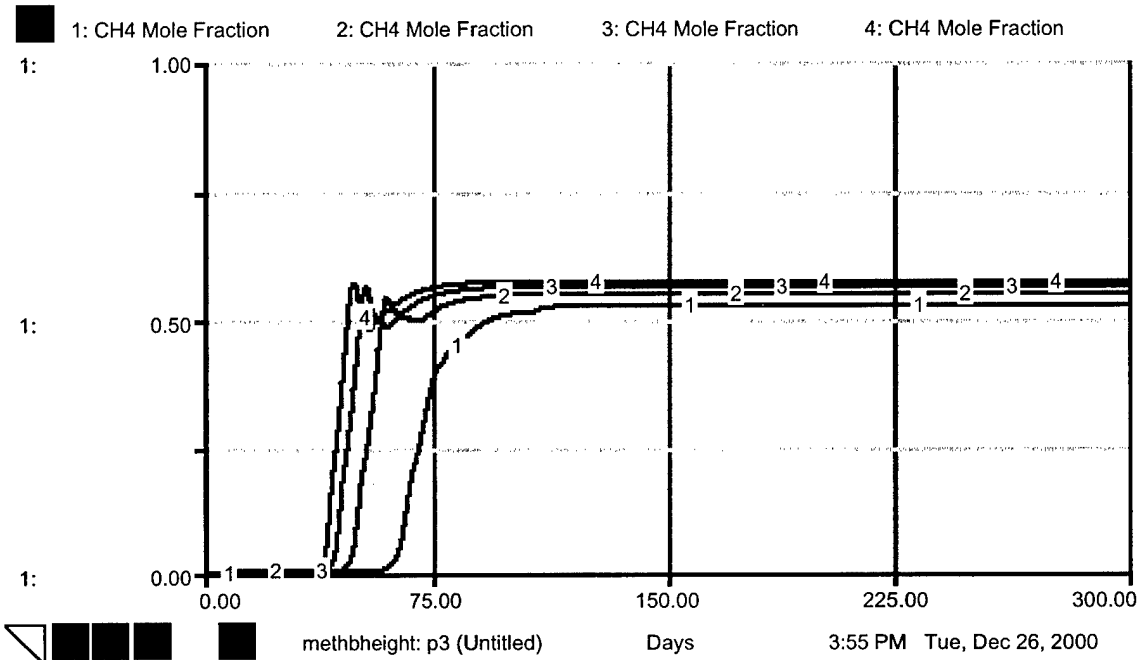
FIGURE 86. CH$_4$ MOLE FRACTION WITH VARIOUS HEIGHT VALUES

ACIDOGEN DECAY STEEPNESS: FIGURES 87-89

1: 1.0   2: 4.67   3: 8.33   4: 12.0

1: CO2 Mole Fraction   2: CO2 Mole Fraction   3: CO2 Mole Fraction   4: CO2 Mole Fraction

acidodecaystepness: p4 (Untitled)   Days   1:47 PM   Fri, Dec 29, 2000

FIGURE 87. CO$_2$ MOLE FRACTION WITH VARIOUS DECAY STEEPNESS VALUES

FIGURE 88. BUTYRATE BIOMASS VARIOUS DECAY STEEPNESS VALUES

FIGURE 89. K_D ACIDOGEN WITH VARIOUS DECAY STEEPNESS VALUES
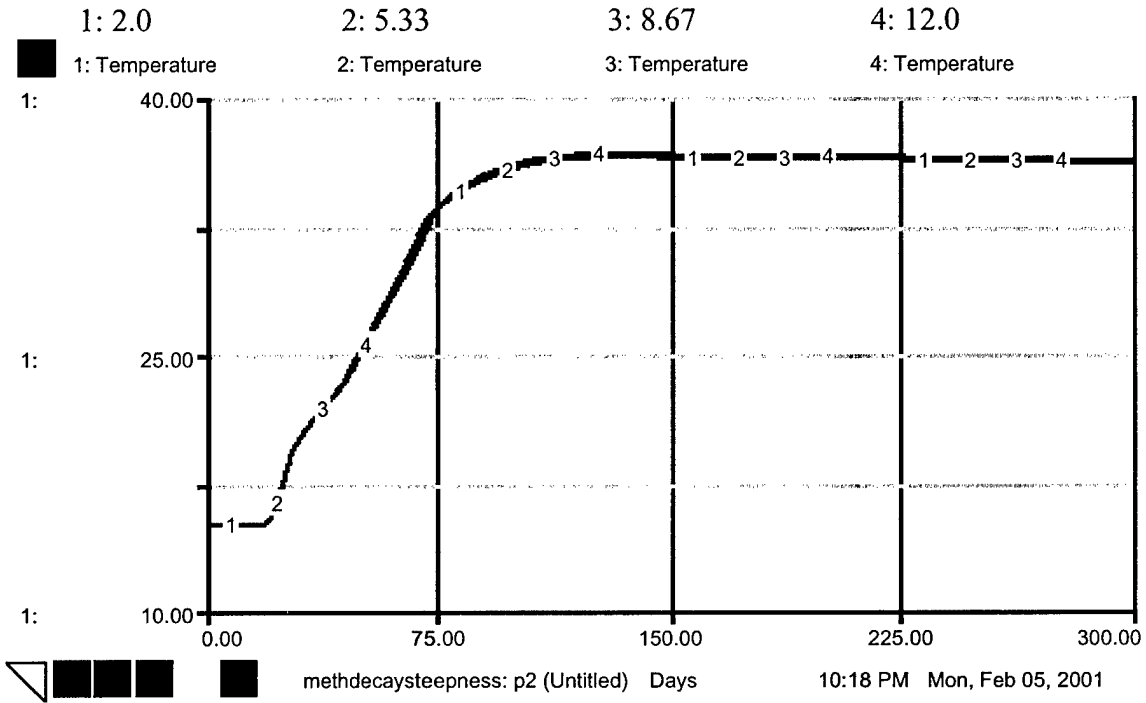
FIGURE 90. TEMPERATURE WITH VARIOUS DECAY STEEPNESS VALUES
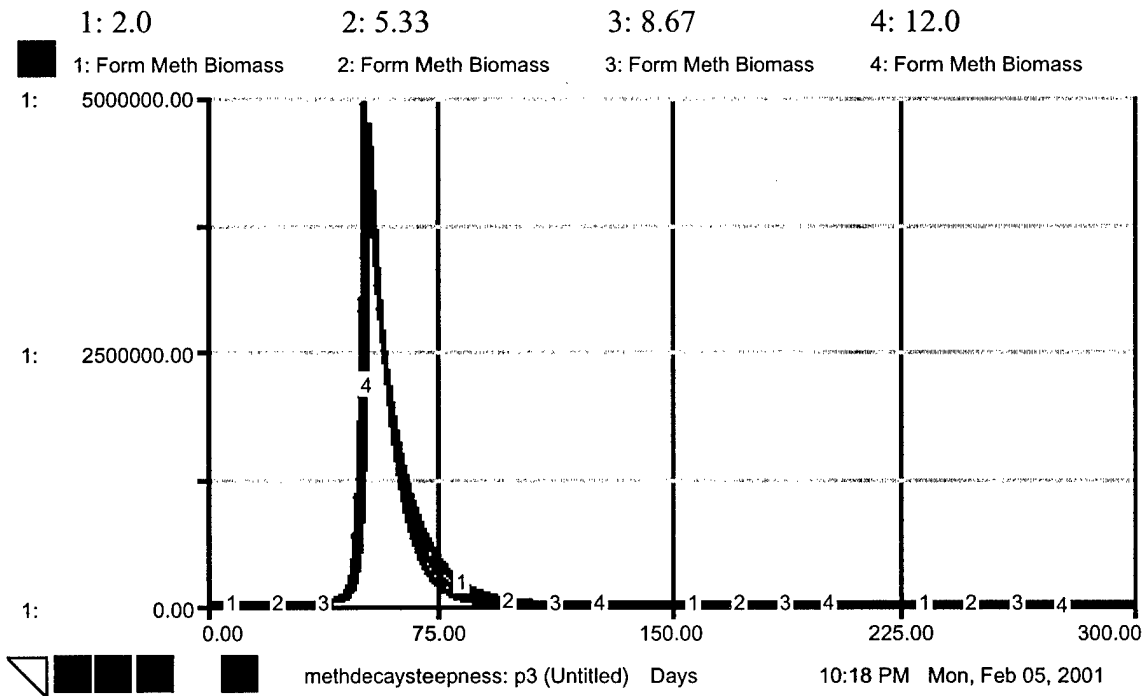
FIGURE 91. FORMATE METH BIOMASS LEVEL WITH VARIOUS DECAY STEEPNESS VALUES

114
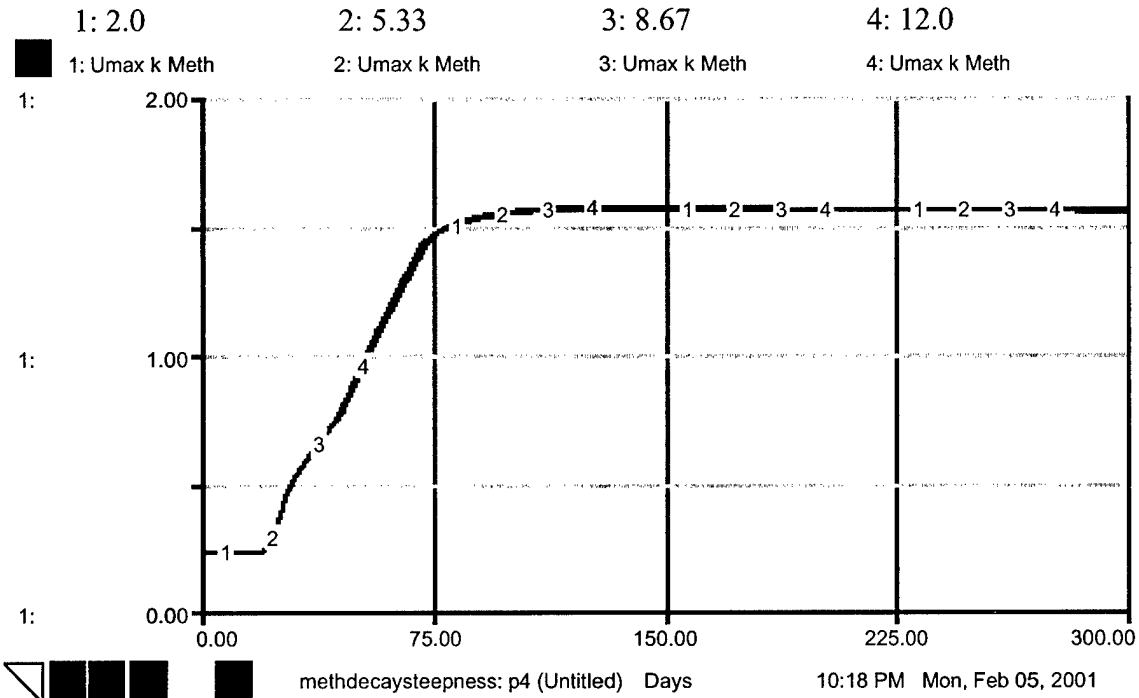
FIGURE 92. U_{MAX} METHANOGEN WITH VARIOUS DECAY STEEPNESS VALUES
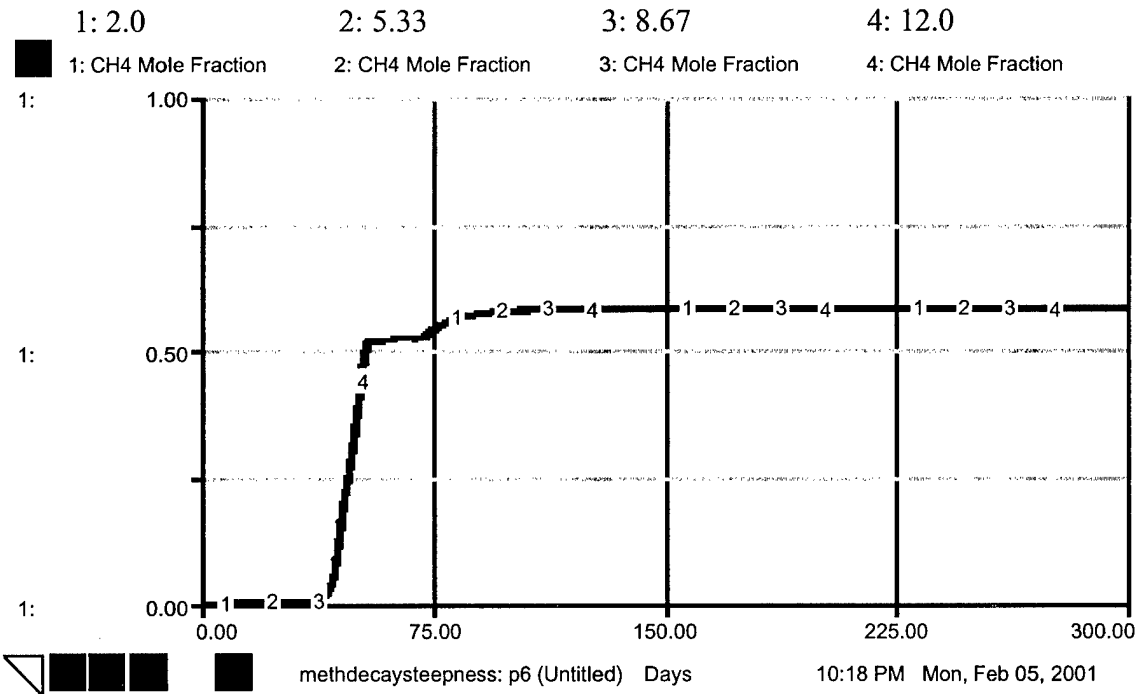
FIGURE 93. CH_4 MOLE FRACTION WITH VARIOUS DECAY STEEPNESS VALUES

115

FIGURE 94. U_{MAX} ACIDOGEN AT VARIOUS TEMPERATURE SPAN VALUES
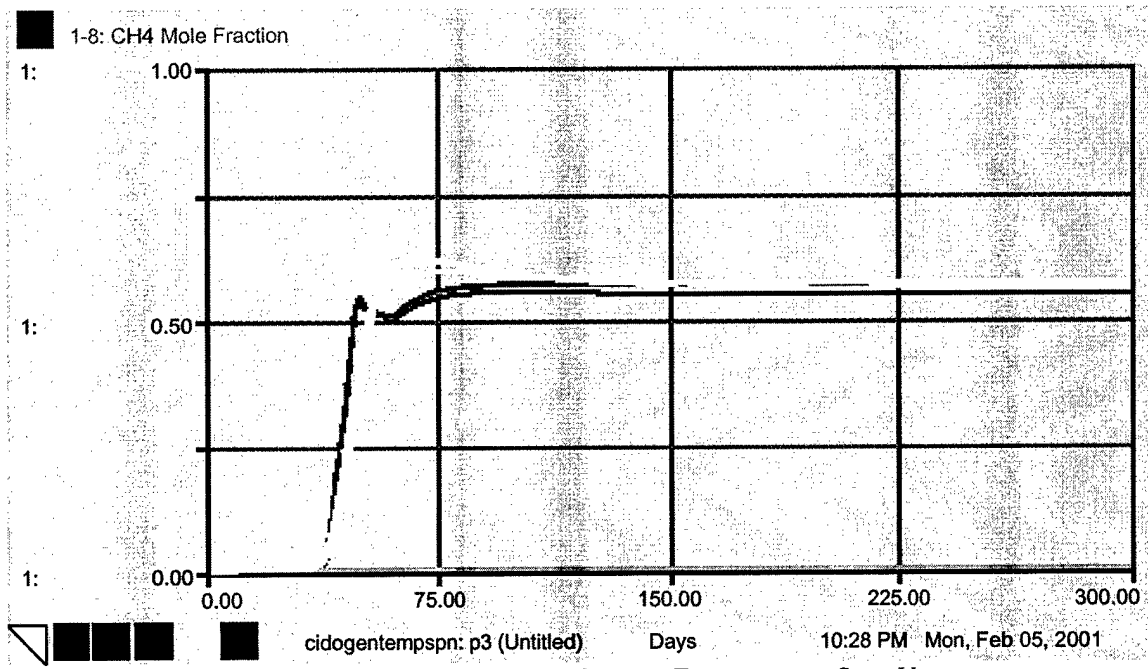
FIGURE 95. CH_4 MOLE FRACTION AT VARIOUS TEMPERATURE SPAN VALUES

116
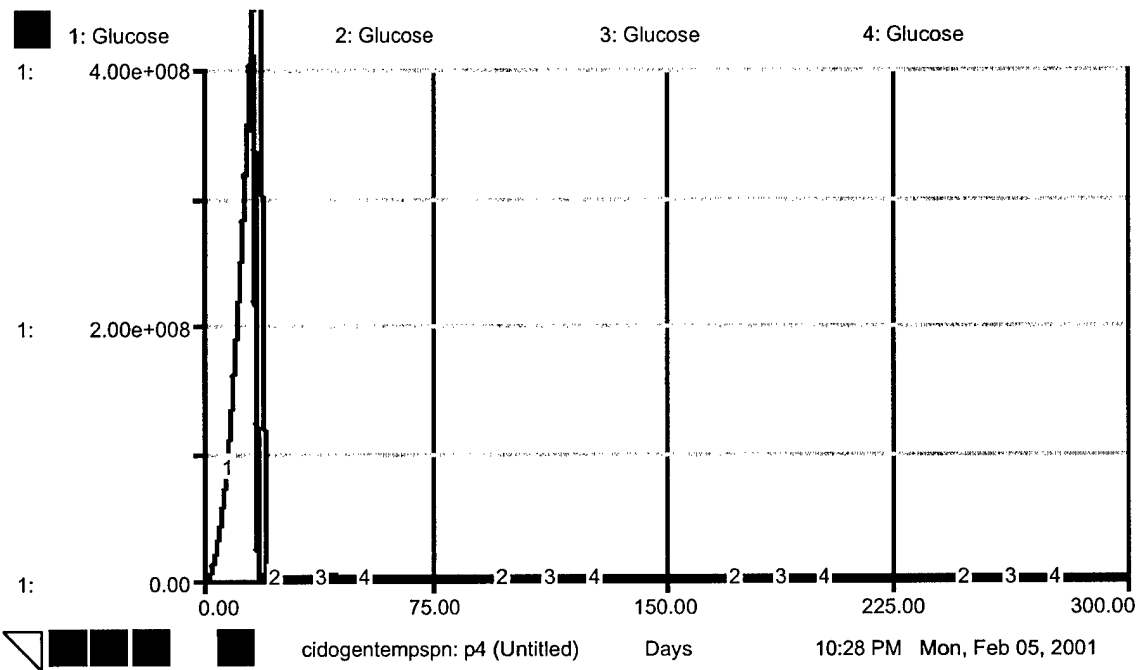
FIGURE 96. GLUCOSE LEVEL AT VARIOUS TEMPERATURE SPAN VALUES

METHANOGEN TEMPERATURE SPAN: FIGURES 97-98
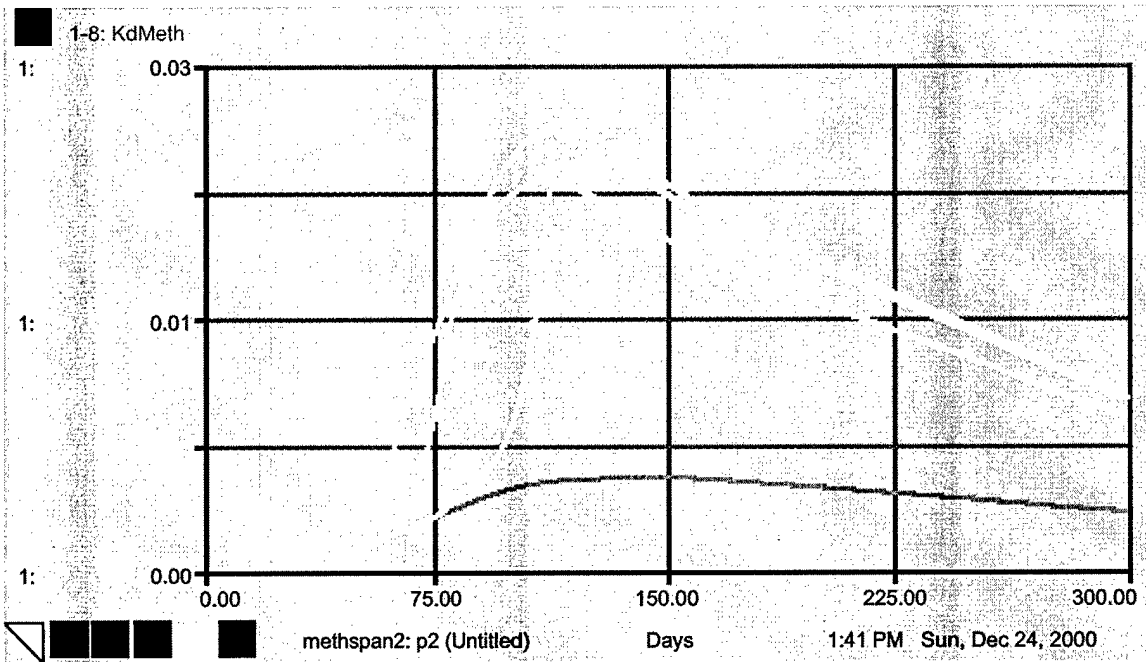
FIGURE 97. K_D METHANOGEN AT VARIOUS TEMPERATURE SPAN VALUES
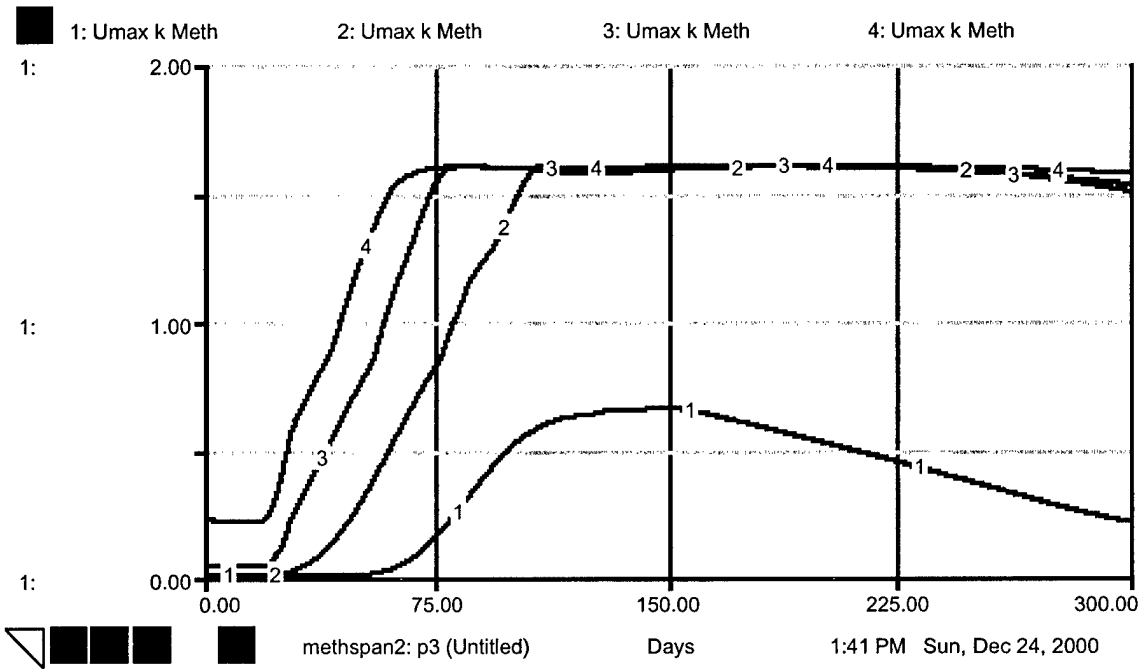
FIGURE 98. U$_{MAX}$ METHANOGEN AT VARIOUS TEMPERATURE SPAN VALUES

METHANOGEN TEMPERATURE SPAN: HC 15 KCAL/MOL GLUCOSE, FIGURES 99-102
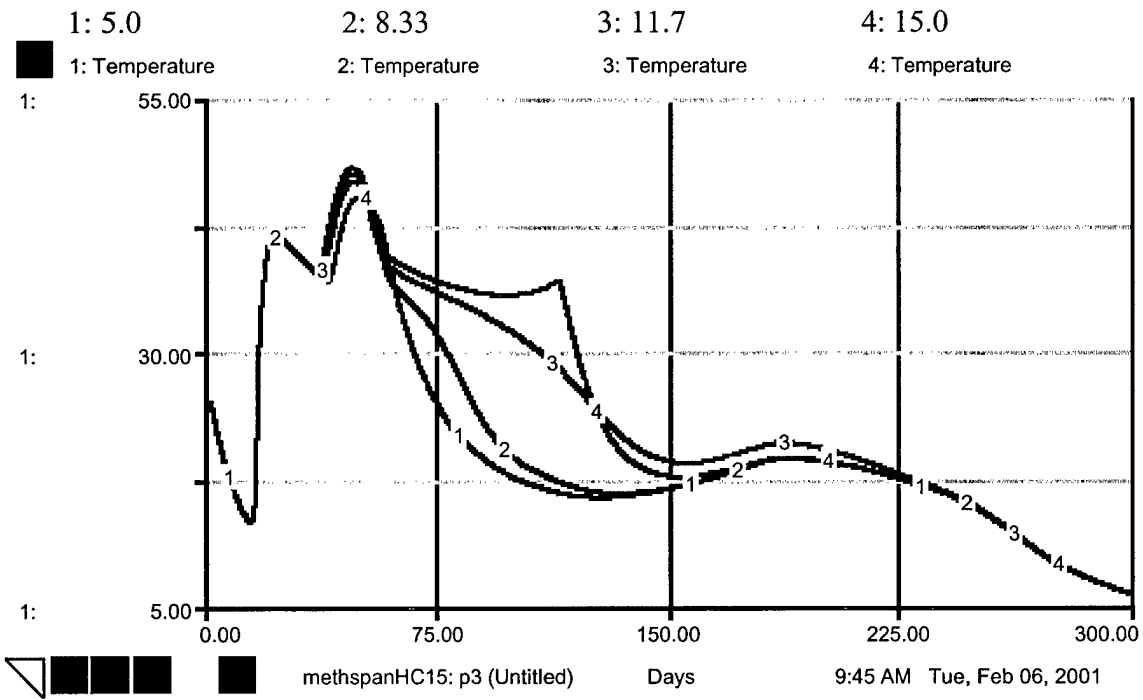
FIGURE 99. TEMPERATURE AT VARIOUS TEMPERATURE SPAN VALUES

118

1: 5.0   2: 8.33   3: 11.7   4: 15.0

1: CO2 Mole Fraction   2: CO2 Mole Fraction   3: CO2 Mole Fraction   4: CO2 Mole Fraction

methspanHC15: p4 (Untitled)   Days   9:45 AM Tue, Feb 06, 2001
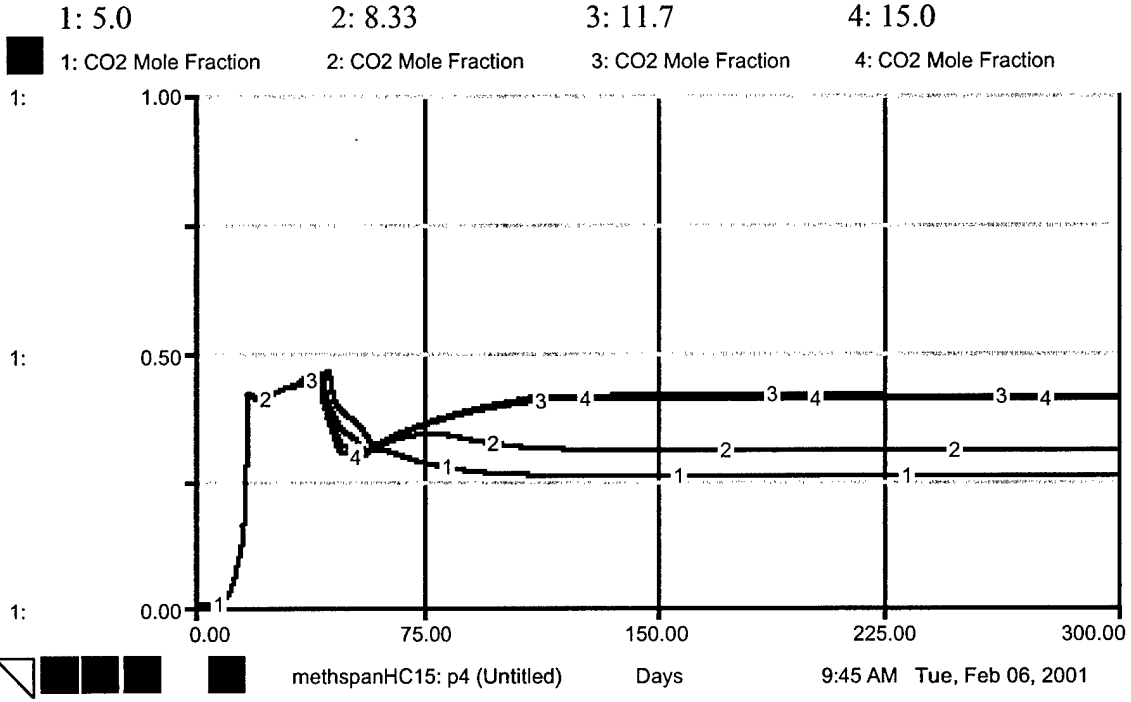
FIGURE 100. CO$_2$ MOLE FRACTION AT VARIOUS TEMPERATURE SPAN VALUES

1: 5.0   2: 8.33   3: 11.7   4: 15.0

1: CH4 Mole Fraction   2: CH4 Mole Fraction   3: CH4 Mole Fraction   4: CH4 Mole Fraction

methspanHC15: p5 (Untitled)   Days   9:45 AM Tue, Feb 06, 2001
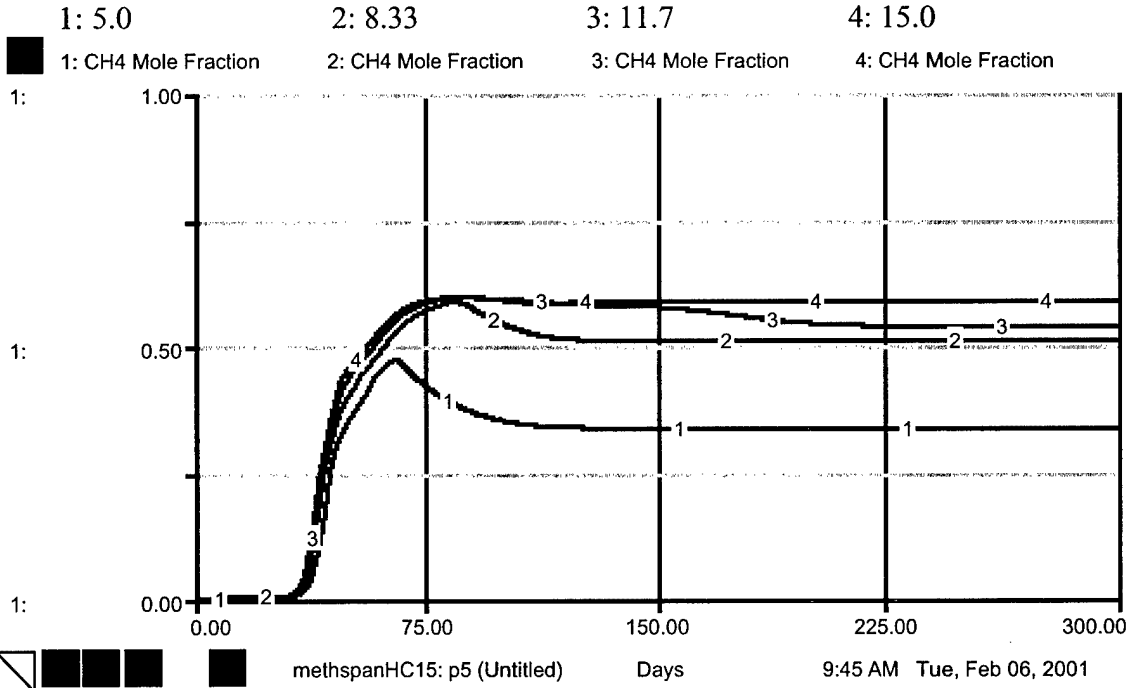
FIGURE 101. CH$_4$ AT VARIOUS TEMPERATURE SPAN VALUES

119

1: Umax k Meth   2: Umax k Meth   3: Umax k Meth   4: Umax k Meth

methspanHC15: p6 (Untitled)   Days   9:45 AM Tue, Feb 06, 2001
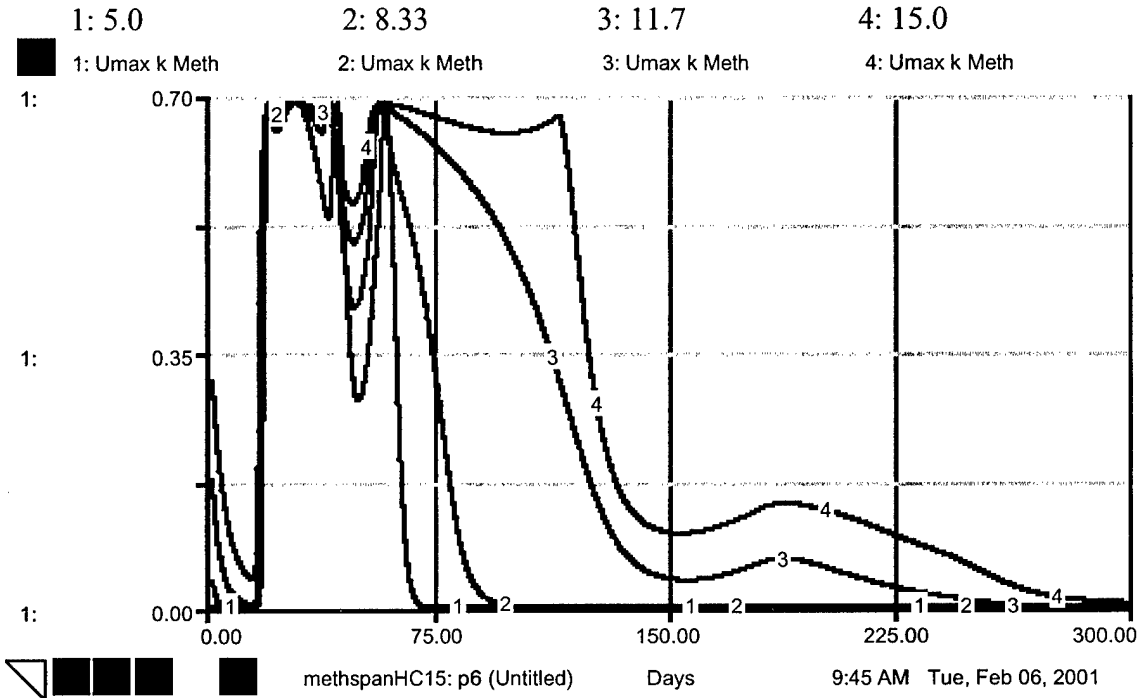
FIGURE 102. U$_{MAX}$ METHANOGEN AT VARIOUS TEMPERATURE SPAN VALUES

METHANOGEN TEMPERATURE SPAN: HC 25 KCAL/MOL GLUCOSE, FIGURES 103-106

1: 5.0   2: 8.33   3: 11.7   4: 15.0

1: Temperature   2: Temperature   3: Temperature   4: Temperature

methspanHC25: p3 (Untitled)   Days   10:14 AM Tue, Feb 06, 2001
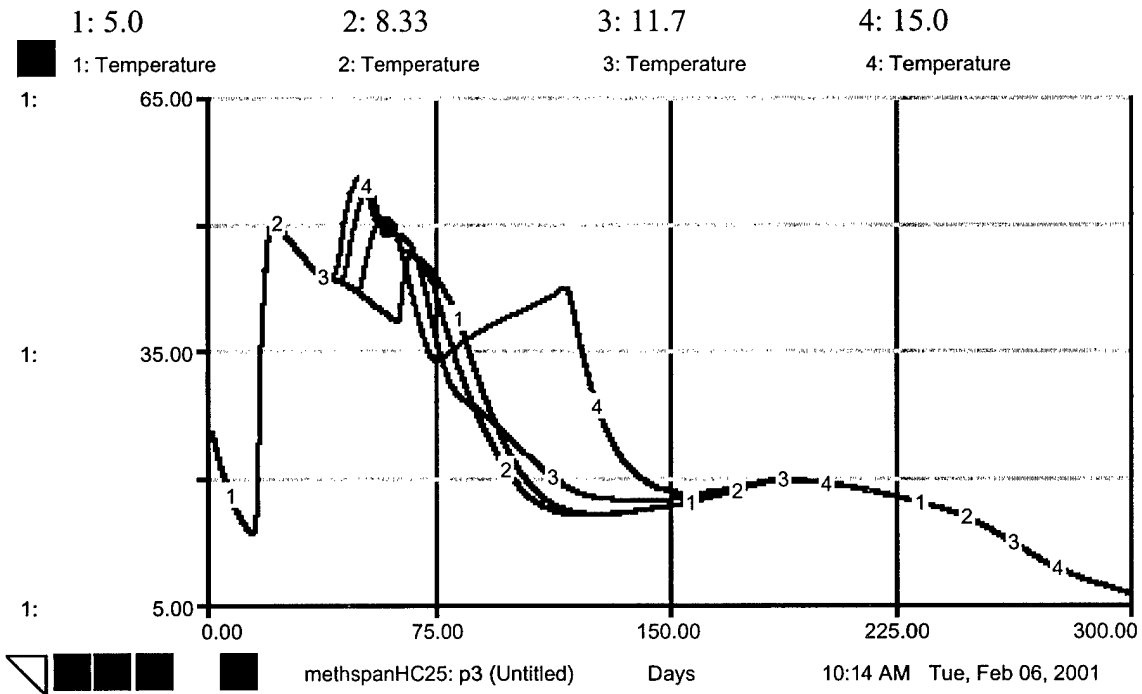
FIGURE 103. TEMPERATURE AT VARIOUS TEMPERATURE SPAN VALUES

120

1: 5.0   2: 8.33   3: 11.7   4: 15.0

1: CH4 Mole Fraction   2: CH4 Mole Fraction   3: CH4 Mole Fraction   4: CH4 Mole Fraction

methspanHC25: p4 (Untitled)   Days   10:14 AM   Tue, Feb 06, 2001
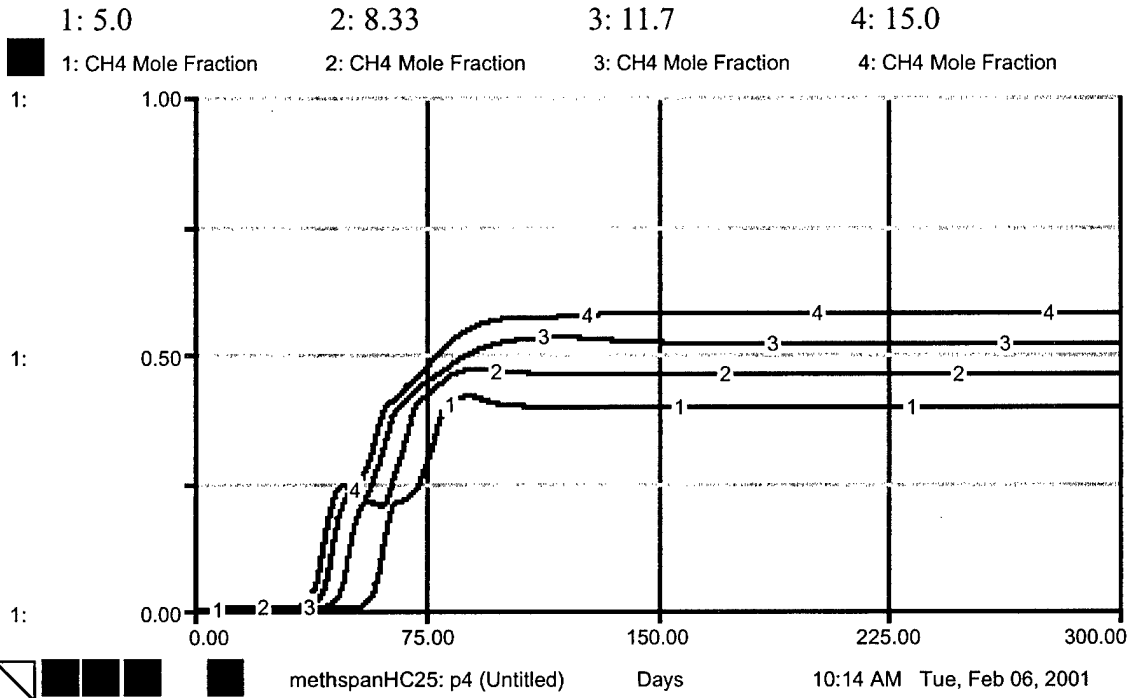
FIGURE 104. CH$_4$ MOLE FRACTION AT VARIOUS TEMPERATURE SPAN VALUES

1: 5.0   2: 8.33   3: 11.7   4: 15.0

1: CO2 Mole Fraction   2: CO2 Mole Fraction   3: CO2 Mole Fraction   4: CO2 Mole Fraction

methspanHC25: p5 (Untitled)   Days   10:14 AM   Tue, Feb 06, 2001
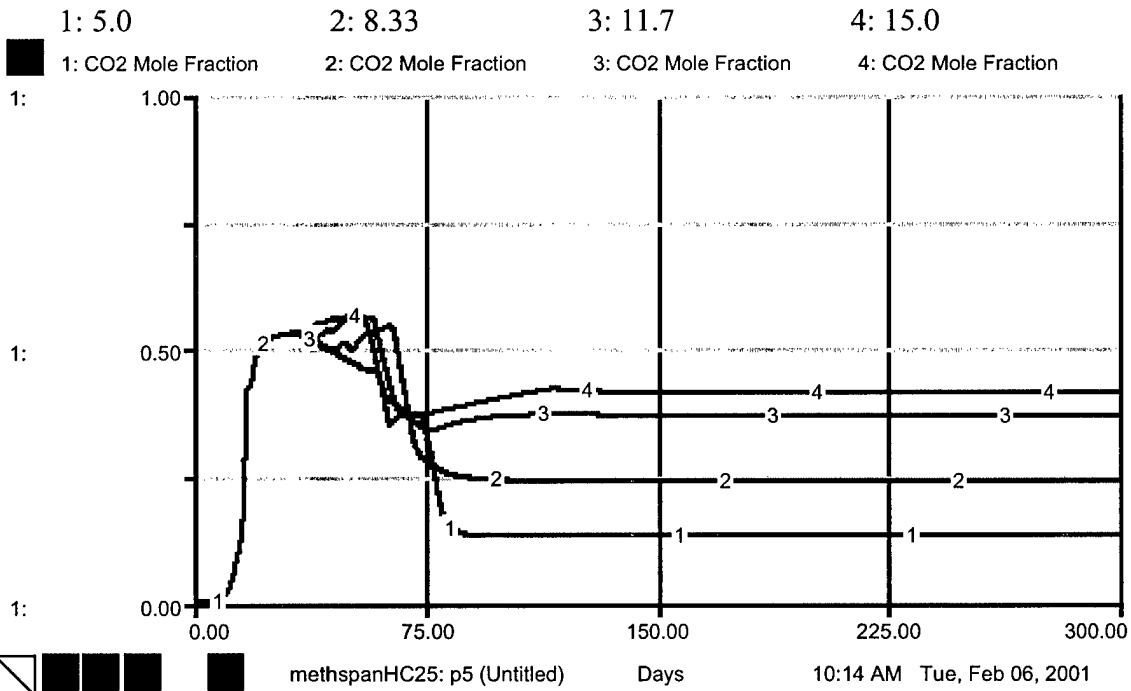
FIGURE 105. CO$_2$ MOLE FRACTION AT VARIOUS TEMPERATURE SPAN VALUES

121
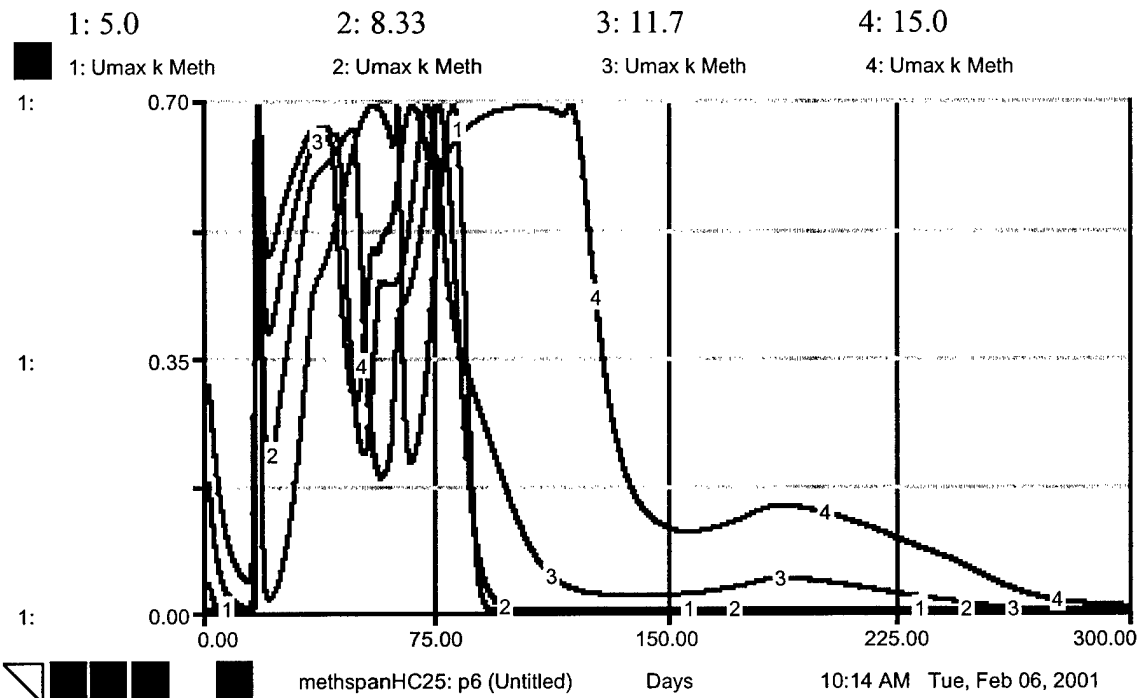
FIGURE 106. U$_{MAX}$ METHANOGEN AT VARIOUS TEMPERATURE SPAN VALUES

122

1: 20.0　　　　2: 25.0　　　　3: 30.0　　　　4: 35.0

■ 1: Umax k Acido　　2: Umax k Acido　　3: Umax k Acido　　4: Umax k Acido

tpeakacid: p6 (Untitled)　　　Days　　　6:15 PM　Sun, Jan 07, 2001

FIGURE 107. U_{MAX} ACIDOGEN AT VARIOUS PEAK TEMPERATURE VALUES

1: 20.0　　　　2: 25.0　　　　3: 30.0　　　　4: 35.0

■ 1: CH4 Mole Fraction　　2: CH4 Mole Fraction　　3: CH4 Mole Fraction　　4: CH4 Mole Fraction

tpeakacid: p1 (Untitled)　　　Days　　　6:15 PM　Sun, Jan 07, 2001
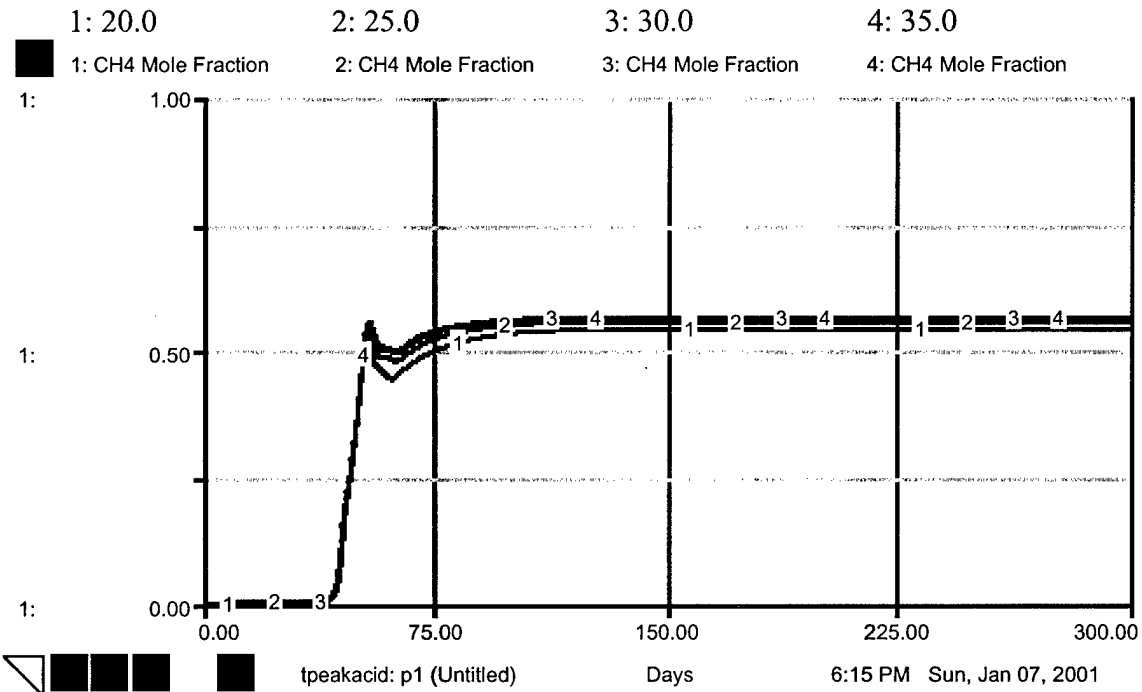
FIGURE 108. CH_4 MOLE FRACTION AT VARIOUS PEAK TEMPERATURE VALUES

123

1: 20.0   2: 25.0   3: 30.0   4: 35.0
■ 1: CO2 Mole Fraction   2: CO2 Mole Fraction   3: CO2 Mole Fraction   4: CO2 Mole Fraction

tpeakacid: p2 (Untitled)   Days   6:15 PM   Sun, Jan 07, 2001
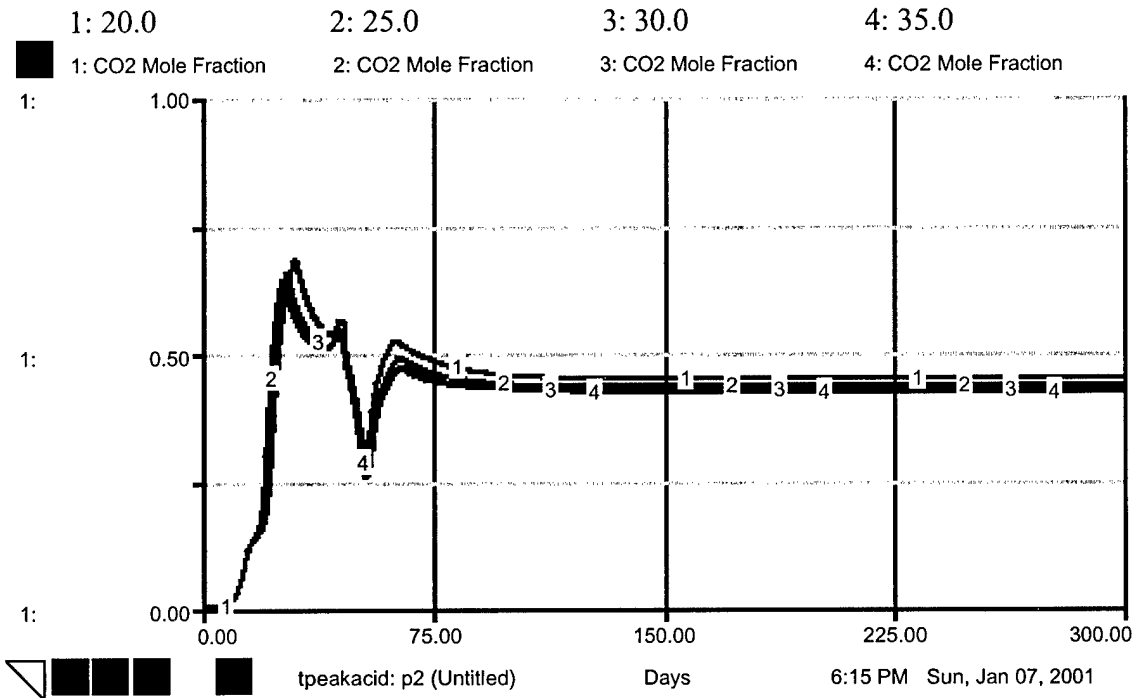
FIGURE 109. CO₂ MOLE FRACTION AT VARIOUS PEAK TEMPERATURE VALUES

METHANOGEN PEAK TEMPERATURE: FIGURES 110-113

1: 30   2: 38.3   3: 46.7   4: 55
■ 1: Temperature   2: Temperature   3: Temperature   4: Temperature

tpeakmeth: p8 (Untitled)   Days   7:15 PM   Sun, Jan 07, 2001
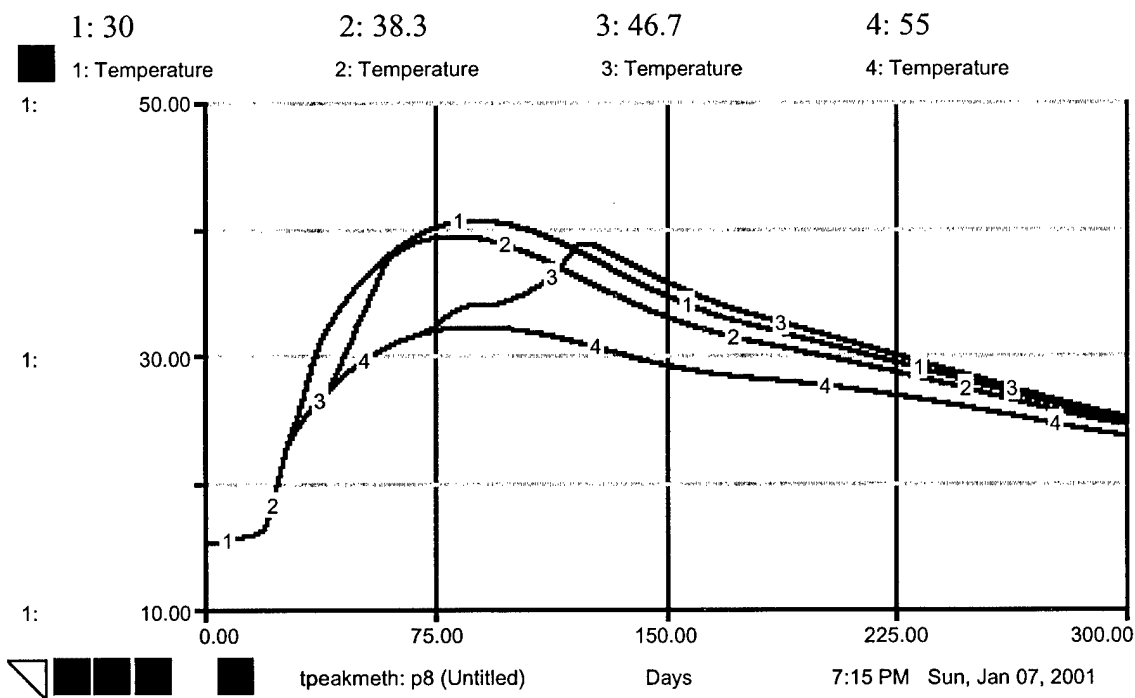
FIGURE 110. TEMPERATURE AT VARIOUS PEAK TEMPERATURE VALUES

124

1: 30   2: 38.3   3: 46.7   4: 55

■ 1: Glucose   2: Glucose   3: Glucose   4: Glucose

1:    7.00e+008

1:    3.50e+008

1:       0.00

        0.00   75.00   150.00   225.00   300.00

◥■■■ ■   tpeakmeth: p1 (Untitled)   Days   7:15 PM   Sun, Jan 07, 2001
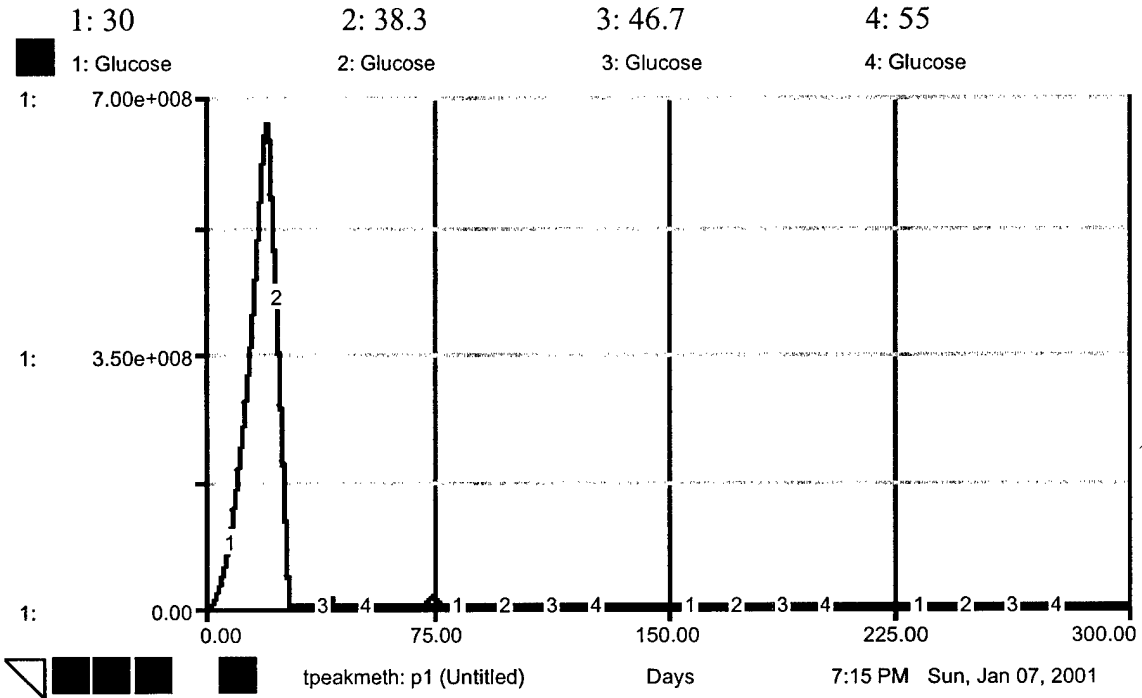
FIGURE 111. GLUCOSE LEVEL AT VARIOUS PEAK TEMPERATURE VALUES

1: 30   2: 38.3   3: 46.7   4: 55

■ 1: CO2 Mole Fraction 2: CO2 Mole Fraction 3: CO2 Mole Fraction 4: CO2 Mole Fraction

1:       1.00

1:       0.50

1:       0.00

        0.00   75.00   150.00   225.00   300.00

◥■■■ ■   tpeakmeth: p3 (Untitled)   Days   7:15 PM   Sun, Jan 07, 2001
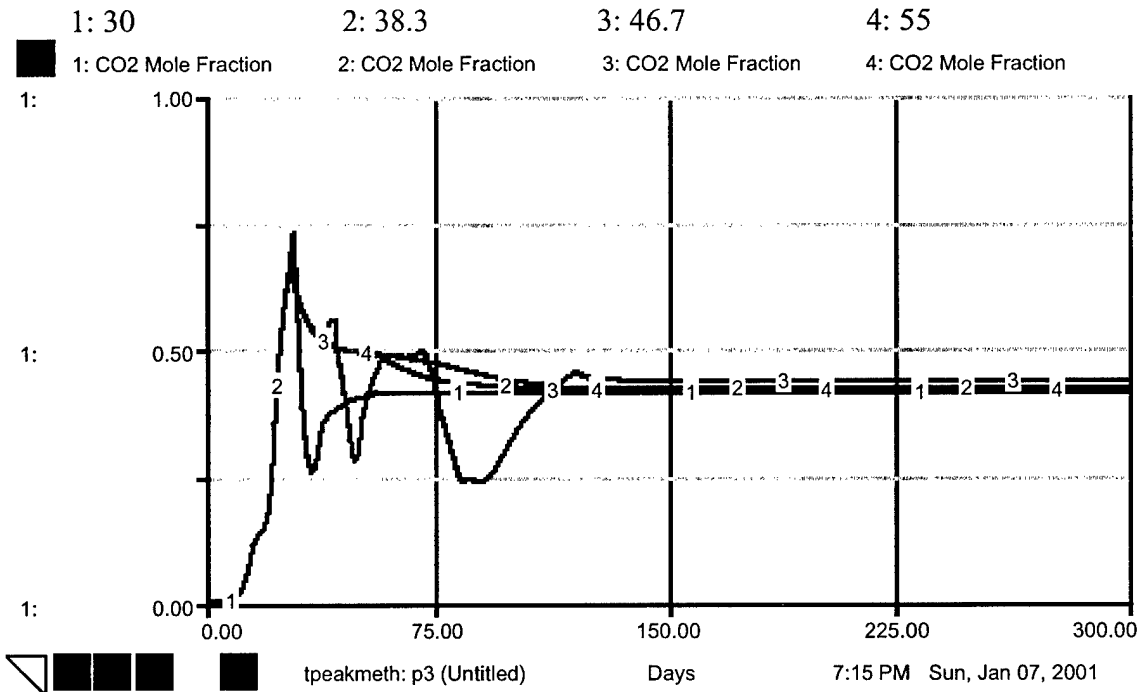
FIGURE 112. CO$_2$ MOLE FRACTION AT VARIOUS PEAK TEMPERATURE VALUES

125

1: Umax k Meth   2: Umax k Meth   3: Umax k Meth   4: Umax k Meth
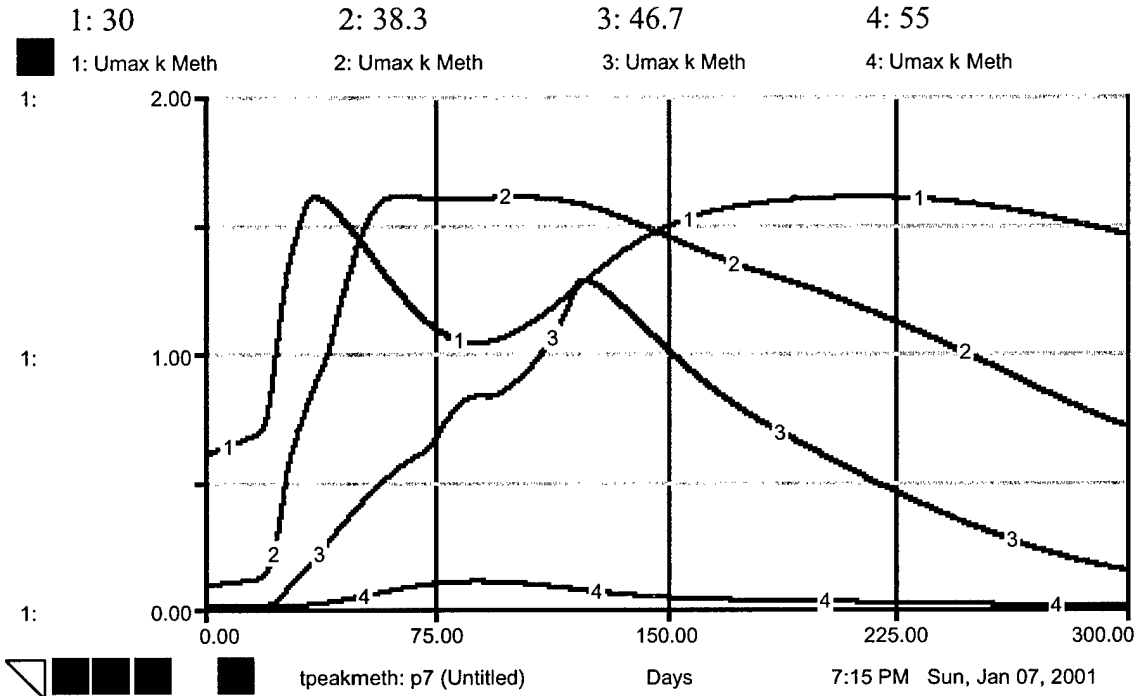
FIGURE 113. U_{MAX} METHANOGEN AT VARIOUS PEAK TEMPERATURE VALUES

ACIDOGEN CRITICAL TEMPERATURE: 114-116

1: 30.0   2: 38.3   3: 46.7   4: 55.0

1: Glucose   2: Glucose   3: Glucose   4: Glucose
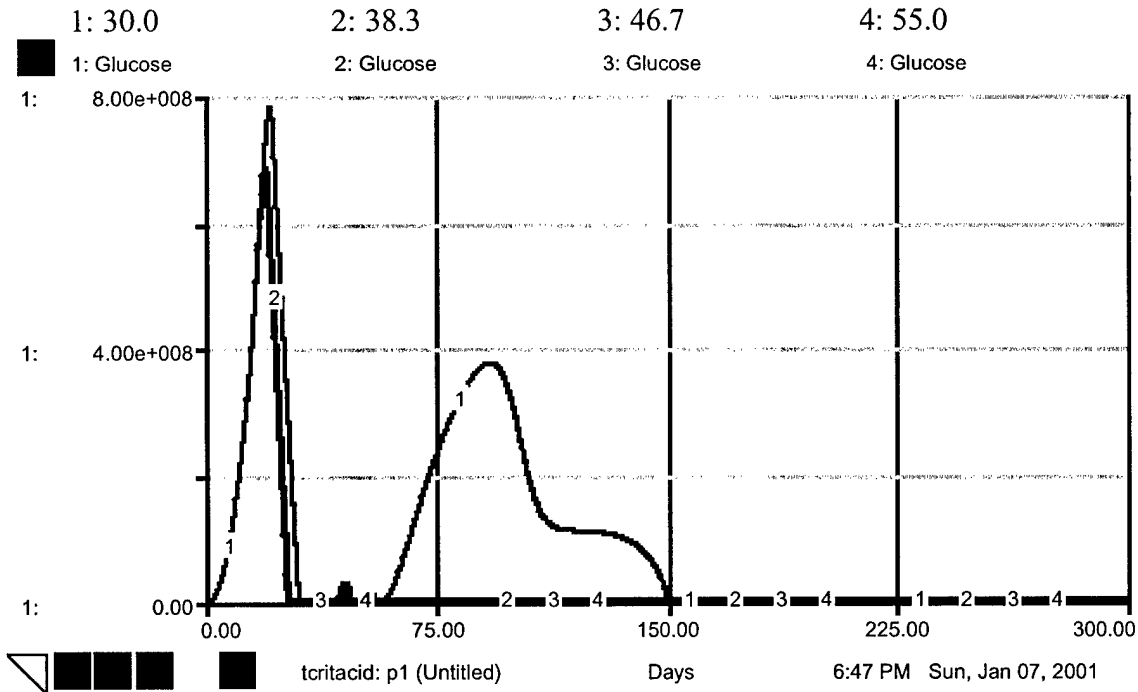
FIGURE 114. GLUCOSE LEVEL AT VARIOUS CRITICAL TEMPERATURE VALUES

■ 1: CO2 Mole Fraction   2: CO2 Mole Fraction   3: CO2 Mole Fraction   4: CO2 Mole Fraction

1:        1.00

1:        0.50

1:        0.00
         0.00   75.00   150.00   225.00   300.00

◣■■■   ■   tcritacid: p3 (Untitled)   Days   6:47 PM   Sun, Jan 07, 2001
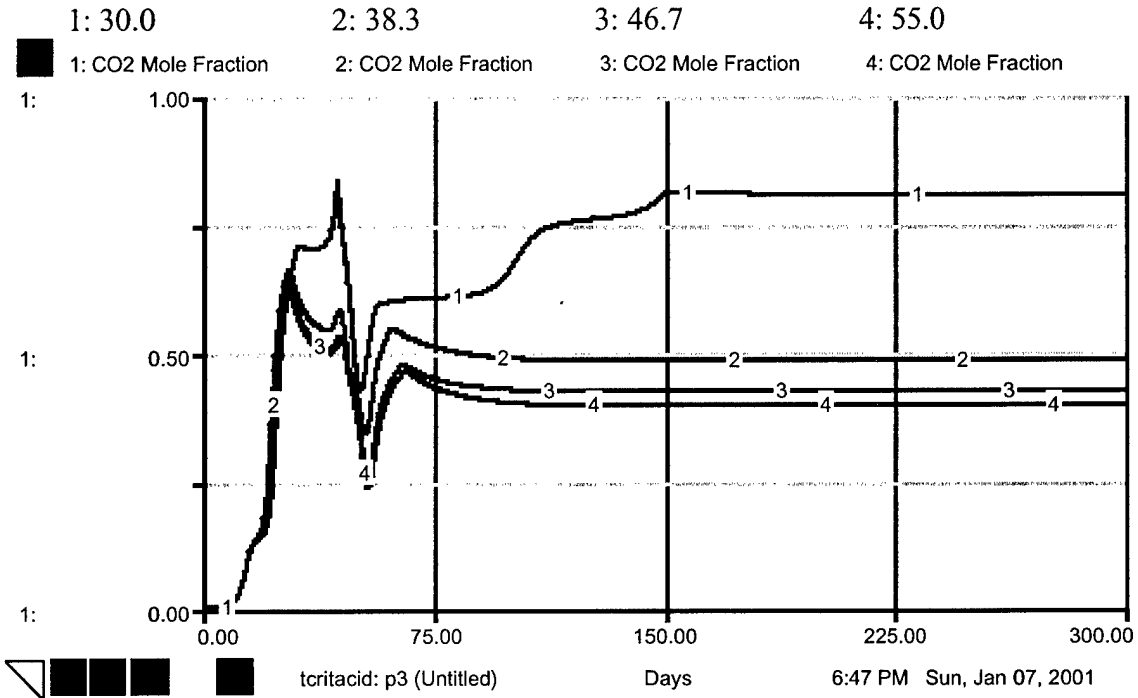
FIGURE 115. CO_2 MOLE FRACTION AT VARIOUS CRITICAL TEMPERATURE VALUES

■ 1: kd Acidog   2: kd Acidog   3: kd Acidog   4: kd Acidog

1:        2.00

1:        1.00

1:        0.00
         0.00   75.00   150.00   225.00   300.00

◣■■■   ■   tcritacid: p7 (Untitled)   Days   6:47 PM   Sun, Jan 07, 2001
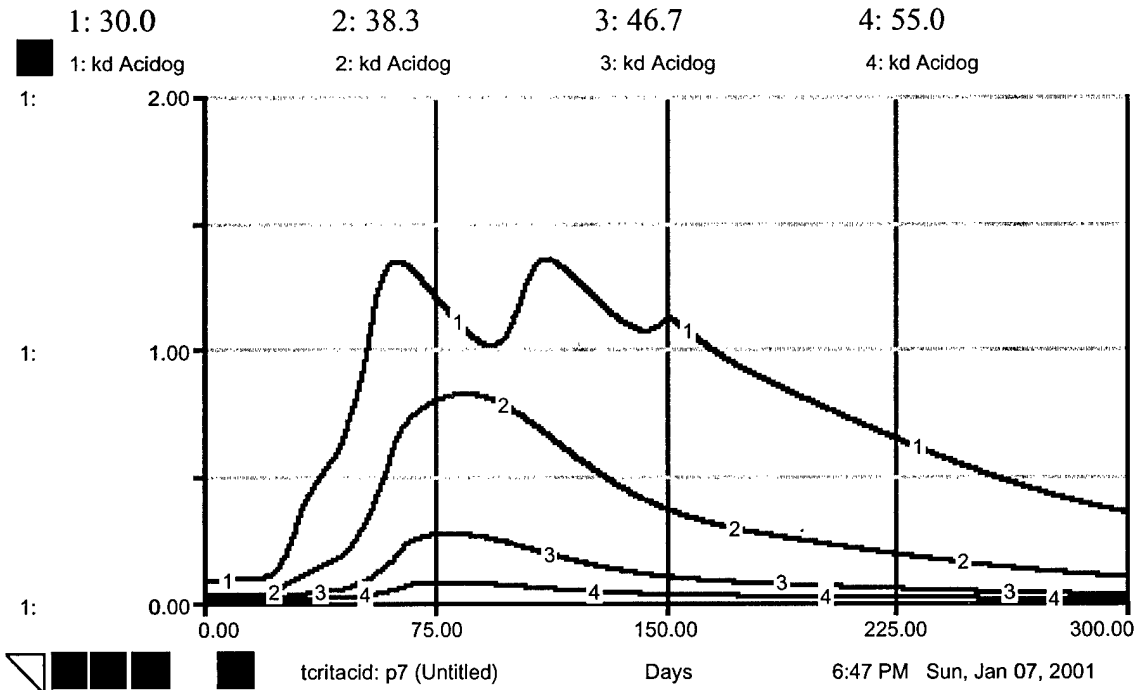
FIGURE 116. K_D METHANOGEN AT VARIOUS CRITICAL TEMPERATURE VALUES

127

FIGURE 117. CH₄ MOLE FRACTION AT VARIOUS CRITICAL TEMPERATURE VALUES
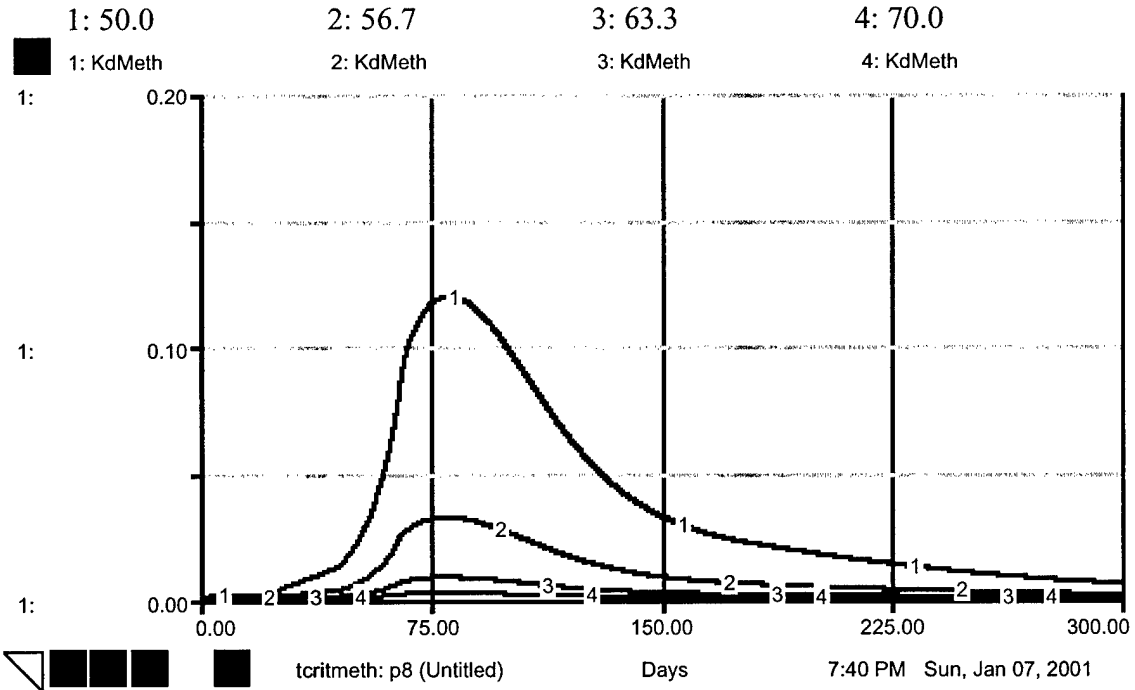
FIGURE 118. K_D METHANOGEN AT VARIOUS CRITICAL TEMPERATURE VALUES

128
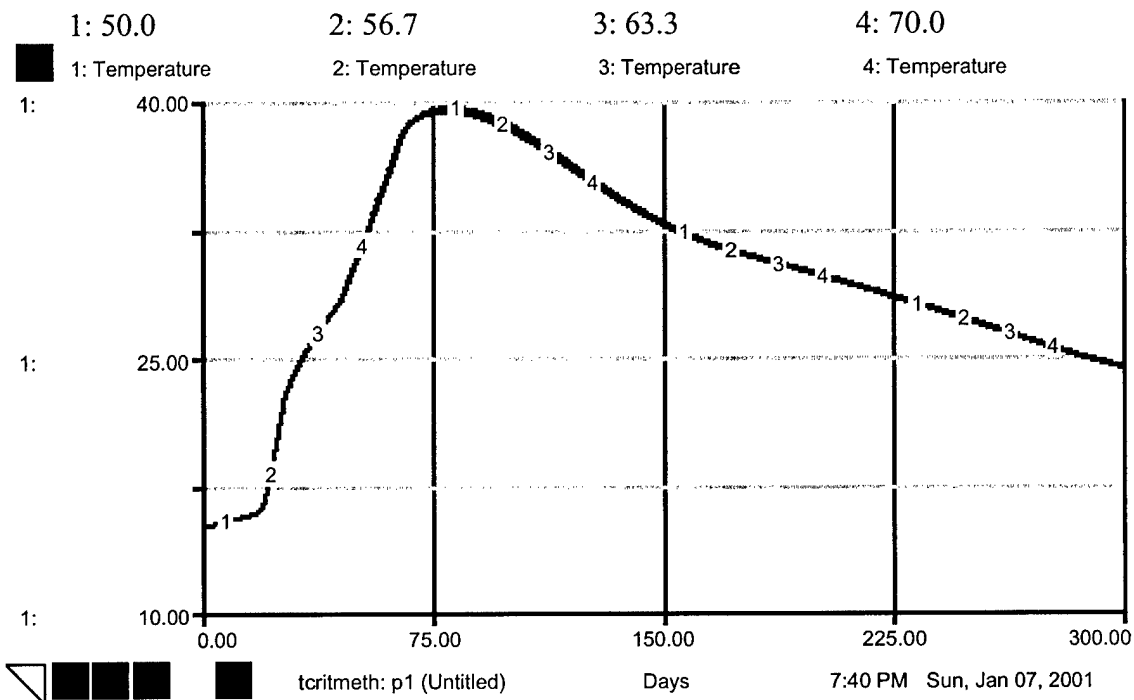
FIGURE 119. TEMPERATURE AT VARIOUS CRITICAL TEMPERATURE VALUES
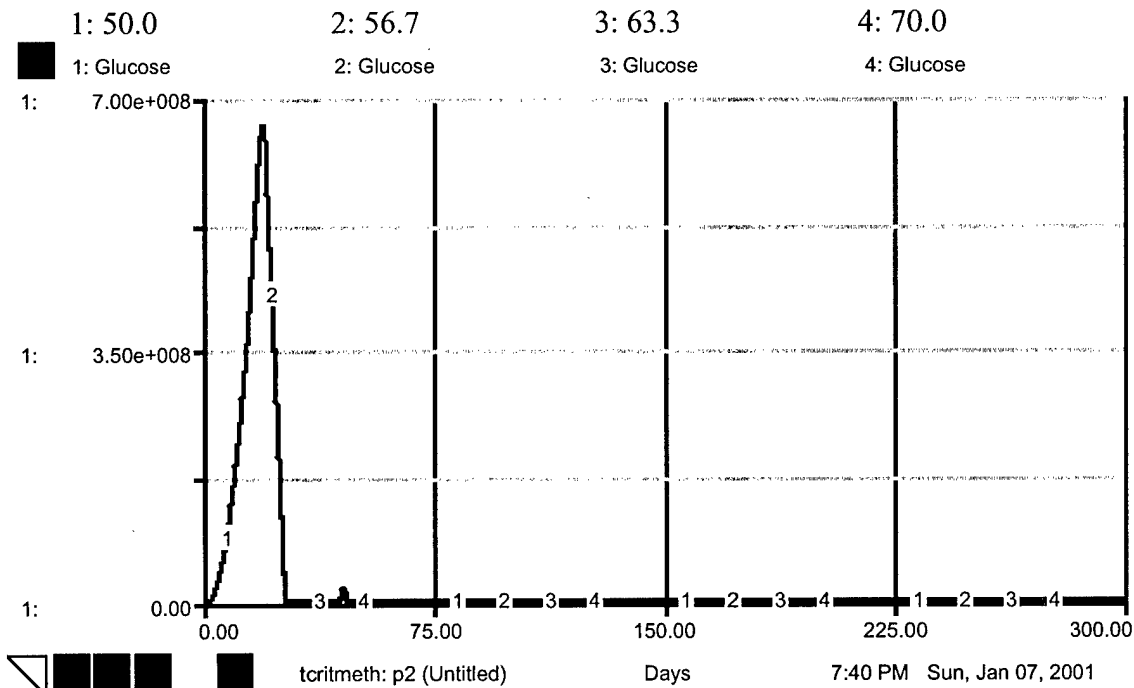
FIGURE 120. GLUCOSE LEVEL AT VARIOUS CRITICAL TEMPERATURE VALUES

129

FIGURE 121. TEMPERATURE WITH VARIOUS HEAT CONSTANT VALUES

FIGURE 122. CO$_2$ MOLE FRACTION WITH VARIOUS HEAT CONSTANT VALUES

1: 5.0	2: 8.33	3: 11.7	4: 15.0
1: Umax k Acido	2: Umax k Acido	3: Umax k Acido	4: Umax k Acido

kansasHC10TC01: p5 (Untitled)   Days   2:33 PM Tue, Feb 06, 2001

FIGURE 123. U$_{MAX}$ ACIDOGEN WITH VARIOUS HEAT CONSTANT VALUES

1: 5.0	2: 8.33	3: 11.7	4: 15.0
1: Glucose	2: Glucose	3: Glucose	4: Glucose

kansasHC10TC01: p1 (Untitled)   Days   2:33 PM Tue, Feb 06, 2001
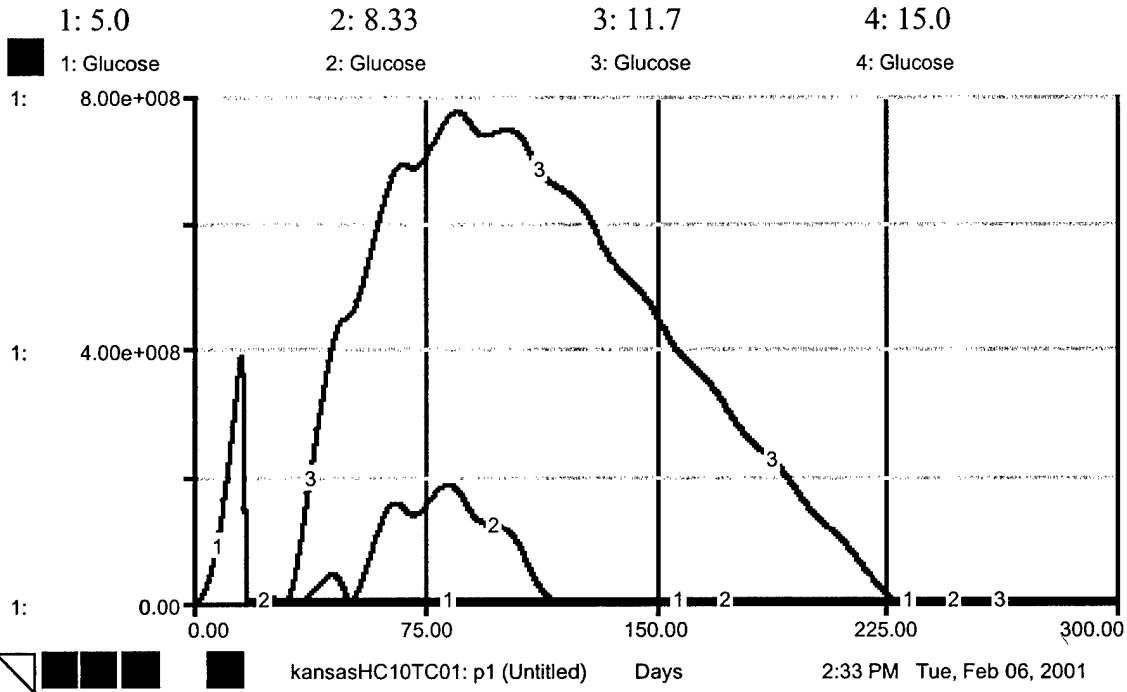
FIGURE 124. GLUCOSE LEVEL WITH VARIOUS HEAT CONSTANT VALUES

131

1: 5.0   2: 8.33   3: 11.7   4: 15.0

■ 1: Umax k Meth   2: Umax k Meth   3: Umax k Meth   4: Umax k Meth
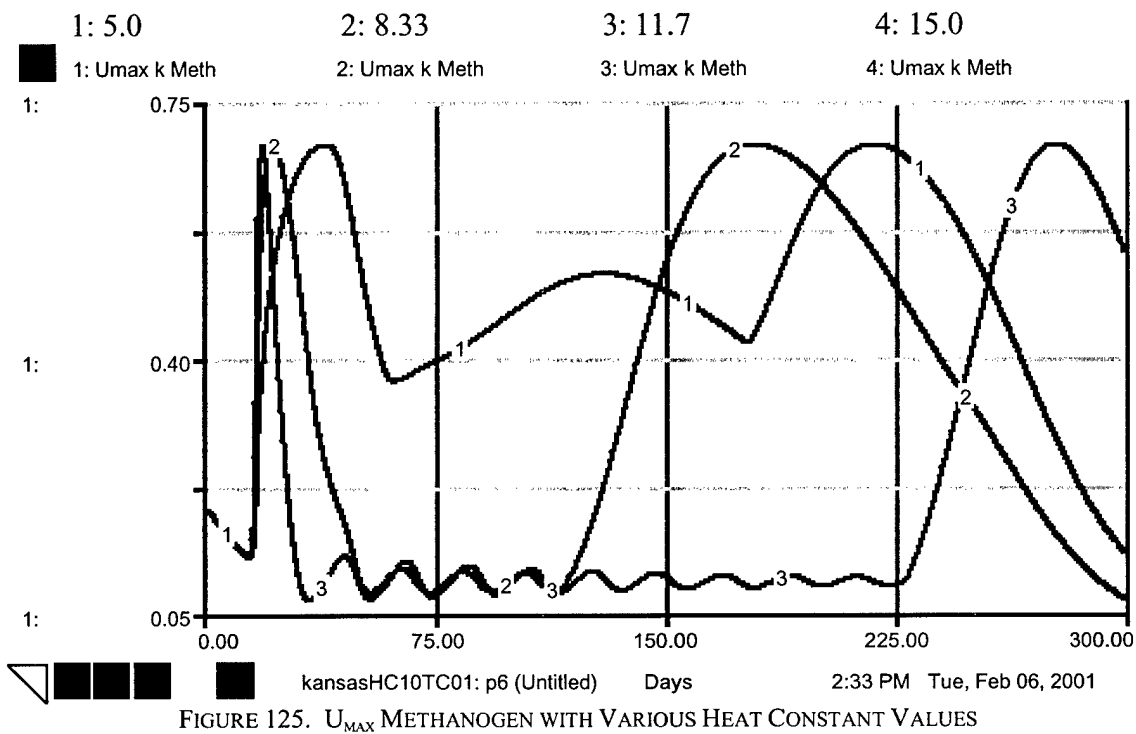
FIGURE 125. U_{MAX} METHANOGEN WITH VARIOUS HEAT CONSTANT VALUES

MOSCOW SOIL PROFILE: TC 0.01, HC 5.0-15.0 KCAL/MOL GLUCOSE FIGURES 126-131

1: 5.0   2: 8.33   3: 11.7   4: 15.0

■ 1: CH4 Mole Fraction   2: CH4 Mole Fraction   3: CH4 Mole Fraction   4: CH4 Mole Fraction
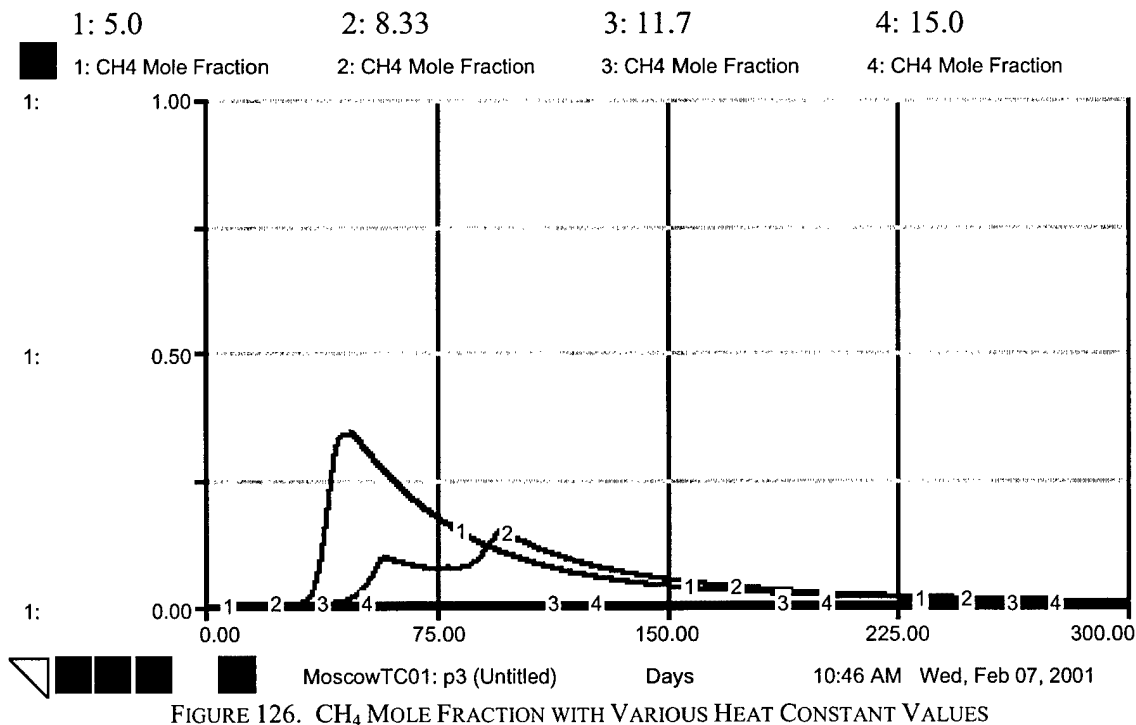
FIGURE 126. CH_4 MOLE FRACTION WITH VARIOUS HEAT CONSTANT VALUES
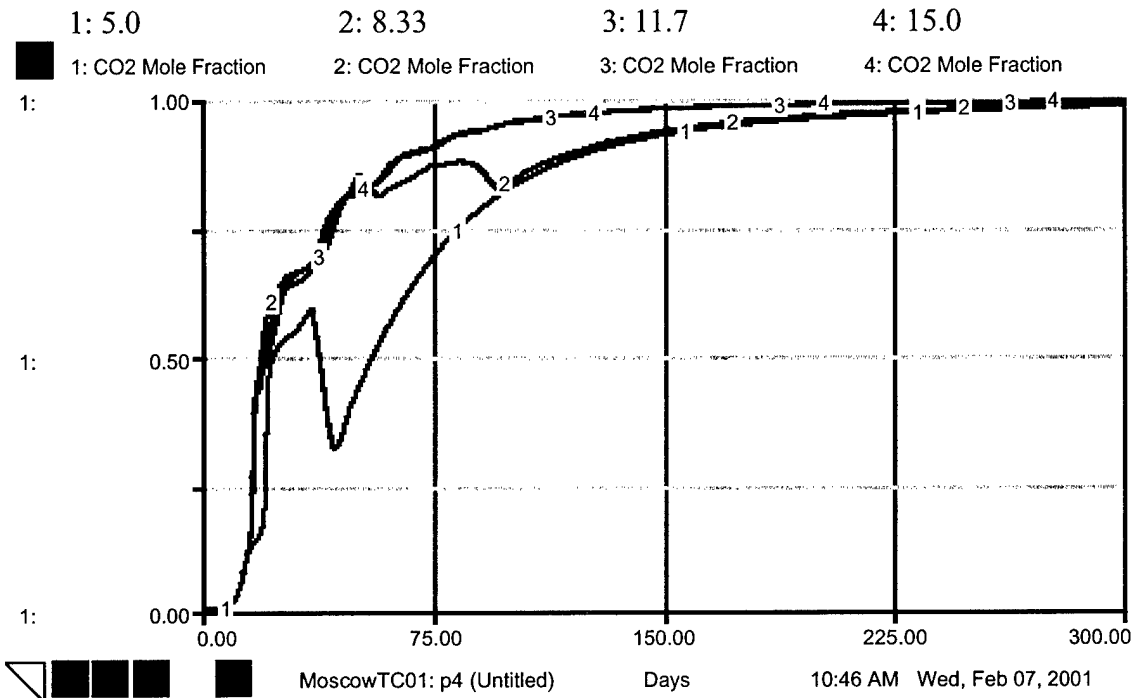
FIGURE 127. CO_2 MOLE FRACTION WITH VARIOUS HEAT CONSTANT VALUES

FIGURE 128. U_{MAX} METHANOGEN WITH VARIOUS HEAT CONSTANT VALUES

1: 5.0   2: 8.33   3: 11.7   4: 15.0

1: Umax k Acido   2: Umax k Acido   3: Umax k Acido   4: Umax k Acido

1:    4.00

1:    3.00

1:    2.00

         0.00   75.00   150.00   225.00   300.00

MoscowTC01: p6 (Untitled)   Days   10:46 AM   Wed, Feb 07, 2001

FIGURE 129. U_{MAX} ACIDOGEN WITH VARIOUS HEAT CONSTANT VALUES

1: 5.0   2: 8.33   3: 11.7   4: 15.0

1: Glucose   2: Glucose   3: Glucose   4: Glucose

1:    1.00e+009

1:    5.00e+008

1:    0.00

         0.00   75.00   150.00   225.00   300.00

MoscowTC01: p1 (Untitled)   Days   10:46 AM   Wed, Feb 07, 2001

FIGURE 130 GLUCOSE LEVEL WITH VARIOUS HEAT CONSTANT VALUES

134

1: 5.0   2: 8.33   3: 11.7   4: 15.0

1: Temperature   2: Temperature   3: Temperature   4: Temperature

MoscowTC01: p2 (Untitled)   Days   10:46 AM   Wed, Feb 07, 2001

FIGURE 131. TEMPERATURE WITH VARIOUS HEAT CONSTANT VALUES

KANSAS SOIL PROFILE: TC 0.1, HC 5.0 –15.0 KCAL/MOL GLUCOSE FIGURES 132-136

1: 5.0   2: 8.33   3: 11.7   4: 15.0

1: CO2 Mole Fraction   2: CO2 Mole Fraction   3: CO2 Mole Fraction   4: CO2 Mole Fraction

kansasTC1: p4 (Untitled)   Days   3:21 PM   Tue, Feb 06, 2001

FIGURE 132. CO_2 MOLE FRACTION WITH VARIOUS HEAT CONSTANT VALUES

1: 5.0	2: 8.33	3: 11.7	4: 15.0
■ 1: Umax k Acido	2: Umax k Acido	3: Umax k Acido	4: Umax k Acido
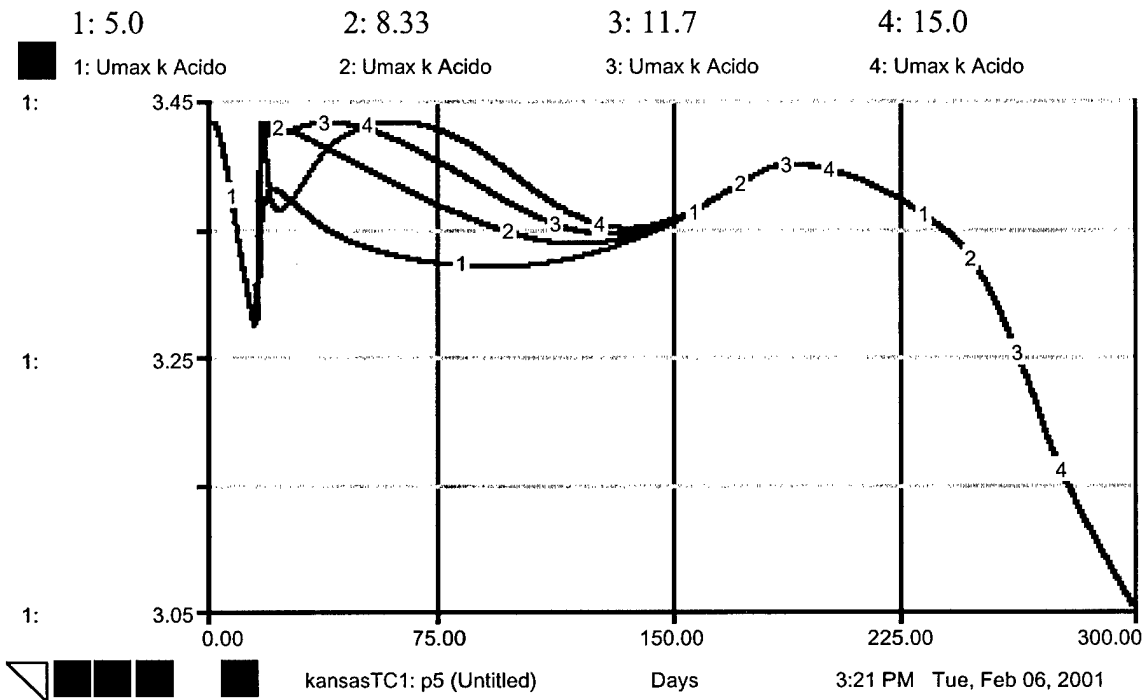
FIGURE 133. U_{MAX} ACIDOGEN WITH VARIOUS HEAT CONSTANT VALUES

1: 5.0	2: 8.33	3: 11.7	4: 15.0
■ 1: Umax k Meth	2: Umax k Meth	3: Umax k Meth	4: Umax k Meth
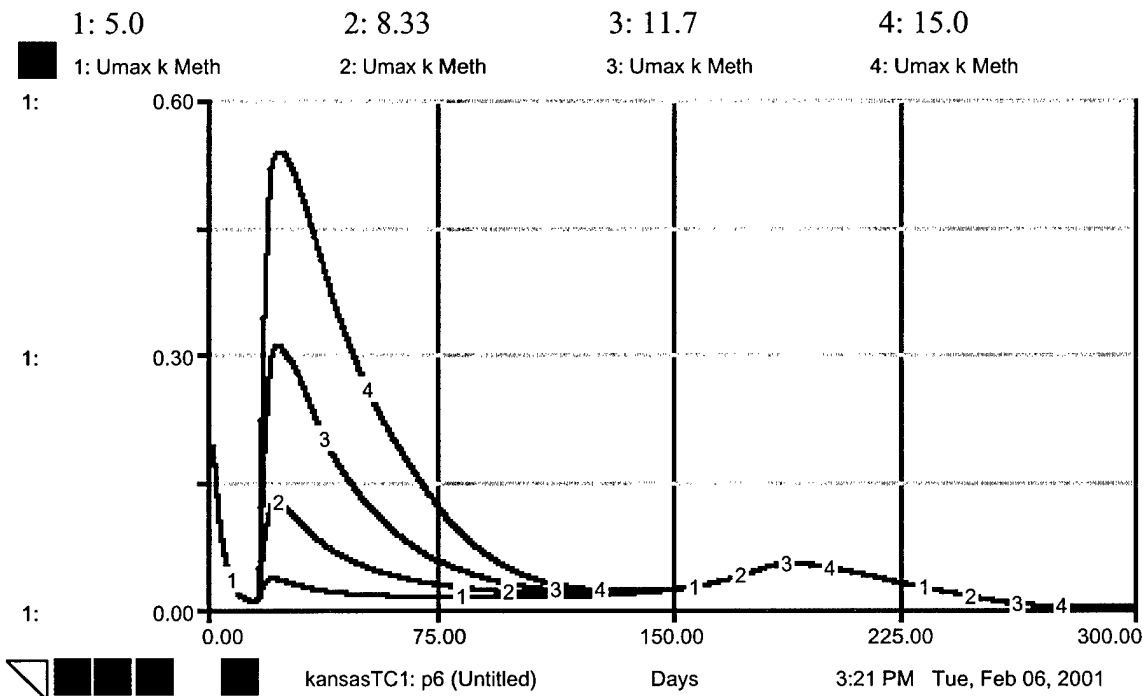
FIGURE 134. U_{MAX} METHANOGEN WITH VARIOUS HEAT CONSTANT VALUES

136

■ 1: Glucose   2: Glucose   3: Glucose   4: Glucose

1:    4.00e+008

1:    2.00e+008

1:    0.00

0.00   75.00   150.00   225.00   300.00

◁ ■■■   ■   kansasTC1: p1 (Untitled)   Days   3:21 PM   Tue, Feb 06, 2001

FIGURE 135. GLUCOSE LEVEL WITH VARIOUS HEAT CONSTANT VALUES

1: 5.0   2: 8.33   3: 11.7   4: 15.0

■ 1: Temperature   2: Temperature   3: Temperature   4: Temperature

1:    35.00

1:    20.00

1:    5.00

0.00   75.00   150.00   225.00   300.00

◁ ■■■   ■   kansasTC1: p2 (Untitled)   Days   3:21 PM   Tue, Feb 06, 2001
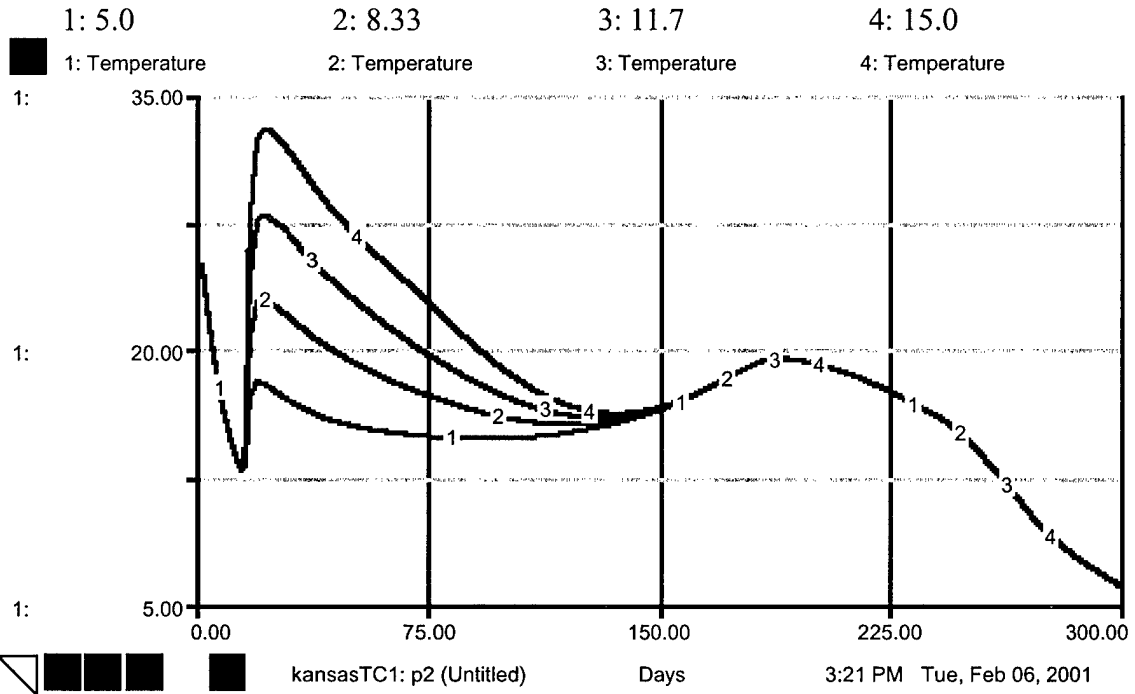
FIGURE 136. TEMPERATURE WITH VARIOUS HEAT CONSTANT VALUES

137

FIGURE 137. UMAX ACIDOGEN WITH VARIOUS HEAT CONSTANT VALUES
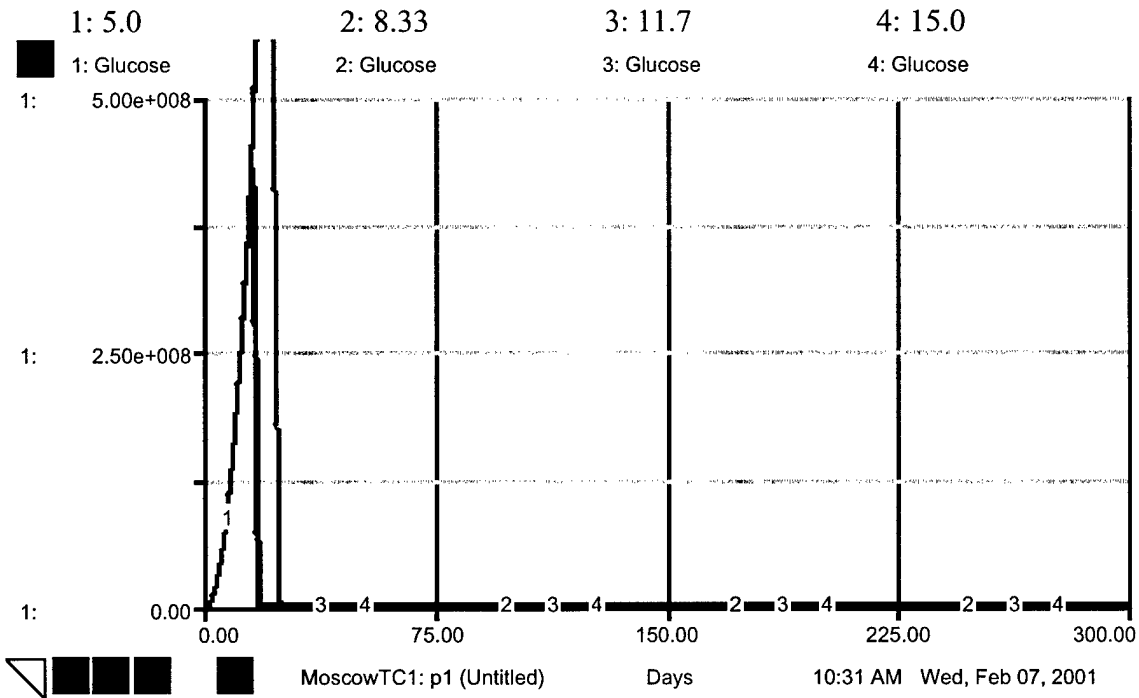
FIGURE 138. GLUCOSE LEVEL WITH VARIOUS HEAT CONSTANT VALUES
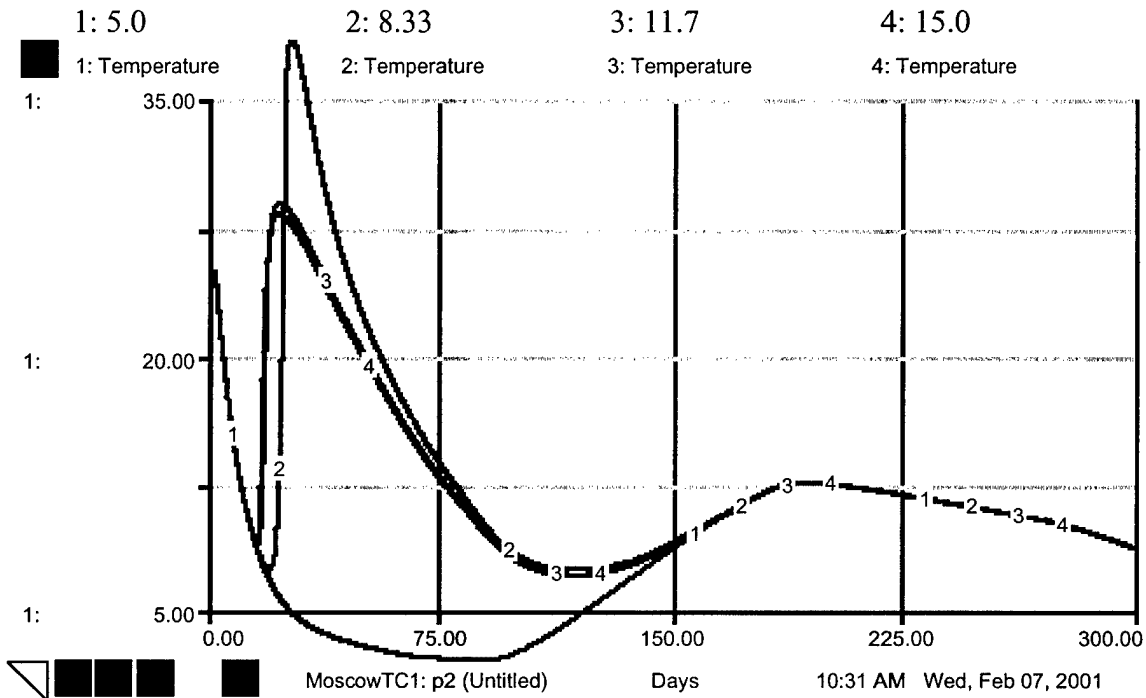
FIGURE 139. TEMPERATURE WITH VARIOUS HEAT CONSTANT VALUES
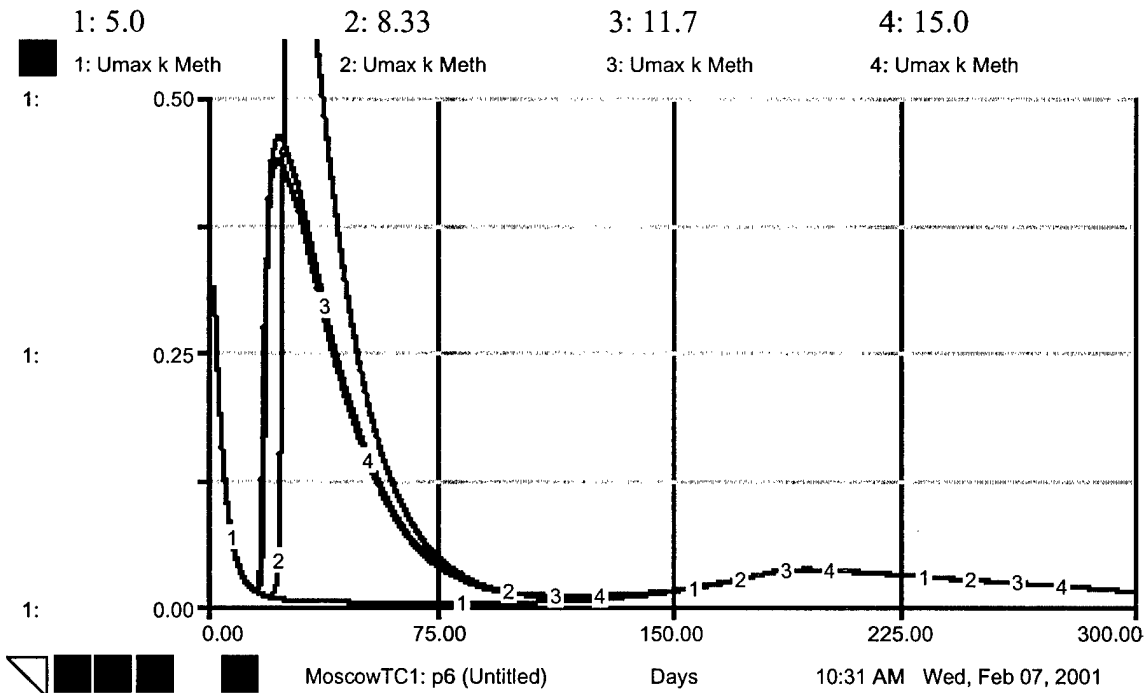
FIGURE 140. U$_{MAX}$ METHANOGEN WITH VARIOUS HEAT CONSTANT VALUES
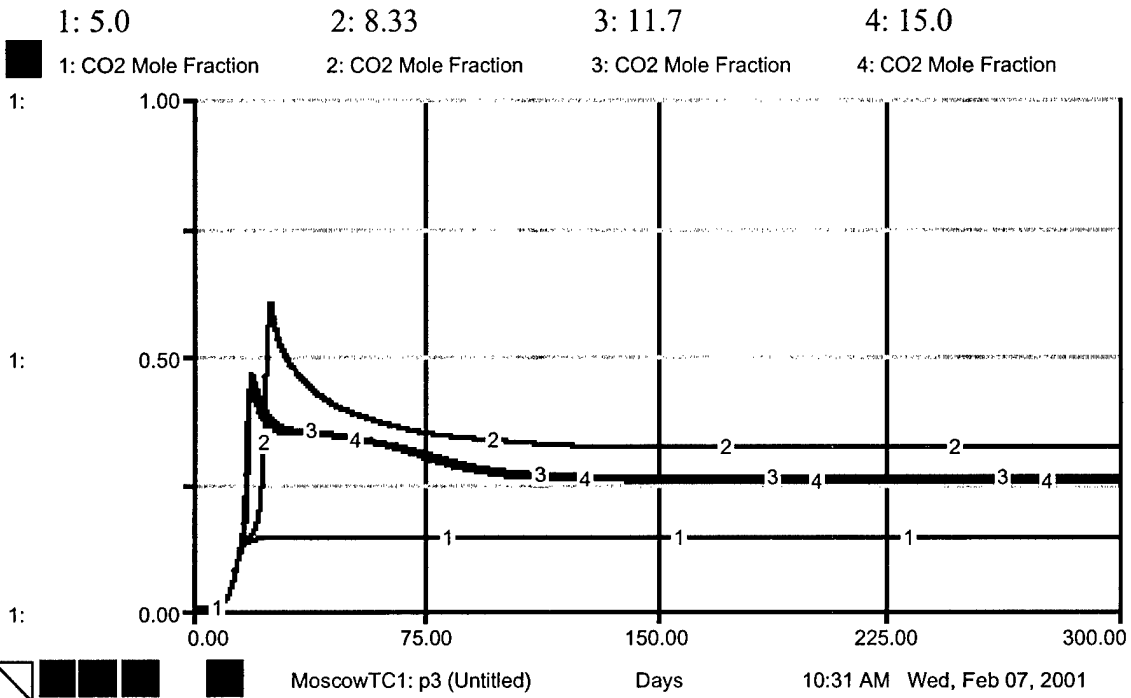
FIGURE 141. CO_2 MOLE FRACTION WITH VARIOUS HEAT CONSTANT VALUES

1: 5.0   2: 8.33   3: 11.7   4: 15.0

■ 1: CO2 Mole Fraction   2: CO2 Mole Fraction   3: CO2 Mole Fraction   4: CO2 Mole Fraction

seasonchangeTC1: p4 (Untitled)   Days   3:04 PM Tue, Feb 06, 2001

FIGURE 142. CO$_2$ MOLE FRACTION WITH VARIOUS HEAT CONSTANT VALUES

1: 5.0   2: 8.33   3: 11.7   4: 15.0

■ 1: Umax k Meth   2: Umax k Meth   3: Umax k Meth   4: Umax k Meth

seasonchangeTC1: p5 (Untitled)   Days   3:04 PM Tue, Feb 06, 2001
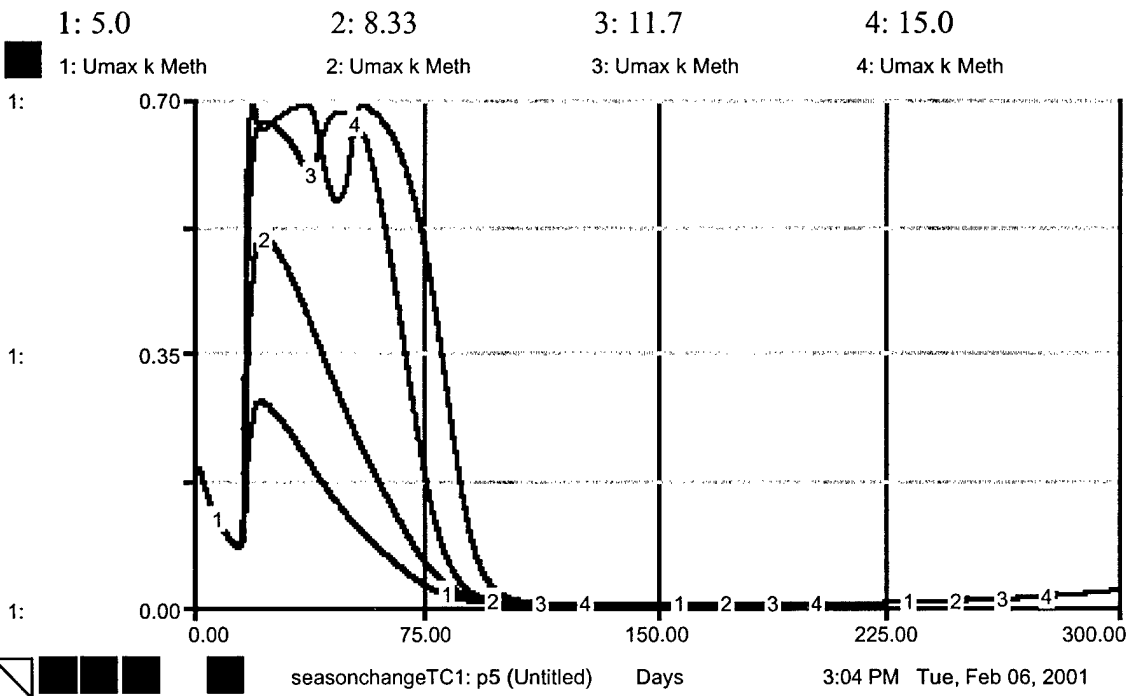
FIGURE 143. U$_{MAX}$ METHANOGEN WITH VARIOUS HEAT CONSTANT VALUES

141
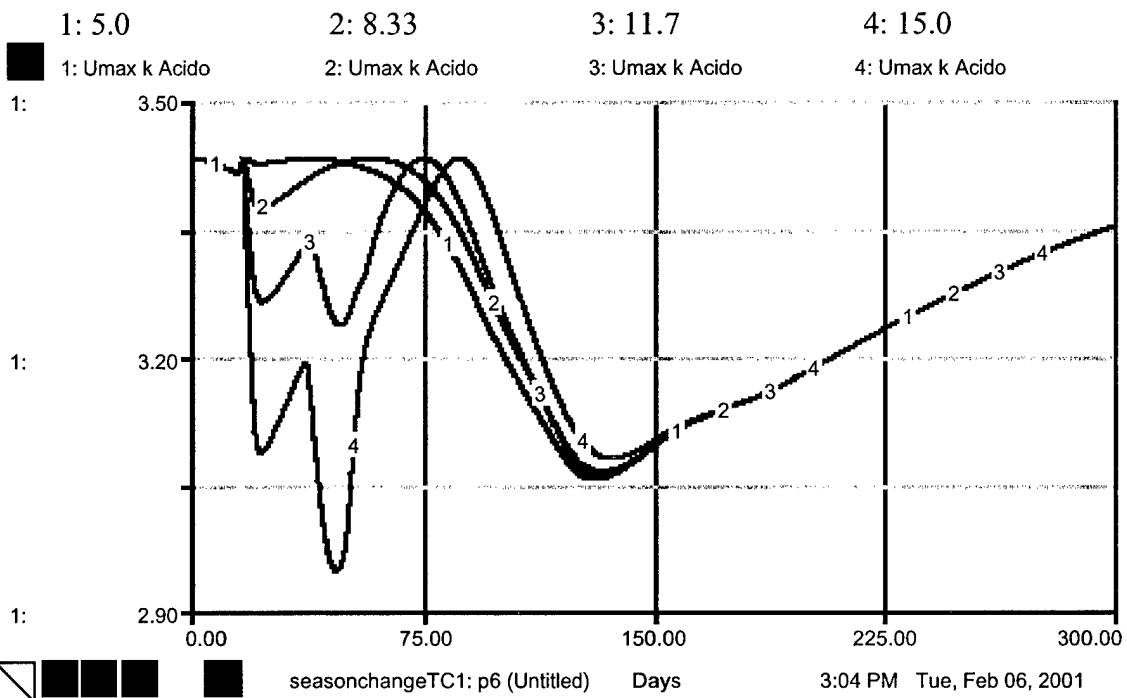
FIGURE 144. U_{MAX} ACIDOGEN WITH VARIOUS HEAT CONSTANT VALUES
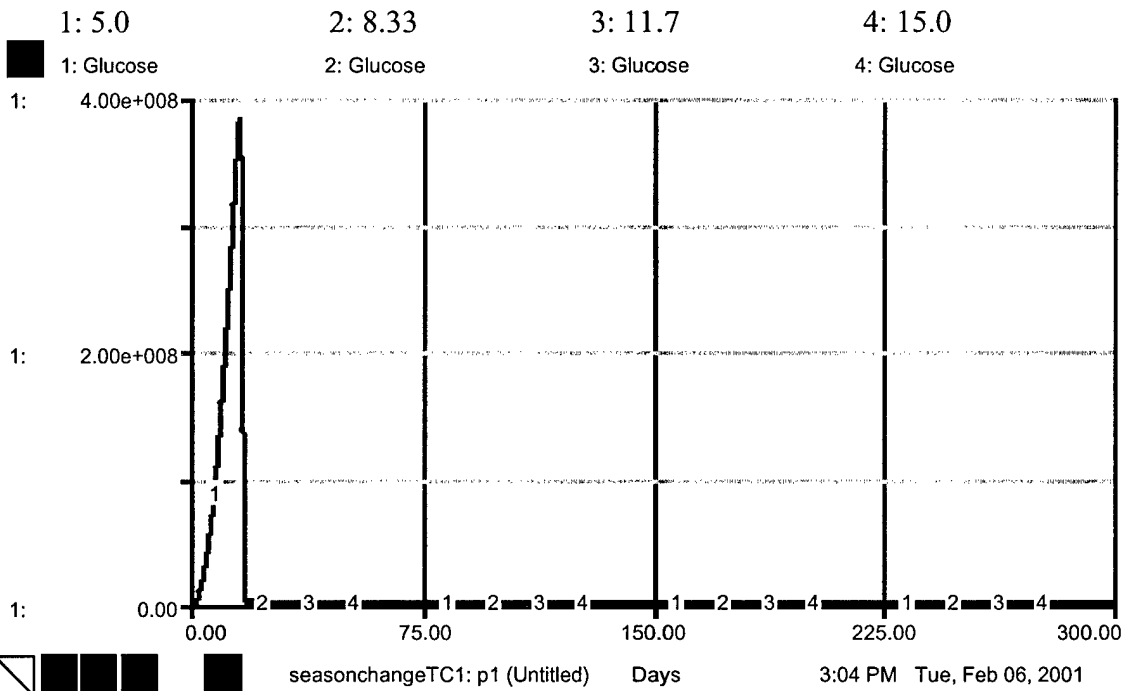
FIGURE 145. GLUCOSE LEVEL WITH VARIOUS HEAT CONSTANT VALUES

1: 5.0   2: 8.33   3: 11.7   4: 15.0
■ 1: Temperature   2: Temperature   3: Temperature   4: Temperature

seasonchangeTC1: p2 (Untitled)   Days   3:04 PM   Tue, Feb 06, 2001
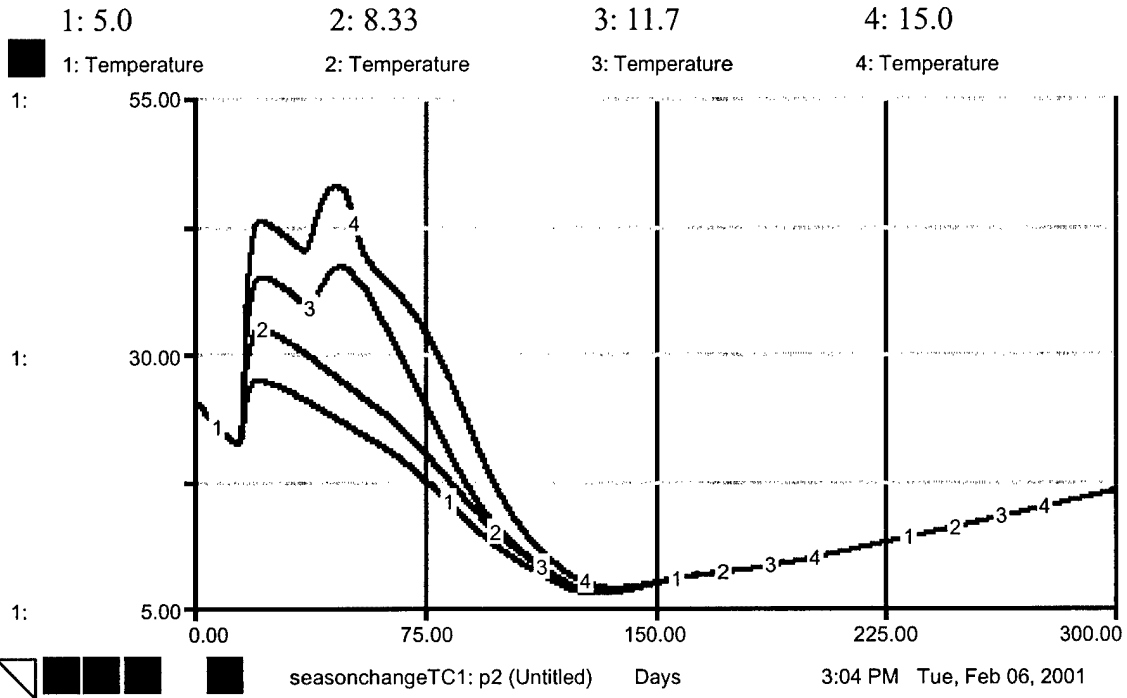
FIGURE 146. TEMPERATURE WITH VARIOUS HEAT CONSTANT VALUES

SEASONAL CHANGE KANSAS: TC 0.01, HC 5.0-15.0 KCAL/MOL GLUCOSE FIGURES 147-151

1: 5.0   2: 8.33   3: 11.7   4: 15.0
■ 1: CO2 Mole Fraction 2: CO2 Mole Fraction 3: CO2 Mole Fraction 4: CO2 Mole Fraction

seasonchangeTC01: p4 (Untitled)   Days   2:46 PM   Tue, Feb 06, 2001
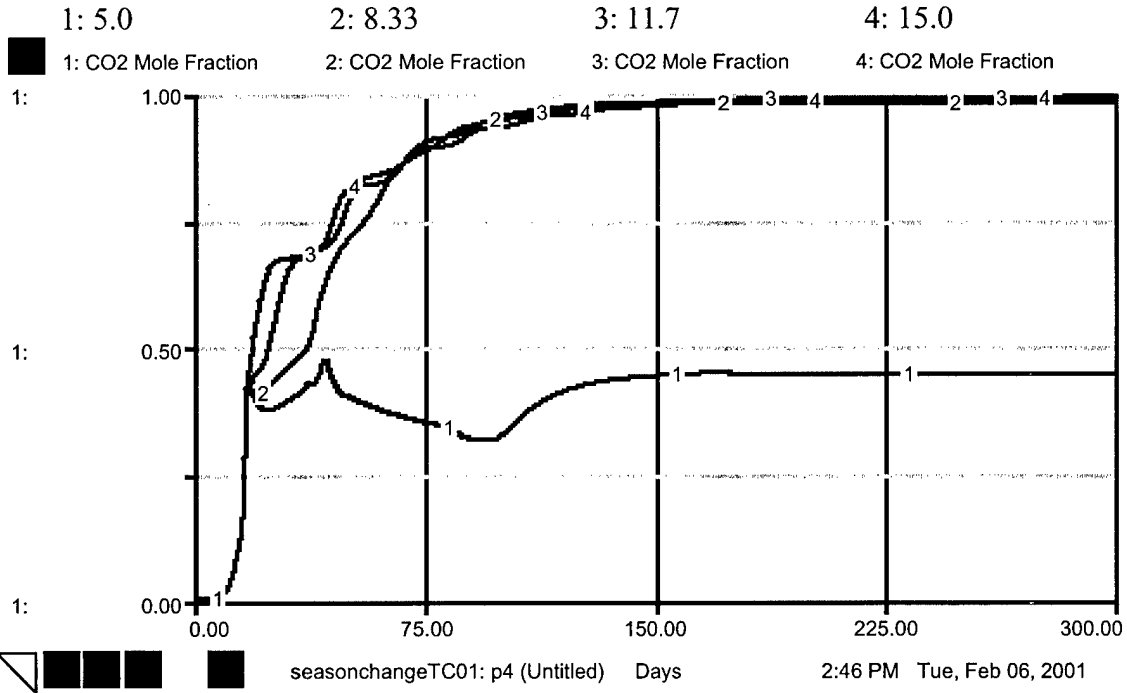
FIGURE 147. CO_2 MOLE FRACTION WITH VARIOUS HEAT CONSTANT VALUES

seasonchangeTC01: p5 (Untitled)   Days   2:46 PM   Tue, Feb 06, 2001
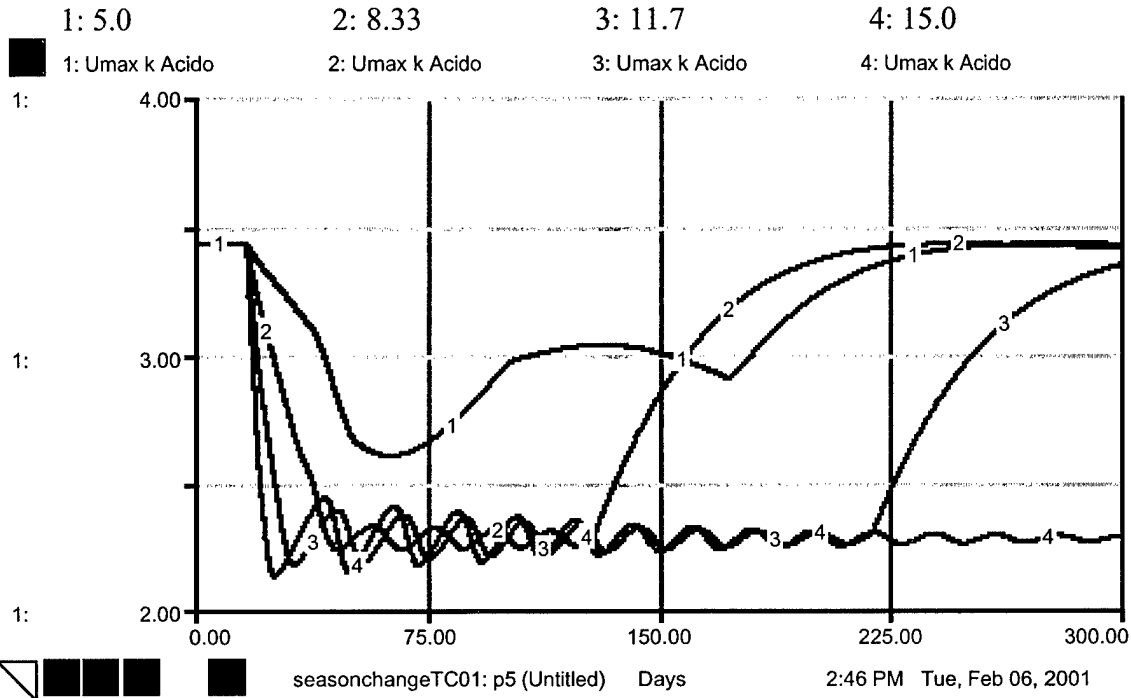
FIGURE 148. U_{MAX} ACIDOGEN WITH VARIOUS HEAT CONSTANT VALUES

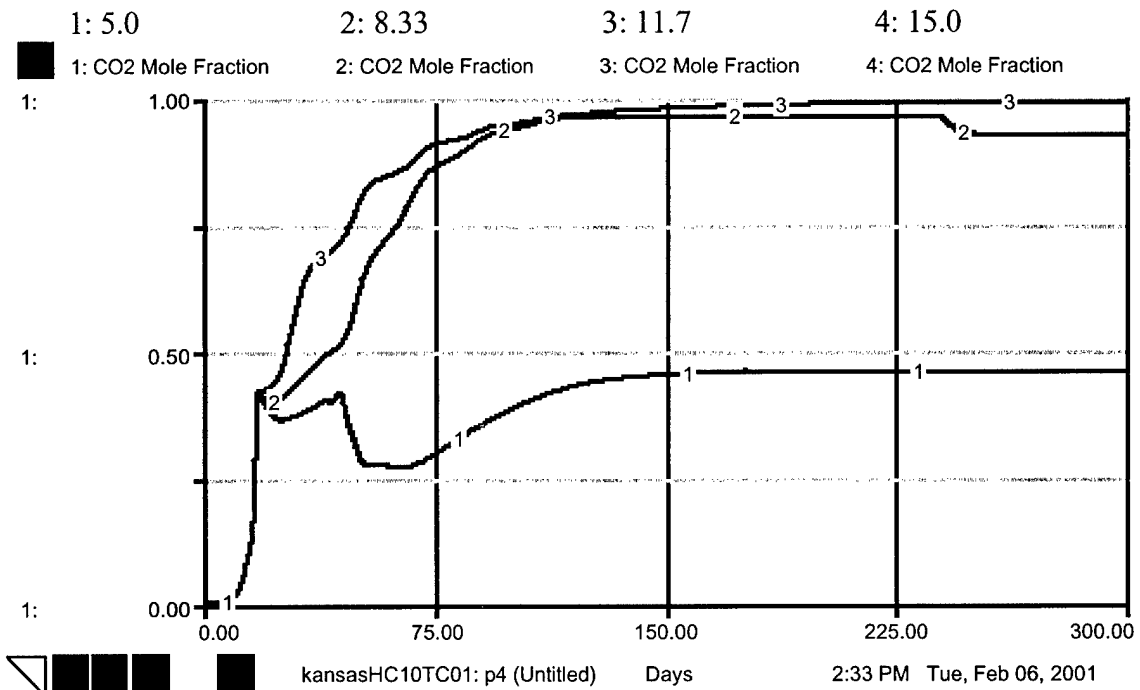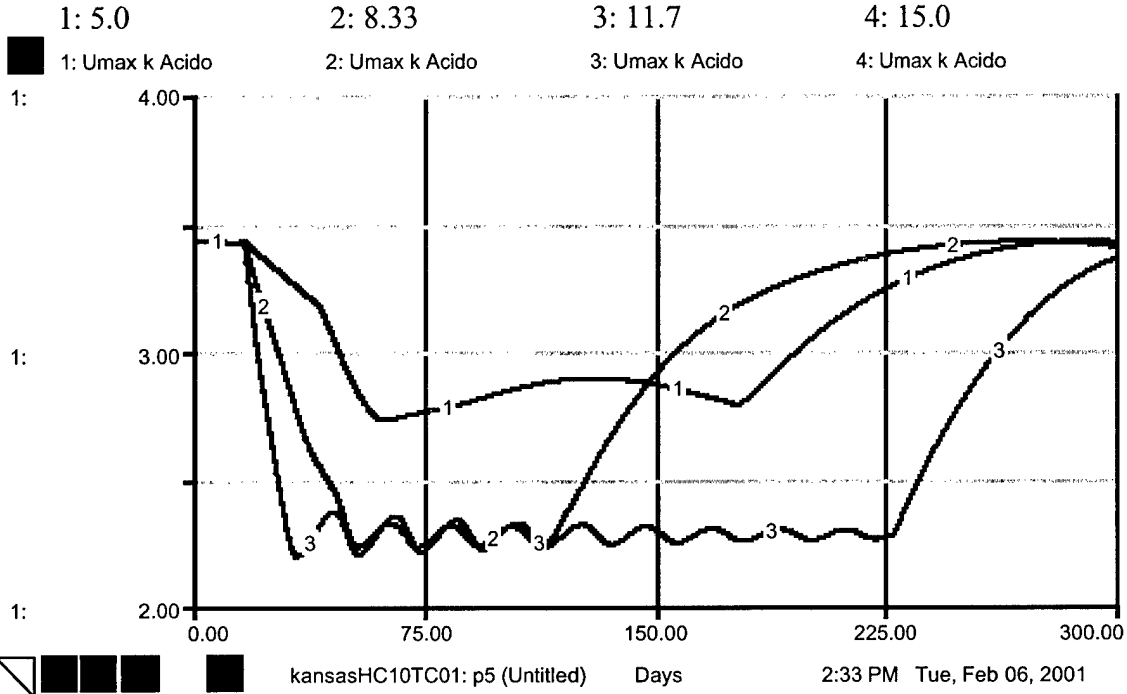seasonchangeTC01: p6 (Untitled)   Days   2:46 PM   Tue, Feb 06, 2001
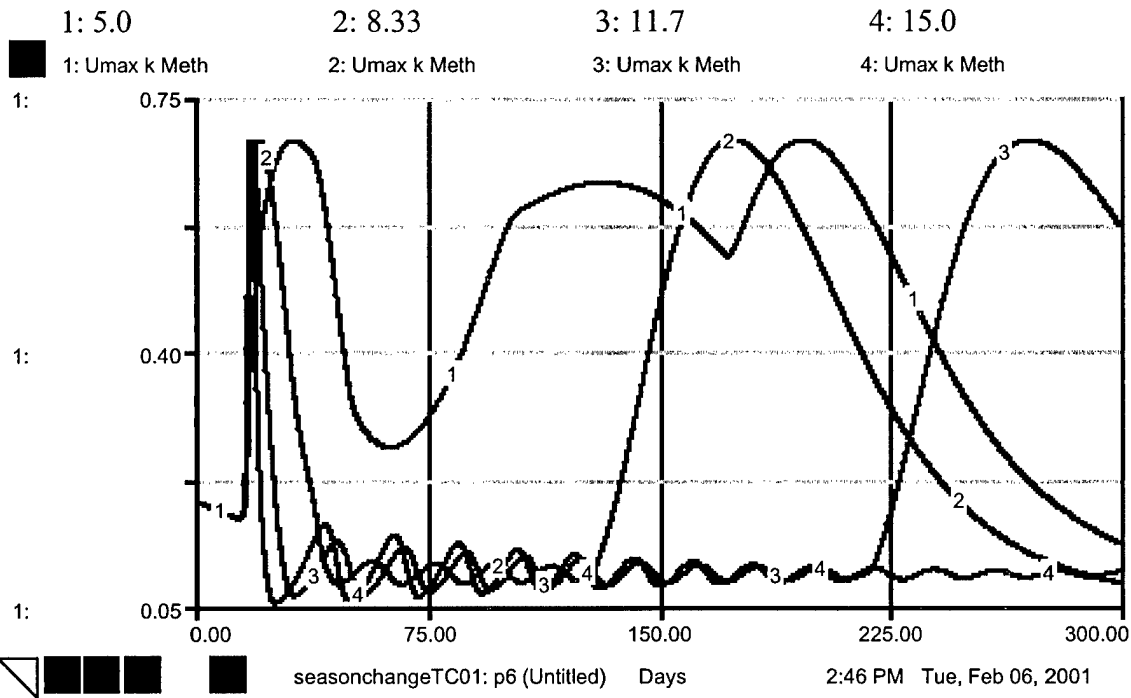
FIGURE 149. U_{MAX} METHANOGEN WITH VARIOUS HEAT CONSTANT VALUES

144
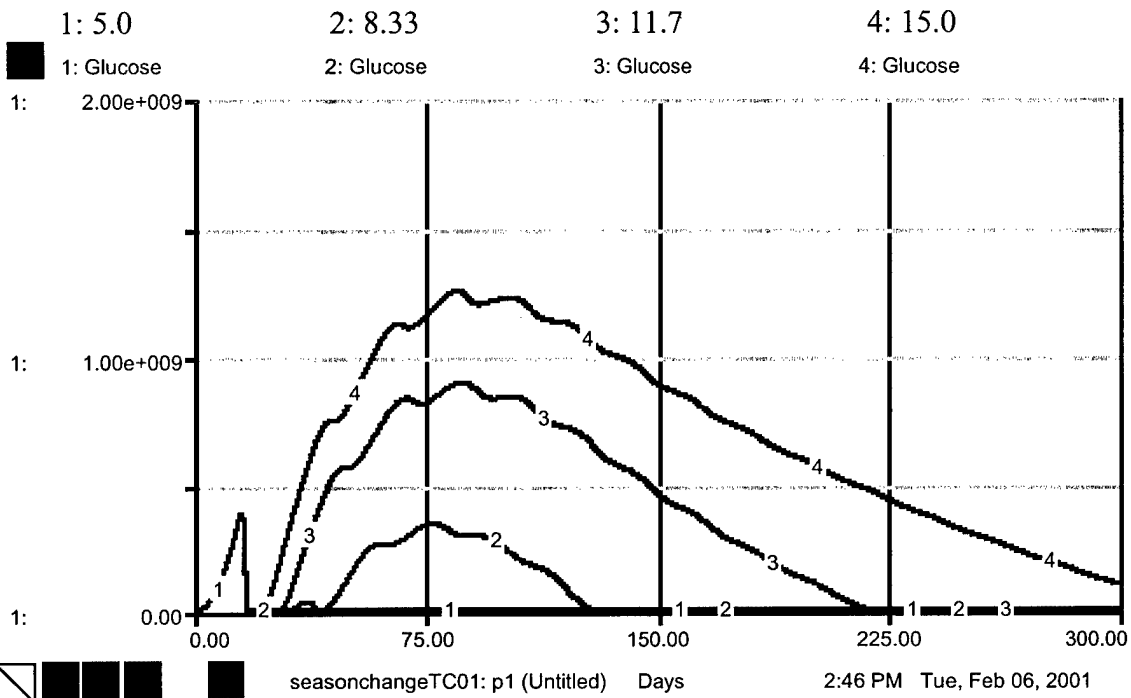
FIGURE 150. GLUCOSE LEVEL WITH VARIOUS HEAT CONSTANT VALUES
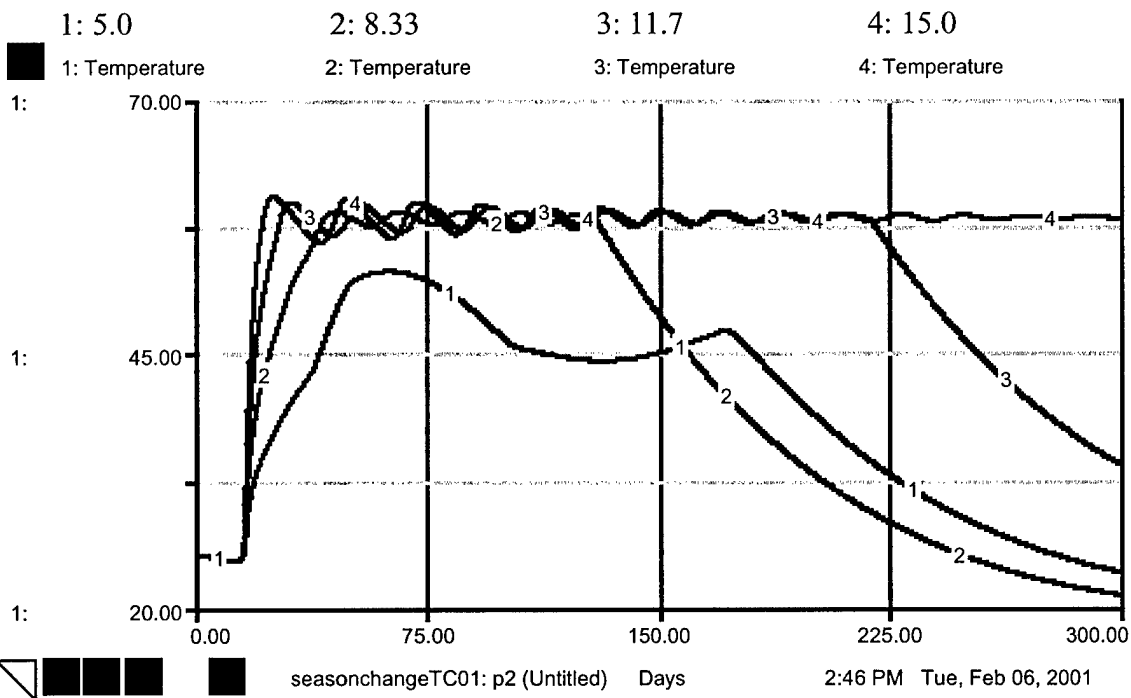
FIGURE 151. TEMPERATURE WITH VARIOUS HEAT CONSTANT VALUES

145

1: 5.0   2: 8.33   3: 11.7   4: 15.0

1: CH4 Mole Fraction   2: CH4 Mole Fraction   3: CH4 Mole Fraction   4: CH4 Mole Fraction

seasonMoscowTC1: p4 (Untitled)   Days   11:23 AM   Wed, Feb 07, 2001

FIGURE 152. CH$_4$ MOLE FRACTION WITH VARIOUS HEAT CONSTANT VALUES

1: 5.0   2: 8.33   3: 11.7   4: 15.0

1: Umax k Meth   2: Umax k Meth   3: Umax k Meth   4: Umax k Meth

seasonMoscowTC1: p5 (Untitled)   Days   11:23 AM   Wed, Feb 07, 2001
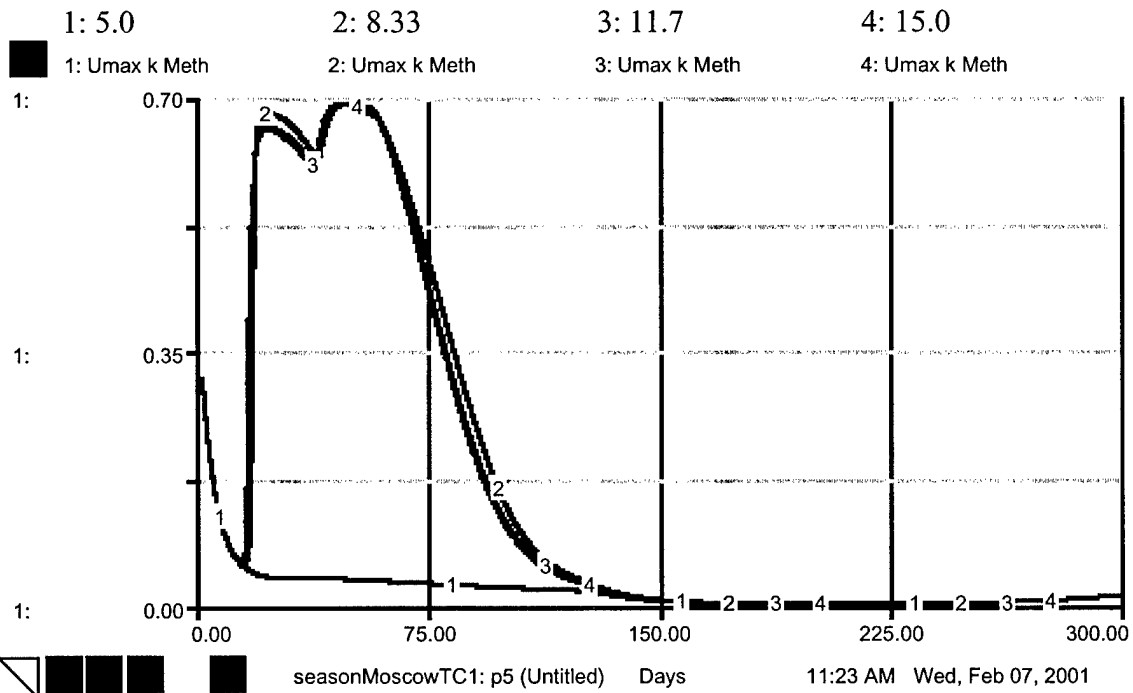
FIGURE 153. U$_{MAX}$ METHANOGEN WITH VARIOUS HEAT CONSTANT VALUES

146

1:    3.50

1:    3.05

1:    2.60

     0.00   75.00   150.00   225.00   300.00

seasonMoscowTC1: p6 (Untitled)   Days   11:23 AM   Wed, Feb 07, 2001

FIGURE 154. U_{MAX} ACIDOGEN WITH VARIOUS HEAT CONSTANT VALUES

1:    4.00e+008

1:    2.00e+008

1:    0.00

     0.00   75.00   150.00   225.00   300.00

seasonMoscowTC1: p1 (Untitled)   Days   11:23 AM   Wed, Feb 07, 2001

FIGURE 155. GLUCOSE LEVEL WITH VARIOUS HEAT CONSTANT VALUES

147
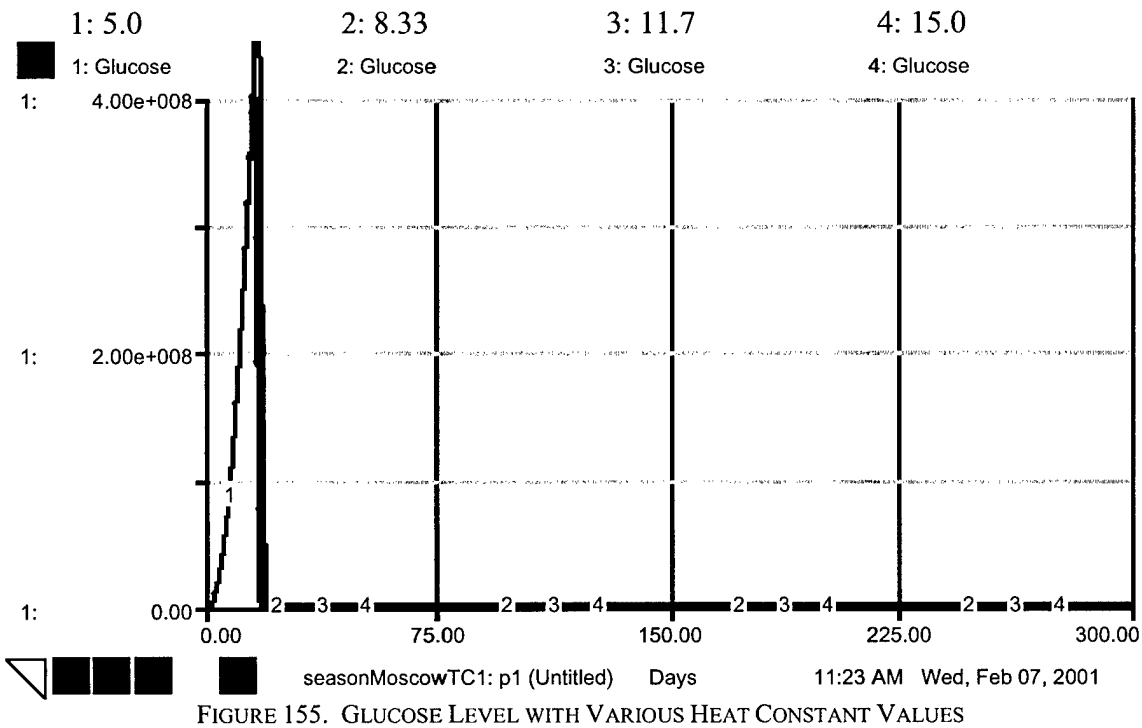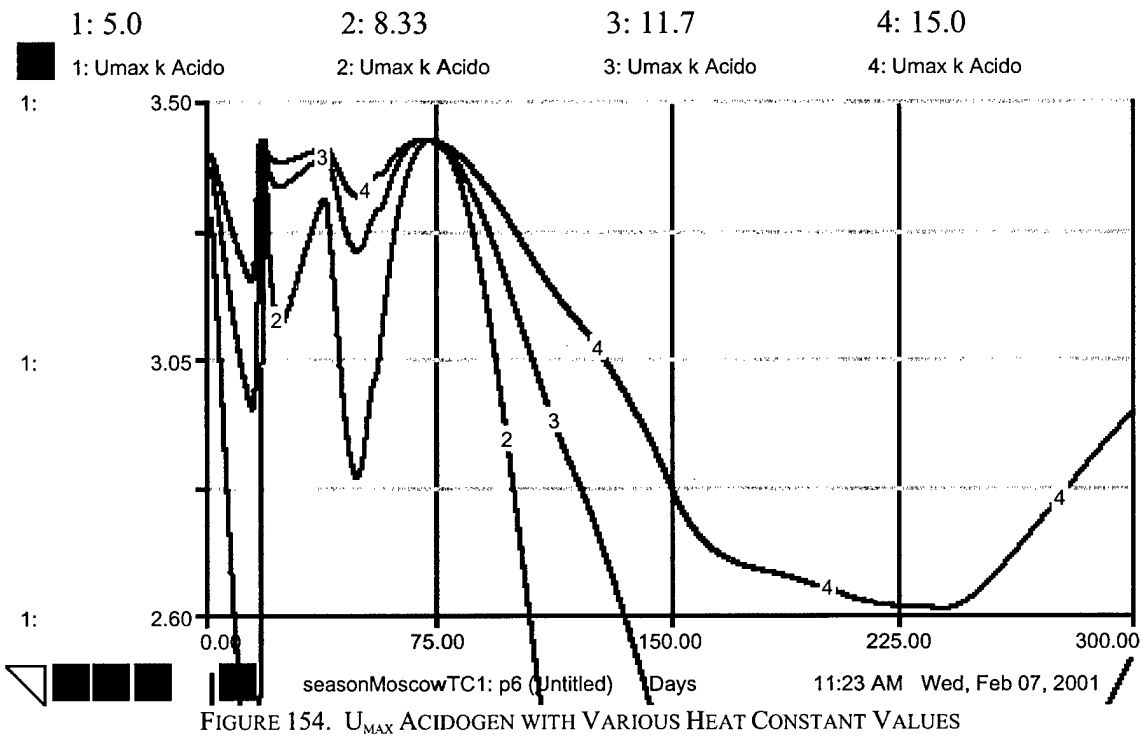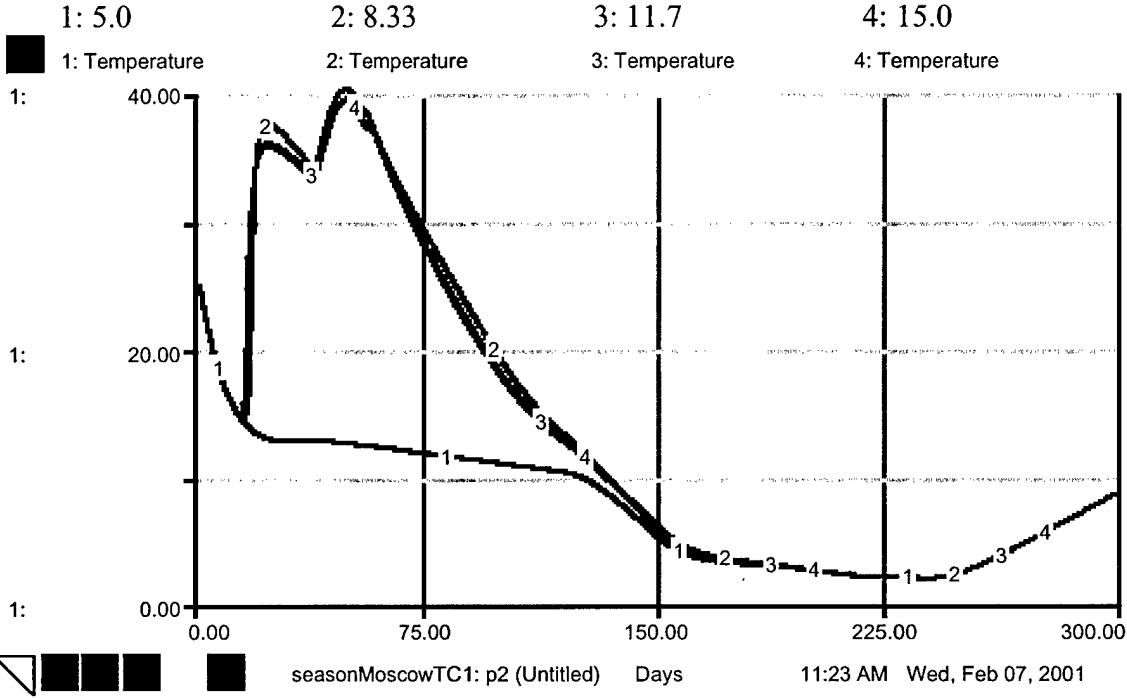
FIGURE 156. TEMPERATURE WITH VARIOUS HEAT CONSTANT VALUES
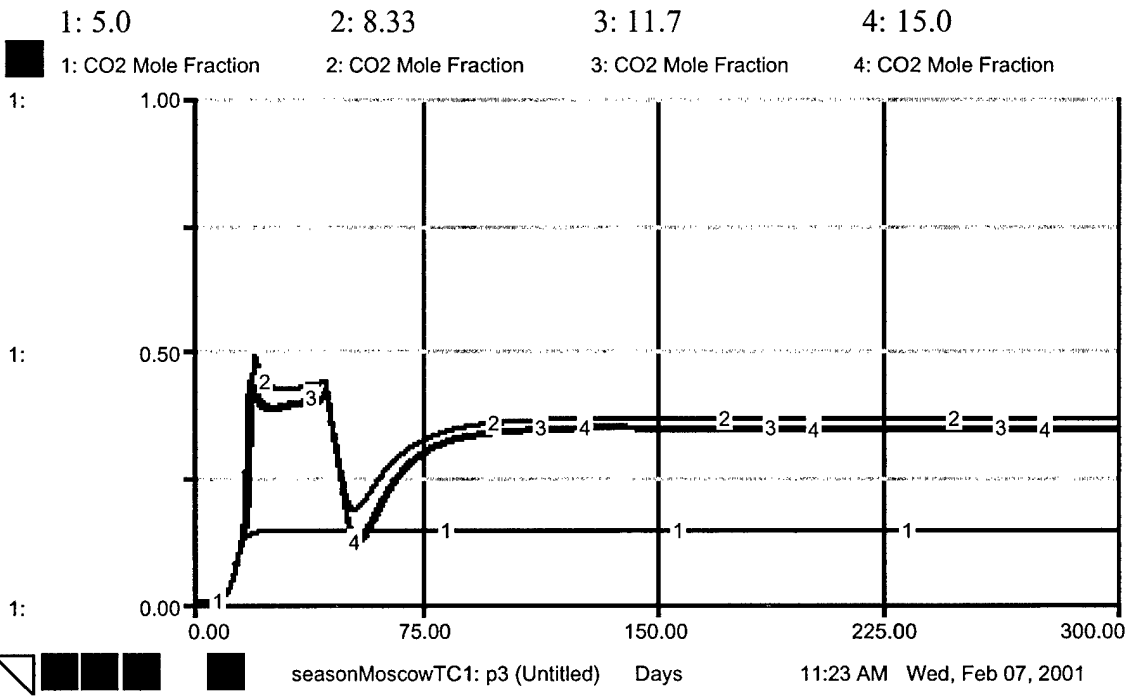
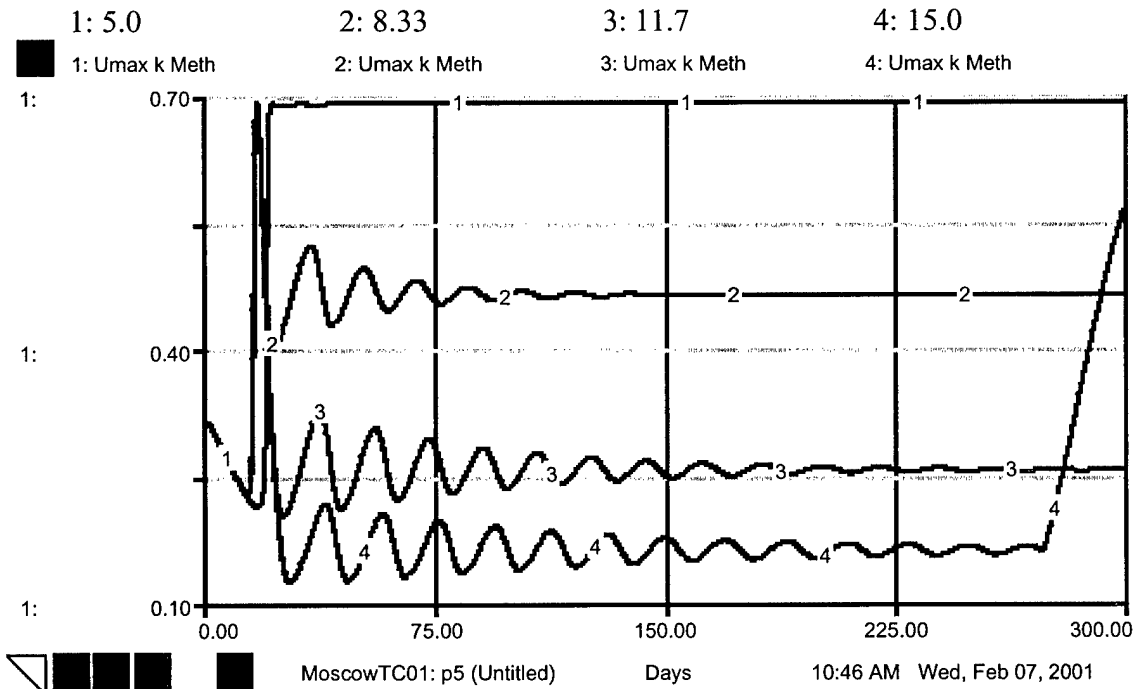FIGURE 157. CO₂ MOLE FRACTION WITH VARIOUS HEAT CONSTANT VALUES

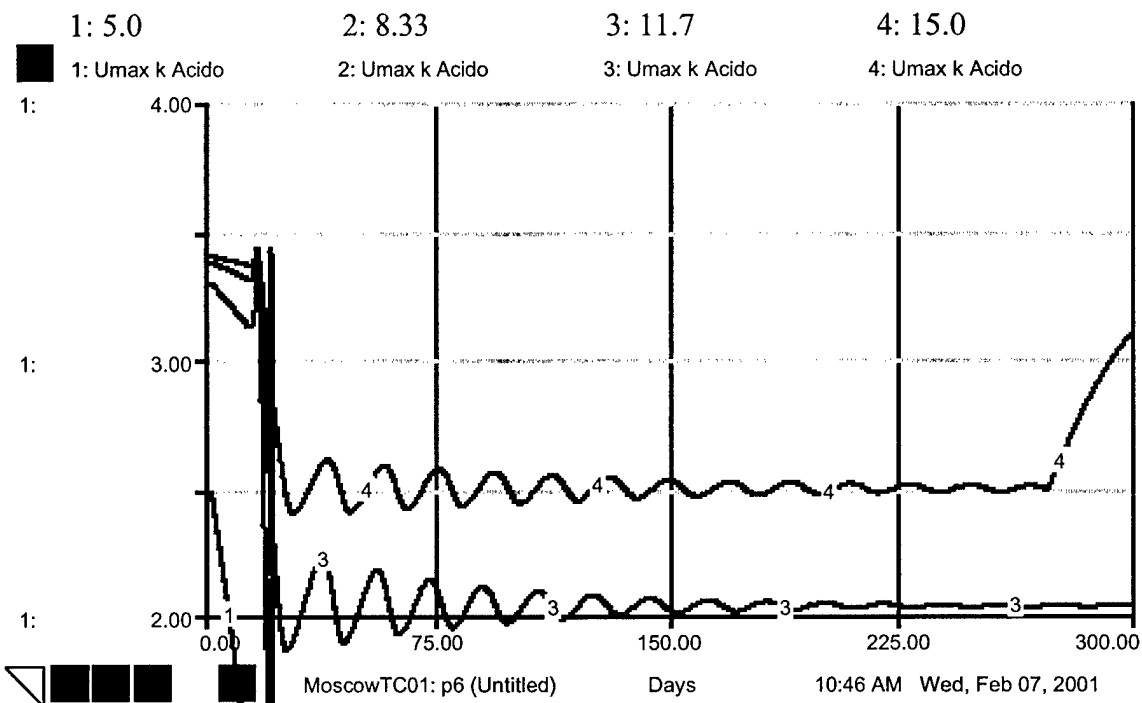FIGURE 158. GLUCOSE LEVEL WITH VARIOUS HEAT CONSTANT VALUES
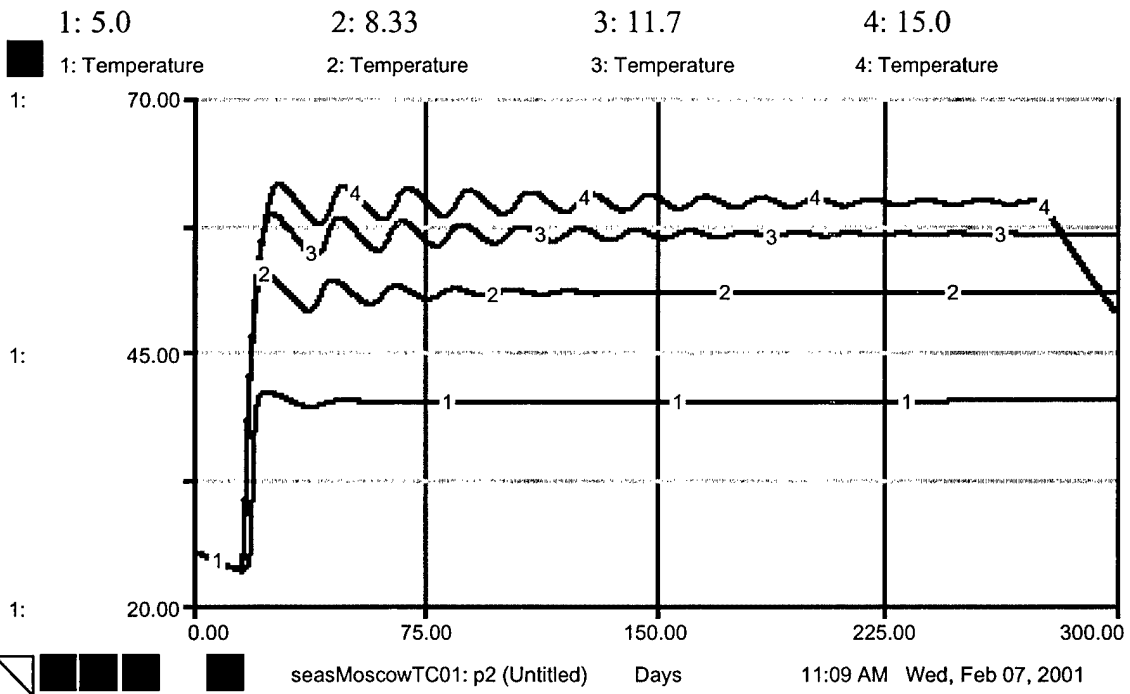
FIGURE 159. TEMPERATURE WITH VARIOUS HEAT CONSTANT VALUES

149
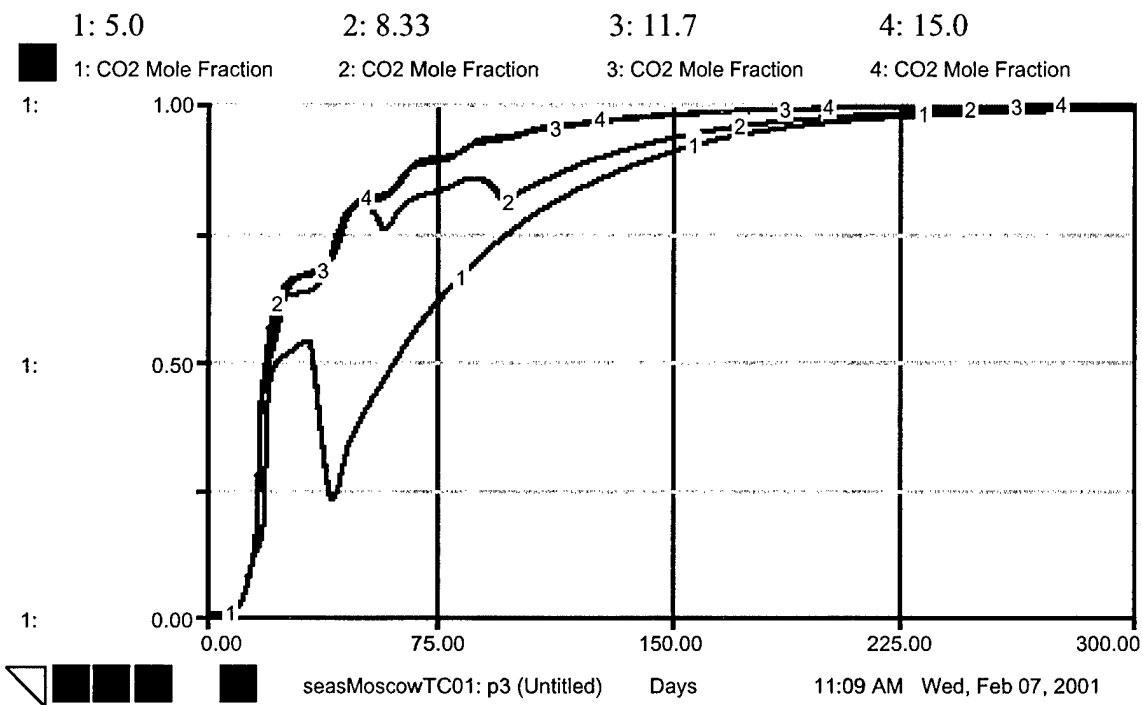
FIGURE 160. CO$_2$ MOLE FRACTION WITH VARIOUS HEAT CONSTANT VALUES
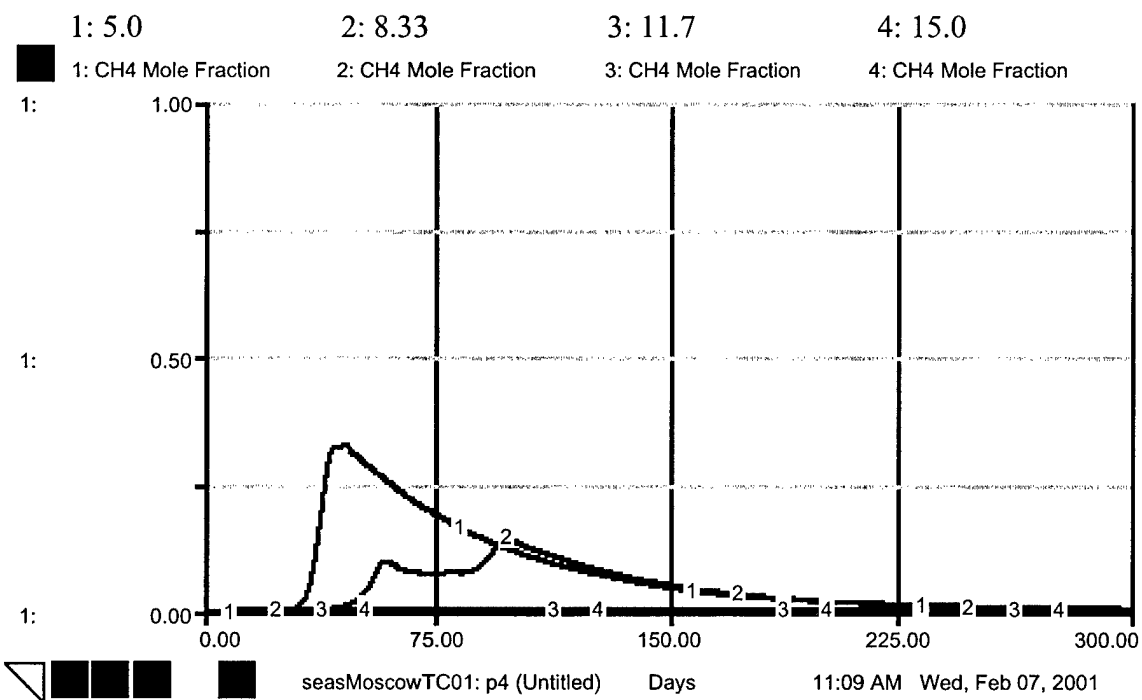
FIGURE 161. CH$_4$ MOLE FRACTION WITH VARIOUS HEAT CONSTANT VALUES

FIGURE 162. U~MAX~ METHANOGEN WITH VARIOUS HEAT CONSTANT VALUES

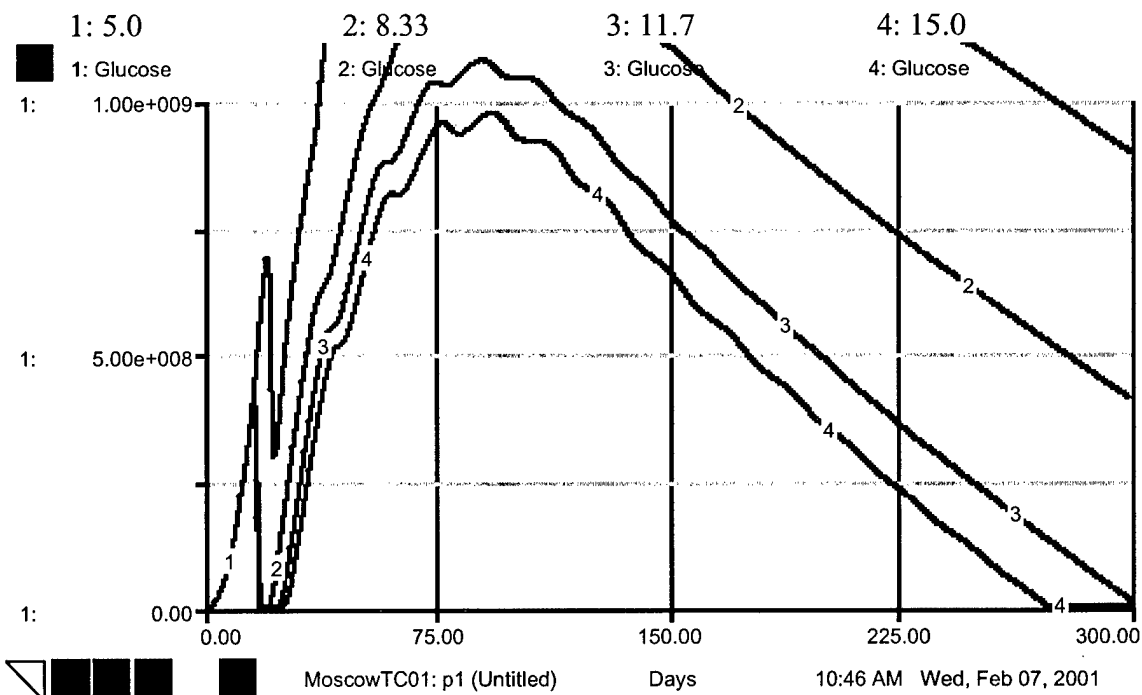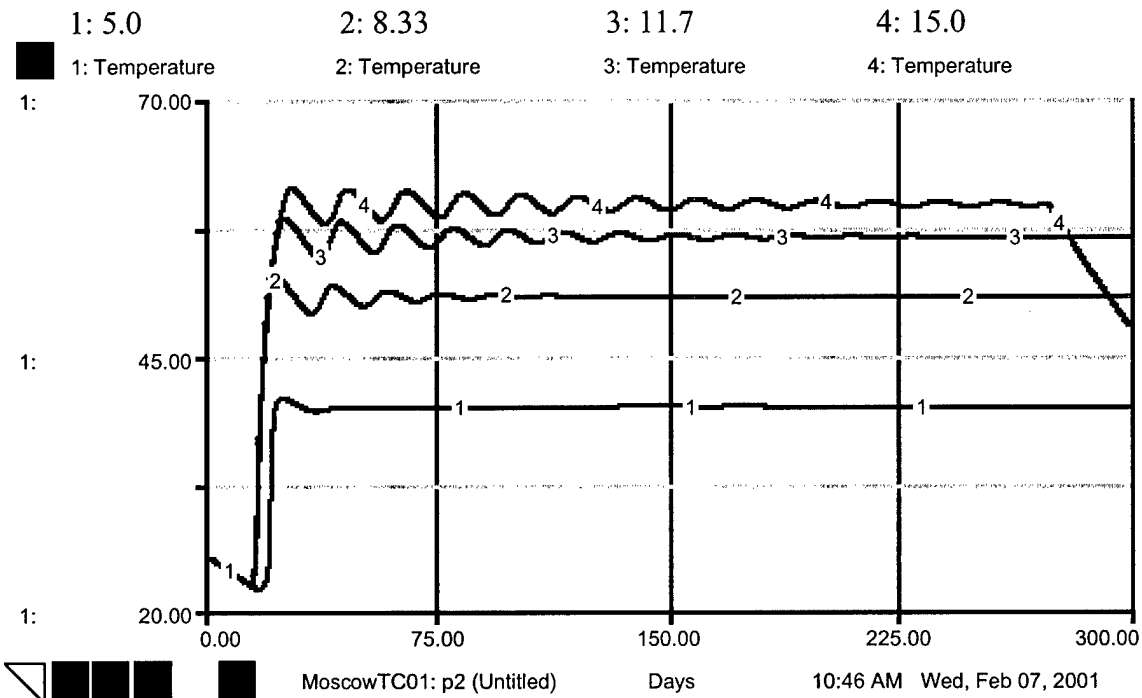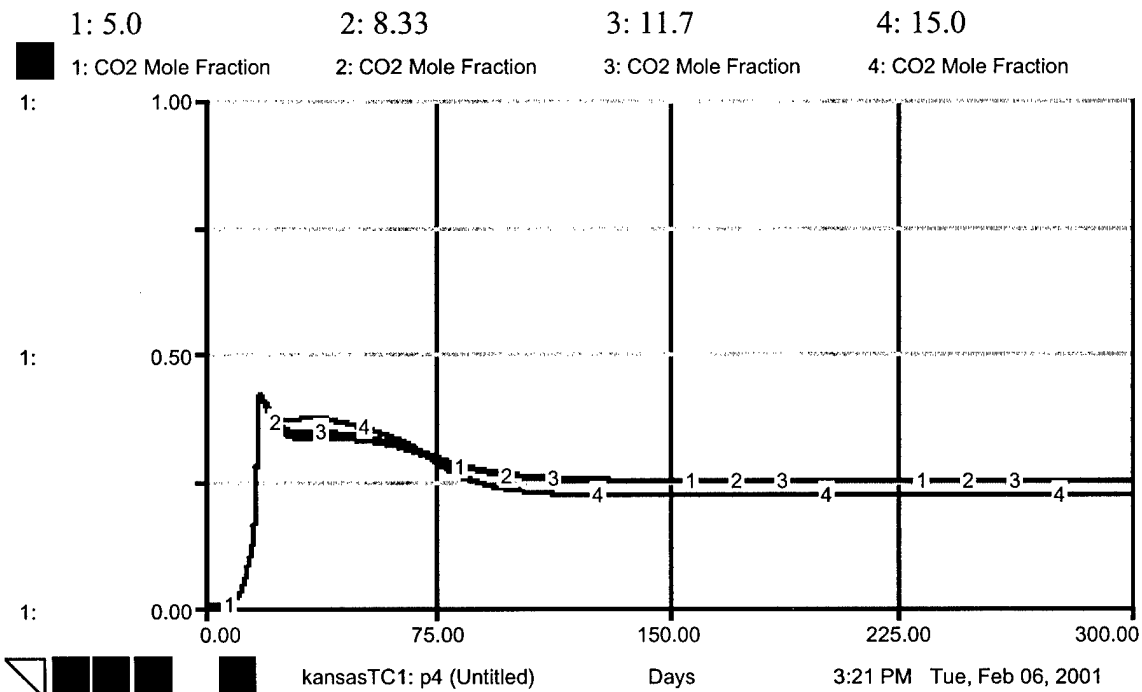FIGURE 163. U~MAX~ ACIDOGEN WITH VARIOUS HEAT CONSTANT VALUES

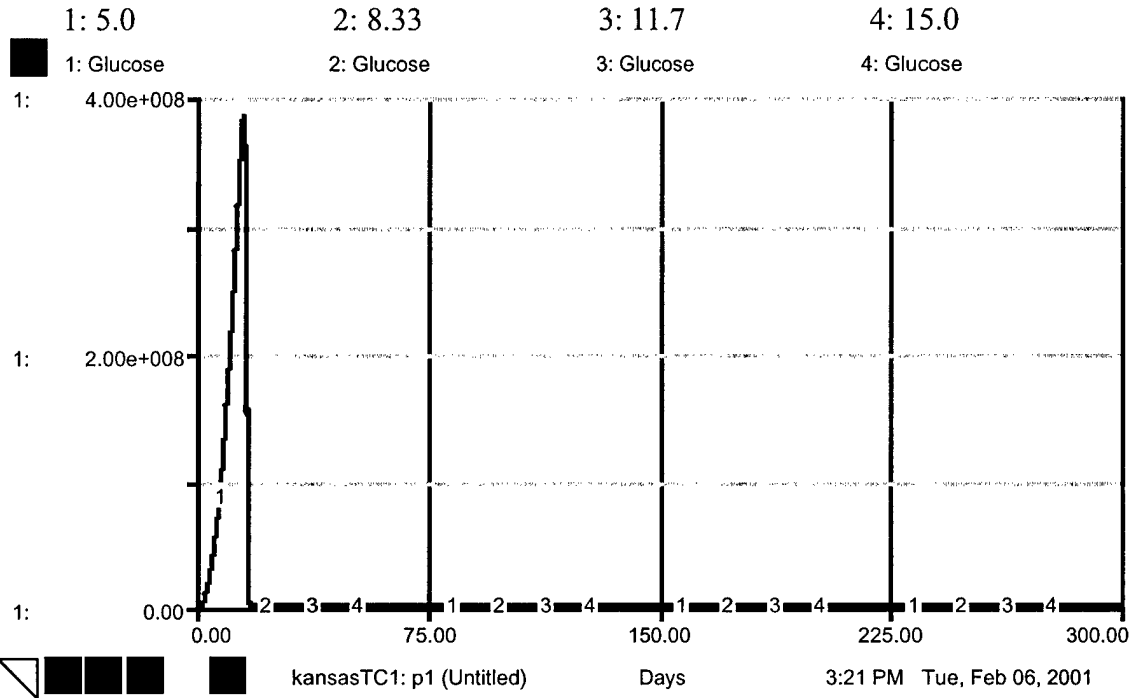# Appendix B: Arrhenius Model Structure

Glucose --> Butyrate + 2CO2 + 2H2

Appendix D Model Structure

The Temperature Sector immediate below was developed for this model, Shelley created the remaining sectors.

Total Gas Mole Capacity

PF Growth Factor

Solid Org Waste

Porosity Factor

Org Sphere Volume

Inorg Waste

Org Sphere Radius

Org Surface Area

Inorg Sphere Number

Initial Radius

Surf Area Exp Factor

Org Waste Fraction

Total Spheres

Cell Volume

Avg Solid Density

Initial Cell Volume

Acet Conc

Organic Waste Volume

Acetate

Aerobic Fract

Initial Sphere Vol

Cell Length

Org Density Factor

Org Sphere Number

Cell Depth

Cell Width

H2 umax inh factor

Cell Porosity Org Waste Density   Inorg Waste Density

pH...

pH Factor

pH   Acet Conc

156

Chemical Characteristics & Stoichiometry

Total Biomass Decay

158

Aerobic Biomass Sector

Clostridial Biomass Sector

Butyrate Biomass Sector

Lactate 1 Biomass Sector

159

Lactate 2 Biomass Sector

Lactate 2 Growth
Lactate 2 Decay
Nutrients
Glu to Lactate 2 Bio
Lactate 2 Biomass
Lactate 2 Decay Rate Factor
Solid Org Waste
Glucose
pH Factor
Th Lactate 2 Growth
Lactate 2 Decay Rate
Lactate 2 umax
Th Lactate 2 Depl
Anaero O2 Factor
Lactate 2 K
Lactate 2 Resp
Umax k Acido
Smth Th Lactate 2 Growth
H2 umax inh factor
Lactate 2 Yield
kd Acidog
Max Fract Lactate 2 Mass

Bifidum Biomass Sector

Bifidum Growth
Bifidum Decay
Nutrients
Glu to Bif Bio
Bifidum Biomass
Bifidum Decay Rate Factor
Solid Org Waste
Glucose
pH Factor
Th Bifidum Growth
Bifidum Decay Rate
Bifidum umax
Th Bifidum Depl
Bifidum K
Bifidum Resp
Anaero O2 Factor
Umax k Acido
Smth Th Bifidum Growth
H2 umax inh factor
Bifidum Yield
kd Acidog
Max Fract Bifidum Mass

Propionate Biomass Sector

Propionate Growth
Propionate Decay
Nutrients
Glu to Prop Bio
Propionate Biomass
Propionate Decay Rate Factor
Solid Org Waste
Glucose
pH Factor
Th Propionate Growth
Propionate Decay Rate
Propionate umax
Th Propionate Depl
Propionate K
Propionate Resp
Anaero O2 Factor
Umax k Acido
Smth Th Propionate Growth
H2 umax inh factor
Propionate Yield
kd Acidog
Max Fract Propionate Mass

Ethanol Biomass Sector

Ethanol Growth
Ethanol Decay
Nutrients
Glu to Eth Bio
Ethanol Biomass
Ethanol Decay Rate Factor
Solid Org Waste
Glucose
pH Factor
Th Ethanol Growth
Ethanol Decay Rate
Ethanol umax
Th Ethanol Depl
Ethanol K
Ethanol Resp
Anaero O2 Factor
Umax k Acido
Smth Th Ethanol Growth
H2 umax inh factor
Ethanol Yield
kd Acidog
Max Fract Ethanol Mass

160

Acetate Biomass Sector

Acetate Growth — Acetate Decay
Nutrients
Glu to Acet Bio — Acetate Biomass
Th Acetate Growth — Glucose
pH Factor — Acetate Decay Rate Factor
Acetate umax — Solid Org Waste
Anaero O2 Factor — Acetate Decay Rate
Acetate K — Th Acetate Depl
Acetate Resp
Smth Th Acetate Growth — H2 umax inh factor
kd Acidog
Acetate Yield — Max Fract Acetate Mass

Mixed Acid Biomass Sector

Mixed Growth — Mixed Decay
Nutrients
Glu to Mixed Bio — Mixed Biomass
Th Mixed Growth — Glucose
pH Factor — umax k Acido — Mixed Decay Rate Factor
Mixed umax — Solid Org Waste
Anaero O2 Factor — Mixed K — Mixed Decay Rate
Th Mixed Depl
Mixed Resp
Smth Th Mixed Growth — H2 umax inh factor
kd Acidog
Mixed Yield — Max Fract Mixed Mass

Butanol Acetone Biomass Sector

Butnl Acet Growth — Butnl Acet Decay
Nutrients
Glu to Butanol Bio — Butnl Acet Biomass
Th Butnl Acet Growth — Glucose
Umax k Acido — Butnl Acet Decay Rate Factor
pH Factor — Butnl Acet umax — Solid Org Waste
Anaero O2 Factor — Butnl Acet K — Butnl Acet Decay Rate
Th Butnl Acet Depl
Butnl Acet Resp
Smth Th Butnl Acet Growth — Smth Glu
kd Acidog
Butnl Acet Yield — Max Fract Butnl Acet Mass

161

Butyrate Acetogen Biomass Sector

Lact to Prop Acetogen Biomass Sector

Propionate Acetogen Biomass Sector

Ethanol Acetogen Biomass Sector

162

Acetate Methanogen Biomass Sector

Formate Methanogen Biomass Sector

Carbopn Dioxide Methanogen Biomass Sector

Total Mass Sector

Butyrate Lactate Acetone Proprionate Butanol Ethanol Formate Hydroxide H Ion H1 BiCarbonate Acetate

Solid Org Waste Glucose Oxygen Hydrogen Carbon Dioxide Methane Water Butyrate Acetogen Biomass

Prop Acetogen Biomass Form Meth Biomass Acetate Meth Biomass CO2 Meth Biomass

Initial Mass Current Mass

Aerobic Biomass Butyrate Biomass Butyl Acet Biomass Lactate 1 Biomass Lactate 2 Biomass Propionate Biomass

Clostridial Biomass Ethanol Biomass Eth Acetogen Biomass Bifidum Biomass Lact to Prop Biomass Mixed Biomass

Mass Balance Sector

H2 Loss CH4 Loss

Net H2 Atm Loss Net CH4 Atm Loss CH4 Atm Loss Percent Mass Deviation Mass Balance Initial Mass

CO2 Loss Net CO2 Atm Loss O2 Loss

H2 Loss to Atm Net O2 Atm Loss Net Gas Loss CO2 Atm Loss O2 Atm Exch Current Mass

Gas Sector

Moisture Sector

Appendix E Model Equations

Acetate Biomass Sector

Acetate_Biomass(t) = Acetate_Biomass(t - dt) + (Acetate_Growth - Acetate_Decay) * dt
INIT Acetate_Biomass = 100000

INFLOWS:
Acetate_Growth = Glu_to_Acet_Bio

OUTFLOWS:
Acetate_Decay = Acetate_Biomass*Acetate_Decay_Rate
Acetate_Decay_Rate = (0.15 + Acetate_Decay_Rate_Factor*((Acetate_umax) - 0.15))+kd_Acidog
Acetate_K = 500
Acetate_Resp = Th_Acetate_Depl - Th_Acetate_Growth
Acetate_umax = Umax_k_Acido
Acetate_Yield = .5
Max_Fract_Acetate_Mass = .01
Smth_Th_Acetate_Growth = SMTH1(Th_Acetate_Growth,1)
Th_Acetate_Depl = Th_Acetate_Growth/Acetate_Yield
Th_Acetate_Growth = IF (Nutrients=1) THEN
pH_Factor*Anaero_O2_Factor*Acetate_Biomass*(Acetate_umax*H2_umax_inh_factor*Glucose)/(Acetat
e_K+Glucose) ELSE 0
Acetate_Decay_Rate_Factor =
GRAPH(Acetate_Biomass/(Max_Fract_Acetate_Mass*INIT(Solid_Org_Waste)))
(0.00, 0.00), (0.1, 0.00), (0.2, 0.00), (0.3, 0.00), (0.4, 0.00), (0.5, 0.185), (0.6, 0.36), (0.7, 0.52), (0.8, 0.7),
(0.9, 0.86), (1, 1.00)

Acetate Methanogen Biomass Sector

Acetate_Meth_Biomass(t) = Acetate_Meth_Biomass(t - dt) + (Acet_Meth_Growth - Acet_Meth_Decay) *
dt
INIT Acetate_Meth_Biomass = 10000

INFLOWS:
Acet_Meth_Growth = Acet_Meth_Bio

OUTFLOWS:
Acet_Meth_Decay = Acetate_Meth_Biomass*Acet_Meth_Decay_Rate
Acet_Meth_Decay_Rate = (0.1 + Acet_Meth_Decay_Rate_Factor*((Acet_Meth_umax) - 0.1))+KdMeth
Acet_Meth_K = 1000
Acet_Meth_Resp = Th_Acet_Meth_Depl - Th_Acet_Meth_Growth
Acet_Meth_umax = Umax_k_Meth
Acet_Meth_Yield = .4
Max_Fract_Acet_Meth_Mass = .01
Smth_Th_Acet_Meth_Growth = SMTH1(Th_Acet_Meth_Growth,1)
Th_Acet_Meth_Depl = Th_Acet_Meth_Growth/Acet_Meth_Yield
Th_Acet_Meth_Growth = IF (Nutrients=1) THEN
Anaero_O2_Factor*Acetate_Meth_Biomass*(Acet_Meth_umax*H2_umax_inh_factor*Acetate)/(Acet_Me
th_K+Acetate) ELSE 0
Acet_Meth_Decay_Rate_Factor =
GRAPH(Acetate_Meth_Biomass/(Max_Fract_Acet_Meth_Mass*INIT(Solid_Org_Waste)))
(0.00, 0.00), (0.1, 0.00), (0.2, 0.00), (0.3, 0.00), (0.4, 0.00), (0.5, 0.185), (0.6, 0.36), (0.7, 0.52), (0.8, 0.7),
(0.9, 0.86), (1, 1.00)

Aerobic Biomass Sector

Aerobic_Biomass(t) = Aerobic_Biomass(t - dt) + (Aerobic_Growth - Aerobic_Decay) * dt
INIT Aerobic_Biomass = 100000

INFLOWS:
Aerobic_Growth = Glu_to_Aero_Bio

OUTFLOWS:
Aerobic_Decay = Aerobic_Biomass*Aero_Decay_Rate
Aero_Decay_Rate = 0.1 + Aero_Decay_Rate_Factor*(Aero_umax - 0.1)
Aero_K = 50
Aero_umax = .6
Aero_Yield = 0.6
Glu_Aero_Resp = Th_Aero_Depl-Th_Aero_Growth
Max_Fract_Aero_Mass = 0.01
Nutrients = 1
Smth_Glu = SMTH1(Glucose,.1)
Smth_Th_Aero_Growth = SMTH1(Th_Aero_Growth,1)
Th_Aero_Depl = Th_Aero_Growth/Aero_Yield
Th_Aero_Growth = IF(Nutrients=1)THEN
(Aero_O2_Factor*Aerobic_Biomass*(Aero_umax*Aerobic_Fract*Glucose)/(Aero_K+Aerobic_Fract*Glucose)) ELSE 0
Aero_Decay_Rate_Factor =
GRAPH(Aerobic_Biomass/(Max_Fract_Aero_Mass*INIT(Solid_Org_Waste)))
(0.00, 0.00), (0.1, 0.00), (0.2, 0.00), (0.3, 0.00), (0.4, 0.00), (0.5, 0.185), (0.6, 0.36), (0.7, 0.52), (0.8, 0.7), (0.9, 0.86), (1, 1.00)

Bifidum Biomass Sector

Bifidum_Biomass(t) = Bifidum_Biomass(t - dt) + (Bifidum_Growth - Bifidum_Decay) * dt
INIT Bifidum_Biomass = 100000

INFLOWS:
Bifidum_Growth = Glu_to_Bif_Bio

OUTFLOWS:
Bifidum_Decay = Bifidum_Biomass*Bifidum_Decay_Rate
Bifidum_Decay_Rate = (0.15 + Bifidum_Decay_Rate_Factor*((Bifidum_umax) - 0.15))+kd_Acidog
Bifidum_K = 500
Bifidum_Resp = Th_Bifidum_Depl - Th_Bifidum_Growth
Bifidum_umax = Umax_k_Acido
Bifidum_Yield = .5
Max_Fract_Bifidum_Mass = .01
Smth_Th_Bifidum_Growth = SMTH1(Th_Bifidum_Growth,1)
Th_Bifidum_Depl = Th_Bifidum_Growth/Bifidum_Yield
Th_Bifidum_Growth = IF (Nutrients=1) THEN
pH_Factor*Anaero_O2_Factor*Bifidum_Biomass*(Bifidum_umax*H2_umax_inh_factor*Glucose)/(Bifidum_K+Glucose) ELSE 0
Bifidum_Decay_Rate_Factor =
GRAPH(Bifidum_Biomass/(Max_Fract_Bifidum_Mass*INIT(Solid_Org_Waste)))
(0.00, 0.00), (0.1, 0.00), (0.2, 0.00), (0.3, 0.00), (0.4, 0.00), (0.5, 0.185), (0.6, 0.36), (0.7, 0.52), (0.8, 0.7), (0.9, 0.86), (1, 1.00)

Butanol Acetone Biomass Sector

Butnl_Acet_Biomass(t) = Butnl_Acet_Biomass(t - dt) + (Butnl_Acet_Growth - Butnl_Acet_Decay) * dt
INIT Butnl_Acet_Biomass = 100000

INFLOWS:
Butnl_Acet_Growth = Glu_to_Butanol_Bio

OUTFLOWS:
Butnl_Acet_Decay = Butnl_Acet_Biomass*Butnl_Acet_Decay_Rate
Butnl_Acet_Decay_Rate = (0.15 + Butnl_Acet_Decay_Rate_Factor*((Butnl_Acet_umax) -
0.15))+kd_Acidog
Butnl_Acet_K = 500
Butnl_Acet_Resp = Th_Butnl_Acet_Depl - Th_Butnl_Acet_Growth
Butnl_Acet_umax = Umax_k_Acido
Butnl_Acet_Yield = .5
Max_Fract_Butnl_Acet_Mass = .01
Smth_Th_Butnl_Acet_Growth = SMTH1(Th_Butnl_Acet_Growth,1)
Th_Butnl_Acet_Depl = Th_Butnl_Acet_Growth/Butnl_Acet_Yield
Th_Butnl_Acet_Growth = IF (Nutrients=1) THEN
pH_Factor*Anaero_O2_Factor*Butnl_Acet_Biomass*(Butnl_Acet_umax*Glucose)/(Butnl_Acet_K+Gluc
ose) ELSE 0
Butnl_Acet_Decay_Rate_Factor =
GRAPH(Butnl_Acet_Biomass/(Max_Fract_Butnl_Acet_Mass*INIT(Solid_Org_Waste)))
(0.00, 0.00), (0.1, 0.00), (0.2, 0.00), (0.3, 0.00), (0.4, 0.00), (0.5, 0.185), (0.6, 0.36), (0.7, 0.52), (0.8, 0.7),
(0.9, 0.86), (1, 1.00)

Butyrate Acetogen Biomass Sector

Butyrate_Acetogen_Biomass(t) = Butyrate_Acetogen_Biomass(t - dt) + (Buty_Acetogen_Growth -
Buty_Acetogen_Decay) * dt
INIT Butyrate_Acetogen_Biomass = 100000

INFLOWS:
Buty_Acetogen_Growth = Buty_to_Acet_Bio

OUTFLOWS:
Buty_Acetogen_Decay = Butyrate_Acetogen_Biomass*Buty_Acetogen_Decay_Rate
Buty_Acetogen_Decay_Rate = (0.1 + Buty_Acetogen_Decay_Rate_Factor*(Buty_Acetogen_umax) -
0.1)+kd_Acidog
Buty_Acetogen_K = 750
Buty_Acetogen_Resp = Th_Buty_Acetogen_Depl - Th_Buty_Acetogen_Growth
Buty_Acetogen_umax = Umax_k_Acido
Buty_Acetogen_Yield = .4
Max_Fract_Buty_Acetogen_Mass = .01
Smth_Th_Buty_Acetogen_Growth = SMTH1(Th_Buty_Acetogen_Growth,1)
Th_Buty_Acetogen_Depl = Th_Buty_Acetogen_Growth/Buty_Acetogen_Yield
Th_Buty_Acetogen_Growth = IF (Nutrients=1) THEN
Anaero_O2_Factor*Butyrate_Acetogen_Biomass*(Buty_Acetogen_umax*H2_umax_inh_factor*Butyrate)
/(Buty_Acetogen_K+Butyrate) ELSE 0
Buty_Acetogen_Decay_Rate_Factor =
GRAPH(Butyrate_Acetogen_Biomass/(Max_Fract_Buty_Acetogen_Mass*INIT(Solid_Org_Waste)))

(0.00, 0.00), (0.1, 0.00), (0.2, 0.00), (0.3, 0.00), (0.4, 0.00), (0.5, 0.185), (0.6, 0.36), (0.7, 0.52), (0.8, 0.7), (0.9, 0.86), (1, 1.00)

Butyrate Biomass Sector

Butyrate_Biomass(t) = Butyrate_Biomass(t - dt) + (Butyrate_Growth - Butyrate_Decay) * dt
INIT Butyrate_Biomass = 100000

INFLOWS:
Butyrate_Growth = Glu_to_Buty_Bio

OUTFLOWS:
Butyrate_Decay = Butyrate_Biomass*Butyrate_Decay_Rate
Butyrate_Decay_Rate = (0.15 + Butyrate_Decay_Rate_Factor*((Butyrate_umax) - 0.15))+kd_Acidog
Butyrate_K = 500
Butyrate_Resp = Th_Butyrate_Depl - Th_Butyrate_Growth
Butyrate_umax = Umax_k_Acido
Butyrate_Yield = .5
Max_Fract_Buty_Mass = .01
Smth_Th_Butyrate_Growth = SMTH1(Th_Butyrate_Growth,1)
Th_Butyrate_Depl = Th_Butyrate_Growth/Butyrate_Yield
Th_Butyrate_Growth = IF (Nutrients=1) THEN
pH_Factor*Anaero_O2_Factor*Butyrate_Biomass*(Butyrate_umax*H2_umax_inh_factor*Glucose)/(Butyrate_K+Glucose) ELSE 0
Butyrate_Decay_Rate_Factor =
GRAPH(Butyrate_Biomass/(Max_Fract_Buty_Mass*INIT(Solid_Org_Waste)))
(0.00, 0.00), (0.1, 0.00), (0.2, 0.00), (0.3, 0.00), (0.4, 0.00), (0.5, 0.185), (0.6, 0.36), (0.7, 0.52), (0.8, 0.7), (0.9, 0.86), (1, 1.00)

Carbopn Dioxide Methanogen Biomass Sector

CO2_Meth_Biomass(t) = CO2_Meth_Biomass(t - dt) + (CO2_Meth_Growth - CO2_Meth_Decay) * dt
INIT CO2_Meth_Biomass = 10000

INFLOWS:
CO2_Meth_Growth = CO2_Meth_Bio

OUTFLOWS:
CO2_Meth_Decay = CO2_Meth_Biomass*CO2_Meth_Decay_Rate
CO2_Meth_Decay_Rate = (0.1 + CO2_Meth_Decay_Rate_Factor*((CO2_Meth_umax) - 0.1))+KdMeth
CO2_Meth_K = 1000
CO2_Meth_Resp = Th_CO2_Meth_Depl - Th_CO2_Meth_Growth
CO2_Meth_umax = Umax_k_Meth
CO2_Meth_Yield = .4
H2_to_CO2 = IF(Carbon_Dioxide>0)THEN (Hydrogen/Carbon_Dioxide) ELSE (0.18)
Max_Fract_CO2_Meth_Mass = .01
Smth_H2 = SMTH1(Hydrogen,1)
Th_CO2_Meth_Depl = Th_CO2_Meth_Growth/CO2_Meth_Yield
Th_CO2_Meth_Growth = IF ((Nutrients=1)) THEN
Anaero_O2_Factor*CO2_umax_inh_factor*CO2_Meth_Biomass*CO2_Meth_umax*Carbon_Dioxide*Smth_H2/((CO2_Meth_K+Carbon_Dioxide)*(CO2_Meth_K+Smth_H2)) ELSE 0
CO2_Meth_Decay_Rate_Factor =
GRAPH(CO2_Meth_Biomass/(Max_Fract_CO2_Meth_Mass*INIT(Solid_Org_Waste)))

169

(0.00, 0.00), (0.1, 0.00), (0.2, 0.00), (0.3, 0.00), (0.4, 0.00), (0.5, 0.185), (0.6, 0.36), (0.7, 0.52), (0.8, 0.7),
(0.9, 0.86), (1, 1.00)
CO2_umax_inh_factor = GRAPH(H2_to_CO2)
(0.00, 1.00), (0.1, 0.745), (0.2, 0.5), (0.3, 0.25), (0.4, 0.00), (0.5, 0.00), (0.6, 0.00), (0.7, 0.00), (0.8, 0.00),
(0.9, 0.00), (1, 0.00)

Chemical Characteristics & Stoichiometry

Acetate_MW = 60
Acetone_MW = 58
Acet_Co2_Cnv = 1*CO2_MW/Acetate_MW
Acet_Meth_Cnv = 1*CH4_MW/Acetate_MW
Acet_Prod = Glu_Acet_Prop_Cnv*Propionate_Path + Lact_Acet_Cnv*Lact_to_Prop
Aero_H2O_Cnv = 6*Water_MW/Glu_MW
BiCarb_Cnv = 1*BiCarb_MW/Propionate_MW
BiCarb_MW = 61
Butanol_MW = 74
Butyrate_MW = 88
Buty_Acet_Cnv = 2*Acetate_MW/Butyrate_MW
Buty_H2O_Cnv = 2*Water_MW/Butyrate_MW
Buty_H2_Cnv = 1*H2_MW/Butyrate_MW
Buty_Ion_Cnv = 2*H1_MW/Butyrate_MW
CH4_MW = 16
CO2_H2O_Cnv = 2*Water_MW/CO2_MW
CO2_Meth_Cnv = 1*CH4_MW/CO2_MW
CO2_MW = 44
CO2_Prod = Acet_Co2_Cnv*Meth_from_Acetate + Form_CO2_Cnv*Meth_from_Form +
Glu_CO2_Butnl_Cnv*Butanol_Acetone_Path + Glu_CO2_Buty_Cnv*Butyrate_Path +
Glu_CO2_Eth_Cnv*Ethanol_Path + Glu_CO2_Lact2_Cnv*Lactate2_Path +
Glu_CO2_Mx_Cnv*Mixed_Acid_Path + Glu_CO2_Prop_Cnv*Propionate_Path +
Lact_CO2_Cnv*Lact_to_Prop
Ethanol_MW = 46
Eth_Acet_Cnv = 1*Acetate_MW/Ethanol_MW
Eth_H2O_Cnv = 1*Water_MW/Ethanol_MW
Eth_H2_Cnv = 2*H2_MW/Ethanol_MW
Formate_MW = 46
Form_CO2_Cnv = 3*CO2_MW/(4*Formate_MW)
Form_H2O_Cnv = 0.5*Water_MW/Formate_MW
Form_Meth_Cnv = 0.25*CH4_MW/Formate_MW
Glu_Acetone_Cnv = 0.5*Acetone_MW/Glu_MW
Glu_Acet_Bif_Cnv = 3*Acetate_MW/(2*Glu_MW)
Glu_Acet_Cnv = 3*Acetate_MW/Glu_MW
Glu_Acet_Prop_Cnv = 2*Acetate_MW/(3*Glu_MW)
Glu_Butanol_Cnv = 0.5*Butanol_MW/Glu_MW
Glu_Buty_Cnv = 1*Butyrate_MW/Glu_MW
Glu_CO2_Aero_Cnv = 6*CO2_MW/Glu_MW
Glu_CO2_Butnl_Cnv = 5*CO2_MW/(2*Glu_MW)
Glu_CO2_Buty_Cnv = 2*CO2_MW/Glu_MW
Glu_CO2_Clos_Cnv = 6*CO2_MW/Glu_MW
Glu_CO2_Eth_Cnv = 2*CO2_MW/Glu_MW
Glu_CO2_Lact2_Cnv = 1*CO2_MW/Glu_MW
Glu_CO2_Mx_Cnv = 180*CO2_MW/(100*Glu_MW)
Glu_CO2_Prop_Cnv = 2*CO2_MW/(3*Glu_MW)

Glu_Eth_Cnv = 2*Ethanol_MW/Glu_MW
Glu_Eth_Lact2_Cnv = 1*Ethanol_MW/Glu_MW
Glu_Eth_Mx_Cnv = 75*Ethanol_MW/(100*Glu_MW)
Glu_Form_Cnv = 60*Formate_MW/(100*Glu_MW)
Glu_H2O_Aero_Cnv = 6*Water_MW/Glu_MW
Glu_H2O_Mx_Cnv = 95*Water_MW/(100*Glu_MW)
Glu_H2O_Prop_Cnv = 2*Water_MW/(3*Glu_MW)
Glu_H2_Butnl_Cnv = 2*H2_MW/Glu_MW
Glu_H2_Buty_Cnv = 2*H2_MW/Glu_MW

Glu_H2_Mx_Cnv = 200*H2_MW/(100*Glu_MW)
Glu_Lact_1_Cnv = 2*Lactate_MW/Glu_MW
Glu_Lact_2_Cnv = 1*Lactate_MW/Glu_MW
Glu_Lact_Bif_Cnv = 1*Lactate_MW/Glu_MW
Glu_MW = 180
Glu_O2_Cnv = 6*O2_MW/Glu_MW
Glu_OH_Cnv = 1*OH_MW/Glu_MW
Glu_Prop_Cnv = 4*Propionate_MW/(3*Glu_MW)
Glu_Prop_Mx_Cnv = 70*Propionate_MW/(100*Glu_MW)
H1_Cnv = 24*H1_MW/Glu_MW
H1_MW = 1
H2O_Glu_Aero_Cnv = 1*Water_MW/Glu_MW
H2O_Glu_Anaero_Cnv = 0.5*Water_MW/Glu_MW
H2_Meth_Cnv = 4*H2_MW/CO2_MW
H2_MW = 2
H2_Prod = Glu_H2_Buty_Cnv*Butyrate_Path + Glu_H2_Butnl_Cnv*Butanol_Acetone_Path +
Glu_H2_Mx_Cnv*Mixed_Acid_Path + Prop_H2_Cnv*Aceto_from_Prop +
Buty_H2_Cnv*Aceto_from_Butyrate + Eth_H2_Cnv*Aceto_from_Eth - H2_Meth_Cnv*Meth_from_CO2
Lactate_MW = 90
Lact_Acet_Cnv = 1*Acetate_MW/(3*Lactate_MW)
Lact_CO2_Cnv = 1*CO2_MW/(3*Lactate_MW)
Lact_H2O_Cnv = 1*Water_MW/(3*Lactate_MW)
Lact_Prop_Cnv = 2*Propionate_MW/(3*Lactate_MW)
N2_MW = 28
O2_CO2_Cnv = 6*O2_MW/CO2_MW
O2_Glu_Cnv = 0.25*O2_MW/Glu_MW
O2_MW = 32
OH_MW = 17
Propionate_MW = 74
Prop_Acet_Cnv = 1*Acetate_MW/Propionate_MW
Prop_H2O_Cnv = 3*Water_MW/Propionate_MW
Prop_H2_Cnv = 3*H2_MW/Propionate_MW
Prop_Ion_Cnv = 1*H1_MW/Propionate_MW
Water_MW = 18

Clostridial Biomass Sector

Clostridial_Biomass(t) = Clostridial_Biomass(t - dt) + (Clostridial_Growth - Clostridial_Decay) * dt
INIT Clostridial_Biomass = 100000

INFLOWS:
Clostridial_Growth = Glu_to_Clostr_Bio

OUTFLOWS:
Clostridial_Decay = Clostridial_Biomass*Clostridial_Decay_Rate

Clostridial_Decay_Rate = (0.1 + Clostridial_Decay_Rate_Factor*((Clostridial_umax) - 0.1))+kd_Acidog
Clostridial_K = 500
Clostridial_Resp = Th_Clostridial_Depl - Th_Clostridial_Growth
Clostridial_umax = Umax_k_Acido
Clostridial_Yield = .5
Max_Fract_Clostridial_Mass = .02
Smth_Th_Clostridial_Growth = SMTH1(Th_Clostridial_Growth,1)
Th_Clostridial_Depl = Th_Clostridial_Growth/Clostridial_Yield
Th_Clostridial_Growth = IF (Nutrients=1) THEN
Anaero_O2_Factor*Clostridial_Biomass*(Clostridial_umax*Aerobic_Fract*Glucose)/(Clostridial_K+Aero
bic_Fract*Glucose) + Clostridial_Biomass*(Clostridial_umax*(1-
Aerobic_Fract)*Glucose)/(Clostridial_K+(1-Aerobic_Fract)*Glucose) ELSE 0

Clostridial_Decay_Rate_Factor =
GRAPH(Clostridial_Biomass/(Max_Fract_Clostridial_Mass*INIT(Solid_Org_Waste)))
(0.00, 0.00), (0.1, 0.00), (0.2, 0.00), (0.3, 0.00), (0.4, 0.00), (0.5, 0.145), (0.6, 0.285), (0.7, 0.42), (0.8,
0.61), (0.9, 0.78), (1, 1.00)

Ethanol Acetogen Biomass Sector

Eth_Acetogen_Biomass(t) = Eth_Acetogen_Biomass(t - dt) + (Eth_Acetogen_Growth -
Eth_Acetogen_Decay) * dt
INIT Eth_Acetogen_Biomass = 100000

INFLOWS:
Eth_Acetogen_Growth = Eth_to_Acet_Bio

OUTFLOWS:
Eth_Acetogen_Decay = Eth_Acetogen_Biomass*Eth_Acetogen_Decay_Rate
Eth_Acetogen_Decay_Rate = (0.1 + Eth_Acetogen_Decay_Rate_Factor*((Eth_Acetogen_umax) -
0.1))+kd_Acidog
Eth_Acetogen_K = 750
Eth_Acetogen_Resp = Th_Eth_Acetogen_Depl - Th_Eth_Acetogen_Growth
Eth_Acetogen_umax = Umax_k_Acido
Eth_Acetogen_Yield = .4
Max_Fract_Eth_Acetogen_Mass = .01
Smth_Th_Eth_Acetogen_Growth = SMTH1(Th_Eth_Acetogen_Growth,1)
Th_Eth_Acetogen_Depl = Th_Eth_Acetogen_Growth/Eth_Acetogen_Yield
Th_Eth_Acetogen_Growth = IF (Nutrients=1) THEN
Anaero_O2_Factor*Eth_Acetogen_Biomass*(Eth_Acetogen_umax*H2_umax_inh_factor*Ethanol)/(Eth_
Acetogen_K+Ethanol) ELSE 0
Eth_Acetogen_Decay_Rate_Factor =
GRAPH(Eth_Acetogen_Biomass/(Max_Fract_Eth_Acetogen_Mass*INIT(Solid_Org_Waste)))
(0.00, 0.00), (0.1, 0.00), (0.2, 0.00), (0.3, 0.00), (0.4, 0.00), (0.5, 0.185), (0.6, 0.36), (0.7, 0.52), (0.8, 0.7),
(0.9, 0.86), (1, 1.00)

Ethanol Biomass Sector

Ethanol_Biomass(t) = Ethanol_Biomass(t - dt) + (Ethanol_Growth - Ethanol_Decay) * dt
INIT Ethanol_Biomass = 100000

INFLOWS:
Ethanol_Growth = Glu_to_Eth_Bio

OUTFLOWS:
Ethanol_Decay = Ethanol_Biomass*Ethanol_Decay_Rate

Ethanol_Decay_Rate = (0.15 + Ethanol_Decay_Rate_Factor*((Ethanol_umax) - 0.15))+kd_Acidog
Ethanol_K = 500
Ethanol_Resp = Th_Ethanol_Depl - Th_Ethanol_Growth
Ethanol_umax = Umax_k_Acido
Ethanol_Yield = .5
Max_Fract_Ethanol_Mass = .01
Smth_Th_Ethanol_Growth = SMTH1(Th_Ethanol_Growth,1)
Th_Ethanol_Depl = Th_Ethanol_Growth/Ethanol_Yield
Th_Ethanol_Growth = IF (Nutrients=1) THEN
pH_Factor*Anaero_O2_Factor*Ethanol_Biomass*(Ethanol_umax*H2_umax_inh_factor*Glucose)/(Ethan
ol_K+Glucose) ELSE 0
Ethanol_Decay_Rate_Factor =
GRAPH(Ethanol_Biomass/(Max_Fract_Ethanol_Mass*INIT(Solid_Org_Waste)))

(0.00, 0.00), (0.1, 0.00), (0.2, 0.00), (0.3, 0.00), (0.4, 0.00), (0.5, 0.185), (0.6, 0.36), (0.7, 0.52), (0.8, 0.7),
(0.9, 0.86), (1, 1.00)

Formate Methanogen Biomass Sector

Form_Meth_Biomass(t) = Form_Meth_Biomass(t - dt) + (Form_Meth_Growth - Form_Meth_Decay) * dt
INIT Form_Meth_Biomass = 10000

INFLOWS:
Form_Meth_Growth = Form_Meth_Bio

OUTFLOWS:
Form_Meth_Decay = Form_Meth_Biomass*Form_Meth_Decay_Rate
Form_Meth_Decay_Rate = (0.1 + Form_Meth_Decay_Rate_Factor*((Form_Meth_umax) - 0.1))+KdMeth
Form_Meth_K = 1000
Form_Meth_Resp = Th_Form_Meth_Depl - Th_Form_Meth_Growth
Form_Meth_umax = Umax_k_Meth
Form_Meth_Yield = .4
Max_Fract_Form_Meth_Mass = .01
Smth_Th_Form_Meth_Growth = SMTH1(Th_Form_Meth_Growth,1)
Th_Form_Meth_Depl = Th_Form_Meth_Growth/Form_Meth_Yield
Th_Form_Meth_Growth = IF (Nutrients=1) THEN
Anaero_O2_Factor*Form_Meth_Biomass*(Form_Meth_umax*H2_umax_inh_factor*Formate)/(Form_Me
th_K+Formate) ELSE 0
Form_Meth_Decay_Rate_Factor =
GRAPH(Form_Meth_Biomass/(Max_Fract_Form_Meth_Mass*INIT(Solid_Org_Waste)))
(0.00, 0.00), (0.1, 0.00), (0.2, 0.00), (0.3, 0.00), (0.4, 0.00), (0.5, 0.185), (0.6, 0.36), (0.7, 0.52), (0.8, 0.7),
(0.9, 0.86), (1, 1.00)

Gas Sector

Nitrogen(t) = Nitrogen(t - dt) + (- N2_Atm_Exch) * dt
INIT Nitrogen = .8*Total_Gas_Mole_Capacity*N2_MW

OUTFLOWS:
N2_Atm_Exch = IF(Excess_Gas>0) THEN (N2_Mole_Fraction*Gas_Diff_Rate*Excess_Gas*N2_MW)
ELSE IF (Excess_Gas<0) THEN (.8*Gas_Diff_Rate*Excess_Gas*N2_MW) ELSE
(N2_Mole_Fraction*Gas_Diff_Rate*Neutral_Gas_Exch*N2_MW -
.8*Gas_Diff_Rate*Neutral_Gas_Exch*N2_MW)
Oxygen(t) = Oxygen(t - dt) + (- O2_Depletion - O2_Atm_Exch) * dt

INIT Oxygen = .2*Total_Gas_Mole_Capacity*O2_MW

OUTFLOWS:
O2_Depletion = O2_Glu_Cnv*Aero_Hydr + Glu_O2_Cnv*Aerobic_Degrade
O2_Atm_Exch = IF(Excess_Gas>0) THEN (O2_Mole_Fraction*Gas_Diff_Rate*Excess_Gas*O2_MW)
ELSE IF (Excess_Gas<0) THEN (0.2*Gas_Diff_Rate*Excess_Gas*O2_MW) ELSE
(O2_Mole_Fraction*Gas_Diff_Rate*Neutral_Gas_Exch*O2_MW -
.2*Gas_Diff_Rate*Neutral_Gas_Exch*O2_MW)
CH4_Exch = IF(Excess_Gas>0) THEN (CH4_Mole_Fraction*Gas_Diff_Rate*Excess_Gas*CH4_MW)
ELSE IF (Excess_Gas<0) THEN (0) ELSE
(CH4_Mole_Fraction*Gas_Diff_Rate*Neutral_Gas_Exch*CH4_MW)
CH4_Moles = Methane/CH4_MW
CH4_Mole_Fraction = CH4_Moles/Total_Gas_Moles
CH4_Wt_Fract = Methane/Total_Gas

CO2_Exch = IF(Excess_Gas>0) THEN (CO2_Mole_Fraction*Gas_Diff_Rate*Excess_Gas*CO2_MW)
ELSE IF (Excess_Gas<0) THEN (0) ELSE
(CO2_Mole_Fraction*Gas_Diff_Rate*Neutral_Gas_Exch*CO2_MW)
CO2_Moles = Carbon_Dioxide/CO2_MW
CO2_Mole_Fraction = CO2_Moles/Total_Gas_Moles
CO2_Wt_Fract = Carbon_Dioxide/Total_Gas
Excess_Gas = Total_Gas_Moles-Total_Gas_Mole_Capacity
Gas_Diff_Rate = 1
H2_Exch = IF(Excess_Gas>0) THEN (H2_Mole_Fraction*Gas_Diff_Rate*Excess_Gas*H2_MW) ELSE
IF (Excess_Gas<0) THEN (0) ELSE (H2_Mole_Fraction*Gas_Diff_Rate*Neutral_Gas_Exch*H2_MW)
H2_Moles = Hydrogen/H2_MW
H2_Mole_Fraction = H2_Moles/Total_Gas_Moles
H2_Wt_Fract = Hydrogen/Total_Gas
N2_Moles = Nitrogen/N2_MW
N2_Mole_Fraction = N2_Moles/Total_Gas_Moles
N2_Wt_Fract = Nitrogen/Total_Gas
Neutral_Gas_Exch = 100
O2_Moles = Oxygen/O2_MW
O2_Mole_Fraction = O2_Moles/Total_Gas_Moles
O2_Wt_Fract = Oxygen/Total_Gas
Total_Gas = Oxygen+Carbon_Dioxide+Hydrogen+Methane+Nitrogen
Total_Gas_Moles = CH4_Moles+CO2_Moles+H2_Moles+N2_Moles+O2_Moles
Aero_O2_Factor = GRAPH(Oxygen/INIT(Oxygen))
(0.00, 0.00), (0.1, 0.045), (0.2, 0.16), (0.3, 0.46), (0.4, 0.795), (0.5, 1.00), (0.6, 1.00), (0.7, 1.00), (0.8,
1.00), (0.9, 1.00), (1, 1.00)
Anaero_O2_Factor = GRAPH(Oxygen/INIT(Oxygen))
(0.00, 1.00), (0.1, 0.895), (0.2, 0.795), (0.3, 0.695), (0.4, 0.57), (0.5, 0.455), (0.6, 0.32), (0.7, 0.205), (0.8,
0.105), (0.9, 0.00), (1, 0.00)
H2_umax_inh_factor = GRAPH(Hydrogen/Initial_Cell_Volume)
(0.00, 1.00), (0.1, 0.97), (0.2, 0.935), (0.3, 0.895), (0.4, 0.845), (0.5, 0.795), (0.6, 0.745), (0.7, 0.67), (0.8,
0.595), (0.9, 0.52), (1, 0.41)
Meth_H2_Factor = GRAPH(H2_Mole_Fraction)
(0.00, 0.7), (0.1, 1.00), (0.2, 1.00), (0.3, 1.00), (0.4, 1.00), (0.5, 1.00), (0.6, 1.00), (0.7, 1.00), (0.8, 1.00),
(0.9, 1.00), (1, 1.00)

Lact to Prop Acetogen Biomass Sector

Lact_to_Prop_Biomass(t) = Lact_to_Prop_Biomass(t - dt) + (Lact_to_Prop_Growth -
Lact_to_Prop_Decay) * dt
INIT Lact_to_Prop_Biomass = 100000

INFLOWS:
Lact_to_Prop_Growth = Lact_to_Prop_Bio

OUTFLOWS:
Lact_to_Prop_Decay = Lact_to_Prop_Biomass*Lact_to_Prop_Decay_Rate
Lact_to_Prop_Decay_Rate = (0.1 + Lact_to_Prop_Decay_Rate_Factor*((Lact_to_Prop_umax) -
0.1))+kd_Acidog
Lact_to_Prop_K = 500
Lact_to_Prop_Resp = Th_Lact_to_Prop_Depl - Th_Lact_to_Prop_Growth
Lact_to_Prop_umax = Umax_k_Acido
Lact_to_Prop_Yield = .5
Max_Fract_Lact_to_Prop_Mass = .01
Smth_Th_Lact_to_Prop_Growth = SMTH1(Th_Lact_to_Prop_Growth,1)
Th_Lact_to_Prop_Depl = Th_Lact_to_Prop_Growth/Lact_to_Prop_Yield
Th_Lact_to_Prop_Growth = IF (Nutrients=1) THEN
Anaero_O2_Factor*Lact_to_Prop_Biomass*(Lact_to_Prop_umax*H2_umax_inh_factor*Lactate)/(Lact_to
_Prop_K+Lactate) ELSE 0
Lact_to_Prop_Decay_Rate_Factor =
GRAPH(Lact_to_Prop_Biomass/(Max_Fract_Lact_to_Prop_Mass*INIT(Solid_Org_Waste)))
(0.00, 0.00), (0.1, 0.00), (0.2, 0.00), (0.3, 0.00), (0.4, 0.00), (0.5, 0.185), (0.6, 0.36), (0.7, 0.52), (0.8, 0.7),
(0.9, 0.86), (1, 1.00)

Lactate 1 Biomass Sector

Lactate_1_Biomass(t) = Lactate_1_Biomass(t - dt) + (Lactate_1_Growth - Lactate_1_Decay) * dt
INIT Lactate_1_Biomass = 100000

INFLOWS:
Lactate_1_Growth = Glu_to_Lactate_1_Bio

OUTFLOWS:
Lactate_1_Decay = Lactate_1_Biomass*Lactate_1_Decay_Rate
Lactate_1_Decay_Rate = (0.15 + Lactate_1_Decay_Rate_Factor*((Lactate_1_umax) - 0.15))+kd_Acidog
Lactate_1_K = 500
Lactate_1_Resp = Th_Lactate_1_Depl - Th_Lactate_1_Growth
Lactate_1_umax = Umax_k_Acido
Lactate_1_Yield = .5
Max_Fract_Lactate_1_Mass = .01
Smth_Th_Lactate_1_Growth = SMTH1(Th_Lactate_1_Growth,1)
Th_Lactate_1_Depl = Th_Lactate_1_Growth/Lactate_1_Yield
Th_Lactate_1_Growth = IF (Nutrients=1) THEN
pH_Factor*Anaero_O2_Factor*Lactate_1_Biomass*(Lactate_1_umax*H2_umax_inh_factor*Glucose)/(L
actate_1_K+Glucose) ELSE 0
Lactate_1_Decay_Rate_Factor =
GRAPH(Lactate_1_Biomass/(Max_Fract_Lactate_1_Mass*INIT(Solid_Org_Waste)))
(0.00, 0.00), (0.1, 0.00), (0.2, 0.00), (0.3, 0.00), (0.4, 0.00), (0.5, 0.185), (0.6, 0.36), (0.7, 0.52), (0.8, 0.7),
(0.9, 0.86), (1, 1.00)

Lactate 2 Biomass Sector

Lactate_2_Biomass(t) = Lactate_2_Biomass(t - dt) + (Lactate_2_Growth - Lactate_2_Decay) * dt
INIT Lactate_2_Biomass = 100000

INFLOWS:
Lactate_2_Growth = Glu_to_Lactate_2_Bio

OUTFLOWS:
Lactate_2_Decay = Lactate_2_Biomass*Lactate_2_Decay_Rate
Lactate_2_Decay_Rate = (0.15 + Lactate_2_Decay_Rate_Factor*((Lactate_2_umax) - 0.15))+kd_Acidog
Lactate_2_K = 500
Lactate_2_Resp = Th_Lactate_2_Depl - Th_Lactate_2_Growth
Lactate_2_umax = Umax_k_Acido
Lactate_2_Yield = .5
Max_Fract_Lactate_2_Mass = .01
Smth_Th_Lactate_2_Growth = SMTH1(Th_Lactate_2_Growth,1)
Th_Lactate_2_Depl = Th_Lactate_2_Growth/Lactate_2_Yield
Th_Lactate_2_Growth = IF (Nutrients=1) THEN
pH_Factor*Anaero_O2_Factor*Lactate_2_Biomass*(Lactate_2_umax*H2_umax_inh_factor*Glucose)/(L
actate_2_K+Glucose) ELSE 0
Lactate_2_Decay_Rate_Factor =
GRAPH(Lactate_2_Biomass/(Max_Fract_Lactate_2_Mass*INIT(Solid_Org_Waste)))

(0.00, 0.00), (0.1, 0.00), (0.2, 0.00), (0.3, 0.00), (0.4, 0.00), (0.5, 0.185), (0.6, 0.36), (0.7, 0.52), (0.8, 0.7),
(0.9, 0.86), (1, 1.00)

Mass Balance Sector
Net_CH4_Atm_Loss(t) = Net_CH4_Atm_Loss(t - dt) + (CH4_Loss) * dt
INIT Net_CH4_Atm_Loss = 0

INFLOWS:
CH4_Loss = CH4_Atm_Loss
Net_CO2_Atm_Loss(t) = Net_CO2_Atm_Loss(t - dt) + (CO2_Loss) * dt
INIT Net_CO2_Atm_Loss = 0

INFLOWS:
CO2_Loss = CO2_Atm_Loss
Net_H2_Atm_Loss(t) = Net_H2_Atm_Loss(t - dt) + (H2_Loss) * dt
INIT Net_H2_Atm_Loss = 0

INFLOWS:
H2_Loss = H2_Loss_to_Atm
Net_O2_Atm_Loss(t) = Net_O2_Atm_Loss(t - dt) + (O2_Loss) * dt
INIT Net_O2_Atm_Loss = 0

INFLOWS:
O2_Loss = O2_Atm_Exch
Mass_Balance = Current_Mass+Net_Gas_Loss
Net_Gas_Loss = Net_CH4_Atm_Loss+Net_CO2_Atm_Loss+Net_H2_Atm_Loss+Net_O2_Atm_Loss
Percent_Mass_Deviation = 100*(Mass_Balance-Initial_Mass)/Initial_Mass

Mixed Acid Biomass Sector
Mixed_Biomass(t) = Mixed_Biomass(t - dt) + (Mixed_Growth - Mixed_Decay) * dt
INIT Mixed_Biomass = 100000

INFLOWS:
Mixed_Growth = Glu_to_Mixed_Bio

OUTFLOWS:
Mixed_Decay = Mixed_Biomass*Mixed_Decay_Rate
Max_Fract_Mixed_Mass = .01

Mixed_Decay_Rate = (0.15 + Mixed_Decay_Rate_Factor*((Mixed_umax) - 0.15))+kd_Acidog
Mixed_K = 500
Mixed_Resp = Th_Mixed_Depl - Th_Mixed_Growth
Mixed_umax = Umax_k_Acido
Mixed_Yield = .5
Smth_Th_Mixed_Growth = SMTH1(Th_Mixed_Growth,1)
Th_Mixed_Depl = Th_Mixed_Growth/Mixed_Yield
Th_Mixed_Growth = IF (Nutrients=1) THEN
pH_Factor*Anaero_O2_Factor*Mixed_Biomass*(Mixed_umax*H2_umax_inh_factor*Glucose)/(Mixed_K+Glucose) ELSE 0
Mixed_Decay_Rate_Factor =
GRAPH(Mixed_Biomass/(Max_Fract_Mixed_Mass*INIT(Solid_Org_Waste)))
(0.00, 0.00), (0.1, 0.00), (0.2, 0.00), (0.3, 0.00), (0.4, 0.00), (0.5, 0.185), (0.6, 0.36), (0.7, 0.52), (0.8, 0.7), (0.9, 0.86), (1, 1.00)

Moisture Sector

Water(t) = Water(t - dt) + (Aerobic_H2O_Production + Other_H20_Production - H2O_Lost_to_Hydrolysis - Aceto_H2O_Consumption - Ferm_H2O_Consump) * dt
INIT Water = (Initial_Percent_Moisture/100)*(Solid_Org_Waste/Org_Waste_Fraction)

INFLOWS:
Aerobic_H2O_Production = Aero_H2O_Cnv*Aerobic_Degrade
Other_H20_Production = CO2_H2O_Cnv*Meth_from_CO2 + Form_H2O_Cnv*Meth_from_Form + Glu_H2O_Prop_Cnv*Propionate_Path + Lact_H2O_Cnv*Lact_to_Prop

OUTFLOWS:
H2O_Lost_to_Hydrolysis = H2O_Glu_Aero_Cnv*Aero_Hydr + H2O_Glu_Anaero_Cnv*Anaero_Hydro
Aceto_H2O_Consumption = Eth_H2O_Cnv*Aceto_from_Eth + Buty_H2O_Cnv*Aceto_from_Butyrate + Prop_H2O_Cnv*Aceto_from_Prop
Ferm_H2O_Consump = Glu_H2O_Aero_Cnv*Clostridial_Path + Glu_H2O_Mx_Cnv*Mixed_Acid_Path
Initial_Percent_Moisture = 25
Moisture =
Acetate+Acetone+BiCarbonate+Butanol+Butyrate+Ethanol+Formate+Glucose+Lactate+Proprionate+Water
Percent_Moisture = Moisture / (Solid_Org_Waste+Inorg_Waste+Moisture)
Moisture_Factor = GRAPH(Percent_Moisture)
(0.00, 0.00), (0.1, 0.45), (0.2, 0.66), (0.3, 0.8), (0.4, 0.865), (0.5, 0.89), (0.6, 0.905), (0.7, 0.925), (0.8, 0.95), (0.9, 0.975), (1, 0.995)

pH Sector
pH = GRAPH(Acet_Conc)
(0.00, 7.80), (5.00, 7.10), (10.0, 6.45), (15.0, 5.95), (20.0, 5.55), (25.0, 5.55), (30.0, 5.55), (35.0, 5.55), (40.0, 5.55), (45.0, 5.55), (50.0, 5.55)
pH_Factor = GRAPH(pH)
(5.00, 0.00), (5.50, 0.845), (6.00, 1.00), (6.50, 1.00), (7.00, 1.00), (7.50, 1.00), (8.00, 1.00), (8.50, 0.855), (9.00, 0.00), (9.50, 0.00), (10.0, 0.00)

Physical Dimensions Sector
Acet_Conc = Acetate/Initial_Cell_Volume
Aerobic_Fract = 1
Avg_Solid_Density = 1350/(1 - Porosity_Factor*Cell_Porosity)

177

Cell_Depth = 3
Cell_Length = 1000
Cell_Porosity = (8-(4/3)*PI) / 8
Cell_Volume = Org_Sphere_Number*(2*Org_Sphere_Radius)^3 + (Total_Spheres-
Org_Sphere_Number)*(2*Initial_Radius)^3
Cell_Width = 1000
Initial_Cell_Volume = Cell_Depth*Cell_Length*Cell_Width
Initial_Radius = .07
Initial_Sphere_Vol = (4*PI*Initial_Radius^3)/3
Inorg_Sphere_Number = (1 - Org_Waste_Fraction)*Total_Spheres
Inorg_Waste = Inorg_Sphere_Number*Initial_Sphere_Vol*Inorg_Waste_Density
Inorg_Waste_Density = Org_Waste_Density/Org_Density_Factor
Organic_Waste_Volume = Solid_Org_Waste/Org_Waste_Density
Org_Density_Factor = .75
Org_Sphere_Number = Org_Waste_Fraction*Total_Spheres
Org_Sphere_Radius = (3*Org_Sphere_Volume/(4*PI))^(1/3)
Org_Sphere_Volume = Organic_Waste_Volume/Org_Sphere_Number
Org_Surface_Area = Org_Sphere_Number*4*PI*(Org_Sphere_Radius)^2
Org_Waste_Density = Avg_Solid_Density/(Org_Waste_Fraction + (1 -
Org_Waste_Fraction)/Org_Density_Factor)

Org_Waste_Fraction = .75
PF_Growth_Factor = (Initial_Sphere_Vol + (1-Porosity_Factor)*Cell_Porosity*(2*Initial_Radius)^3) /
Initial_Sphere_Vol
Porosity_Factor = .1
Surf_Area_Exp_Factor = .01
Total_Gas_Mole_Capacity = Cell_Porosity*Initial_Cell_Volume*1000/22.4*Porosity_Factor *
PF_Growth_Factor
Total_Spheres = Initial_Cell_Volume/((2*Initial_Radius)^3) * PF_Growth_Factor

Propionate Acetogen Biomass Sector

Prop_Acetogen_Biomass(t) = Prop_Acetogen_Biomass(t - dt) + (Prop_Acetogen_Growth -
Prop_Acetogen_Decay) * dt
INIT Prop_Acetogen_Biomass = 100000

INFLOWS:
Prop_Acetogen_Growth = Prop_Acetogen_Bio

OUTFLOWS:
Prop_Acetogen_Decay = Prop_Acetogen_Biomass*Prop_Acetogen_Decay_Rate
Max_Fract_Prop_Acetogen_Mass = .01
Prop_Acetogen_Decay_Rate = (0.1 + Prop_Acetogen_Decay_Rate_Factor*((Prop_Acetogen_umax) -
0.1))+kd_Acidog
Prop_Acetogen_K = 750
Prop_Acetogen_Resp = Th_Prop_Acetogen_Depl - Th_Prop_Acetogen_Growth
Prop_Acetogen_umax = Umax_k_Acido
Prop_Acetogen_Yield = .4
Smth_Th_Prop_Acetogen_Growth = SMTH1(Th_Prop_Acetogen_Growth,1)
Th_Prop_Acetogen_Depl = Th_Prop_Acetogen_Growth/Prop_Acetogen_Yield
Th_Prop_Acetogen_Growth = IF (Nutrients=1) THEN
Anaero_O2_Factor*Prop_Acetogen_Biomass*(Prop_Acetogen_umax*H2_umax_inh_factor*Proprionate)/
(Prop_Acetogen_K+Proprionate) ELSE 0
Prop_Acetogen_Decay_Rate_Factor =
GRAPH(Prop_Acetogen_Biomass/(Max_Fract_Prop_Acetogen_Mass*INIT(Solid_Org_Waste)))

(0.00, 0.00), (0.1, 0.00), (0.2, 0.00), (0.3, 0.00), (0.4, 0.00), (0.5, 0.185), (0.6, 0.36), (0.7, 0.52), (0.8, 0.7), (0.9, 0.86), (1, 1.00)

Propionate Biomass Sector

Propionate_Biomass(t) = Propionate_Biomass(t - dt) + (Propionate_Growth - Propionate_Decay) * dt
INIT Propionate_Biomass = 100000

INFLOWS:
Propionate_Growth = Glu_to_Prop_Bio

OUTFLOWS:
Propionate_Decay = Propionate_Biomass*Propionate_Decay_Rate
Max_Fract_Propionate_Mass = .01
Propionate_Decay_Rate = (0.15 + Propionate_Decay_Rate_Factor*((Propionate_umax) - 0.15))+kd_Acidog
Propionate_K = 500
Propionate_Resp = Th_Propionate_Depl - Th_Propionate_Growth
Propionate_umax = Umax_k_Acido
Propionate_Yield = .5
Smth_Th_Propionate_Growth = SMTH1(Th_Propionate_Growth,1)
Th_Propionate_Depl = Th_Propionate_Growth/Propionate_Yield

Th_Propionate_Growth = IF (Nutrients=1) THEN
pH_Factor*Anaero_O2_Factor*Propionate_Biomass*(Propionate_umax*H2_umax_inh_factor*Glucose)/(Propionate_K+Glucose) ELSE 0
Propionate_Decay_Rate_Factor =
GRAPH(Propionate_Biomass/(Max_Fract_Propionate_Mass*INIT(Solid_Org_Waste)))
(0.00, 0.00), (0.1, 0.00), (0.2, 0.00), (0.3, 0.00), (0.4, 0.00), (0.5, 0.185), (0.6, 0.36), (0.7, 0.52), (0.8, 0.7), (0.9, 0.86), (1, 1.00)

Substrate Mass Flow

Acetate(t) = Acetate(t - dt) + (Bifidum_Path + Other_Acet_Prod + Aceto_from_Butyrate + Aceto_from_Prop + Aceto_from_Eth + Acetate_Pathway - Meth_from_Acetate - Acet_Meth_Bio) * dt
INIT Acetate = 0

INFLOWS:
Glu_Acet_Bif_Cnv = 3*Acetate_MW/(2*Glu_MW)
Other_Acet_Prod = Acet_Prod
Buty_Acet_Cnv = 2*Acetate_MW/Butyrate_MW
Prop_Acet_Cnv = 1*Acetate_MW/Propionate_MW
Eth_Acet_Cnv = 1*Acetate_MW/Ethanol_MW
Glu_Acet_Cnv = 3*Acetate_MW/Glu_MW

OUTFLOWS:
Meth_from_Acetate(o) = Acet_Meth_Resp
Acet_Meth_Bio = Th_Acet_Meth_Depl - Meth_from_Acetate
Acetone(t) = Acetone(t - dt) + (Acetone_from_Butanol_Acet_Path) * dt

INIT Acetone = 0

INFLOWS:
Acetone_from_Butanol_Acet_Path = Glu_Acetone_Cnv*Butanol_Acetone_Path
BiCarbonate(t) = BiCarbonate(t - dt) + (HCO3_Form) * dt

INIT BiCarbonate = 0

INFLOWS:
HCO3_Form = BiCarb_Cnv*Aceto_from_Prop
Butanol(t) = Butanol(t - dt) + (Butanol_Acetone_Path) * dt

INIT Butanol = 0

INFLOWS:
Glu_Butanol_Cnv = 0.5*Butanol_MW/Glu_MW
Butyrate(t) = Butyrate(t - dt) + (Butyrate_Path - Aceto_from_Butyrate - Buty_to_Acet_Bio) * dt

INIT Butyrate = 0

INFLOWS:
Glu_Buty_Cnv = 1*Butyrate_MW/Glu_MW

OUTFLOWS:
Aceto_from_Butyrate(o) = Buty_Acetogen_Resp
Buty_to_Acet_Bio = Th_Buty_Acetogen_Depl - Aceto_from_Butyrate
Carbon_Dioxide(t) = Carbon_Dioxide(t - dt) + (Clostridial_Path + Aerobic_Degrade + Other_CO2_Prod -
Meth_from_CO2 - CO2_Atm_Loss - CO2_Meth_Bio) * dt

INIT Carbon_Dioxide = 0

INFLOWS:
Glu_CO2_Clos_Cnv = 6*CO2_MW/Glu_MW
Glu_CO2_Aero_Cnv = 6*CO2_MW/Glu_MW
Other_CO2_Prod = CO2_Prod

OUTFLOWS:
Meth_from_CO2(o) = CO2_Meth_Resp
CO2_Atm_Loss = CO2_Exch
CO2_Meth_Bio = Th_CO2_Meth_Depl - Meth_from_CO2
Ethanol(t) = Ethanol(t - dt) + (Ethanol_Path + Other_Ferm_to_Eth - Aceto_from_Eth - Eth_to_Acet_Bio) *
dt

INIT Ethanol = 0

INFLOWS:
Glu_Eth_Cnv = 2*Ethanol_MW/Glu_MW
Other_Ferm_to_Eth = Glu_Eth_Mx_Cnv*Mixed_Acid_Path + Glu_Eth_Lact2_Cnv*Lactate2_Path

OUTFLOWS:
Aceto_from_Eth(o) = Eth_Acetogen_Resp
Eth_to_Acet_Bio = Th_Eth_Acetogen_Depl - Aceto_from_Eth
Formate(t) = Formate(t - dt) + (Mixed_Acid_Path - Meth_from_Form - Form_Meth_Bio) * dt

INIT Formate = 0

INFLOWS:
Glu_Form_Cnv = 60*Formate_MW/(100*Glu_MW)

OUTFLOWS:
Meth_from_Form = Form_Meth_Resp
Form_Meth_Bio = Th_Form_Meth_Depl - Meth_from_Form
Glucose(t) = Glucose(t - dt) + (Aero_Hydr + Anaero_Hydro + Org_from_Bio - Butanol_Acetone_Path -
Butyrate_Path - Lactate1_Path - Propionate_Path - Ethanol_Path - Bifidum_Path - Mixed_Acid_Path -
Clostridial_Path - Aerobic_Degrade - Lactate2_Path - Glu_to_Aero_Bio - Glu_to_Buty_Bio -
Glu_to_Butanol_Bio - Glu_to_Lactate_1_Bio - Glu_to_Lactate_2_Bio - Glu_to_Prop_Bio -
Glu_to_Clostr_Bio - Glu_to_Eth_Bio - Glu_to_Bif_Bio - Glu_to_Mixed_Bio - Acetate_Pathway -
Glu_to_Acet_Bio) * dt

INIT Glucose = 0

INFLOWS:
Aero_Hydr = IF (Oxygen>0.05*INIT(Oxygen)) THEN
Growth_Lag*Aero_Hyd_Rate*Org_Surface_Area*Surf_Area_Exp_Factor ELSE 0
Anaero_Hydro = IF (Oxygen<0.1*INIT(Oxygen)) THEN
(Growth_Lag*An_Hyd_Rate*Org_Surface_Area) ELSE
(Growth_Lag*An_Hyd_Rate*Org_Surface_Area*(1 - Surf_Area_Exp_Factor))
Org_from_Bio = Total_Decay

OUTFLOWS:
Butanol_Acetone_Path(o) = Butnl_Acet_Resp
Butyrate_Path(o) = Butyrate_Resp
Lactate1_Path(o) = Lactate_1_Resp

Propionate_Path(o) = Propionate_Resp
Ethanol_Path(o) = Ethanol_Resp
Bifidum_Path(o) = Bifidum_Resp
Mixed_Acid_Path(o) = Mixed_Resp
Clostridial_Path(o) = Clostridial_Resp
Aerobic_Degrade(o) = Glu_Aero_Resp
Lactate2_Path(o) = Lactate_2_Resp
Glu_to_Aero_Bio = Th_Aero_Depl-Aerobic_Degrade
Glu_to_Buty_Bio = Th_Butyrate_Depl - Butyrate_Path
Glu_to_Butanol_Bio = Th_Butnl_Acet_Depl - Butanol_Acetone_Path
Glu_to_Lactate_1_Bio = Th_Lactate_1_Depl - Lactate1_Path
Glu_to_Lactate_2_Bio = Th_Lactate_2_Depl - Lactate2_Path
Glu_to_Prop_Bio = Th_Propionate_Depl - Propionate_Path
Glu_to_Clostr_Bio = Th_Clostridial_Depl - Clostridial_Path
Glu_to_Eth_Bio = Th_Ethanol_Depl - Ethanol_Path
Glu_to_Bif_Bio = Th_Bifidum_Depl - Bifidum_Path
Glu_to_Mixed_Bio = Th_Mixed_Depl - Mixed_Acid_Path
Acetate_Pathway(o) = Acetate_Resp
Glu_to_Acet_Bio = Th_Acetate_Depl - Acetate_Pathway
H1(t) = H1(t - dt) + (H1_from_Cloistr) * dt

INIT H1 = 0

INFLOWS:
H1_from_Cloistr = H1_Cnv*Clostridial_Path
Hydrogen(t) = Hydrogen(t - dt) + (Tot_H2_Prod - H2_Loss_to_Atm) * dt

INIT Hydrogen = 0

INFLOWS:
Tot_H2_Prod = H2_Prod

OUTFLOWS:
H2_Loss_to_Atm = H2_Exch
Hydroxide(t) = Hydroxide(t - dt) + (OH_from_Hydr) * dt

INIT Hydroxide = 0

INFLOWS:
OH_from_Hydr = Glu_OH_Cnv*Aero_Hydr
H_Ion(t) = H_Ion(t - dt) + (Ion_Form) * dt

INIT H_Ion = 0

INFLOWS:
Ion_Form = Prop_Ion_Cnv*Aceto_from_Prop + Buty_Ion_Cnv*Aceto_from_Butyrate
Lactate(t) = Lactate(t - dt) + (Lactate1_Path + Lactate2_Path + Other_Ferm_to_Lact - Lact_to_Prop - Lact_to_Prop_Bio) * dt

INIT Lactate = 0

INFLOWS:
Glu_Lact_1_Cnv = 2*Lactate_MW/Glu_MW
Glu_Lact_2_Cnv = 1*Lactate_MW/Glu_MW
Other_Ferm_to_Lact = Glu_Lact_Bif_Cnv*Bifidum_Path

OUTFLOWS:
Lact_to_Prop(o) = Lact_to_Prop_Resp
Lact_to_Prop_Bio = Th_Lact_to_Prop_Depl - Lact_to_Prop
Methane(t) = Methane(t - dt) + (Meth_from_Form + Meth_from_CO2 + Meth_from_Acetate - CH4_Atm_Loss) * dt

INIT Methane = 0

INFLOWS:
Meth_from_Form = Form_Meth_Resp
CO2_Meth_Cnv = 1*CH4_MW/CO2_MW
Acet_Meth_Cnv = 1*CH4_MW/Acetate_MW

OUTFLOWS:
CH4_Atm_Loss = CH4_Exch
Proprionate(t) = Proprionate(t - dt) + (Propionate_Path + Lact_to_Prop + Mx_Prop_Prod - Aceto_from_Prop - Prop_Acetogen_Bio) * dt

INIT Proprionate = 0

INFLOWS:
Glu_Prop_Cnv = 4*Propionate_MW/(3*Glu_MW)
Lact_Prop_Cnv = 2*Propionate_MW/(3*Lactate_MW)
Mx_Prop_Prod = Glu_Prop_Mx_Cnv*Mixed_Acid_Path

OUTFLOWS:

Aceto_from_Prop(o) = Prop_Acetogen_Resp
Prop_Acetogen_Bio = Th_Prop_Acetogen_Depl - Aceto_from_Prop
Solid_Org_Waste(t) = Solid_Org_Waste(t - dt) + (- Anaerobic_Depletion - Aerobic_Hydr_Depl) * dt
INIT Solid_Org_Waste = Org_Sphere_Number*Initial_Sphere_Vol*Org_Waste_Density

OUTFLOWS:
Anaerobic_Depletion = Anaero_Hydro - (H2O_Glu_Anaero_Cnv*Anaero_Hydro)
Aerobic_Hydr_Depl = Aero_Hydr + OH_from_Hydr - (O2_Glu_Cnv*Aero_Hydr) -
(H2O_Glu_Aero_Cnv*Aero_Hydr)
Aero_Hyd_Rate = 50
An_Hyd_Rate = .7
Growth_Lag = GRAPH(TIME)
(0.00, 0.055), (5.00, 0.21), (10.0, 0.51), (15.0, 0.795), (20.0, 0.93), (25.0, 1.00), (30.0, 1.00), (35.0, 1.00),
(40.0, 1.00), (45.0, 1.00), (50.0, 1.00)

Temperature Sector
Heat_Generated(t) = Heat_Generated(t - dt) + (Total_heat_gain - Heat_lose) * dt
INIT Heat_Generated = 0

INFLOWS:
Total_heat_gain =
((Acetate_Pathway/(Glu_MW/1000))*Acetate_Heat)+((Bifidum_Path/(Glu_MW/1000))*Bifidium_Heat)+
((Butanol_Acetone_Path/(Glu_MW/1000))*Butanol_Heat)+((Butyrate_Path/(Glu_MW/1000))*Butyrate_
Heat)+((Clostridial_Path/(Glu_MW/1000))*ClostridialHeat)+((Ethanol_Path/(Glu_MW/1000))*Ethanol_H
eat)+((Lactate1_Path/(Glu_MW/1000))*Lactate_Heat)+((Lactate2_Path/(Glu_MW/1000))*Lactate_Heat)+
((Mixed_Acid_Path/(Glu_MW/1000))*Mixed_Acid_Heat)+((Propionate_Path/(Glu_MW/1000))*Propiona
te_Heat)

OUTFLOWS:
Heat_lose = Temp_Loss*Current_Mass*Specific_heat
Temperature(t) = Temperature(t - dt) + (Temp_Increase - Temp_Loss) * dt

INIT Temperature = 25

INFLOWS:
Temp_Increase = Total_heat_gain/(Specific_heat*Current_Mass)

OUTFLOWS:
Temp_Loss = Temp_Differential*TC
Acetate_Heat = Heat_Constant
Bifidium_Heat = Heat_Constant
Butanol_Heat = Heat_Constant
Butyrate_Heat = Heat_Constant
b_Height_Acidogen = 5
b_Heigth_Meth = 3
ClostridialHeat = Heat_Constant
Decay_Steepness_Acidogen = 6
Decay_Steepness_Meth = 5
Ethanol_Heat = Heat_Constant
Heat_Constant = 30
KdMeth = LOGN(1/1+exp((Temperature-Tcritical_Meth)/Decay_Steepness_Meth))
kd_Acidog = LOGN(1/1+exp((Temperature-Tcrtical_Acidogen)/Decay_Steepness_Acidogen))

183

Lactate_Heat = Heat_Constant
Mixed_Acid_Heat = Heat_Constant
Propionate_Heat = Heat_Constant
Specific_heat = .6
TC = .001
Tcritical_Meth = 60
Tcrtical_Acidogen = 46
Temp_Differential = (Temperature-Soil_Temp)
Temp_Span_Acidogen = 30
Temp_Span_Meth = 12
Tpeak_Acidogen = 25
Tpeak_Meth = 40
Umax_k_Acido = LOGN((1+b_Height_Acidogen*exp(-1*((Temperature-Tpeak_Acidogen)/Temp_Span_Acidogen)^2)))
Umax_k_Meth = LOGN(1+b_Heigth_Meth*exp
(-1*((Temperature-Tpeak_Meth)/Temp_Span_Meth)^2))
Soil_Temp = GRAPH(TIME)
(0.00, 7.00), (30.0, 11.0), (60.0, 19.5), (90.0, 16.8), (120, 12.8), (150, 14.8), (180, 19.8), (210, 18.0), (240, 12.1), (270, 4.50), (300, 2.10)

Total Biomass Decay

Total_Decay =
Bifidum_Decay+Acet_Meth_Decay+Aerobic_Decay+Butyrate_Decay+Buty_Acetogen_Decay+Butnl_Acet_Decay+Clostridial_Decay+CO2_Meth_Decay+Ethanol_Decay+Eth_Acetogen_Decay+Form_Meth_Decay+Lactate_1_Decay+Lactate_2_Decay+Lact_to_Prop_Decay+Mixed_Decay+Propionate_Decay+Prop_Acetogen_Decay+Acetate_Decay

Total Mass Sector

Current_Mass =
Acetate+Bifidum_Biomass+Acetate_Meth_Biomass+Acetone+Aerobic_Biomass+BiCarbonate+Butanol+Butyrate+Butyrate_Acetogen_Biomass+Butyrate_Biomass+Butnl_Acet_Biomass+Carbon_Dioxide+Clostridial_Biomass+CO2_Meth_Biomass+Ethanol+Ethanol_Biomass+Eth_Acetogen_Biomass+Formate+Form_Meth_Biomass+Glucose+H1+Hydrogen+Hydroxide+H_Ion+Lactate+Lactate_1_Biomass+Lactate_2_Biomass+Lact_to_Prop_Biomass+Methane+Mixed_Biomass+Oxygen+Propionate_Biomass+Proprionate+Prop_Acetogen_Biomass+Solid_Org_Waste+Water

Initial_Mass = INIT(Solid_Org_Waste) + INIT(Water) + INIT(Oxygen)

Bibliography

Adeel, Zafar and Audrey D. Levine. "Solubilization and Methanogenesis of a Particulate Industrial Waste: Impact of Solids Loading and temperature," Waste Management, 14: 693-702 (1994).

Attal, A., J. Akunna, P. Camacho, P. Salmon, and I. Paris. "Anaerobic Degradation of Municipal Wastes in Landfill," Water Science Technology, 25: 243-253 (1992).

Barlaz, Morton A. Microbiological and Chemical Dynamics during Refuse Decomposition in a Simulated Sanitary Landfill. Ph.D. dissertation. University of Wisconsin-Madison, 1988 (ON8817111).

Barlaz, Morton A., M.W. Milke, and R.K. Ham. "Gas Production Parameters in a Sanitary Landfill Simulators," Waste Management & Research. 5: 27-39 (1987).

Barlaz, Morton, A., Rober K. Ham, and Daniel M. Schaefer. "Methane Production from Municipal Refuse: A Review of Enhancement Techniques and Microbial Dynamics," Critical Reviews in Environmental Control, 19: 557-585(1990).

Barlaz, Morton A. and Anna C. Palamisano. Microbiology of Solid Waste. Boca Raton FL: CRC Press, 1996.

Bazin, Michael J. Microbial Population Dynamics. Boca Raton, FL: CRC Press, 1982.

Benter, Brian D. Substrate Availability in Solid Waste Landfills. MS Thesis, AFIT/GEE/ENV/99M-03. School of Engineering, Air Force Institute of Technology (AU), Wright-Patterson AFB OH, March 1999

Boeckx, Pascal and Oswald Van Cleempt. "Methane Oxidation in a Neutral Landfill Cover Soil: Influence of Moisture Content, Temperature, and Nitrogen-Turnover," Journal of Environment Quality, 25: 178-183 (1996).

Borjesson, Gunnar, and Bo H. Svensson. "Seasonal and Diurnal Methane Emissions from a Landfill and their Regulation by Methane Oxidation," International Solid Waste Association: 33-54 (1997).

Brock, Thomas D. and others. Biology of Microorganisms. (7th Edition). New Jersey: Prentice Hall, Inc., 1994.

Cha, Cheol Gi and Tatsuya Noike. "Effect of Rapid Temperature Change HRT on Anaerobic Acidogenesis," Water, Science and Technology, 36: 247-253 (1997).

Chang, Jen-Hu. Ground Temperature. Milton, MA: Harvard University, 1958.

Chiampo, F., R. Conti, and Cometto. "Morphological Characterization of MSW Landfills," Resources, Conservation, and Recycling, 17: 37-45 (1996).

Colborn, Philip A. Investigation of Biodegradation Processes in Solid Waste Landfills. MS Thesis, AFIT/GEE/ENV/97D-04. School of Engineering, Air Force Institute of Technologyy (AU), Wright-Patterson AFB OH, December 1997.

Cox, Ricky D. In Situ Warming and Soil Venting to Enhance the Biodegradation of JP-4 in Cold Climates: A Critical Study and Analysis. MS Thesis, AFIT/GEE/ENV/93D-03. School of Engineering, Air Force Institute of Technology (AU), Wright-Patterson AFB OH, December 1995.

Eck, Craig P. Effects of Moisture Content in Solid Waste Landfills. MS Thesis, AFIT/GEE/ENV/00M-03. School of Engineering, Air Force Institute of Technologyy (AU), Wright-Patterson AFB OH, March 2000.

El-Fadel, M., A. N. Findikakis, and J.O. Leckie. "Numerical Modeling of Generation and Transport of Gas and Heat in Landfills I. Model Formulation," Waste Management & Research, 14: 483-504 (1996).

Environmental Protection Agency. Characterization of Municipal Solid Waste in the United States 1996 Update . n. pag. http://www.epa.gov. (July 00).

Forrester, J.W. and P.M. Senge. "Tests for Building Confidence in System Dynamics Models," TIMS Studies in Management Sciences, 14: 209-228 (1980).

Gordon, James A. and Irene A. Watson Craik, and Eric Senior. "Use of a Three-Stage Laboratory Model to Determine the Effects of Temperature on Individual Trophic Groups of Methanogenic Associations Isolated from Anoxic Landfill," Journal of Chemical Technology & Biotechnology, 67: 333-338 (1996).

Gurijala, Rao. K., and Joseph M. Suflita. "Environmental Factors Influencing Methanogenesis from Refuse in Landfill Samples," Environmental Science & Technology, 27: 1176-1181 (1993).

Hartz, Kenneth E., Robert E. Klink, and Robert K. Ham. "Temperature Effects: Methane Generation from Landfill Samples," Journal of Environmental Engineering, 108: 629-638 (1982).

Johnston, G.H., ed. Permafrost Engineering Design and Construction. New York: Jon Wiley & Sons, 1981.

Kasali, George B. and Eric Senior. "Effects of Temperature and Moisture on the Anaerobic Digestion of Refuse," Journal of Chemical Technology and Biotechnology, 44: 31-41 (1989).

Meadows, Donella H. "The Unavoidable A Priori," Elements of the System Dynamics Method. Ed. Jorgen Randers. Cambridge MA: MIT Press, 1980.

Murphy, R. J., D.E. Jones, and R.I. Stessel. "Relationship of Microbial Mass and Activity in Biodegradation of Solid Waste," Waste Management & Research, 13: 485-497 (1995).

Peleg, Micha. "A Model of Temperature Effects on Microbial Populations From Growth to Lethality," Journal of Science, Food, Agriculture, 68: 83-89 (1995).

Senior, Eirc., Irene A. Watson-Craik, and G.B. Kasali. "Control/Promotion of the Refuse Methanogenic Fermentation," Critical Reviews in Biotechnology, 10: 93-118(1990).

Shelley, Michael L. Class Handout, ENVR 642, Environmental System Dynamics Modeling. School of Engineering, Air Force Institute of Technology (AU), Wright-Patterson AFB OH, Spring 2000.

Smith, Lawrence and Robert E. Hinchee. In-Situ Thermal Technologies for Site Remediation. Boca Raton FL: Lewis Publishers, 1993.

STELLA Research. Version 5.1.1, Windows disk. Computer software, High Performance Systems, Inc., Hanover NH, 1998.

Tchobanoglous, George, Hilary Theisen, and Samuel Vigil. (2nd Edition). Integrated Solid Waste Management. New York: McGraw-Hill, Inc., 1993.

Wheeler Environmental Management. "What is Landfill Gas?" Excerpt from unpublished article. 1999 Update. n. pag. http//www.ch4gas.com. (July 00).

Zeikus, J.G. "Microbial Populations in Digesters," Anaerobic Digestion. D.A. Stafford, ed., London: Applied. Aci. Publishers, 1979.

Zwietering, M.W., J.T. De Koos, B.E. Hasenack, J.C. De Wit, and K. Van'triet. "Modeling of Bacterial Growth as a Function of Temperature," Applied and Environmental Microbiology, 57: 1094-1101 (April 1991).

Vita

2nd Lt David A. Jokinen graduated from Rome Free Academy High School in Rome New York in June 1995. He entered undergraduate studies at the Air Force Academy in Colorado Springs where he graduated with a Bachelor of Science degree in Environmental Engineering in June 1999. While at the Academy he was the captain of the Nordic Ski Team and led the team to a third place finish at the National Collegiate Ski Championship.

His first assignment was to the Air Force Institute of Technology, Wright Patterson to pursue his Masters degree in Systems Engineering and Management. In his free to time Lt Jokinen likes to play volleyball and cross country ski. He plays for the base volleyball team which and has represented WPAFB at the AFMC Volleyball tournament in April 2000 at Hill AFB. Upon graduation, he will be assigned to Ellsworth, SD.

					Form Approved
REPORT DOCUMENTATION PAGE					OMB No. 074-0188

The public reporting burden for this collection of information is estimated to average 1 hour per response, including the time for reviewing instructions, searching existing data sources, gathering and maintaining the data needed, and completing and reviewing the collection of information. Send comments regarding this burden estimate or any other aspect of the collection of information, including suggestions for reducing this burden to Department of Defense, Washington Headquarters Services, Directorate for Information Operations and Reports (0704-0188), 1215 Jefferson Davis Highway, Suite 1204, Arlington, VA 22202-4302. Respondents should be aware that notwithstanding any other provision of law, no person shall be subject to an penalty for failing to comply with a collection of information if it does not display a currently valid OMB control number. **PLEASE DO NOT RETURN YOUR FORM TO THE ABOVE ADDRESS.**

1. REPORT DATE *(DD-MM-YYYY)* 20-03-2001	2. REPORT TYPE Master's Thesis		3. DATES COVERED *(From – To)* Aug 1999– Mar 2001

4. TITLE AND SUBTITLE	5a. CONTRACT NUMBER
A SYSTEM DYNAMICS APPROACH TO MODELING TEMPERATURE EFFECTS IN SOLID WASTE LANDFILLS	5b. GRANT NUMBER
	5c. PROGRAM ELEMENT NUMBER

6. AUTHOR(S)	5d. PROJECT NUMBER
Jokinen, David, A., 2 Lt USAF	5e. TASK NUMBER
	5f. WORK UNIT NUMBER

7. PERFORMING ORGANIZATION NAMES(S) AND ADDRESS(S)	8. PERFORMING ORGANIZATION REPORT NUMBER
Air Force Institute of Technology Graduate School of Engineering and Management (AFIT/EN) 2950 P Street, Building 640 WPAFB OH 45433-7765	AFIT/GEE/ENV/01M-05

9. SPONSORING/MONITORING AGENCY NAME(S) AND ADDRESS(ES)	10. SPONSOR/MONITOR'S ACRONYM(S)
	11. SPONSOR/MONITOR'S REPORT NUMBER(S)

12. DISTRIBUTION/AVAILABILITY STATEMENT
APPROVED FOR PUBLIC RELEASE; DISTRIBUTION UNLIMITED.

13. SUPPLEMENTARY NOTES

14. ABSTRACT

The amount of municipal solid waste discarded to landfills is continually increasing even with extensive recycling efforts. The need to understand the behavior of waste in landfills is increased due to the decreasing number of active landfills, communities concern to the potential hazards associated with landfills, and companies or installations with landfills on-site need to understand landfill behavior because they must comply with new legislation concerning design and detecting hazardous material movement of-site.

This research is focused on increasing the understanding of landfill behavior by examining the effects of temperature in a landfill system. A system dynamics approach was used in this research to develop and build structure to produce landfill behavior. Two reference modes using gas generation and a basic microbial growth curve were used as verification mechanisms. Initial verification and validation were preformed in separate sections then added to Shelley's landfill model to verify that the additional temperature structure more accurately modeled landfill behavior.

Results show that an equation responsive to temperature effects on microbial growth and death, more accurately depicts landfill behavior. Increased understanding of how heat is lost from a landfill will increase the usefulness of this model. An inclusive model will help landfill operator's build and manage landfills to optimize performance and biodegradation over the lifetime of a landfill.

15. SUBJECT TERMS
Solid Waste, Temperature, Landfill Gas, Methane, Microbial Processes

16. SECURITY CLASSIFICATION OF:			17. LIMITATION OF ABSTRACT	18. NUMBER OF PAGES	19a. NAME OF RESPONSIBLE PERSON Dr. Michael L. Shelley, ENV
a. REPORT U	b. ABSTRACT U	c. THIS PAGE U	UU	203	19b. TELEPHONE NUMBER *(Include area code)* (937) 255-3636, ext 4594

Standard Form 298 (Rev. 8-98)
Prescribed by ANSI Std. Z39-18